Investigating the mechanism of Tau and Fyn mediated neurodegeneration in Alzheimer's disease

A thesis submitted to the University of Hyderabad in partial fulfilment of the award degree of

DOCTOR OF PHILOSOPHY (Ph.D.)

By

Ravi Kant Yadav

(Regd. No: 13LTPM01)



Supervisor

Dr. Madhubabu Gajula Balija

Department of Biotechnology and Bioinformatics

School of Life Sciences

University of Hyderabad

Hyderabad-500 046, INDIA



Dedicated to

My beloved grandparents Late Shri Suraj Pal Yadav and Late Smt Rambeti Yadav...

While you may not be present to witness this achievement, your essence thrives within each written word and explored concept in these pages. Your profound thinking and dedicated work ethics have not only transformed our family's way of life but have also left an indelible mark on our values and aspirations.

My Chachaji Dr. Mahesh Chandra Yadav...

Your unwavering guidance and nurturing support have illuminated my path, shaping not just my career but the very essence of who I've become. Your wisdom and encouragement continue to be the driving force behind my journey.



University of Hyderabad

(A Central University established in 1974 by act of parliament)

Department of Biotechnology and Bioinformatics

School of Life Sciences

Hyderabad- 500 046,

INDIA

DECLARATION

I, Ravi Kant Yadav, hereby declare that this thesis entitled "Investigating the mechanism of Tau and Fyn mediated neurodegeneration in Alzheimer's disease" submitted by me under the guidance and supervision of Dr. Madhubabu Gajula Balija is a bonafide work.

I also declare that it has not been submitted previously in part or in full to this University or any other University or Institution for the award of any degree or diploma.

Place: Hyderabad Date: 22/8/23

Ravi Kant Yadav Regd. No: 13LTPM01



Department of Biotechnology and Bioinformatics School of Life Sciences University of Hyderabad Hyderabad 500 046, INDIA.

CERTIFICATE

This is to certify that the thesis entitled "Investigating the mechanism of Tau and Fyn mediated neurodegeneration in Alzheimer's disease" submitted by Mr. Ravi Kant Yadav bearing Reg. No. 13LTPM01 in partial fulfilment of the requirements for the award of Doctor of Philosophy in Biotechnology is a bonafide work carried out by him under my supervision and guidance.

The thesis has not been submitted previously in part or in full to this or any other University or Institution for the award of any degree or diploma.

Dr. Madhubabu Gajula Balija Supervisor

Department of Biotechnology and Bioinformatics

Dr. MADHUBABU G.B.

Assistant Professor
Dept. of Biotechnology & Bioinformatics
School of Life Sciences
University of Hyderabad
Gachibowli, Hyderabad-500 046. India.

Prof. J. S. S. Prakash Head

Department of Biotechnology and Bioinformatics

HEAD

Dept. of Biotechnology & Bioinformatics
University of Hyderabad
Hyderabad.

Prof. N. Siva Kumar

News Know

Dean

School of Life Sciences निर्मेश अधिक / Dean

जीव विज्ञान संकास / School of Life Sciences हैदराबाद विश्वविद्यालय/University of Hyderabad हैदराबाद / Hyderabad-500 046.



Department of Biotechnology and Bioinformatics School of Life Sciences University of Hyderabad Hyderabad 500 046, INDIA.

CERTIFICATE

(For Ph.D. Dissertations)

This is to certify that the thesis entitled "Investigating the mechanism of Tau and Fyn mediated neurodegeneration in Alzheimer's disease" Submitted by Mr. Ravi Kant Yadav bearing Reg. No. 13LTPM01 in partial fulfilment of the requirements for award of Doctor of Philosophy in the School of Life Sciences is a bona fide work carried out by him under my supervision and guidance.

This thesis is free from plagiarism and has not been submitted previously in part or in full to this or any other university or institution for award of any degree or diploma.

Publication:

 Ravi Kant Yadav¹, Dushyant Kumar Gautam¹, Chukhu Muj, Madhu Babu Gajula Balija, Indira Paddibhatla. Methotrexate negatively acts on inflammatory responses triggered in Drosophila larva with hyperactive JAK/STAT pathway. Developmental and Comparative Immunology 123 (2021) 104161

Student has made presentations in the following conferences:

Oral presentations:

 Oral presentation entitled as 'Investigating the mechanism of Tau and Fyn mediated neurodegeneration in Alzheimer's disease' at BioAnveshana, Symposium on Frontiers in Biotechnology and Bioinformatics, University of Hyderabad. (National)

Posters presentations:

- Presented a poster entitled as 'Effects of Methotrexate (MTX) on hematopoiesis in Drosophila melanogaster' at Bioquest-2016, School of Life Sciences, University of Hyderabad, India. (National)
- Presented a poster entitled as 'Investigating the mechanism of Tau and Fyn mediated neurodegeneration in Alzheimer's disease' at 5th Asia Pacific Drosophila research

conference and 5th India Drosophila research conference, IISER Pune, India. (International).

Further, the student has passed the following courses towards fulfillment of coursework requirement for Ph.D.

Course Code	Name	Credits	Pass/Fail
BC801	Analytical Techniques	4	Passed
BC802	Research ethics, Data Analysis and Biostatistics	4	Passed
BC803	Research Proposal and Scientific writing	4	Passed

Dr. MADHUBABU G.B.

Assistant Professor Dept. of Biotechnology & Bioinformatics School of Life Sciences

University of Hyderabad

Gachibowli, Hyderabad-500 046. India.

Head of Department

HEAD

Dept. of Biotechnology & Bioinformatics हैदराबाद विश्वविद्यालय/University of Hyderabad University of Hyderabad हैदराबाद / Hyderabad-500 046. Hyderabad.

Bura Kiro संकाय Deam / Dean

जीव विज्ञान संकाय / School of Life Sciences

हैदरावाद / Hyderabad-500 046.

Acknowledgements

I deem it my privilege and honour to consign my gratitude and indebtedness to the following without whose guidance, support and concern I would not have been able to complete my PhD journey. I am very thankful for each one of them who helped sculpting my career in science.

If eel fortunate to express my deep sense of reverence and gratitude to my revered guide, **Dr. Madhubabu Gajula Balija**, for his support, immaculate guidance, constant encouragement and providing requisite facilities to persist my research which otherwise would have remained incomplete. His nurturing and gentle concern has been a stimulus which I will always cherish. I also appreciate his untiring efforts during the entire tenure of my research work and patience during writing of this thesis. I am eternally indebted to him for giving me the exceptional freedom and opportunity to work on several different projects. Our association taught me many important aspects of life apart from research. I have no words to express my gratitude for everything he has contributed to my PhD and without his blessings it was surely impossible for me to finish my work.

The School of Life Sciences, University of Hyderabad has one of the best facilities available. For this I would like to extend my sincere thanks to the present Dean of life sciences, Prof. Siva Kumar Nadimpalli and the previous Deans Prof. Dayananda Siddavattam, Prof. K.V.A. Ramaiah, Prof. P. Reddanna, and Prof. R. P. Sharma, who have provided the necessary facilities and constantly thrived for the betterment of the students.

I would also like to extend my sincere gratitude to our present Head of the Department of Biotechnology and Bioinformatics, Prof. J.S.S Prakash, and the previous heads, Prof. Anand Kumar Kondapi, Prof. KPMSV Padmasree, Prof. Niyaz Ahmed, and Prof. P Prakash Babu, for providing us with good equipment and facilities to carry out the work.

I would like to express my deepest appreciation to my committee, I was very fortunate to have Prof. Anand Kumar Kondapi and Dr Joby Joseph as my doctoral committee member. Their suggestions, positive criticism and rationales were very instrumental in diluting my otherwise emotional biasness towards my work.

I am very much thankful to Dr Joby Joseph for his kind help in ERG recordings, Matlab program writing and data analysis. Without his help, my research work would not have been completed.

My heartfelt thanks to Dr. Indira Paddibhatla for her guidance and moral support. She always helped me out when I got any difficulties or queries regarding experiments. She helped me a lot by taking time out of her busy schedules so that I could improve my presentation skills. I also thank Dr. Rajendra Chilkuri for helping me learning the microinjections, playing with us in our team and always being so welcoming.

I emphatically express my loyal and venerable thanks to Prof. Markus Zweckstetter, Max Planck Institute for Multidisciplinary Sciences, Gottingen, Germany for generously helping us with the compounds for my PhD work.

I also thank Prof. G. Ravi Kumar, Dr Rahul Kumar, Dr Anil Kumar, Prof Suresh Yenugu, Prof.Sharmistha for allowing me to use their lab facilities. I thank Prof Vijay Raghavan, Dr Krishan, Prof Rakesh Mishra for allowing me to use their facilities for learning the fly work, Prof.Krishanu Ray, Dr Manish Jaiswal, Prof. Cheng-Ting and Bloomington *Drosophila* Stock Centre (BDSC) for helping with *Drosophila* stocks. I thank Raghvendra for helping me with the microinjection setup for transgenesis.

I am very thankful to my chachaji Dr. Mahesh C. Yadav for nurturing science in me and guiding me throughout my career. He has been my inspiration and motivation always.

My special thanks to fellow lab mates Ashraf, Ashwani, Enong, Shreya, Ayngarasoruoban, Pratibha, Poojitha and Chhigan, I thank them for their support, encouragement, and cooperation during my research work. I am extremely grateful for the wholehearted support of my lab masters' students C. Muj, Kajal, Supraja, SriRam, Souvik, Anwesha, Manjiri, JD, Mayur, Saran M and Anindita. I am very much thankful to Ashraf for always being there for everything day and night. Special thanks to Saran M, and Pratibha their generous help in work.

I extend my gratitude to my friends, Pratul Kumar, Dushyant Kumar, Rajat Srivastava for their firm support and cooperation during my PhD tenure. I have spent the best moments of life with them, they have been there with me through all ups and downs in my PhD journey. I sincerely thank Dushyant for all his patience and composure during our research work, we have spent many sleepless nights working in lab together. I also thank Rajat for cooking and providing us the best food, I have really enjoyed that. I am indebted to Pratul for all the love, guidance, support and help. I also thank Dr. Nikhil, Dr Akash, Abhishek, Madhulika and Sourabh for their help, support and all the moments to cherish.

I gratefully acknowledge the Council of Scientific and Industrial Research (CSIR), for providing me financial support in the form of fellowship. I am also grateful to thank DBT, ICMR, and UoH-IoE funding for Lab and DST-FIST, DBT-CREBB, UGC-SAP, DST-PURSE funding to school and departmental facilities that aided in my research work.

I thank all the teaching and nonteaching staff members of Department of Biotechnology and Bioinformatics, and School of Life Sciences for all their help and support.

I owe this thesis to my parents, Sh. Rajan Singh Yadav and Smt. Rajwati who always stood by me and provided strength in pursuing this work. I express my deep sense of gratitude to my chachaji Dr. Mahesh C. Yadav and Er. Yatesh Yadav, my chachiji Smt. Anjali and Smt Zebul Nisha for their support and all the love. There are not enough words to express how grateful I am to my bua Smt. Sonam for everything she has done for me, I take this opportunity to thank her from my heart. I express my thanks and love to my brother, Neelansh and my sisters Rashmi, Soni, Shweta, Divyanshi, Gulshan, Muskaan and Anupriya for their love, tremendous moral support and making my life beautiful. My love for Tanu and Aviraj. I am blessed to have you all in my life.

I would like to thank God for giving me strength and encouragement throughout all the challenging moments of completing this thesis and beyond.

Ravi Kant Yadav

Contents

List of Figures	13
List of Tables	16
ABBREVIATIONS	17
Chapter 1: Introduction & Review of Literature	19
1.1 Neurons	19
1.2 Neurodegeneration and neurodegenerative diseases	19
1.3 Alzheimer's disease (AD)	19
1.4 Pathological hallmarks of AD	21
1.5 Tau Protein	23
1.6 Post-translational modifications of Tau affecting AD pathogenicity	25
1.6.1 Tau phosphorylation	25
1.6.2 Other Post-translational modifications of Tau	26
1.7 Tyrosine phosphorylation of Tau	27
1.8 Fyn Kinase	28
1.9 Regulation of activity of Fyn Kinase	29
1.10 Tau and Fyn interaction in AD	30
1.11 The dendritic Tau mediated neurodegeneration	31
1.12 Background of study	32
1.13 Dendritic Arborization in AD	34
1.14 Rho GTPase signalling pathways in Alzheimer's disease	35
1.15 Hypothesis	36
1.16 The system of <i>Drosophila</i> dendritic arborization (DA) neurons to study the	
pathogenetic mechanism	38
1.17 Objectives of the study	40
1.18 Important amino-acid residues chosen for mutagenesis to study the physical and	
functional interaction of Tau and Fvn.	41

1.18.1 PXXP motifs in Tau protein	41
Chapter 2. Materials and Methods	43
2.1 Materials and Reagents	43
2.1.1 Drosophila Stocks	43
2.1.2 Mutagenesis and cloning reagents	44
2.1.3 Squish Buffer for crude extract preparations	44
2.1.4 Bouin's and Paraformaldehyde (PFA) fixing solution	44
2.1.5 Wash Buffer (PBSTx)	44
2.1.6 Blocking Buffer	45
2.1.7 Mounting medium	45
2.2 Methodology	45
2.2.1 Site-directed mutagenesis	45
2.2.2 Mutagenic Primers	46
2.2.3 Cloning of the mutated constructs into pUAST-attB Vector	46
2.2.4 Microinjection of the WT and mutated construct into <i>Drosophila</i> embryos	47
2.2.5 Post Injection care	48
2.2.6 Screening of the transgenic flies	48
2.2.7 Single fly PCR for genotypic screening	49
2.2.8 Single fly genomic PCR with flanking primer for confirming site-specific	
integration	49
2.2.9 Generation of Tau and Fyn coexpression fly stocks	49
2.2.10 Scanning Electron Microscopy	50
2.2.11 Locomotion assay	50
2.2.12 Nail Paint imprinting	51
2.2.13 Electroretinograms	51
2.2.14 Western Blotting	52
2.2.15 C4da neurons dissections and staining	53

2.2.16 Immunofluoroscence and confocal microscopy	53
2.2.17 C4da neurons analysis and quantification	.54
2.2.18 Compounds treatment and analysis	55
2.2.19 Statistical analysis	56
Chapter 3. Results	57
3.1 Isolation of WT Fyn Kinase from human glioblastoma cell lines and cloning it into	
pUAST-attB vector	57
3.2 Cloning of Tau into pUAST-attB vector	58
3.3 Mutagenesis of Tau P216A	59
3.4 Mutagenesis of Tau P219A	.61
3.5 Mutagenesis of Tau P233A	62
3.6 Mutagenesis of Tau P236A	62
3.7 Mutagenesis of Tau P216A-P219A	63
3.8 Mutagenesis of Tau P233A-P236A	64
3.9 Subcloning of the mutated Tau and Fyn Construct into pUAST-attB vector	65
3.10 Subcloning of the Tau P216A into pUAST-attB vector	65
3.11 Subcloning of the Tau P219A into pUAST-attB vector	66
3.12 Subcloning of the Tau P233A into pUAST-attB vector	67
3.13 Subcloning of the Tau P236A into pUAST-attB vector	68
3.14 Subcloning of the Tau P216A-P219A into pUAST-attB vector	69
3.15 Subcloning of the Tau P233A-P236A into pUAST-attB vector	70
3.16 Microinjection of the WT and mutated MAPT constructs into <i>Drosophila</i> embryos	
3.17 Screening for transgenic flies after microinjections	72
3.18 Generation and confirmation of Tau and Fyn coexpression stocks	
3.19 WT and mutated Tau together with Fyn overexpression in <i>Drosophila</i> causes	
locomotor defects in aged flies	80
3.20 WT and mutated Tau and Fyn overexpression in <i>Drosophila</i> causes fused and	
disrupted ommatidia	82

3.21 Tau overexpression in <i>Drosophila</i> causes rough eye and the loss of Inter On	ımatidial
Bristles	85
3.22 WT Tau mediated depletion in retinal neuron function is improved by reduc	ing Fyn
and Tau interaction (Tau P216A and Tau P216AP219A)	88
3.23 WT and mutated Tau overexpression reduces C4da neurons dendritic arbori.	zation95
3.24 WT Tau overexpression affects Rho1 and Rac1 levels	98
3.25 Drug Dosage and Treatment	101
3.26 Screening of the compounds for protective effects on Tau toxicity	102
3.27 SEM to check the effects of drug compounds on degeneration of eye	111
3.28 Compounds treatment rescues Tau mediated neurodegeneration in retinal ne	urons
(ERGs)	112
apter 4: Discussion	116
1. Generation of <i>Drosophila</i> model of AD: Generation of stable transgenic flies e	expressing
Wild Type (WT) & mutated human Tau and Fyn for studying functional interacti	on116
2. Genetic analysis to understand the mechanism of Tau-Fyn mediated neurotoxic	city118
3. Repurposing the drugs used in oncotherapy for checking the neuroprotective ex	ffects in
Drosophila model of AD	120
apter 5: Conclusions	122
PPENDIX	123
Matlab program codes for processing ERG recording data	123
Matlab code for reading Heka file	130
Matlab program code to check traces and mean	131
EFERENCES	133

List of Figures

Figure 1. Common neurodegenerative diseases	19
Figure 2. Morphological differences between healthy and AD brain	21
Figure 3. Pathological hallmarks of AD.	22
Figure 4. Schematic representing human MAPT gene structure and alternative splice	cing of the
full-length 2N4R Tau Protein.	24
Figure 5. Domain structure of the Tau protein.	24
Figure 6. Post-translational modifications of Tau.	25
Figure 7. Schematic representing domain structure of human Fyn Kinase.	29
Figure 8. Regulation of the activity of the Fyn kinase by auto phosphorylation of T	yr420 and
dephosphorylation of Tyr531 residues	30
Figure 9. Schematic representing the background of our study	34
Figure 10. Graphical representation of our proposed hypothesis.	37
Figure 11. Schematic representation of the Rho GTPases mediated Tau-Fyn induced	d dendritic
and spines degeneration.	38
Figure 12. C4da neurons dendritic arborization as a model to study dendrites in D	Prosophila.
	39
Figure 13. Selected important sites for site-directed mutagenesis for studying the ph	nysical and
functional interaction of Tau and Fyn.	42
Figure 14. Strategy for site-directed mutagenesis and cloning into fly specific pU	JAST-attB
vector	45
Figure 15. Graphical summary of the microinjection procedure.	47
Figure 16. Strategy for screening of the microinjected flies for transgenic	48
Figure 17. Genotypic screening of the transgenic <i>Drosophila</i>	49
Figure 18. Site-specific integration of the microinjected construct.	49
Figure 19. Pictorial representation of the preparation of flies for SEM.	50
Figure 20. Schematic representing the strategy for climbing assay	51
Figure 21. ERG set up, mounting of fly and recording of ERG.	
	52
Figure 22. Quantification of the dendritic arborization and branching pattern of the	
Figure 22. Quantification of the dendritic arborization and branching pattern of the of the C4da neuron.	e dendrites

Figure 24. Analysis of the neurotoxicity on the <i>Drosophila</i> eye as a primary screening for the
compounds treatments
Figure 25. Isolation of WT Fyn Kinase from human glioblastoma cell lines and cloning it into
pUAST-attB vector
Figure 26. Cloning of Tau into pUAST-attB vector
Figure 27. Mutagenesis of Tau P216A.
Figure 28. Mutagenesis of Tau P219A61
Figure 29. Mutagenesis of Tau P233A
Figure 30. Mutagenesis of Tau P236A
Figure 31. Mutagenesis of Tau P216A-P219A64
Figure 32. Mutagenesis of Tau P233A-P236A65
Figure 33. Subcloning of the Tau P216A into pUAST-attB vector
Figure 34. Subcloning of the Tau P219A into pUAST-attB vector
Figure 35. Subcloning of the Tau P233A into pUAST-attB vector
Figure 36. Subcloning of the Tau P236A into pUAST-attB vector
Figure 37. Subcloning of the Tau P216A-P219A into pUAST-attB vector70
Figure 38. Subcloning of the Tau P233A-P236A into pUAST-attB vector71
Figure 39. Single Fly PCR for Tau and Fyn transgenic flies
Figure 40. Single Fly PCR for site-specific integration of Tau and Fyn in generated transgenic
flies
Figure 41. Tau primers are specific to transgene and does not amplify dTau75
Figure 42. Generation of Tau and Fyn coexpression fly stocks
Figure 43. Western blot analysis for protein expression confirmation of generated Tau and Fyn
transgenic flies
Figure 44. Tau and Fyn synergistically affect locomotion in an age-dependent manner81
Figure 45. WT and mutated Tau and Fyn overexpression in Drosophila causes fused and
disrupted ommatidia84
Figure 46. WT Tau overexpression in Drosophila causes rough eye and loss of Inter
Ommatidial Bristles87
Figure 47. WT Tau and WT Tau-Fyn overexpression reduces the receptor potential between
photoreceptor cells94
Figure 48. WT and mutated Tau overexpression reduces C4da neurons dendritic arborization
and branching pattern97
Figure 49. WT Tau overexpression affects Rho1 and Rac1 levels99

Figure 50. Full eyes light microscopy imaging of the compounds treated flies and control flies.
110
Figure 51. Scanning electron microscopy of the compounds treated flies and control flies .112
Figure 52. Compounds treatment rescues Tau mediated neurodegeneration in retinal neurons
TERGs)

List of Tables

Table 1. Primers with point mutations for site-directed mutagenesis	46
Table 2. Tau and Fyn mutants generated.	
<u>Table 3. Transgenic flies generated.</u>	72
Table 4. Compounds and their concentrations used in primary screening.	102
Table 5. Compounds used for SEM.	111
Table 6. Compounds used for ERG.	113

ABBREVIATIONS

AD Alzheimer's disease

ALS Amyotrophic Lateral Sclerosis

Aβ Amyloid-β

APP Amyloid precursor protein

ANOVA Analysis of Variance

attB Attachment site B

attP Attachment site P

APPL Amyloid-beta-like protein

BACE β -site APP-cleaving enzyme

C4da neurons Class IV dendritic arborization neurons

ELAV Embryonic Lethal Abnormal Visual System

FDA Food and Drug Administration

FTDP Frontotemporal Dementia and Parkinsonism

GMR Glass Multiple Reporter

GFP Green fluorescent protein

HD Huntington's disease

LRRK 2 Leucine-rich repeat kinase 2

NFTs Neurofibrillary tangles

NMJ Neuromuscular junction

Ommatidia Clusters of photoreceptors and supporting cells that compose

the adult eye.

PD Parkinson's disease

PAGE Polyacrylamide Gel Electrophoresis

PBS Phosphate Buffered Saline

PCR Polymerase Chain Reaction

Phi-C31 Bacteriophage Phi-C31

pTAU Phosphorylated Tau

PPK Pickpocket

RFP Red Fluorescent Protein

RT–PCR Reverse transcription PCR

SEM Scanning Electron Microscopy

UAS Upstream activating sequence

WT Wildtype

Chapter 1: Introduction & Review of Literature

1.1 Neurons

Neurons are cells in the nervous system that receive and transmit signals to other cells. Structurally, neurons consist of cells body or soma and the neurites which distinguishes the neurons from other cells. Functionally, neurons can convert chemical signals to electrical signals and transmit them across their lengths as action potentials. Neurites are the projections from the cell body of the neurons which can be either axon or dendrites. Dendrites are highly branched structures having high levels of protein synthesis activity, and are responsible for forming connections with other neurons.

1.2 Neurodegeneration and neurodegenerative diseases

Neurodegeneration is age associated progressive loss of neuronal structure and function. It ultimately leads to the cognitive decline and dementia which are associated with age dependent neurodegenerative diseases. Neurodegeneration leads several diseases such as Alzheimer's disease (AD), Amyotrophic Lateral Sclerosis (ALS), Huntington's disease (HD), Parkinson's disease (PD) and Batten Disease (Figure 1).

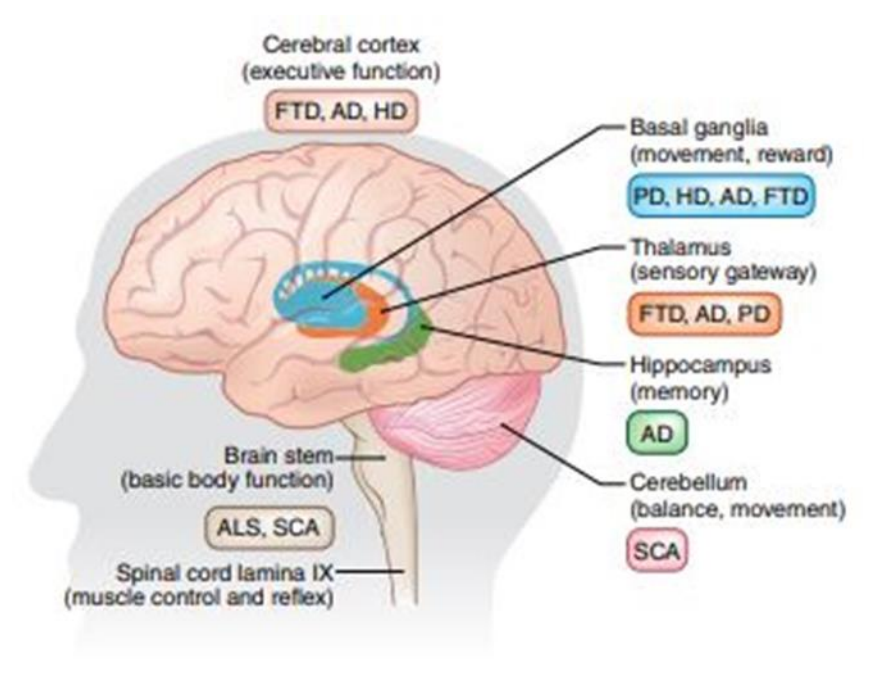


Figure 1. Common neurodegenerative diseases (Gan et al., 2018).

1.3 Alzheimer's disease (AD)

Alois Alzheimer was a famous German psychiatrist first described Alzheimer's disease in 1907. He observed that his patient, Auguste Deter 51-year-old woman had severely impaired

her memory. After her death, Alois Alzheimer observed her brain histology by staining the sections with silver stain. He found some cellular inclusions which were called amyloid-beta plaques and neurofibrillary tangles (Bondi et al., 2017). These findings provided the foundation for the researchers to study and investigate the mechanisms of the formation of the amyloid-beta plaques and neurofibrillary tangles. In initial period of the AD related studies, research was focused mainly on $A\beta$ plaques as primary reason for AD. Later as the research progressed, the formation and mechanisms of the NFTs and its association to the AD pathogenicity was studied.

AD is an age dependent neurodegenerative disorder associated with loss of memory, learning and cognitive impairment. Mostly people older than 65 years are more at risk for AD, but it's not only disease of old people, about 5 % of people with disease have early onset AD. Early onset disease symptoms occurs at theirs 40s and 50s (Alzheimer's Association, https://www.alz.org/alzheimers-dementia/facts-figures). AD is mainly caused due to the aggregation of the abnormally processed Amyloid-β (Aβ) and hyper-phosphorylated Tau protein (Lee et al., 2004). Some other risk factors for AD are aging, family history and heredity. The age-related alterations in AD include shrinkage of certain brain parts, inflammation, production of free radicals, and mitochondrial dysfunction. There are greater chances of AD if there is AD patient family (Alzheimer's any in association, https://www.alz.org/alzheimers disease causes risk factors.asp). AD brain show shrinkage in the hippocampus and cortex reason as well as enlargement of the ventricles (Figure 2) leading to the impairments in the memory, learning and cognition.

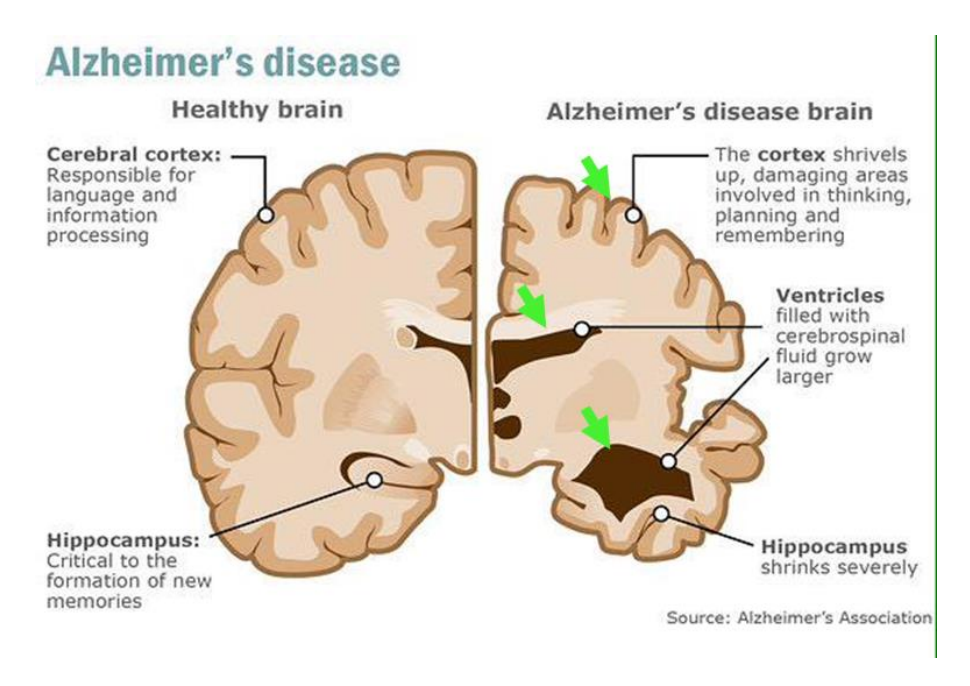


Figure 2. Morphological differences between healthy and AD brain (Source: Alzheimer's association). Green arrows highlight the shrinked cortex, hippocampus and enlarged ventricles.

The pathological hallmarks of AD are Amyloid plaques and the neurofibrillary tangles (NFTs) (Grundke-iqbal et al., 1986; Grundke-Iqbal et al., 1986b). These are abundantly present in the degenerating neurons. Amyloid plaques are composed of the Amyloid peptides differentially cleaved from Amyloid precursor protein (APP) (Lee et al., 2004). β -site APP-cleaving enzyme (BACE) and γ -secretases increases the formation of the Amyloid peptides by proteolytic cleavage of the APP. Neurofibrillary tangles are formed by abnormally phosphorylated Tau proteins within the affected neurons (Grundke-Iqbal et al., 1986b; Kotzbauer et al., 2004; Lee et al., 2004).

Memory and cognitive loss are most common clinical symptoms of the AD. Cognitive symptoms of AD includes mental decline, difficulty in thinking and understanding, or inability to remember common things. AD causes poor judgement, vision problems, forgetting people and changes in mood, personality and behaviour. Patient often withdraws from social or work activities.

There is no treatment available to cure the disease effectively. Patient needs special care and attention. Aricept is the only treatment approved by the FDA for all mild, moderate, and severe stages of Alzheimer's disease. Some other drugs which are currently being used for treating AD are Razadyne and Memantine.

1.4 Pathological hallmarks of AD

Alzheimer's disease brain is diagnosed with the presence of extracellular plaques known as Amyloid plaques and the neurofibrillary tangles (NFTs) (Figure 3). The formation of these plaques and tangles are distinctive hallmarks of AD and ultimately cause the death of affected cells.

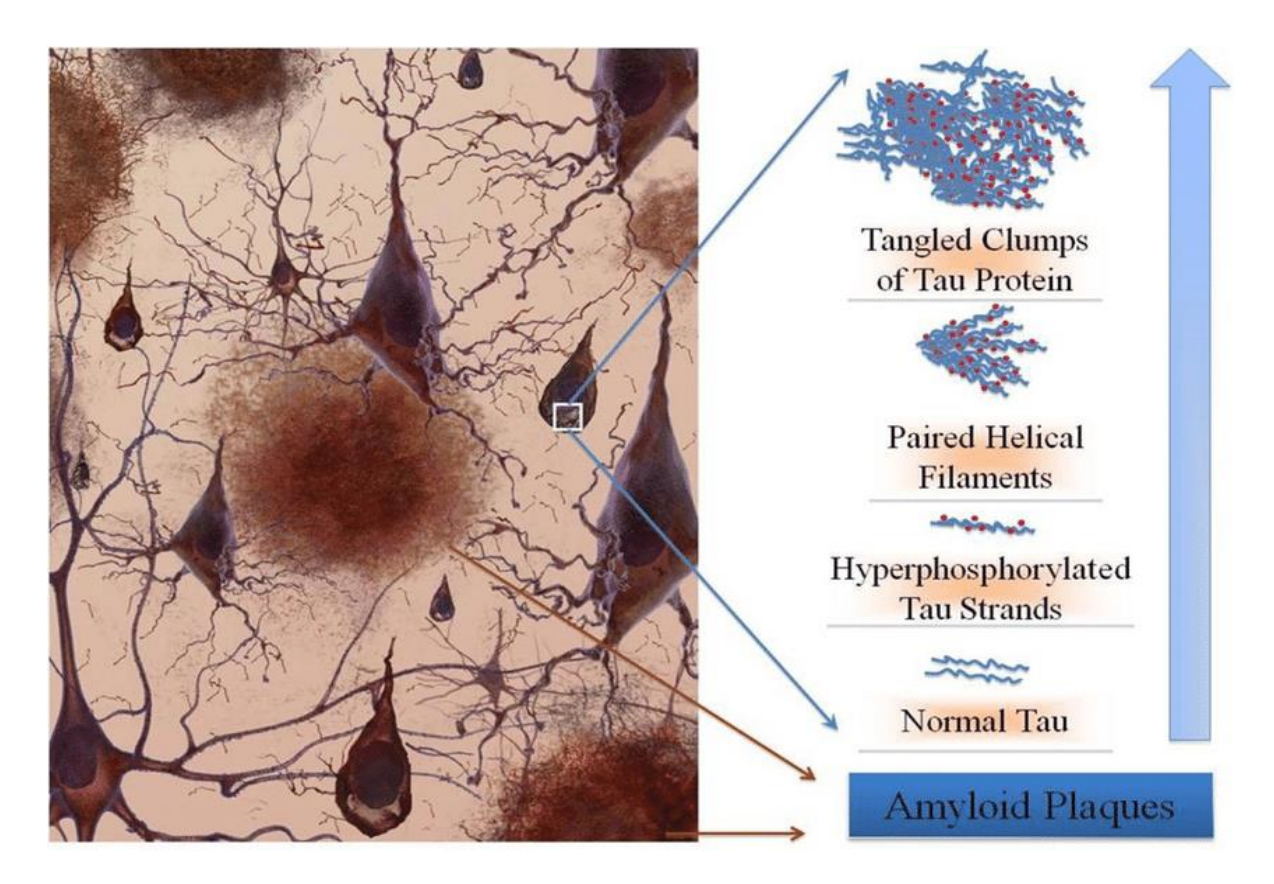


Figure 3. Pathological hallmarks of AD. Amyloid plaques are present extracellularly and NFTs (Tangles) are intracellular clumps of Tau protein. Arrow indicates the series of events involved in the formation of the NFTs (Jaruszewski et al., 2012).

Amyloid Plaques

Amyloid plaques are formed through abnormally processed amyloid protein by BACE and γ -secretases. Abnormally processed amyloid protein forms insoluble oligomers which are toxic to the neurons. These plaques are present extracellularly and lead to the initiation of toxicity in the neurons. Cleavage of the APP by β -secretase (BACE1) and γ -secretase leads to the formation of the amyloid- β (A β) peptides of different lengths including the A β 40 and A β 42 (Hardy and Selkoe, 2002; Jin et al., 2011; Selkoe and Hardy, 2016). A β 42 is main player in pathogenicity of AD as it is more likely to form the aggregates.

One of the major factor in the AD pathogenicity is the ratio of A β 40 to A β 42. Healthy individuals have high amount of A β 40 and lower amount of the A β 42. In diseased condition, this healthy ratio of the A β 40 to A β 42 is disturbed and A β 42 levels are elevated. As A β 42 have high tendency to aggregate and form the fibrils, increased levels of A β 42 in diseased condition leads to the formation of aggregates, protofibrils and ultimately amyloid plaques (Chévez-Gutiérrez et al., 2012; Hardy and Selkoe, 2002; Jin et al., 2011).

Neurofibrillary Tangles (NFTs)

NFTs are present in the affected neurons. These tangles are formed due to the presence of abnormally phosphorylated Tau protein (Grundke-iqbal et al., 1986). Tau protein when abnormally phosphorylated, disintegrates from microtubules and actin and forms toxic insoluble oligomers (Pope et al., 1994; Takahashi et al., 1999a). Physiologically Tau binds and stabilizes the microtubules but the hyperphosphorylation aggregates Tau into insoluble structures forming the straight filaments (SFs) and paired helical filaments (PHFs) (Grundke-Igbal et al., 1986b; Igbal et al., 1998). SFs are the short Tau filaments whereas PHFs are composed of two or more twisted helical filaments of the abnormally hyperphosphorylated Tau protein. These PHFs aggregate together leading to the formation of the NFTs and can be characterized by the abnormal accumulation of Tau in the cytoplasm (Kobayashi et al., 2017; Li and Götz, 2017a). Other than destabilization of the microtubules, NFTs causes neuronal degeneration (Bramblett et al., 1993; Falke et al., 2003; Sun et al., 2016; Williams et al., 2000), synaptic dysfunction, abnormal axonal transport, mitochondrial dysfunction and reduced mitophagy (DuBoff et al., 2012; Fang et al., 2019; Kerr et al., 2017; McInnes et al., 2018; Pooler et al., 2014). The load of the NFTs is directly related to the severity of the diseases, as the load and formation and spreading of the NFTs increases the severity of the Alzheimer's disease and cognitive impairments also increases (Braak and Braak, 1991).

1.5 Tau Protein

In 1975, Kirshner laboratory was dealing with tubulin polymerisation they found a heat stable protein called Tau, which is important for tubulin polymerisation initiation and growth. They isolated Tau protein which is associated with tubulin from porcine brain capable of microtubule seedling ,assembly and stabilization (Weingarten et al., 1975)(Witman et al., 1976). Tau protein is encoded by human Microtubule Associated Protein Tau (MAPT) gene (Grundke-iqbal et al., 1986). MAPT gene is located on human chromosome 17q21 position and consists of total 16 exons out of which 11 exons encode six different isoforms of Tau protein through alternative splicing. Exon no 2 and 3 encodes for the two inserts at N-terminal end and exon no 10 encodes for the repeat 2. Alternative splicing of exon no 2, 3 and 10 leads to six different isoforms of protein Tau (Caillet-Boudin et al., 2015). We are interested in full length 441 amino acid long isoform protein which is encoded by mRNA transcript variant 2 (Figure 4).

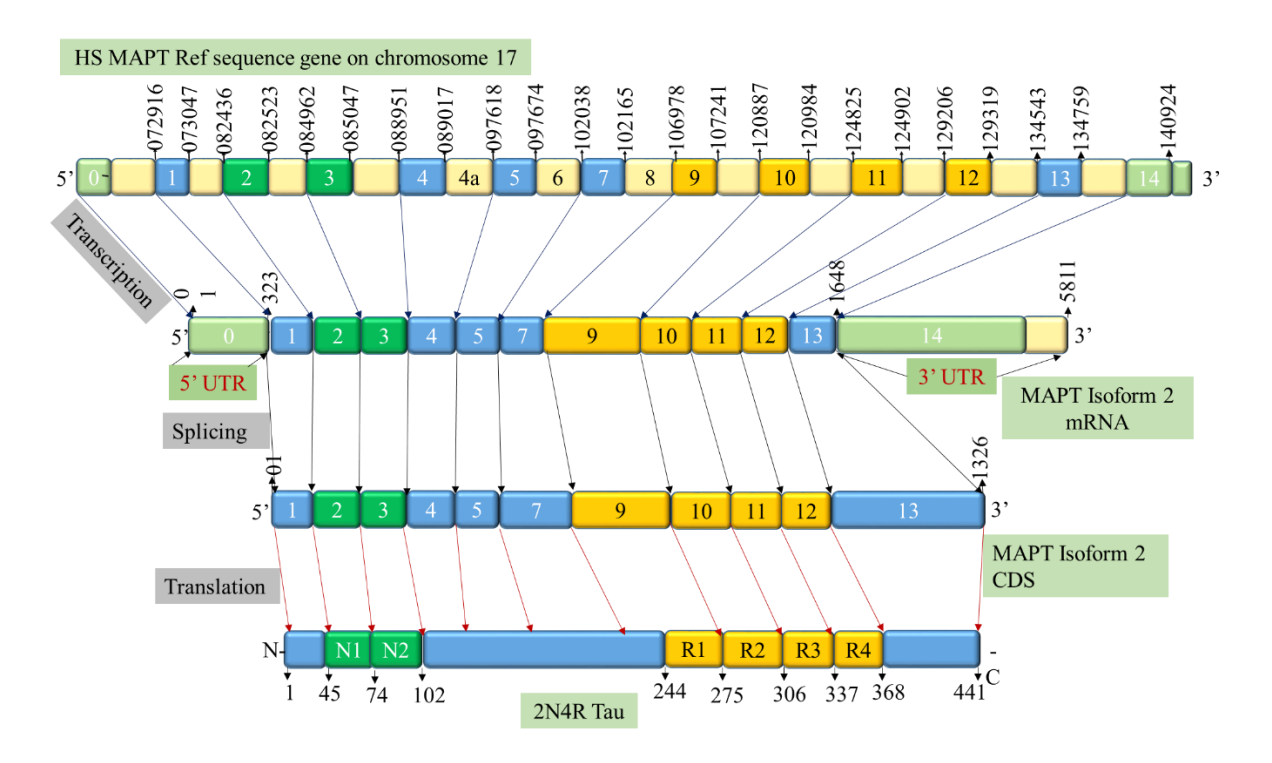


Figure 4. Schematic representing human MAPT gene structure and alternative splicing of the full-length 2N4R Tau Protein.

Tau is microtubule (MT) associated protein. It binds to microtubules and stabilizes them. The binding affinity of Tau to microtubules is regulated by the Tau protein phosphorylation. Tau is phosphorylated at MT binding site by Fyn kinase (Lee et al., 2004). When the Tau is hyperphosphorylated, it detaches from MT and aggregates. This consequently leads to the formation of Neurofibrillary tangles (NFTs). NFTs are toxic to cell and causes degeneration of the affected neurons (Bhaskar et al., 2005; Lee, 2005).

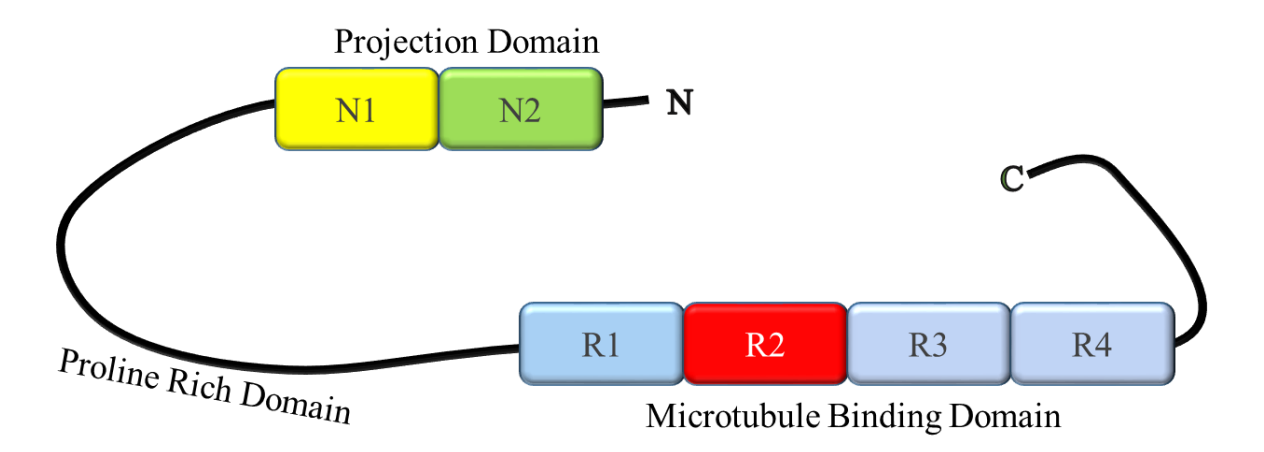


Figure 5. Domain structure of the Tau protein. Tau has N-terminal projection domain which assists in binding of Tau to microtubules and provides stability, proline rich domain which facilitates the interaction with other proteins and microtubule binding.

1.6 Post-translational modifications of Tau affecting AD pathogenicity

Tau protein undergoes several post translational modifications (PTM) like phosphorylation, nitration, glycosylation, acetylation, and ubiquitinylation for performing various physiological functions. During AD disease progression, phosphorylation is the most severely affected PTM of Tau which is altered aberrantly leading to the formation of toxic insoluble oligomers and tangles of Tau (Grundke-Iqbal et al., 1986b, 1986a; Lee et al., 2004). Other PTM such as acetylation, ubiquitination, and glycosylation (Liu et al., 2002), are also affected in AD, but their role in AD is not well studied yet. In AD progression and pathogenicity, there can be possible cross talk between two or more PTM which influences and increases the aggregation and formation of the NFTs leading to Tau toxicity (Martin et al., 2011). Following figure depicts the important post translational modifications of Tau which are associated with the progression of AD (Figure 6).

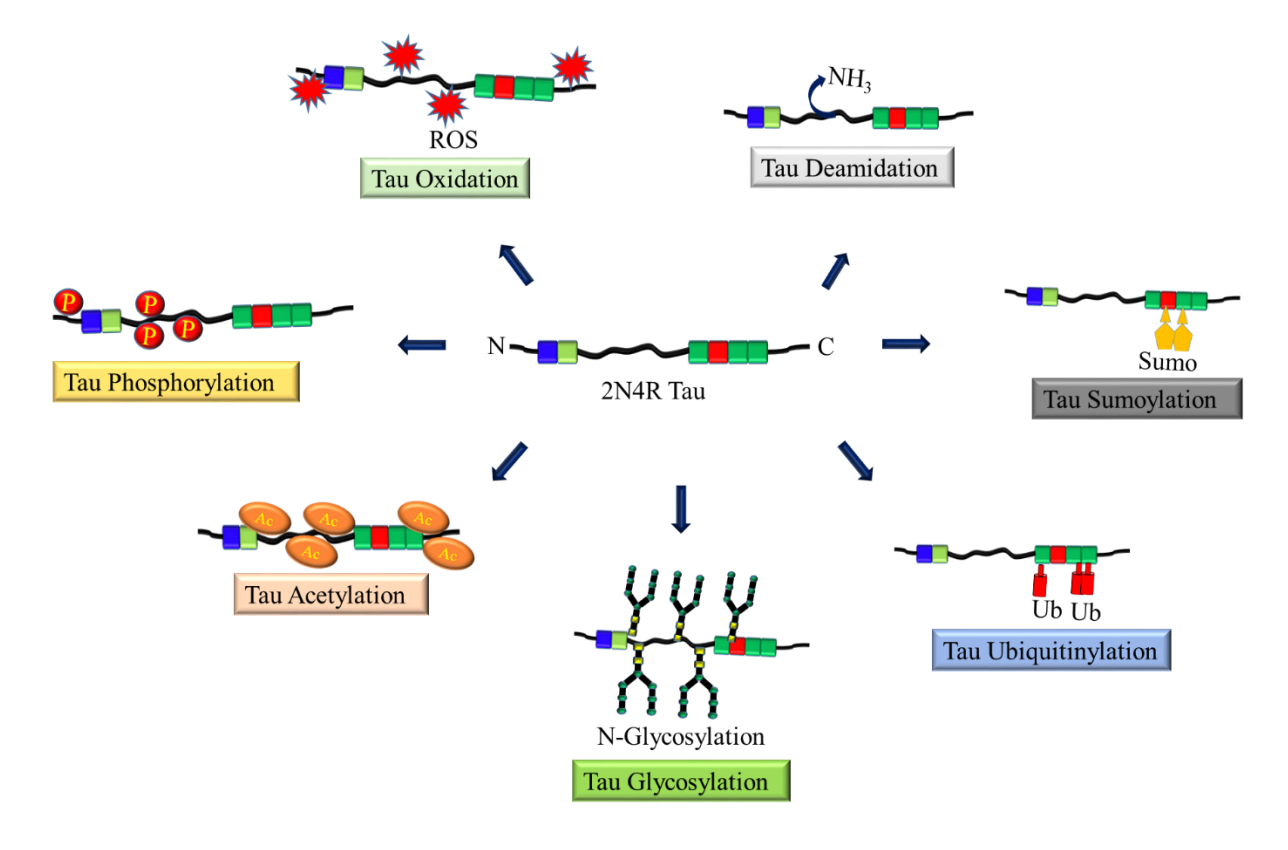


Figure 6. Post-translational modifications of Tau.

1.6.1 Tau phosphorylation

Tau has total 85 phosphorylation sites out of which 45 are serine, 35 are threonine and 5 are tyrosine residues (Buée et al., 2000; Hanger et al., 2009; Sergeant et al., 2008). Physiological levels of Tau phosphorylation are maintained by the balanced activity of protein kinases and protein phosphatases. AD brain studies have revealed the increased activity of the

GSK-3β kinase as it is hyperactive in diseased condition and causes hyperphosphorylation of Tau (Hye et al., 2004; Leroy et al., 2007; Swatton et al., 2004). GSK3β phosphorylates Tau at T231 which further enhances aberrant phosphorylation at C-terminal of Tau and promotes the NFTs formation (Cho and Johnson, 2003; Rudrabhatla and Pant, 2010). Other Ser/Thr kinases such as cyclin dependent kinase 1 (CDK1) (Patrick et al., 1999; Swatton et al., 2004; Tandon et al., 2003), dual specificity tyrosine phosphorylation and regulated kinase 1A (DYRK1A) (Dowjat et al., 2007; Kimura et al., 2007; Ryoo et al., 2008), have also been found with increased activity and also elevated levels of p38 (Johnson and Bailey, 2003; Swatton et al., 2004) were found in AD brain studies. Casein Kinase 1 (CK1) (Schwab et al., 2000; Yasojima et al., 2000) and MAPKs (Feijoo et al., 2005) also phosphorylate Tau and their increased activity hyperphosphorylates Tau protein leading to the formation of the NFTs (Zhu et al., 2000). Other than Ser/Thr, Tau is also hyperphosphorylated at tyrosine residues by various kinases such as Src (Lee, 2005), Lck (Williamson et al., 2002), Syk (Lebouvier et al., 2008), Fyn (Lee et al., 2004) and C-abl kinase (Derkinderen et al., 2005). Balance of these kinases activity and phosphorylated Tau levels are maintained by the activity of protein phosphatases. During AD pathogenesis, the activity of the protein phosphatases is reduced or inhibited. Protein Phosphatase 2A (PP2A) is the most common and widely used phosphatase which dephosphorylates Tau protein (Gong et al., 1993, 2005; Kuszczyk et al., 2009). PP2A activity is reported to be reduced by 50% in AD brains(Gong et al., 1993). Another study revealed the presence of inhibitors 1/2 of PP2A (I₁PP2A & I₁PP2A) in AD brains suggesting that inhibition of PP2A activity in AD pathogenicity (Chen et al., 2008; Tanimukai et al., 2005). Reduced activity of phosphatases may induce the aberrant activity of protein kinases which imbalances the phosphorylation levels of Tau leading to hyperphosphorylated Tau which is the major cause for the formation of the NFTs and AD progression.

1.6.2 Other Post-translational modifications of Tau

Tau has four reported nitration sites so far. Nitration is involved in aggregation of Tau (Horiguchi et al., 2003). In diseased condition, both soluble and insoluble fractions of Tau are nitrated at tyr29 (Cappelletti et al., 2004; Reynolds et al., 2006a). Nitration of Tau at tyr29 reduces the tubulin binding ability of Tau (Reynolds et al., 2006b) leading to the formation of the NFTs (Zhang et al., 2005). Tau protein is also nitrated at Y18 (Reyes et al., 2008), Y197 and Y394 residues (Reynolds et al., 2005) but further studies are required to understand their role in Tau pathogenicity.

Tau protein is also found to be aberrantly glycosylated in AD brain (Takahashi et al., 1999b; Wang et al., 1996). Tau phosphorylation and glycosylation are negatively related to each other, O-glycosylation of Tau protein reduces its phosphorylation (Lefebvre et al., 2003; Liu et al., 2009). A study by Liu et al also found that Tau glycosylation phosphorylation of Tau by GSK3β, CDK5 and PKA (Wei and Liu, 2002). Tau has total eleven glycosylation sites out of which four sites are found to be glycosylated (Shane Arnold et al., 1996). Tau glycosylation may protect the hyperphosphorylation of Tau and reduce the formation of the NFTs.

Tau protein is ubiquitinated at K253, K254, K311 and at C-ter domain of Tau for its degradation (Cripps et al., 2006; Morishima-Kawashima et al., 1993). AD brain studies had revealed the presence of the polyubiquitinated Tau in paired helical fragments (PHFs) (Iqbal et al., 1998; Iqbal and Grundke-Iqbal, 1991).

Tau oxidation can happen at C322 in R3 domain (Schweers et al., 1995) and oxidation of Tau can lead to the formation of the PHFs (Landino et al., 2004; Schweers et al., 1995). Further studies are required to understand the effect of Tau oxidation on AD pathogenesis. During disease progression, Tau also undergo prolyl-isomerization (Bulbarelli et al., 2009; Zhou et al., 2000) and truncation (Basurto-Islas et al., 2008; Horowitz et al., 2004) as disease associated post translational modifications.

Other than these modifications, Tau protein is also modulated by several interactive partners which affects the Tau pathogenicity in AD.

1.7 Tyrosine phosphorylation of Tau

Serine and threonine residues phosphorylation and their implications in AD has been studied widely and their role in disease progression is very much know but recent studies and evidences suggests the involvement of the Tyr phosphorylation in the AD (Derkinderen et al., 2005; Lee et al., 2004; Usardi et al., 2011a; Wang et al., 2013), but the exact mechanisms and impacts of tyrosine phosphorylation in AD progression are not known yet. Abnormal Tyrosine phosphorylation of the Tau also leads to the formation of the NFTs, which is also considered as a pathological hallmark of AD (Lee et al., 2004).

Physiologically, tyrosine phosphorylation of the Tau plays an important role in signal transduction and cell communication (Lee et al., 1998; Li and Götz, 2017b). In AD, dysregulation and increased activity of the Src kinases such as Src, Abl and Fyn leads to the tyrosine hyperphosphorylation and NFTs formation (Bhaskar et al., 2010; Lars M. Ittner et al., 2010a; Lee et al., 2004; Trepanier et al., 2012). Further, tyrosine phosphorylation may

influence the serine/threonine phosphorylation and have a synergistic effect on the Tau hyperphosphorylation, NFTs formation and AD progression. One of the important Src kinase which phosphorylates Tau at tyrosine is Fyn. It has been found in AD brain studies that increased activity of the Fyn kinase causes the hyperphosphorylation of Tau at tyrosine leading to the AD (Chin et al., 2005; Lee et al., 2004; Liu et al., 2020; Poulsen et al., 2017; Usardi et al., 2011a).

Taking together, the mechanism and implications of the tyrosine phosphorylation on NFTs formation and AD progression are not well understood. Further studies are required to elucidate the importance of the tyrosine phosphorylation of Tau and its mechanism in AD progression or Tauopathies. Understanding the mechanism and signalling cascades involved in Fyn mediated tyrosine phosphorylation of Tau will offer better opportunities and therapeutic targets for AD and Tauopathies.

1.8 Fyn Kinase

Human FYN kinase is a Src-family non-receptor tyrosine kinase. Src family kinases have modular nature and consist a unique N-terminal sequence. They play a key role in regulating signal transduction. Excess activity of Fyn kinase causes disorders such as Alzheimer's and Parkinson's disease (Lee et al., 2004; Matsushima et al., 2016). Fyn kinase has four domains, SH1 domain at C-terminal, two central SH2 and SH3 domains and SH4 domain at N-terminal end (Boggon and Eck, 2004). SH1 domain is also known as kinase domain and regulates the activity of the kinase. SH2 and SH3 domains mediate protein-protein interaction and SH4 domain facilitates the membrane binding through palmitoylation of its 'Met-Gly-Cys' motif (Usardi et al., 2011b)(Lau et al., 2016). Kinase activity is controlled by phosphorylation and dephosphorylation of Tyr531 and Tyr420 at the C-terminal tail. When this Tyr-531 residue at C-terminal tail is phosphorylated by Csk kinase, it represses the kinase activity. At the level of transcription, two isoforms are generated through alternative splicing of exon-7 in human: FynT and FynB. FynT is found in T-cells and has exon 7B whereas FynB is found in brain cells and has exon 7A (Nygaard et al., 2014). The difference between the two is of 50 amino acids at the end of SH2 and beginning of kinase domain. This 50 amino acid sequence encompasses the linker sequences that differentiates T & B isoforms of Fyn (Koc et al., 2017).

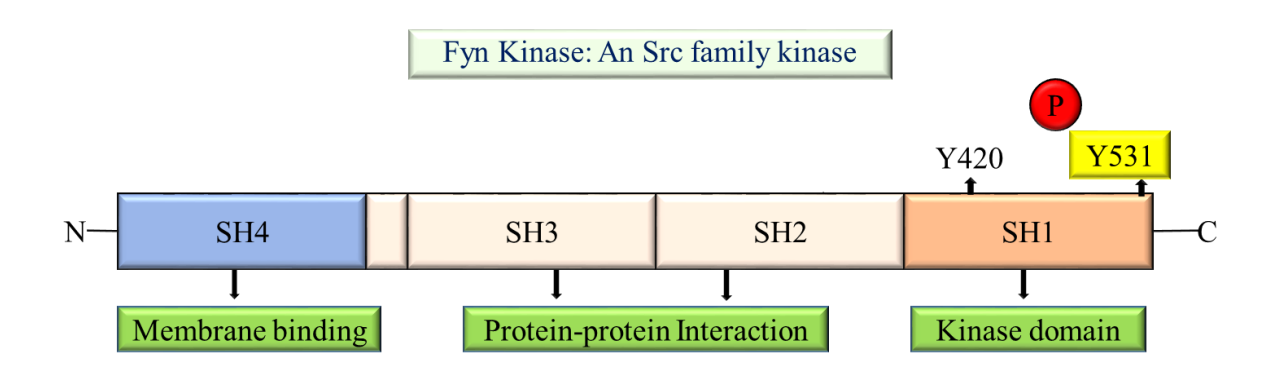


Figure 7. Schematic representing domain structure of human Fyn Kinase. Fyn kinase has four Src homology domains. SH1 domain is kinase domain which contain two phosphorylation sites at Y420 and Y531. Y531 is inhibitory phosphorylation site whereas Y420 is activation phosphorylation site.

1.9 Regulation of activity of Fyn Kinase

Fyn kinase has a kinase or activity domain (SH1) at the C-terminal end which regulates the activity of Fyn kinase. It has two regulatory tyrosine residues, Tyr420 and Tyr531. Fyn kinase was regulated by two tyrosine residue Y531 and Y420 present at the C-terminal region (Nguyen et al., 2002). The phosphorylation at the 531-tyrosine residue inactivates the Fyn kinase activity and sequester the SH2 and SH3 domains of the Fyn. Csk (C-terminal src kinase) is one of the kinases for inhibitory phosphorylation of Fyn (Gerbec et al., 2015). The auto phosphorylation of 420th tyrosine residue of Fyn stabilize the active states (Krämer-Albers and White, 2011). PTPα (Protein Tyrosine Phosphatase alpha) and SHP1 (Src Homology 2 Domain-containing Phosphatase 1) dephosphorylates Fyn at tyrosine 531 which exposes the tyrosine 420 for auto phosphorylation and activation of the Fyn kinase (Chin et al., 2005; Sontag et al., 2012; Yang et al., 2011) (Figure 8).

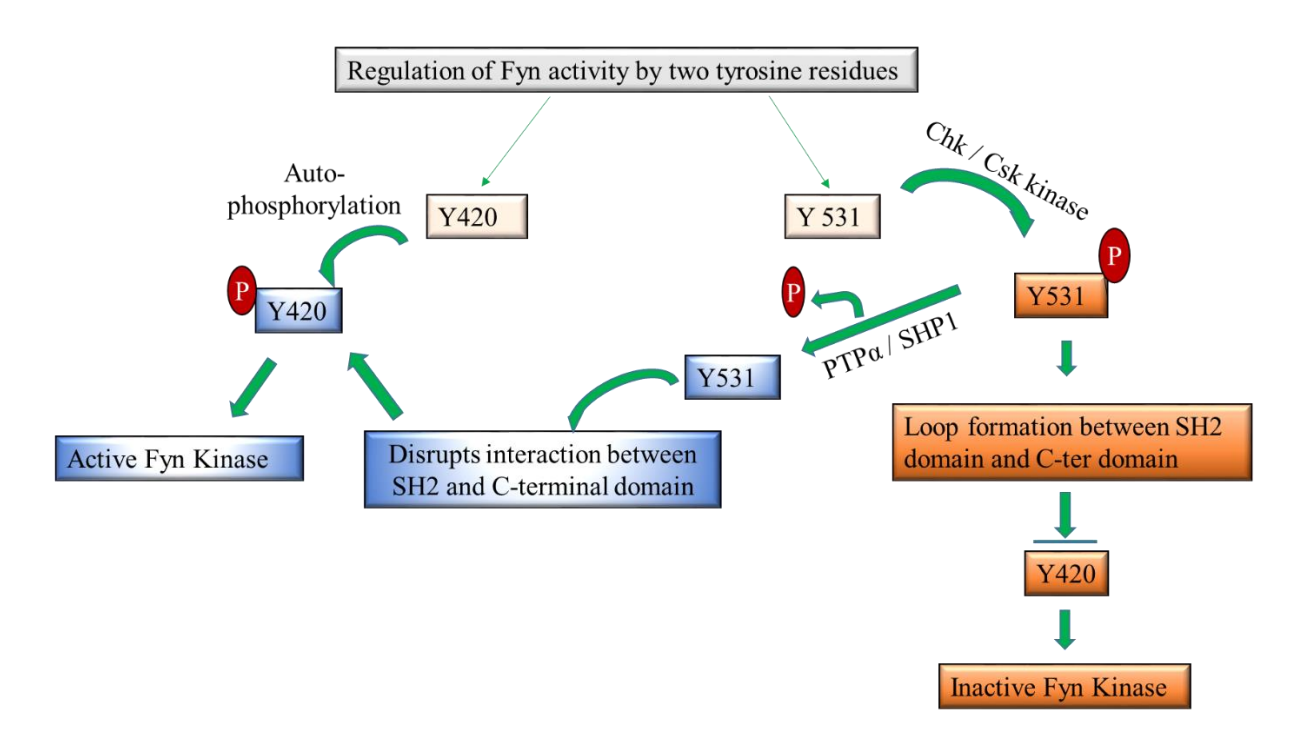


Figure 8. Regulation of the activity of the Fyn kinase by auto phosphorylation of Tyr420 and dephosphorylation of Tyr531 residues. PTP α (Protein Tyrosine Phosphatase alpha) and SHP1 (Src Homology 2 Domain-containing Phosphatase 1) are the negative regulators of Fyn kinase which dephosphorylates tyrosine in Fyn and regulates its activity.

1.10 Tau and Fyn interaction in AD

The upregulated Fyn positive neuron was shown hyperphosphorylated Tau in the hippocampus region of AD patient brain (Shern K; John G., 1993). Fyn can directly phosphorylate Tau in co-transfected COS7 cell lines and indirectly phosphorylate Tau by activation of GSK3β through Fyn kinase (Lee et al., 1998; Lesort et al., 1999). Fyn kinase mediated tyrosine 18 phosphorylation of Tau may influence the phosphorylation of the serine/threonine phosphorylation but the mechanism by which tyrosine 18 phosphorylation affects the serine/threonine phosphorylation is not known yet.

Recent observations from Guangxiu Lu and group (Liu et al., 2016), show that microRNA (miR-106b) suppress the Fyn kinase activity which in turn leads to decreased Tau phosphorylation and ameliorates neurodegeneration (Liu et al., 2016). The knock out study of miR-369 in AD mice model shows that increased Fyn kinase activity leads to hyperphosphorylation of Tau and enhanced cognitive impairment (Yao et al., 2020). Similarly, increase in activity of Fyn kinase was observed in miR-106b knock-out and Aβ induced SHSY5Y cell-lines whereas miR-106b overexpression suppressed tyrosine-18 phosphorylation and Fyn kinase activity (Liu et al., 2016). Expression of miR-369 and miR-106b was found to

be less in AD patients, and restoring of microRNA levels reduces phosphorylation state of the Tau in AD models. Both microRNA can be potential therapeutic targets for the treatment of AD.

Tau and Fyn interaction is very critical for AD pathogenesis (Lee et al., 1998). The interaction between Fyn and Tau is important for oligodendrocytes outgrowth and myelination (Klein et al., 2002). During physiological development, Fyn phosphorylates Tau at the Tyr-18 residue in the early neuronal development of mice, but no Tyr-18 phosphorylation was observed in the adult mice. Even though the Fyn mediated phosphorylation of Tyr-18 was observed in the AD brain (Lee et al., 2004). The constitutively activated Fyn can accumulate at the spines and activate NMDA receptor leads to downstream phosphorylation of Tau at the S202/T205 position (Xia and Götz, 2014). Fyn also mediates somatodendritic translation and accumulation of Tau (Li and Götz, 2017b), suggesting the dendritic neurotoxicity of Tau Psuedophosphorylation of Tau at T231/S235, S262/S356 or S396/404 can target Tau to spine compartment (Xia et al., 2015) suggesting the possible role of dendritic Tau in dendritic neurodegeneration.

1.11 The dendritic Tau mediated neurodegeneration

Recent studies have shown the importance of the extrasynaptic signalling in dendrites in AD (Bordji et al., 2010; Li et al., 2011). Studies with AD brain and AD models has shown that dendritic abnormalities such as dystrophic dendrites (Cochran et al., 2014; Southard, 1910), simplified dendritic branching and complexity (Baloyannis, 2009; Mehraein et al., 1975), and loss of spines (de Ruiter and Uylings, 1987; Flood et al., 1987) are associated with progression of the AD. Tau is physiologically an axonal protein and present in dendrites at very low levels which is non detectable. Physiologically Tau is enriched in axons (Zempel et al., 2010) but also present in lower amount in dendrites and synapses (Chabrier et al., 2012; Lars M. Ittner et al., 2010b; Mondragón-Rodríguez et al., 2012a). During early pathogenesis of AD, Tau is found to be mislocalized in the dendrites (Zempel et al., 2010). Whereas Aβ treatment to the neurons and hyperphosphorylation of Tau also leads to its mislocalization into the dendrites (Congdon et al., 2008; Zempel et al., 2010; Zempel and Mandelkow, 2012). Several studies found that phosphorylation of the Tau at KXGS motifs by MARK/PAR-1 kinases promotes synaptotoxicity and dendritic spine abnormalities (Gu et al., 2013; Mairet-Coello et al., 2013). Also, phosphorylation of Tau at Ser 202 and Ser 205 correlates with the dendritic Tau mislocalization (Li et al., 2011; Zempel et al., 2010). Both of these facts state that phosphorylation of Tau at both KXGS motifs and AT8 sites (Ser 202 and Ser 205) is associated

with dendritic mislocalization and abnormalities and dendritic functions. Elevated soluble Tau in dendritic region targets Fyn aberrantly to the synapse leading to the abnormal increased phosphorylation of NR2B subunit of NMDA receptors which promotes excitotoxicity (Nakazawa et al., 2001; Rong et al., 2001). Taking together, all these observations suggest that mislocalization of Tau into dendritic region elicits the aberrant Fyn mediated signalling leading to the dendritic abnormalities in AD pathogenesis.

1.12 Background of study

Tau functions as a microtubule-associated protein, effectively binding to microtubules to provide stability, thus aiding in the formation of the cytoskeleton. Beyond its role in microtubule stabilisation, Tau also interacts with actin, contributing to the creation of a functional cytoskeleton. Interaction of Tau with microtubules is facilitated by its microtubule binding domain (MTB domain), enabling proper integration and stabilization. However, in conditions like Alzheimer's disease or other pathological states, Tau protein undergoes abnormal hyperphosphorylation, leading to the aggregation of insoluble structures known as paired helical filaments (PHFs).) (Grundke-Iqbal et al., 1986b; Iqbal et al., 1998). PHFs are composed of two or more twisted helical filaments of the hyperphosphorylated Tau protein. These PHFs aggregates together leading to the formation of the NFTs and can be characterized by the abnormal accumulation of Tau in the cytoplasm (Kobayashi et al., 2017; Li and Götz, 2017a).

NFTs are pathological hallmarks of AD, which are composed of the abnormally phosphorylated Tau protein and its aggregates. Research has revealed that hyperphosphorylated Tau loses its ability to interact with microtubules and actins via its binding domains. Consequently, the hyperphosphorylation of Tau results in the breakdown of the cytoskeleton and the emergence of neurofibrillary tangles. Ultimately, these tangles play a pivotal role in driving cellular degeneration and eventual cell death (Grundke-Iqbal et al., 1986a, 1986b; Iqbal et al., 1998; Russell et al., 2016).

Tau protein is phosphorylated at Ser/Thr residues and also Tyr residues for their normal function. In AD, it has been found that Tau is hyperphosphorylated at Ser/Thr residues. While there are total 85 phosphorylation sites out of which 45 are serine, 35 are threonine, there are only five Tyrosine residues that can be phosphorylated. Tau is also known to be hyperphosphorylated at Tyrosine residues, particularly at the Tyrosine-18 (Tyr 18) residue. Many studies so far have been focused on the role and effects of Ser/Thr hyperphosphorylation in AD, however, not much is known about the role of Tyrosine phosphorylation in physiology

and pathology of Tau. Recently, it has been found that hyperphosphorylated of Tau at Tyr18 inhibits its interaction or binding with the microtubules (Lau et al., 2016; Lee et al., 2004). Abnormally phosphorylated Tau is also known to affect other key cellular processes in neurons like mitochondrial transport, fusion and fission (DuBoff et al., 2012; Guo et al., 2017; Lustbader et al., 2004; Stojakovic et al., 2021) (Figure 9).

In addition to the tyrosine phosphorylation of Tau, Fyn kinase also mediates the Amyloid- β toxicity through modulating the glutamate neurotransmitter release (Um et al., 2012). Phosphorylation of the GluN2B subunits of N-methyl-D-aspartate receptor (NMDAR) by Fyn initiates the binding of Post-Synaptic Density 95 (PSD-95) protein for the formation of stable complex. This interaction increases the signalling cascade for the release of the glutamate. A β binds to the NMDA receptors of the glutamate and disturbs the calcium homeostasis which triggers excitotoxicity (Chen et al., 2013; Talantova et al., 2013).

Accumulation of abnormally phosphorylated of Tau takes place within the neuron's cell body. Within the somatic dendritic region, it cannot stabilize actin structures and additionally contributes to the presence of unusually elongated mitochondria (DuBoff et al., 2012; Li and Götz, 2017a). Hyperphosphorylated Tau also binds and helps in the translocation of Fyn kinase to the dendrites (Lars M. Ittner et al., 2010b). In dendrites, Fyn kinase interacts and phosphorylates NMDAR. Activated NMDAR makes a complex with PSD-95, activated Fyn and Tau which triggers the toxic pathways involved in synaptic dysfunction (Snyder et al., 2005), excitotoxicity (Milnerwood et al., 2010; Palop et al., 2007; Roberson et al., 2011), Tau hyperphosphorylation (Lars M Ittner et al., 2010; Nisbet et al., 2015), and synaptic protein trafficking (Melom and Littleton, 2011; Tönnies and Trushina, 2017), leading to the degeneration of the dendrites and ultimately leading to the neurodegeneration. Based on the importance of the Fyn kinase in modulating the toxicity in AD (Poulsen et al., 2017; Yang et al., 2011) and poorly understood mechanism of pathogenicity, we wanted to study the mechanism of Tau and Fyn interaction and their effects on dendritic degeneration. Given Fyn's significant but unknown role in the pathogenesis of Alzheimer's disease (AD), investigating into the fundamental mechanisms underlying their interaction holds the potential to uncover enhanced therapeutic strategies for effectively addressing this condition.

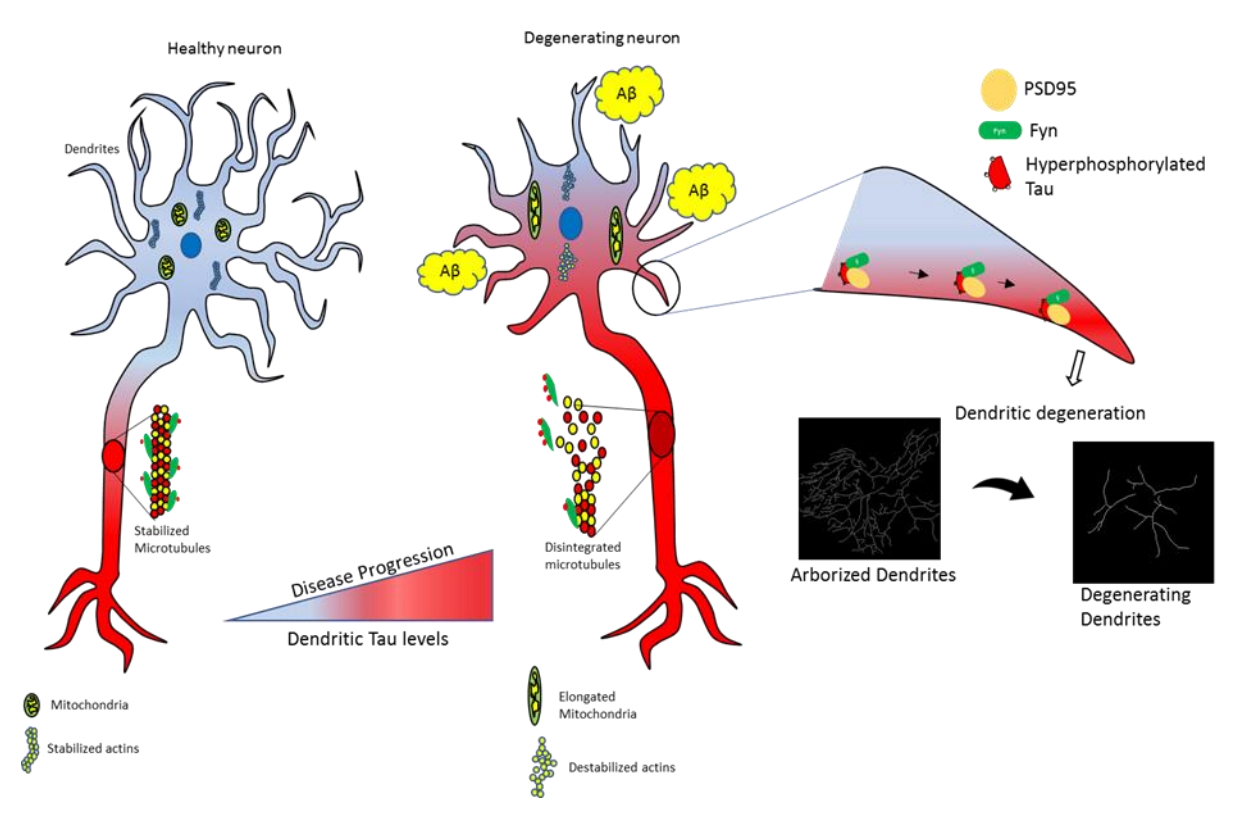


Figure 9. Schematic representing the background of our study. The role of Tau phosphorylation in maintaining the cytoskeleton and abnormalities leading to the AD pathogenicity.

1.13 Dendritic Arborization in AD

Neurons in the brain arborize in different patterns in accordance with their specific functions and form synapses. Proper dendritic arborization is crucial for the integration and processing of the incoming signals. But dendritic arborization has been found to be affected and reduced in the subiculum in the AD brain. Reduction in the arborization is negatively related to the NFTs containing hyperphosphorylated Tau (Falke et al., 2003). NFTs in the AD brain cause reduction in the pyramidal layer leading to the reduction in the neurons density (Falke et al., 2003). The process of dendritic development is tightly regulated by the combination of intrinsic transcription factors (such as Hamlet, Spineless, cut and abrupt (Parrish et al., 2007)) and extracellular signals such as neuronal activity, extrinsic cues and cell contacts (Urbanska et al., 2008). Extracellular signals activate different cascades of intracellular pathways which affects the development and branching of dendrites.

One example of extrinsic cue which is important for dendritic morphology is Semaphorin (Polleux et al., 2000). Semaphorins are both secreted, and membrane bound proteins which share the Sema domain and are guidance cues for axonal transport as well as dendritic branching. Class 3 Semaphorin 3A (Sema 3A) promotes the cytoskeleton

rearrangement, endocytosis and axonal transport (Morita et al., 2006). Sema3A genetically interacts with Fyn for spine maturation in the cerebral cortex and induces the PSD-95 clusters formation and also increases the PSD-95 clusters diameter (Morita et al., 2006) which also correlates with our hypothesis for the role of Fyn in NMDAR-PSD95 complex formation and neurotoxicity.

Regulation of the actin and microtubule cytoskeleton rearrangements regulates the cell morphology. Rho family GTPases such as Rho1, Rac1 and cdc42 are main players for the maintenance and regulation of the actin and microtubule rearrangements (Burridge and Wennerberg, 2004). Studies claim that increased activity of the Rho1 and decreased activity of Rac1 and cdc42 results in the reduction in the branching of the dendritic trees in neurons (Nakayama et al., 2000; Threadgill et al., 1997a), whereas increased activity of the Rac1 and Cdc42 results in the increased complexity of the arbors (Li et al., 2002; Nimchinsky et al., 2002).

There are certain signalling pathways which affect arborization by inhibiting Rho1 activity. One such pathway is mediated by the Abl-1 kinase. Abl-1, non-receptor tyrosine kinase, positively regulates the dendrogenesis via inhibition of the Rho1 activity leading to the increased dendritic complexity (Jones et al., 2004). As Fyn is also a tyrosine kinase like Abl, this hints that Fyn kinase can modulate the activity of Rho GTPases. Along with the regulation of the actin cytoskeleton, Rho GTPases also regulates the microtubule dynamics and mediates the interaction of the actin and microtubules. Rac1 helps in the stabilization of the microtubules via JNK1 dependent phosphorylation of the MAP2 protein and increased levels of the cypin protein mediates the Rho1 dependent alteration of the microtubule cytoskeleton (Chen and Firestein, 2007).

In this context, we propose here that increased Fyn activity could cause increased Rho1 activity, and reduced the activities of Rac1 and cdc42. These disturbed functions of Rho1, Rac1, and cdc42 GTPases might contribute to the impairment of dendritic arborization, spine formation, and spine maturation

1.14 Rho GTPase signalling pathways in Alzheimer's disease

Abnormal Rho GTPases signalling has been associated with several neurodegenerative diseases (Aguilar et al., 2017; Bolognin et al., 2014; Borin et al., 2018; Duman et al., 2021). Recent studies in the human AD brain have found the association of the diminished activity of the Rho family GTPases with disease progression. Reduced Rac1 expression was observed in

AD brains obtained from patients early in disease (Zhao et al., 2006). Rho1 levels were reduced in human AD brains and as well as in the Swedish APP double mutant transgenic mice brain. Rho1 was also found to be decreased in synapses of AD mice, its expression was increased in degenerating neurites which is consistent with the involvement of Rho1 in neurite retraction (Huesa et al., 2010).

1.15 Hypothesis

Within dendrites, the Fyn kinase interacts and phosphorylates NMDA receptor. This activated NMDA receptor subsequently forms a complex with PSD95, active Fyn, and Tau, which triggers pathways that leads to dendritic degeneration and ultimately neurodegeneration.

The importance and role of Tau-Fyn functional interaction is not clear in Tau mediated neurodegeneration in AD. Whether the interaction of Tau and Fyn is toxic and sufficient to cause disease, or the phosphorylation of Tau by Fyn is more pathogenic? The connection between Tau-Fyn interaction, Fyn mediated Tau phosphorylation, and Fyn's effect on neurodegeneration in AD remains to be elucidated.

Therefore, we wanted to study the mechanism of Tau and Fyn interaction and their effects on dendritic degeneration.

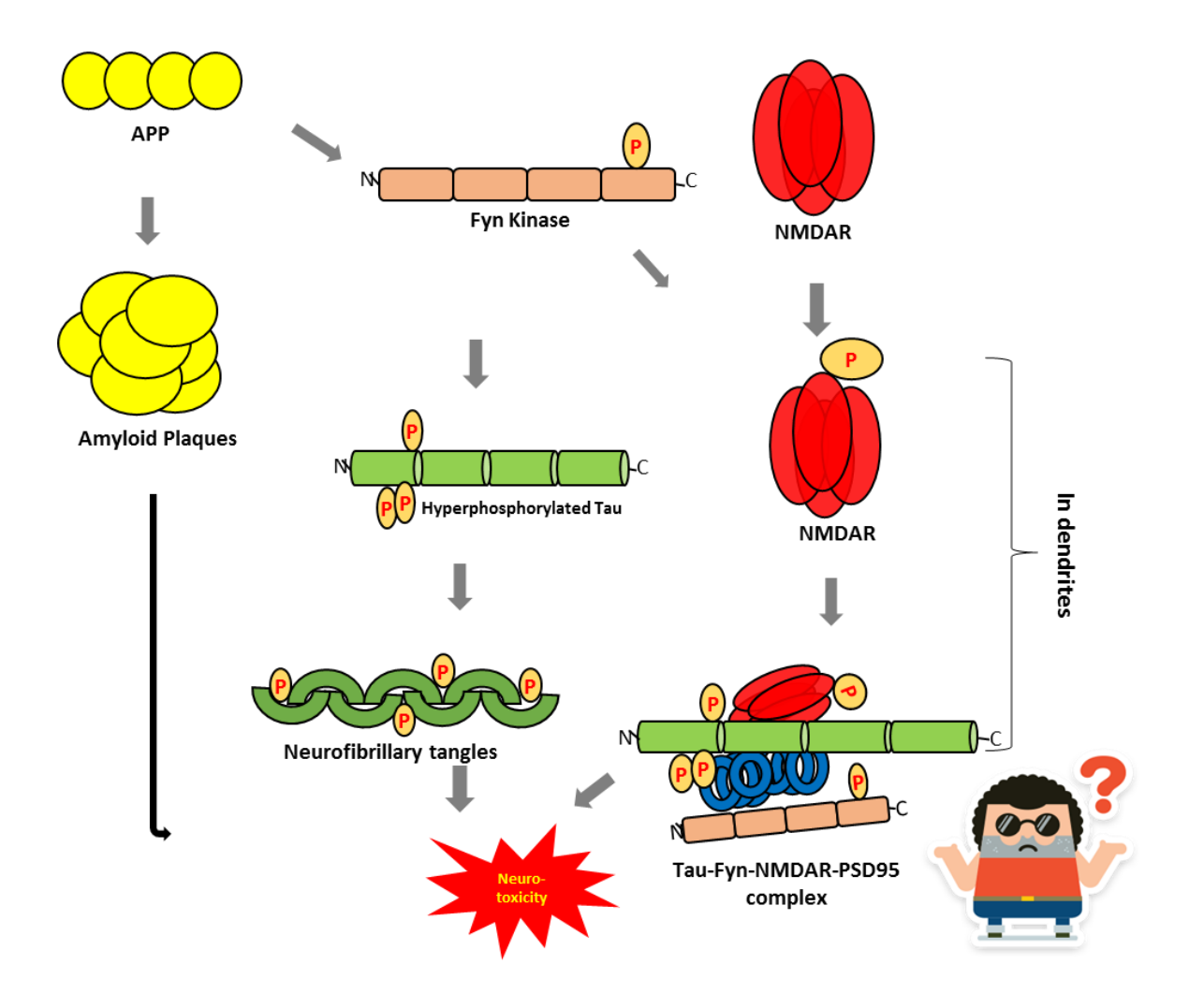


Figure 10. Graphical representation of our proposed hypothesis.

We have set out to identify new molecular players in Tau and Fyn mediated neurotoxicity. In dendrites, based on known association of Rho GTPases with AD, we also hypothesized that there is possibility of the Tau-Fyn interaction affecting the Rho GTPases activity at the dendrites leading to the reduction in the spine formation, dendritic arborization and synaptic function.

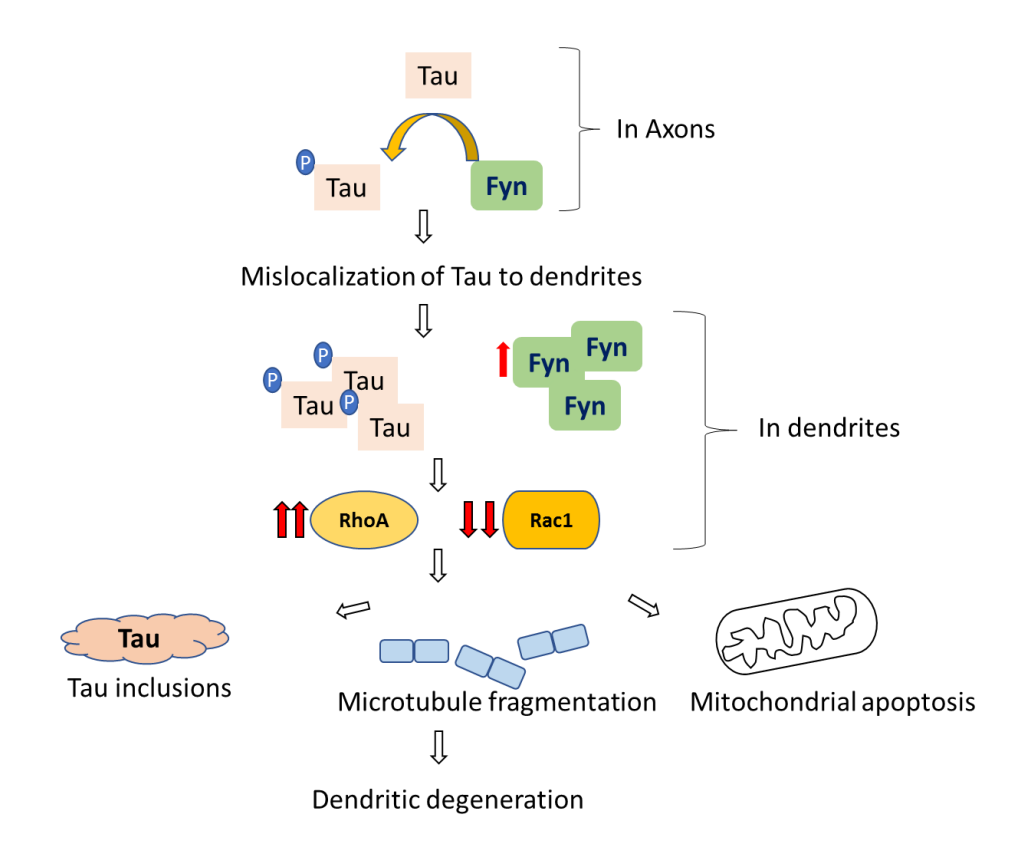
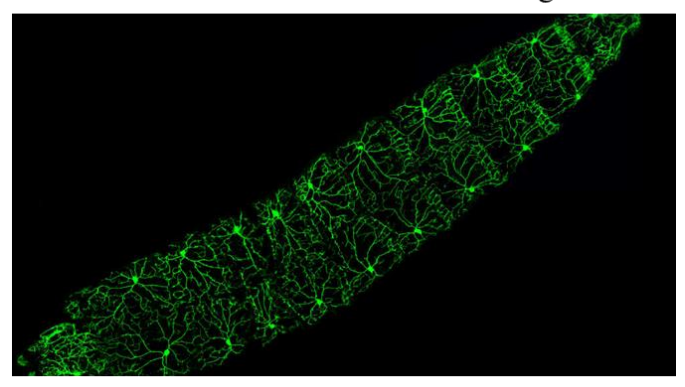


Figure 11. Schematic representation of the Rho GTPases mediated Tau-Fyn induced dendritic and spines degeneration.

1.16 The system of *Drosophila* dendritic arborization (DA) neurons to study the pathogenetic mechanism

Dendritic arborization (DA) neurons are insect sensory neurons in the peripheral nervous system and spread multiple branches across the body wall. *Drosophila* DA neurons are subdivided into four different classes based on the branching complexity and density. Class I DA neurons are the simplest neurons and Class IV being the most complex and dense dendritic branching. These DA Neurons form complex and specific dendritic pattern which can be easily visualized and quantified. *Drosophila* DA neurons have become an ideal model to study pathogenic mechanisms causing degeneration of neurons which is a fundamental characteristic of several neurodegenerative diseases (Iseki et al., 2001; Sáchez-Soriano et al., 2007).

A. C4da neurons in 3rd instar wandering larvae



B. Arborization of C4da neurons

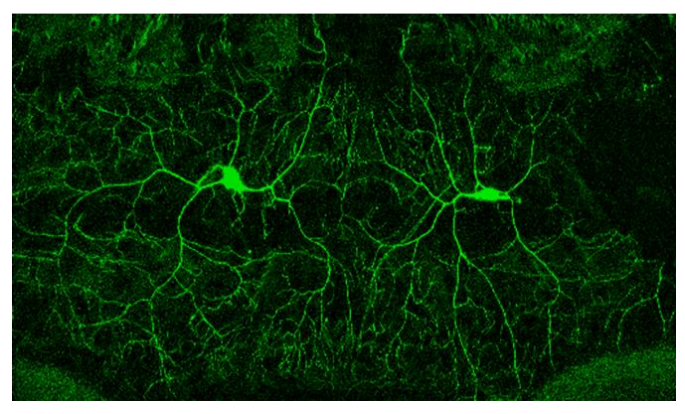


Figure 12. C4da neurons dendritic arborization as a model to study dendrites in *Drosophila*.

(Source of the above image (A): Dr. Chun Han/University of California, San Francisco. Lower C4da arborization image (B) was captured in this study.)

1.17 Objectives of the study

To study the functional mechanism of Tau and Fyn mediated neurodegeneration, we needed to generate the *Drosophila* model with mutations in the amino acid residues of Tau important for Tau-Fyn interaction. To achieve our goal of studying the Tau and Fyn interaction and to study the effect of repurposed drugs on Tau mediated neurotoxicity, we framed following objectives:

- 1. Generation of *Drosophila* model of AD: Generation of stable transgenic flies expressing Wild Type (WT) & mutated human Tau and Fyn for studying functional interaction.
- 2. Genetic analysis to understand the mechanism of Tau-Fyn mediated neurotoxicity.
- 3. Repurposing the drugs used in oncotherapy for checking the neuroprotective effects in *Drosophila* model of AD.

1.18 Important amino-acid residues chosen for mutagenesis to study the physical and functional interaction of Tau and Fyn.

Recent studies have stated that Tau and Fyn kinases interact with each other through their Proline rich domains (PXXP motifs) and SH3 domains, respectively (Lau et al., 2016; Mondragón-Rodríguez et al., 2012b; Usardi et al., 2011b). Tau protein has seven PXXP motifs out of which sixth and seventh domain are found to be important for Tau and Fyn Interaction. Protein binding domain of Fyn Kinase (SH3 domain) binds to the PXXP motifs of Tau protein and phosphorylates the protein at Tyrosine residues. Tau has seven PXXP motifs, and five tyrosine residues, of which Tyr18 is found to be abnormally phosphorylated in AD (Miyamoto et al., 2017). The role of remaining tyrosine residues needs to be studied to understand the mechanisms better. For studying the functional interaction of Tau and Fyn proteins in *Drosophila*, we choose sixth PXXP motif (P216-X-X-P219) and Y18 amino acid residues in Tau protein, to mutate and study their effect on interaction Tau and Fyn.

1.18.1 PXXP motifs in Tau protein

Tau protein has seven P-X-X-P motifs: P176-X-X-P179, P179-X-X-P182, P200-X-X-P203, P203-X-X-P206, P213-X-X-P216, P216-X-X-P219, and P233-X-X-P236 (Lau et al., 2016; Usardi et al., 2011b). Sixth and seventh PXXP motifs are formed by P216-P219 and P233-P236 residues respectively. So, we decided to mutate these proline residues individually as well as in combination with their partner to study to their importance and effect on interaction and Tau pathogenicity.

Fyn kinase is a tyrosine kinase, it phosphorylates the Tau protein at Tyr residues (Miyamoto et al., 2017). In AD, hyperphosphorylation of Tau at Tyr18 is one of the important events and importance of other tyrosine residues is not known yet. So, we also mutated these tyrosine residues in Tau protein to phenylalanine to study if they have any role in Tau pathogenicity.

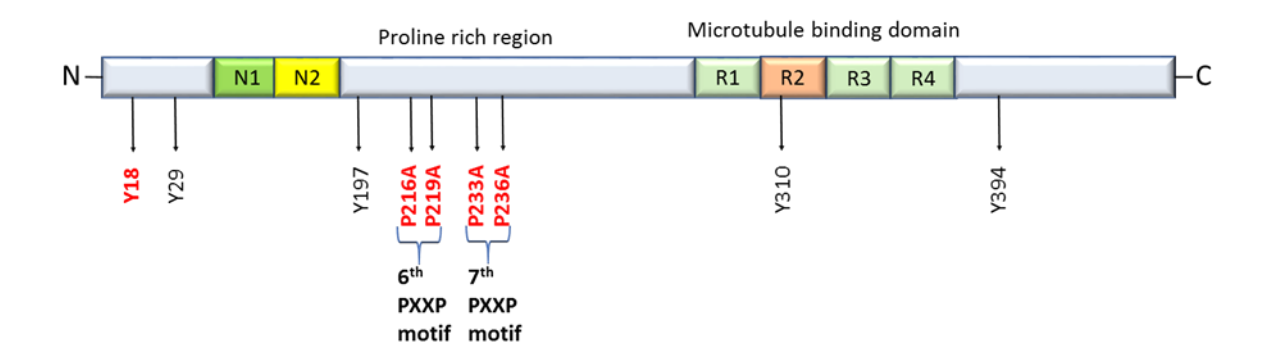


Figure 13. Selected important sites (highlighted in red) for site-directed mutagenesis for studying the physical and functional interaction of Tau and Fyn.

As mentioned before, we have introduced mutations in critical sites for Tau and Fyn interaction (highlighted in figure 13 in red), and created a transgenic *Drosophila* model expressing these altered proteins. Subsequently, we examined the neurodegeneration and evaluated the impact of modulating the Tau-Fyn interaction on the severity of different phenotypes.

Chapter 2. Materials and Methods

2.1 Materials and Reagents

2.1.1 Drosophila Stocks

Following stocks were used in this study:

Sr.	Drosophila	Genotype	Source
No	Stock		
1.	attP landing	y[1] M{RFP[3xP3.PB] GFP[E.3xP3]=vas-	BDSC; Stock
	site	int.Dm}ZH-2A w[*]; M{3xP3-RFP.attP}ZH-86Fb	Number 24749
2.	attP landing	y[1] M{RFP[3xP3.PB] GFP[E.3xP3]=vas-	BDSC; Stock
	site	int.Dm}ZH-2A w[*]; M{3xP3-RFP.attP'}ZH-51C	Number 24482
3.	attP landing	y[1] w[*] P{y[+t7.7]=nanos-phiC31\int.NLS}X;	BDSC; Stock
	site	P{y[+t7.7]=CaryP}Msp300[attP40]	Number 79604
4.	GMR-Gal4	w[*]; P{w[+mC]=GAL4-ninaE.GMR}12	BDSC; Stock
			Number 1104
5.	Elav-Gal4	Elav Gal4 on third chromosome	BDSC; Stock
			Number 8760
6.	PPK-Gal4	w[*]; P{w[+mC]=ppk-GAL4.G}3	BDSC; Stock
			Number 32079
7.	WT Tau	y[1] M{RFP[3xP3.PB] GFP[E.3xP3]=vas-	Generated in
		int.Dm}ZH-2A w[*]; M{3xP3-RFP.WT-Tau}ZH-	this study
		86Fb	
8.	Tau P216A	y[1] M{RFP[3xP3.PB] GFP[E.3xP3]=vas-	Generated in
		int.Dm}ZH-2A w[*]; M{3xP3-RFP.Tau	this study
		P216A}ZH-86Fb	
9.	Tau Y18F	y[1] M{RFP[3xP3.PB] GFP[E.3xP3]=vas-	Generated in
		int.Dm}ZH-2A w[*]; M{3xP3-RFP.Tau Y18F}ZH-	this study
		86Fb	
10.	Tau P216A-	y[1] M{RFP[3xP3.PB] GFP[E.3xP3]=vas-	Generated in
	P219A	int.Dm}ZH-2A w[*]; M{3xP3-RFP.Tau P216A-	this study
		P219A}ZH-86Fb	
	I		

11.	WT Fyn	$y[1]$ w[*] $P{y[+t7.7]=nanos-phiC31\setminus int.NLS}X;$	Generated in
		P{y[+t7.7]=CaryP}WT Fyn[attP40]	this study

2.1.2 Mutagenesis and cloning reagents

For generating the mutants of the Tau, we purchased WT MAPT in pBSK construct from GeneScript USA. We used this construct for site-directed mutagenesis. For amplification of the constructs through Inverse PCR, we used Phusion high fidelity DNA polymerase, from NEB. For transformation and culturing of the mutated constructs, we used XL-Blue competent cells. For digesting the constructs EcoRI, XbaI restriction enzymes were used. For digesting the parental methylated DNA strands from the inverse PCR amplified product, DpnI restriction enzyme was used.

2.1.3 Squish Buffer for crude extract preparations

For preparation of the crude extract for single fly PCR, we crushed the flies in squish buffer. 1M Tris of pH 8.2, 1M EDTA and 25 mM NaCl was used for the preparation of squish buffer. 10 μ g/ml Proteinase K was added to the squish buffer to inactivate the other proteins and in the extract. Single fly was crushed in 50 μ l of squish buffer and debris was separated by centrifugation. Collected supernatant was stored in -20 0 C and used as template for the single fly PCR.

2.1.4 Bouin's and Paraformaldehyde (PFA) fixing solution

Bouin's fixative was used for fixing the dissected third instar larvae for studying the NMJs and 4% paraformaldehyde was used for fixing larval C4da neurons. 100 ml Bouin's fixative was prepared by adding 75 ml saturated picric acid, 25 ml Formalin (37% aqueous solution of Formaldehyde) and 5 ml glacial acetic acid. Similarly, 4% PFA was prepared by diluting the 37% aqueous solution of Formaldehyde. Both fixatives were prepared in the PBS solution.

2.1.5 Wash Buffer (PBSTx)

Wash buffer was prepared by adding 0.3% Triton X-100 in 1XPBS solution. Wash buffer was used for washing the tissue samples after fixing and staining as mentioned in immunofluorescence section.

2.1.6 Blocking Buffer

Blocking buffer was prepared by adding $100 \mu l$ of 10X BSA in $900 \mu l$ 1XPBSTx. Blocking buffer was used for blocking the tissue samples and also for diluting the antibodies used for staining.

2.1.7 Mounting medium

VECTASHIELD Mounting medium (Vector Laboratories, Cat no H-1000) was used for mounting the tissue samples for microscopy.

2.2 Methodology

2.2.1 Site-directed mutagenesis

We used Inverse PCR for creating the site-specific mutations in human Fyn kinase and Tau. Constructs were amplified using mutagenic primers with Phusion high fidelity DNA polymerase. Amplified plasmid was digested with DpnI enzyme to digest the parental template DNA. DpnI digested sample was transformed into XL-B competent cells. Positive colonies were screened through colony PCR and insert was further confirmed through double digestion of the isolated plasmid. Mutation at specific desired position was confirmed through the sequencing.

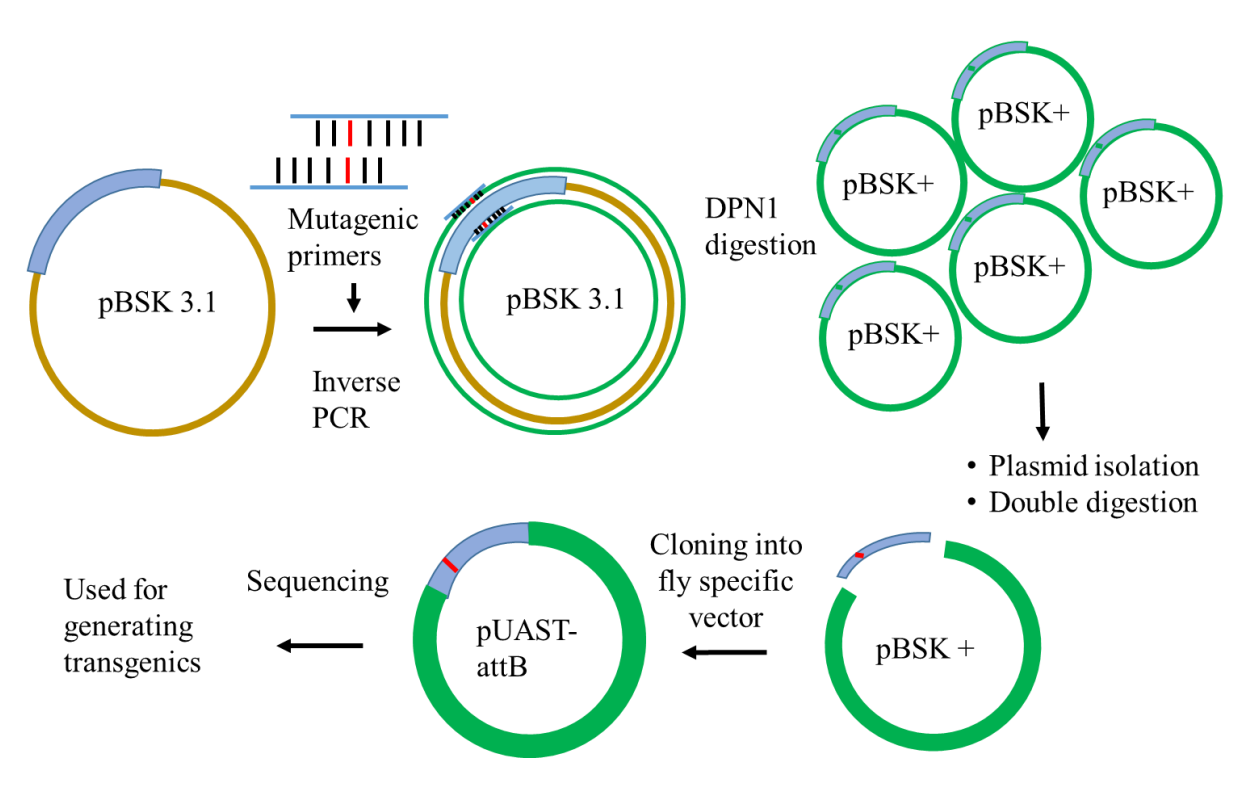


Figure 14. Strategy for site-directed mutagenesis and cloning into fly specific pUAST-attB vector. Mutagenic primers (containing point mutation) were used for amplifying the full pBSK plasmid containing gene, through inverse PCR. Amplified plasmid was digested with DpnI restriction enzyme

to cut the parental methylated strand. This digested plasmid was transformed into XL-Blue competent cells and colonies were screened through colony PCR. Positive colonies were cultured and plasmid was isolated. Isolated plasmid was confirmed through double digestion and sequencing. After sequencing confirmation, construct was ready for microinjection.

2.2.2 Mutagenic Primers

For creating site-specific mutations through inverse PCR, we created primers with point mutations. These mutagenic primers were specific for binding to the target site and introduced point mutations during amplification. Following primers were used in this study:

Table 1. Primers with point mutations for site-directed mutagenesis.

WT Human MAPT primers:				
Forward primer: WT MAPT	ATTGAATTCATGGCTGAGCCCCGCCAG			
Reverse Primer: WT MAPT	ATTTCTAGATCACAAACCCTGCTTGGCCAGG			
WT Human FYN primers:				
Forward primer: WT Fyn	ATAGAATTCATGGCCTGTGTGCAATGTAAGG			
Reverse Primer: WT Fyn	ATATCTAGATTACAGGTTTTCACCAGGTTGG			
Mutagenic primers for MAPT				
Forward primer: MAPT P216A	CCGTCCCTT GCA ACCCCACCCACCCGG			
Reverse Primer: MAPT P216A	TGGGGT TGC AAGGGACGGGGTGCGGGAGCG			
Forward primer: MAPT P219A	CCAACCCCA GCC ACCCGGGAGCCCAAGAAG			
Reverse Primer: MAPT P219A	CCGGGT GG TTGGAAGGGACGG			
Forward primer: MAPT P233A	CGTACTCCA GCC AAGTCGCCGTCTTCCGCC			
Reverse Primer: MAPT P233A	CGGCGACTT GGC TGGAGTACGGACCACTGC			
Forward primer: MAPT P236A	CCCAAGTCG GCG TCTTCCGCCAAGAGCCGC			
Reverse Primer: MAPT P236A	GGCGGAAGA CGC CGACTTGGGTGGAGTACG			
Forward primer: MAPT P216-219A	TCCCTT GCA ACCCCA GCC ACCCGGGAGCCCAAG			
Reverse primer: MAPT P216-219A	CCGGGT GG CTGGGGT TGC AAGGGACGGGGTGCG			
Forward primer: MAPT P233-236A	ACTCCA GCC AAGTCG GCG TCTTCCGCCAAG			
Reverse primer: MAPT P233-236A	GGAAGA CGC CGACTT GGC TGGAGTACGGACCAC			
Forward primer: MAPT Y18F	GCTGGGACG TTC GGGTTGGGGGACAGGAAAGAT			
Reverse Primer: MAPT Y18F	CCCCAACCCGAACGTCCCAGCGTGATCTTCCATCAC			

2.2.3 Cloning of the mutated constructs into pUAST-attB Vector

For inserting the construct into *Drosophila* genome, we cloned WT and mutated constructs into *Drosophila* specific pUAST-attB vector. After confirming the mutation through sequencing, we digested out the mutated construct from pcDNA vector and ligated into pUAST-attB vector at EcoRI and XbaI restriction enzymes sites. This ligated product was transformed into competent cells and grown colonies were screened for the presence of the

insert through colony PCR. Positive colonies were cultured, and the plasmid was isolated. This isolated plasmid was confirmed for the presence for the insert through double digestion and expected band (of 1.5 kb) of Fyn was obtained. Finally, this insert in pUAST-attB vector was also confirmed for the desired mutation through sequencing, and desired results were obtained.

2.2.4 Microinjection of the WT and mutated construct into Drosophila embryos

For generating the transgenic flies expressing human Fyn kinase transgene, we microinjected the WT Fyn cloned in pUAST-attB into *Drosophila* embryos. Fresh flies were taken two days before injections and feed with fresh food and yeast paste. On the day injections, Flies were kept for egg laying in cylindrical tube containing food plate at one end and fine mesh at another end. Flies were kept for 15-20 mins for egg laying and then moved to another egg laying chamber.

We collected the *Drosophila* embryos of 15-20 mins age and processed them for the microinjection. Embryos were aligned on the agarose gel slab in straight line so that all embryos were having their posterior ends on same side. Aligned embryos were transferred to the glass slide containing double sided adhesive tape. Embryos were then merged in halocarbon oil for maintain the proper moisture and oxygen supply. Embryos merged in halocarbon oil were then microinjected with PLI-90 Pico-injector from Harvard apparatus.

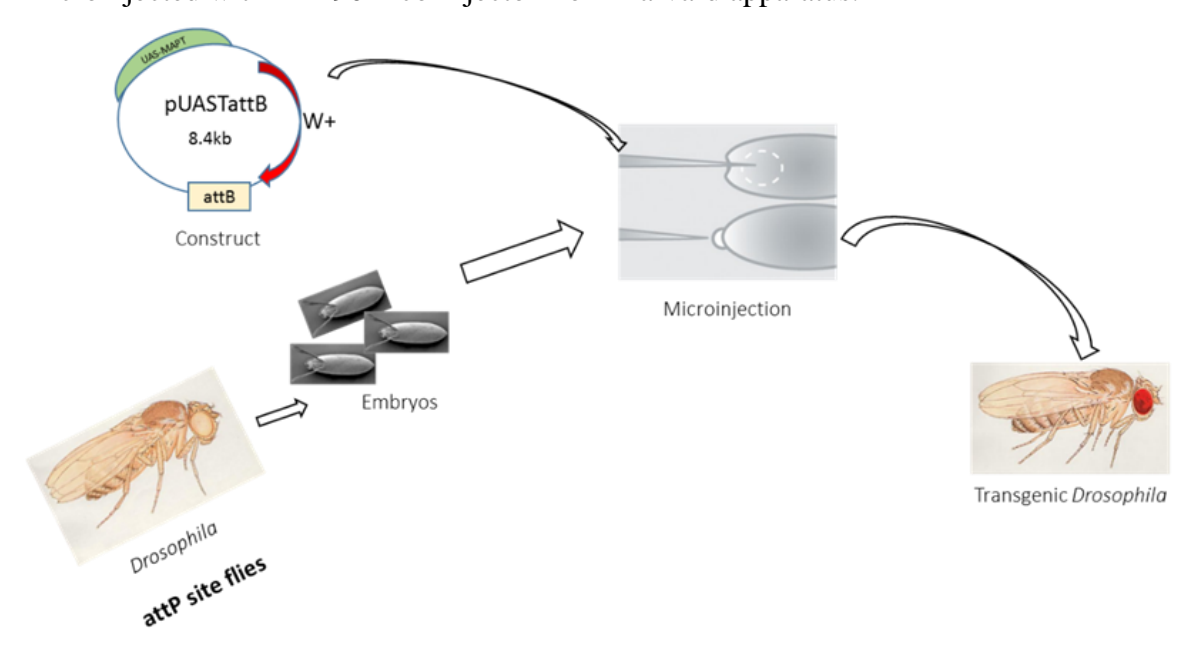


Figure 15. Graphical summary of the microinjection procedure. *Drosophila* stock containing attP landing sites were used for getting embryos which were further processed and microinjected at the posterior end with the help of picoinjector. Progenies were screened for the red eye colour phenotype.

2.2.5 Post Injection care

After microinjecting the construct, embryos were cultured at lower temperature (18°C) for their proper healing and growth. Next day, embryos were collected from injection slide, halocarbon oil was wiped off and embryos were transferred to food vial for further development and kept at 25°C. Once flies were eclosed from injected larvae or pupa, they were screened for the transgenic fly.

2.2.6 Screening of the transgenic flies

After microinjecting the construct, embryos were cultured at lower temperature for their proper healing and growth. After eclosion, injected (G₀) flies were collected (virgins for female) and crossed with specific balancer chromosome stock for inhibiting the possible recombination of the homologous chromosomes. This cross was referred as parental cross. Progeny of this cross was collected as F1 generation and screened for the red eyes, as red eyes will be due the insertion of the pUAST-attB into white eye *Drosophila* (attP site containing flies) background.

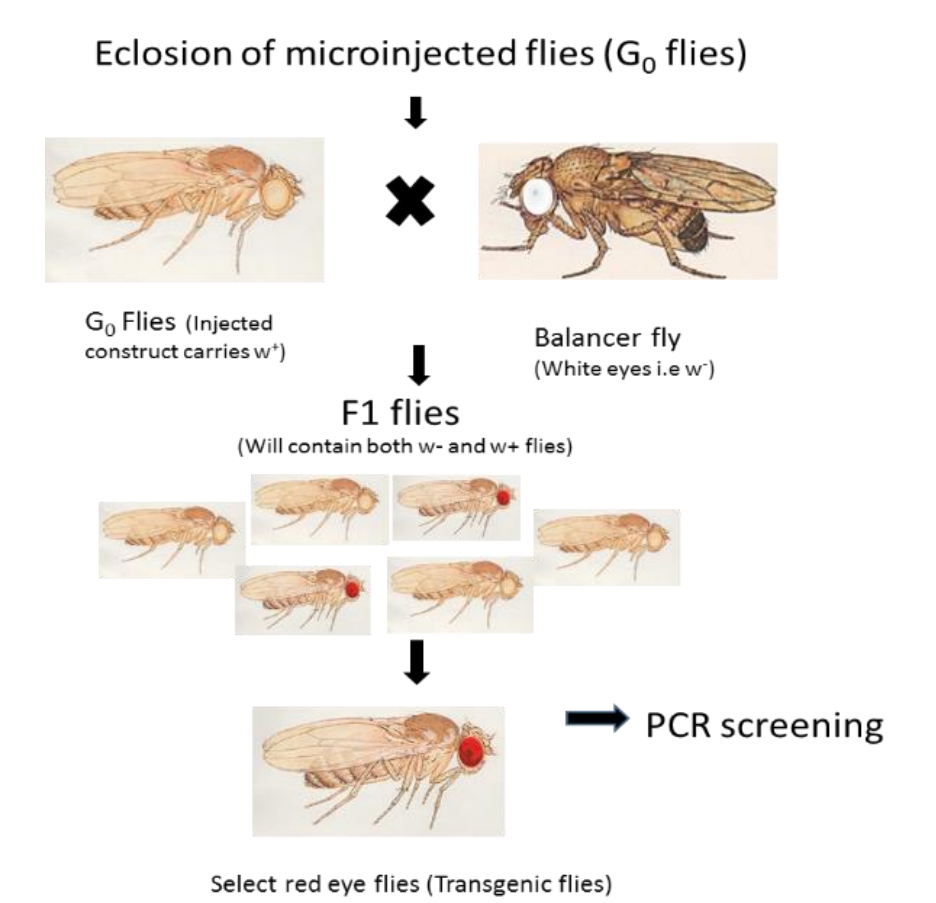


Figure 16. Strategy for screening of the microinjected flies for transgenic.

2.2.7 Single fly PCR for genotypic screening

After phenotypic screening through red eye phenotype, flies were also confirmed through single fly PCR for genotypic screening. Individual single flies were crushed in squish buffer and crude extract was prepared. This crude extract was used for the single fly PCR with WT human MAPT primers. Positive flies for the human transgene were then screened for the site-specific integration (figure 17).

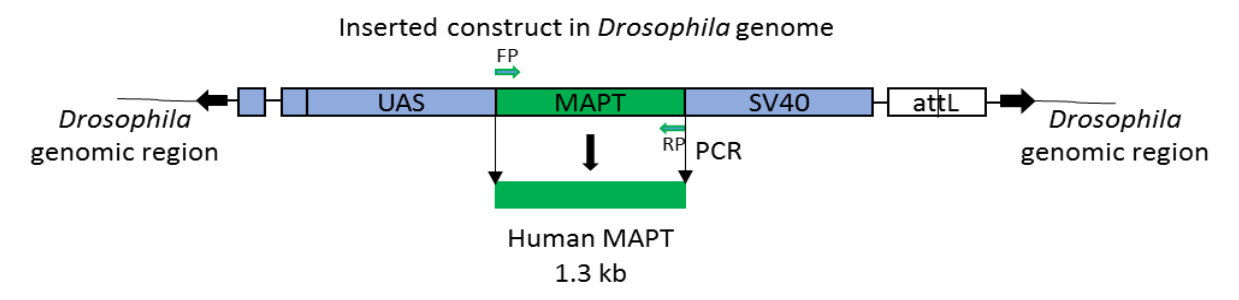


Figure 17. Genotypic screening of the transgenic *Drosophila*. WT MAPT primers were used for single fly PCR and confirmation of the transgene in *Drosophila* genome.

2.2.8 Single fly genomic PCR with flanking primer for confirming site-specific integration

For confirming site-specific integration, we designed forward primer from transgene and reverse primer from flanking region of the insertion. So, if the transgene is inserted at particular site, we will get a higher size band as depicted in the following figure (figure 18).

Inserted construct in Drosophila genome

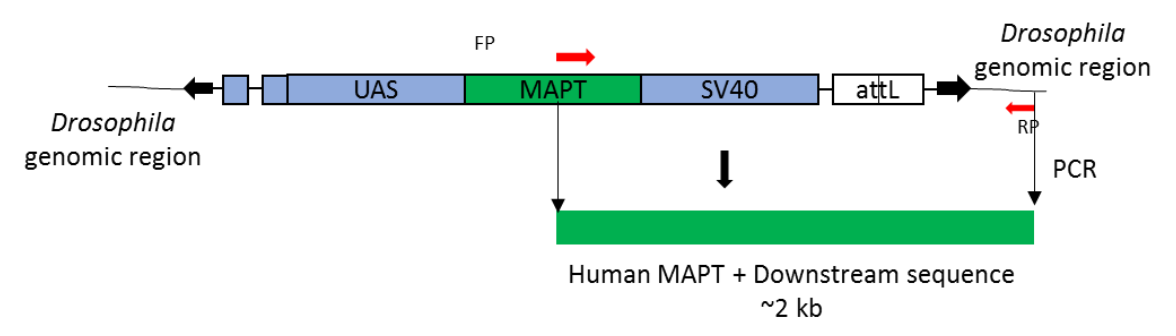


Figure 18. Site-specific integration of the microinjected construct. Primers were designed from transgene (forward primer) and flanking region (reverse primer).

2.2.9 Generation of Tau and Fyn coexpression fly stocks

To study the synergistic effects of both Tau and Fyn overexpression we need both transgene is one fly therefore we generated the fly stock having both Tau and Fyn in one fly. We generated transgenic flies which are having Tau on its third chromosome and Fyn transgene on second chromosome (figure 42).

2.2.10 Scanning Electron Microscopy

Flies with UAS-transgene were crossed with GMR or Ey-Gal4 for the expression in *Drosophila* eyes. F1 progeny was collected and aged as separate pools for different ages. After the eclosion, treated and control flies were fixed in 1% formaldehyde for two hours, followed by serial dehydration steps of 12hrs each in 25%, 50%, 75% and 100% ethanol were carried out (figure 19). Flies were stored in 100% ethanol and dried with CPD (Critical Point Dryer) before mounting on the stab for imaging. Eye Images were captured at 150X and analysed using Infinity Analyze software plotted with Graph Pad Prism 8.

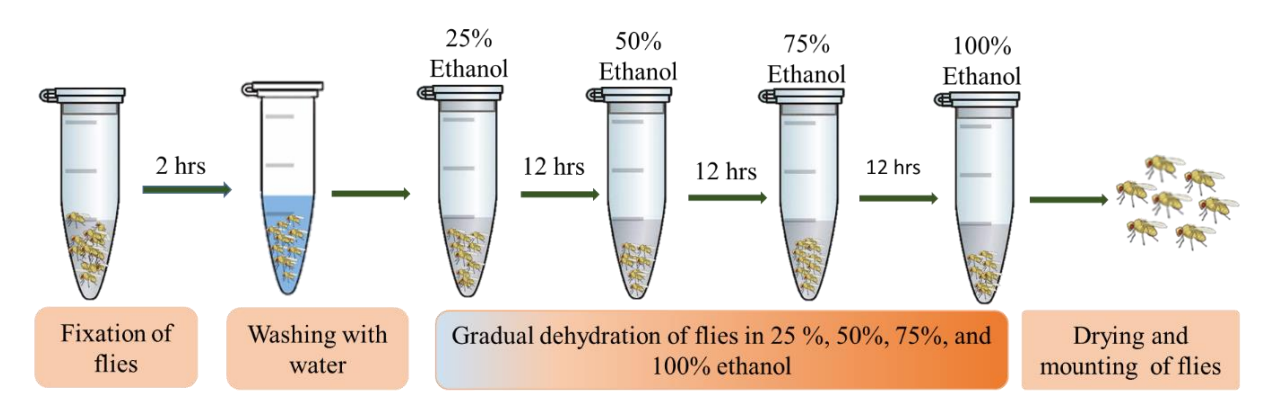


Figure 19. Pictorial representation of the preparation of flies for SEM.

2.2.11 Locomotion assay

Flies with UAS transgene were crossed with pan neuronal Gal4 driver (Elav-Gal4) and F1 progeny was collected for different age pools. 20 flies were in each batch used for assaying the locomotion. Flies were transferred to 20 cm long tube and open end was plugged with cotton. Flies were left in tube for 30 mins to get used to the environment. For recording climbing assay, tube was tapped gently so that all flies were at bottom of tube and then flies climbing up to 20 cm mark in 20 seconds was counted. Experiment was repeated three times for each batch for one reading. Total percentage of flies crossing 20 cm mark in 20 sec was counted and we defined it as climbing Index (figure 20).

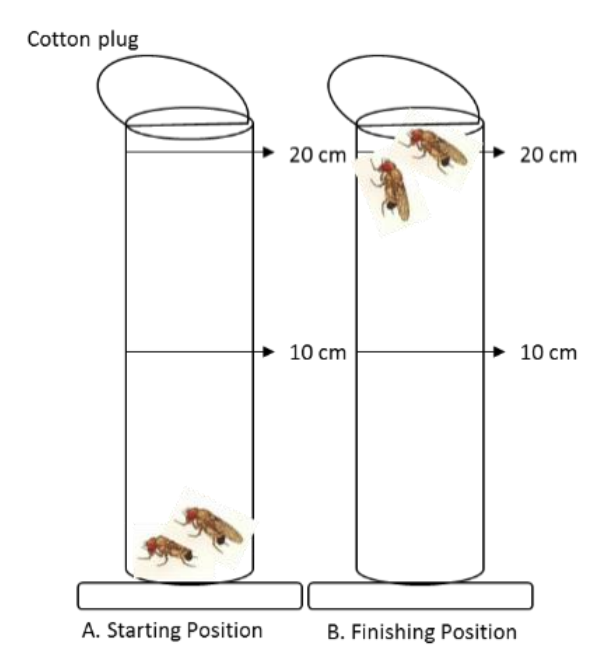


Figure 20. Schematic representing the strategy for climbing assay. Flies were tapped so that every fly is at starting position and percentage of flies crossed 20 cm mark in 20 seconds was counted.

2.2.12 Nail Paint imprinting

Flies with UAS transgenes (human WT Tau, Tau P216A, Tau Y18F with Fyn) were crossed with GMR gal4. The F1 progeny was used for analysing the outer surface of the eyes with nail paint imprinting as described by Arya and Lakhotia (Arya and Lakhotia, 2006). F1 progeny of 1 day, 10 days, 20 days, and 30 days were used. Flies' heads were detached from body and dipped in nail paint. After drying of the paint, the outer layer of the paint covering the eyes were peeled off carefully. This nail paint layer has the exact replica of the outer surface of the eye morphology. We imaged this imprints with light inverted microscope at 4X, 10X, 20X and 40X for analysing the outer surface morphology of the eye.

2.2.13 Electroretinograms

Flies expressing WT and mutant Tau along with Fyn were used for recording ERGs at 1-day, 10-day, 20-day and 30-day age. ERG procedures has been described previously (Dolph et al., 2011). Flies were treated as mentioned in treatment section. 1-day old flies were used for ERG recordings. Flies were immobilized by ice cooling and mounted on top of tip so that only head was popping out and fixed with wax. Reading and reference electrodes were filled with ringer's solution and placed on the cornea of eye and near proboscis respectively (figure 21). Flies were adapted to dark for 10 mins at least before recording ERGs. The stimulus was given by white LED placed approximately 4 cm above the fly head facing towards fly. The light stimulus of 1 sec was given and 10 trials were recorded at inter-trial interval of 15 seconds for

each fly. The recordings were carried out using DAGAN BVC-700A current clamp amplifier with the gain of 100X and digitized using National Instruments 16bit digitizer, sampled at 15 kHz.

ERG traces were analysed through custom written MATLAB scripts to quantify Ontransients. The highest voltage value within 100msec after light stimulus onset was recorded as ON .transients. Mean of 200msec of samples 667msec after stimulus onset was used as receptor potential; and the minimum voltage value within 150msec after switching off light stimulus was recorded as OFF transients. 10-15 flies were used for each genotype or treatment. ERG and average traces were plotted after three individual repeats. Statistical analyses were performed using the Graph Pad Prism 8.0.

ERG: Set up and recording

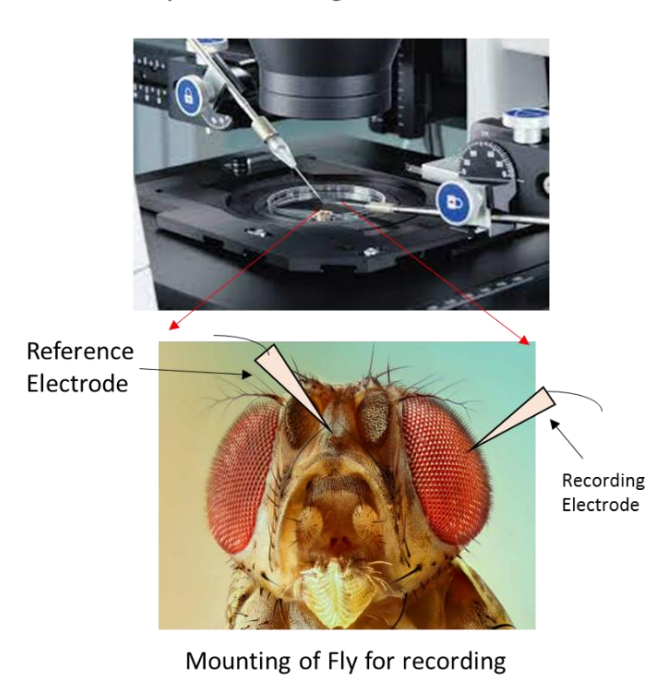


Figure 21. ERG set up, mounting of fly and recording of ERG.

2.2.14 Western Blotting

Flies were freezed in liquid nitrogen and decapitated by removing heads. Heads were collected and crushed in ice cold radioimmunoprecipitation assay (RIPA) buffer (Sigma) in the presence of 1X protease inhibitor cocktail (Cell signalling technologies). Crude extract was centrifuged at 14000 rpm for 15 minutes and supernatent was collected. Equal amount of protein for each sample was loaded in 10% SDS gel and electrophoresed. Basic western blotting methodolgy was followed (Mahmood and Yang, 2012). Protein were transferred to Immobilon

PVDF membrane from MERCK according to supplier's guidelines through wet transfer. After transfer, membrane was blocked in 5% BSA for an hour and then incubated for overnight with with primary antibody at 4°C. Membranes were stained for Tau with HT7 (1:2000, Mouse from Invitrogen, Cat no MN1000), Fyn with Fyn antibody (1:2000, Mouse BD Biosciences, Cat no 610163), Rac with Rac/Cdc antibody (1:2000, Cell Signalling Technology, Cat no 4651), Rho with P1D9 Rho antibody (1:2000, DSHB) and Actin with D6A8 actin antibody (1:2000, Cell Signalling Technology, Cat no 8457). Primary antobody incubation was followed by 3-5 washes with 1xTBST. Secondary antibodies, Goat anti-mouse secondary antibody HRP conjugated (1:20000, Invitrogen Cat No 626520) and Goat anti-rabbit secondary antibody HRP conjugated (1:20000, Invitrogen Cat no 656120) were incubated for 2 hours at room temprature. Membrane was washed with 1xTBST 3-5 times at room temprature and blot was developed in Chemiluminiscence (Biorad) using FemtoLucent detection kit from GBioSciences (Cat no 786-003) according to supplier guidelines.

2.2.15 C4da neurons dissections and staining

We crossed PPK-Gal4 driver line with UAS-GFP (BDSC Stock no 5137) and generated the PPK-Gal4;UAS-GFP homozygous viable stock. We crossed this PPK-Gal4;UAS-GFP homozygous stock with UAS-Tau lines for overexpressing the WT and mutant Tau proteins in the C4da neurons of the flies. Third instar wandering larvae were dissected for C4da neurons analysis as described by (Wang et al., 2019). Briefly, third instar wandering larvae were collected and washed with 1xPBS>70% ethanol> double distilled water> 1xPBS for cleaning and removing the food from the larvae body. Larvae was placed on silicon elastomer petriplate and ice-cold PBS was added and we pinned the larve on both anterior and posterior ends with dorsal side facing up. one small incision was made on the posterior end and cut was made along dorsal line between two tracheas upto anterior end. Two small cuts were made on the anterior end and larvae was streched out and pinned at four corners. Sample was fixed in the 4% PFA for 25 minutes at room temprature. After fixing, gut, faybody glands, and other parts were removed and sample was washed thrice in 1xPBST. Sample was stained with primary and secondary antibodies as mentioned in immunofluoroscence and confocal microscopy section.

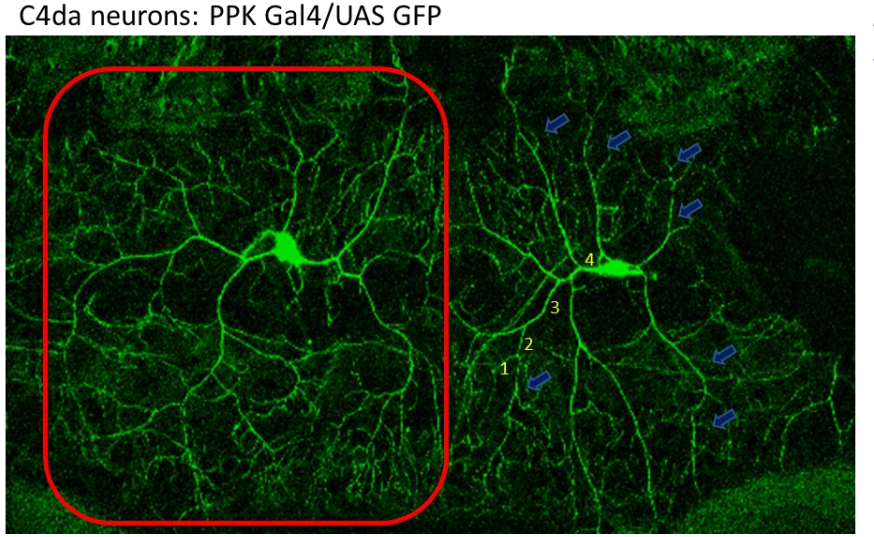
2.2.16 Immunofluoroscence and confocal microscopy

Immunofluoroscence was performed to detect Tau and Fyn proteins in neurons as earlier described (Grueber et al., 2002). Third instar wandering larvae were used. Dissected and fixed samples were incubated in the primary antibody at 4°C overnight. Sample was stained for Tau with HT7 (1:200, Mouse from Invitrogen, Cat no MN1000), Fyn with Fyn antibody

(1:200, Mouse BD Biosciences, Cat no 610163). After overnight incubation with primary antibody, samples were washed thrice in 1xPBST at room temprature followed by staining with secondary antibody goat anti-mouse alexa flour 488 (1:1000, life technologies cat no A11001), goat anti-mouse alexa fluor 568 (1:1000, life technologies cat no 11004), goat anti-rabbit alexa fluor 488 (1;1000, life technologies cat no 110088) and goat anti-rabbit alexa fluor 568 (1:1000, life technologies cat no 11011) for three hours at room temprature. After incubation with secondary antibody samples were washed thrice for 25 minutes each at room temprature. Sample was mounted with vectashield anti-fade mounting medium and sealed the coverslip with transparent nail paint. Carl Zeiss Laser Scanning Confocal microscope (LSM 710) was used for imaging. For capturing dendrite arborization neurons 20x air objective was used.

2.2.17 C4da neurons analysis and quantification

C4da neuron image analysis was performed with the help of Fiji software as described by (Wang et al., 2019). Flouroscent Z-series images were taken with the laser scanning confocal microscope. Dendritic length were quatified with Fiji software as described in (Wang et al., 2019) using simple neurite tracer plugin (Pool et al., 2008). Dendrites length, arbor surface area and number of branches were calculated for each neuron individually and respective average length, arbor surface area and number of branches for all neurons were plotted for each genotype and analyzed with graph pad prism. For analyzing the branching pattern, strahler analysis was used (Strahler, A. (1953)). Percentage of neurons with primary, secondary, tertiary and quaternary branches was calculated with strahler analysis and plotted for analysis (figure 22).



Quantification:

- Total Length of dendrites
- Total no of branches
- Arbor surface area
- Branching Pattern

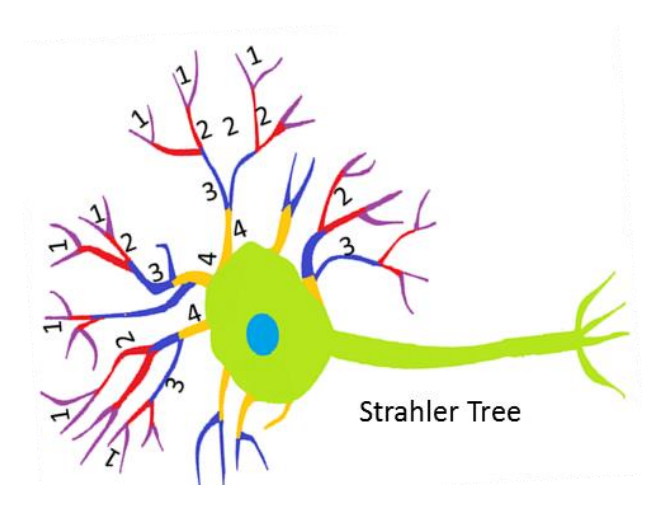


Figure 22. Quantification of the dendritic arborization and branching pattern of the dendrites of the C4da neuron. A. A confocal microscopic image of the C4da neuron. Total length of dendrite, number of branches (blue arrows), arbor surface area (red rectangle box) and pattern of dendritic branching (yellow numbers and below figure) were quantified.

2.2.18 Compounds treatment and analysis

Compound treatments were performed earlier described in (Yadav et al., 2021). Compounds were dissloved in either DMSO or double distilled water according to their chemical nature. This dissolved stock is termed as stock solution and stored in -20°C till use for further dilutions. Reference dose is calculated for larvae body weight for each compound according to the dose recommeded for human body weight. Compound is mixed in the food to get one final reference dose and two higher concentrations as shown in the figure 23.

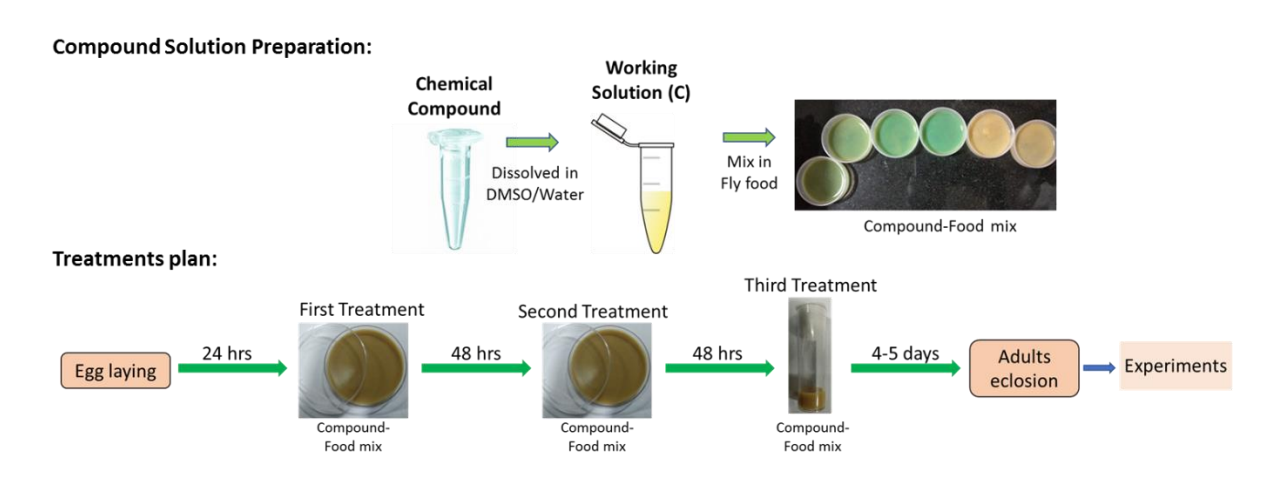


Figure 23. Strategy and planning of the compounds dilution and treatments.

Age synchronized first instar larvae were transferred to the fresh compound-food plate, this is termed as first treatment. After ~ 48 hours of the first treatment, second instar larvae from first treatment plate were transferred to the fresh compound-food plate for second

treatment. Similarly, after ~48 hours of the second treatment, third treatment was given to the larvae. After three treatments, larvae were pupariated. As adult flies eclosed from pupa, we checked and calculated the degenerated surface area of the compounds treated flies and untreated flies. We compared the percentage of the degenerated surface area between compounds treated and untreated flies (Figure 23 and 25).

Analysis of the neurotoxicity:

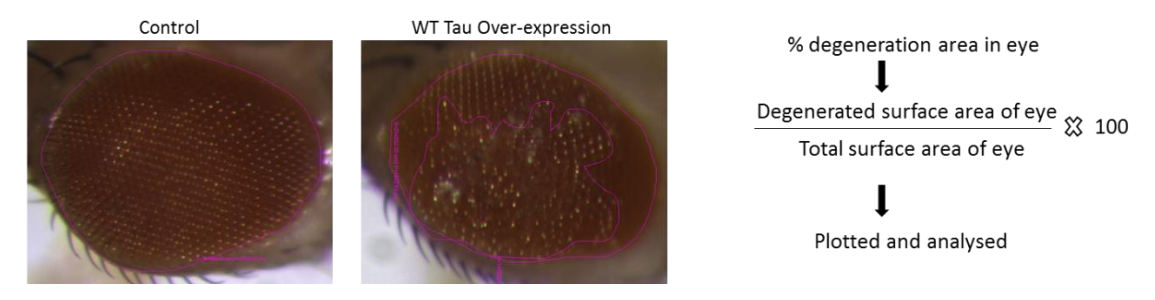


Figure 24. Analysis of the neurotoxicity on the *Drosophila* eye as a primary screening for the compounds treatments.

2.2.19 Statistical analysis

Graph pad prism version 8.0 was used for statistical analysis of the samples. For comparing the difference between two groups, parametric t-test was used as column analysis with 95% confidence interval. Bar graphs represented the SEM. Data was considered significant if the p-value was ≤ 0.05 . P value are ns if P > 0.05, * if P ≤ 0.05 , ** if P ≤ 0.01 , *** if P ≤ 0.001 and **** if P ≤ 0.0001 .

Chapter 3. Results

Objective 1: Generation of Drosophila model of AD.

Generation of stable transgenic flies expressing Wild Type (WT) & mutated human Tau and Fyn for studying functional interaction.

To study the functional interaction of Tau and Fyn and its role in neurodegeneration we have generated the *Drosophila* AD model by overexpressing human Tau and Fyn. We selected the amino acid residues which are important for the interaction of Tau and Fyn for mutagenesis. We mutated Tau Tyrosine-18 to Phenylalanine (Y18F); Proline 216 to Alanine (P216A); and Proline 216, 219 to Alanine 216, 219 (P216A-P219A). We also mutated the seventh PXXP motif of Proline 233 to alanine (P233A); Proline 236 to Alanine (P236A); and Proline 233, 236 to Alanine 233,236 (P233-236A). We used inverse PCR with mutagenic primers for creating the site-specific mutations in human Fyn kinase and Tau. Transformed colonies were screened through colony PCR and insert was further confirmed through double digestion of the isolated plasmid. Mutation at specific desired position was confirmed through the sequencing.

3.1 Isolation of WT Fyn Kinase from human glioblastoma cell lines and cloning it into pUAST-attB vector

For generating transgenic flies expressing human Tau and Fyn, we started with cloning of human Tau and Fyn kinase into pBSKII+ vector. Human glioblastoma cell lines were used for isolation of human Fyn kinase, from these cell lines total RNA was isolated and cDNA was synthesized for amplification of Fyn gene. WT Fyn kinase primers were used for amplification of Fyn Kinase from cDNA. Amplified Fyn kinase gene was ligated into digested pUAST-attB vector. Fyn kinase ligated into pUAST-attB vector was transformed into DH5α competent cells. Colonies containing Fyn Kinase gene insert were screened through colony PCR. Positive colonies were cultured overnight and plasmid was isolated. Presence of gene in isolated plasmid was confirmed through double digestion and expected bands of gene and vector were observed. Finally clone was also confirmed through sequencing. This confirmed clone was further used microinjection into *Drosophila* embryos for generating transgenic flies and also for mutagenesis of Fyn Kinase (figure 25).

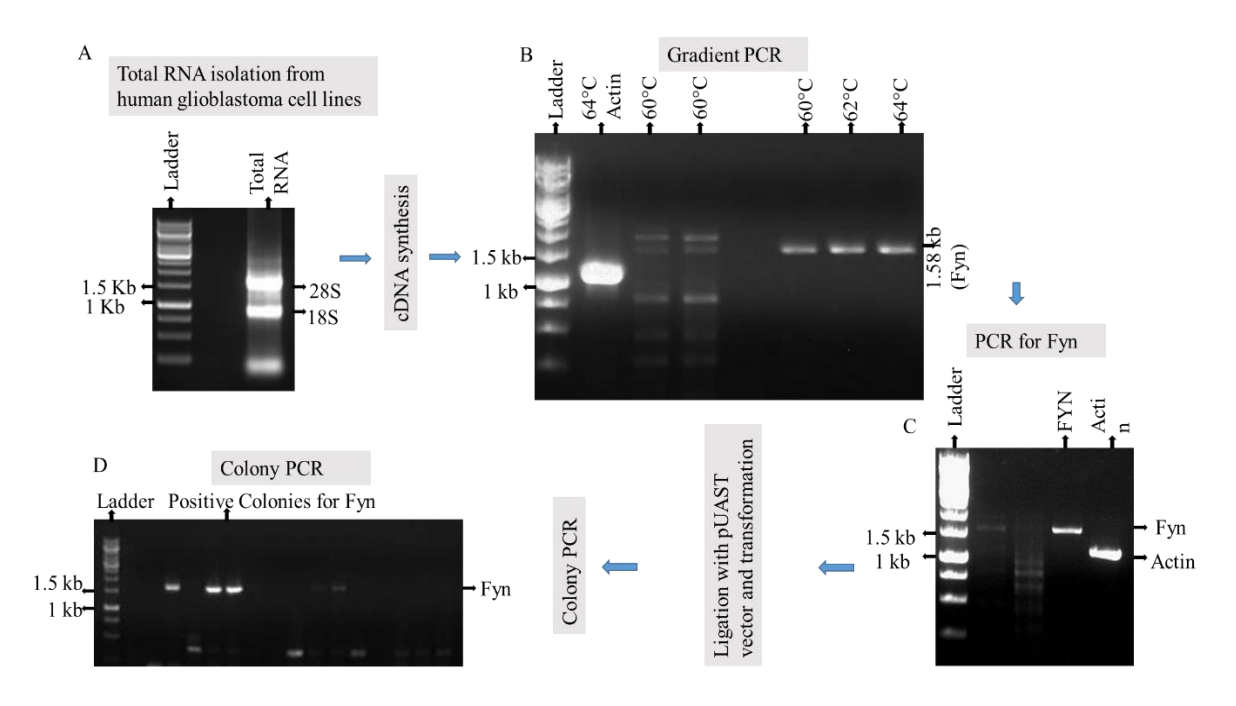


Figure 25. Isolation of WT Fyn Kinase from human glioblastoma cell lines and cloning it into pUAST-attB vector. Total RNA isolation (A) and gradient PCR for amplification of Fyn kinase (B). This amplified Fyn (C) was ligated into pUAST-attB vector and colonies was confirmed through colony PCR (D) and also confirmed through double digestion.

3.2 Cloning of Tau into pUAST-attB vector

For cloning the Tau gene into pUAST-attB vector, we purchased the human Tau clone (Clone ID H98616 from GenScript). Tau gene was amplified from this construct and ligated into pUAST-attB vector. This ligated construct was transformed into DH5α competent cells. Positive colonies for Tau gene were screened through colony PCR and cultured overnight for plasmid isolation. Isolated plasmid was also confirmed through double digestion and then with sequencing. Confirmed construct in pUAST-attB was used for microinjections into *Drosophila* embryos and for Tau mutagenesis (figure 26).

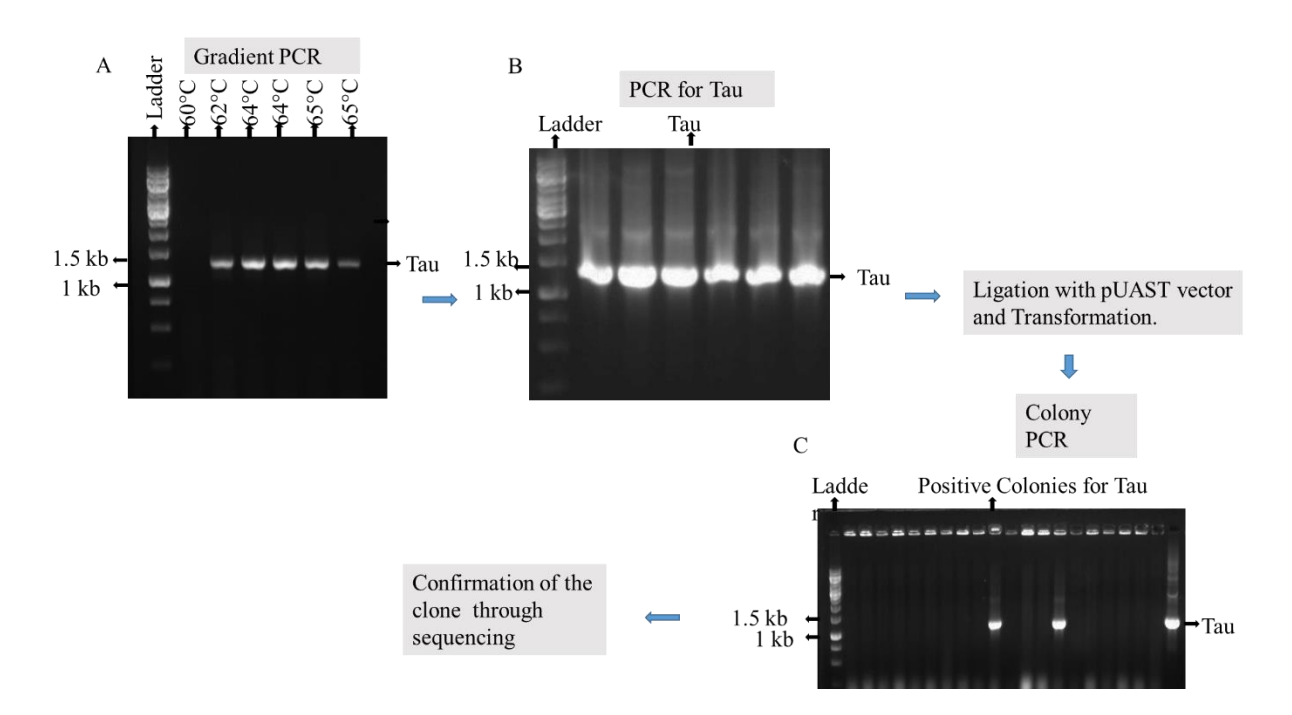


Figure 26. Cloning of Tau into pUAST-attB vector. Tau gene was amplified from Tau in pBSKII+ construct (A and B). Amplified Tau gene was ligated into the pUAST-attB vector and transformed into DH5α cells and positive colonies screened through colony PCR (C).

3.3 Mutagenesis of Tau P216A

Proline 216 was mutated to Alanine by inverse PCR using the mutagenic primers (mentioned in page no.44, Table 1). Tau in pBSK construct was amplified with mutagenic primers for creating the P216A point mutations. This amplified plasmid was digested with DpnI enzyme for cutting the parental plasmid DNA strands. This PCR product was then transformed into XL-B competent cells and positive colonies was screened through colony PCR and double digestion. Point mutation was also confirmed through sequencing (figure 27).

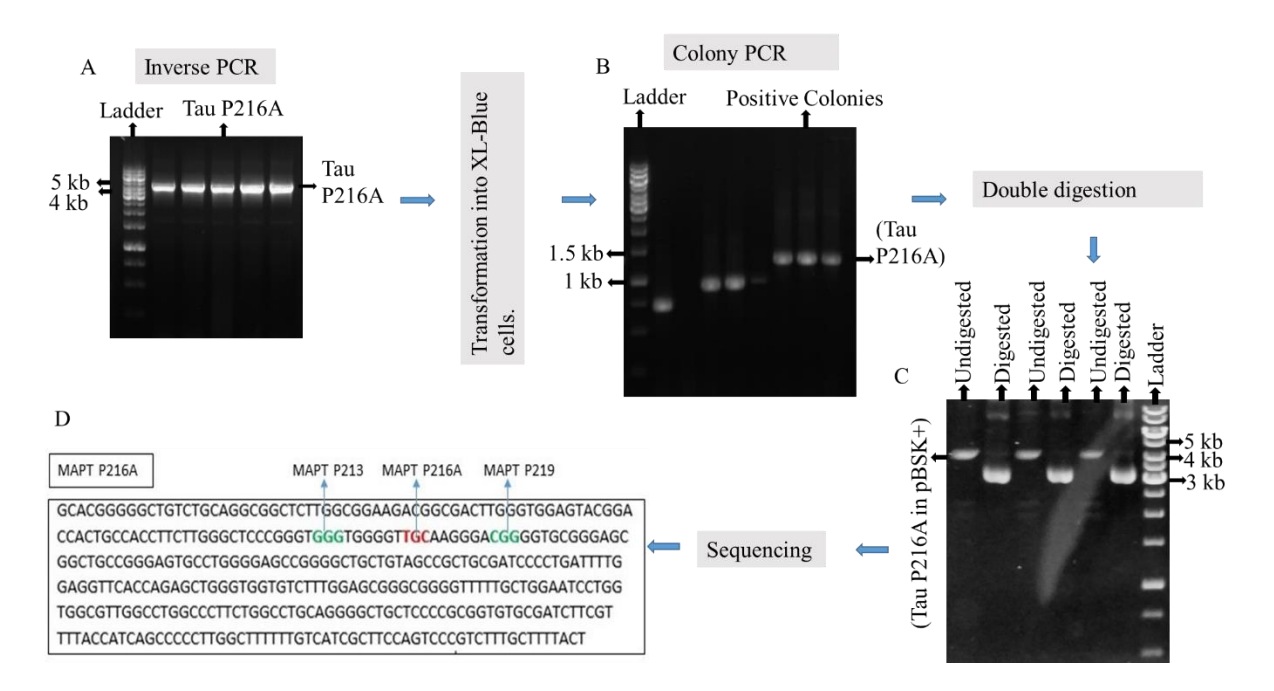


Figure 27. Mutagenesis of Tau P216A. The plasmid containing Tau in pBSK was amplified through inverse PCR. Positive colonies for Tau P216A in pBSK was screened through colony PCR and also through double digestion. Confirmed P216A through sequencing was further used for generating transgenic flies through microinjection.

3.4 Mutagenesis of Tau P219A

Tau gene was mutated at proline residues in PXXP motifs for studying the importance of the proline residues in regulating the interaction of Tau and Fyn protein. Proline 219 was mutated to Alanine by inverse PCR using the mutagenic primers (mentioned in page no. 44, Table 1). Tau in pBSK construct was amplified with mutagenic primers for creating the P219A point mutations. This amplified plasmid was digested with DpnI enzyme for cutting the parental strands. This PCR product was transformed into XL-B competent cells and positive colonies was screened through colony PCR and double digestion. Point mutation was also confirmed through sequencing (figure 28).

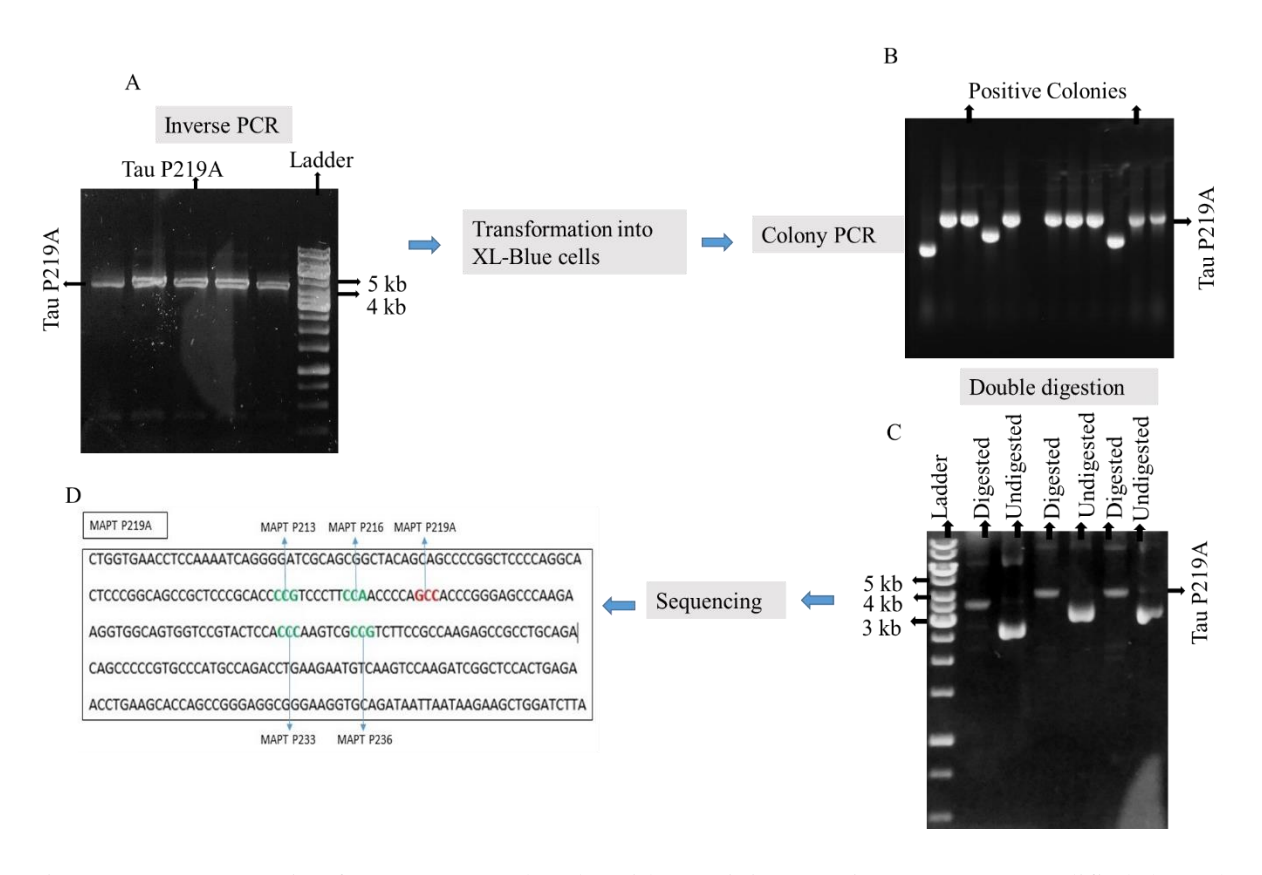


Figure 28. Mutagenesis of Tau P219A. The plasmid containing Tau in pBSK was amplified through inverse PCR (A). Positive colonies for Tau P21PA in pBSK was screened through colony PCR (B) and also through double digestion (C). Confirmed P219A point mutation through sequencing (D).

3.5 Mutagenesis of Tau P233A

Proline 233 and 236 are involved in forming the seventh PXXP motif. Therefore, P233 was by inverse PCR using the mutagenic primers (mentioned in page no. 44, Table 1). Tau in pBSK construct was amplified with mutagenic primers for creating the P233A point mutations. This amplified plasmid was digested with DpnI enzyme for cutting the parental strands. This PCR product was transformed into XL-B competent cells and positive colonies was screened through colony PCR and double digestion. Point mutation was also confirmed through sequencing (figure 29).

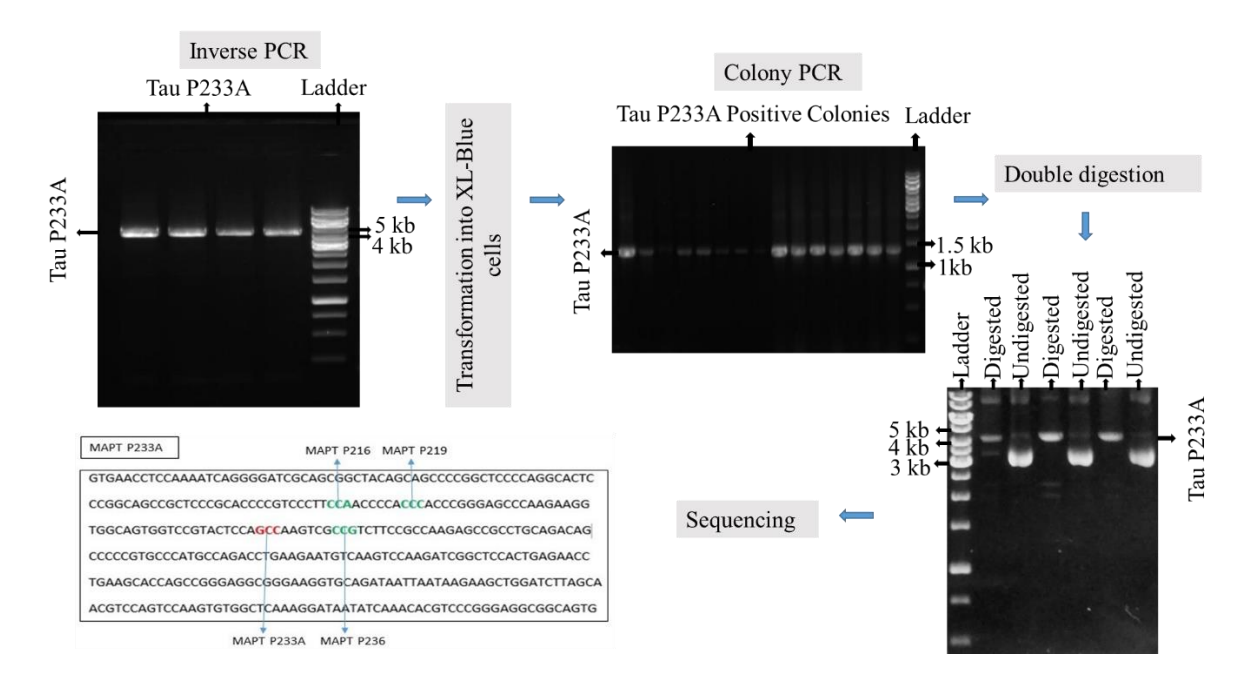


Figure 29. Mutagenesis of Tau P233A. The plasmid containing Tau in pBSK was amplified through inverse PCR (A). Positive colonies for Tau P233A in pBSK was screened through colony PCR (B) and also through double digestion (C). Confirmed P233A point mutation through sequencing (D).

3.6 Mutagenesis of Tau P236A

Second proline for seventh PXXP motif is P236. So, P236 was mutated to alanine by inverse PCR using the mutagenic primers (mentioned in page no. 44, Table 1). Tau in pBSK construct was amplified with mutagenic primers for creating the P236A point mutations. This amplified plasmid was digested with DpnI enzyme for digesting the parental strands. This PCR product was transformed into XL-B competent cells and positive colonies was screened through colony PCR and double digestion. Point mutation was also confirmed through sequencing (figure 30).

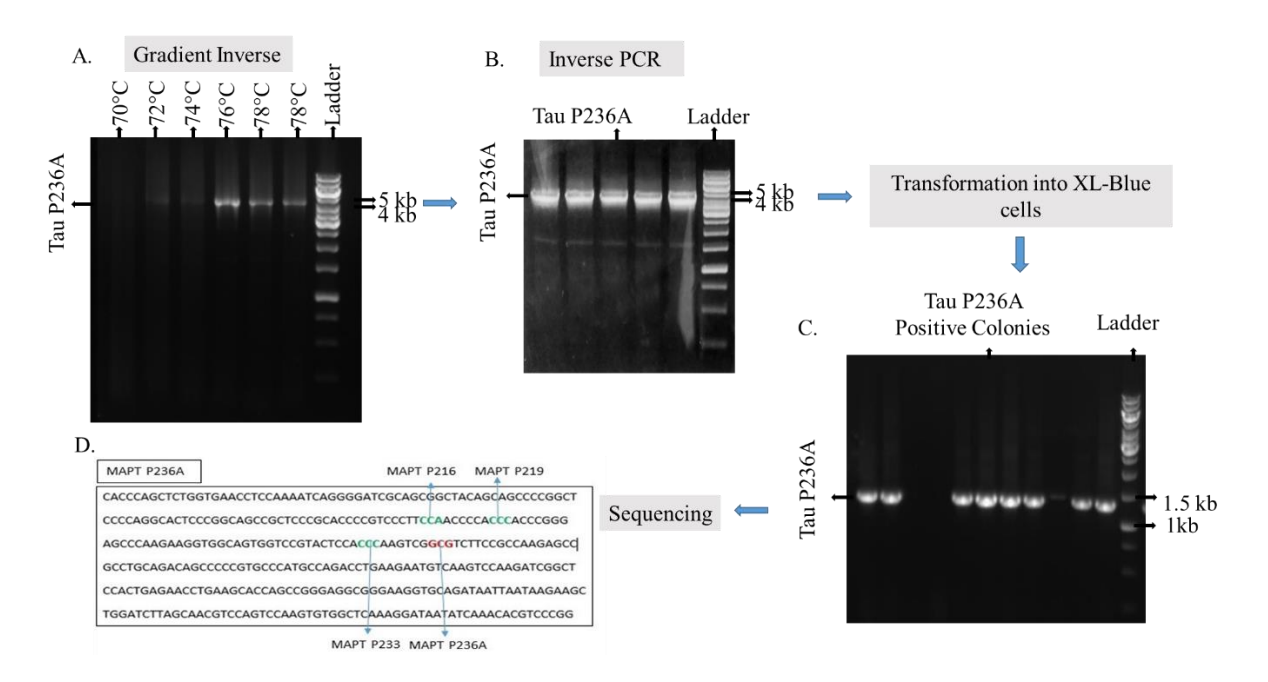


Figure 30. Mutagenesis of Tau P236A. The plasmid containing Tau in pBSK was amplified through inverse PCR (A and B). Positive colonies for Tau P236A in pBSK was screened through colony PCR (C) and also confirmed P236A through sequencing (D).

3.7 Mutagenesis of Tau P216A-P219A

Along with mutating the single partner of sixth and seventh PXXP motifs, we also mutated PXXP motifs as whole. Both the proline partners were mutated to alanine to create the double mutant. P216 and P219 were mutated to Alanine by inverse PCR using the mutagenic primers (Table 1). Tau in pBSK construct was amplified with mutagenic primers for creating the P216A-P219A point mutations. This amplified plasmid was digested with DpnI enzyme for digesting the parental strands. This PCR product was transformed into XL-B competent cells and positive colonies was screened through colony PCR and double digestion. Point mutation was also confirmed through sequencing (figure 31).

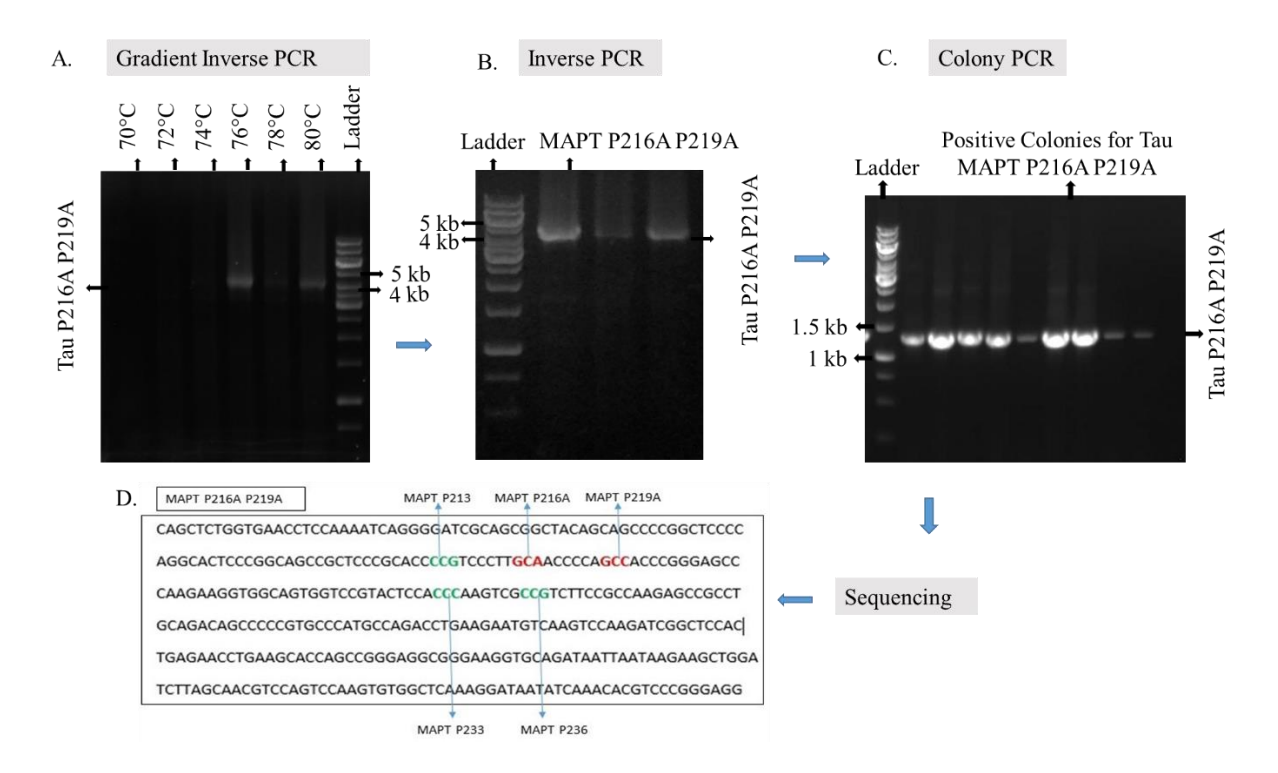


Figure 31. Mutagenesis of Tau P216A-P219A. The plasmid containing Tau in pBSK was amplified through inverse PCR (A and B). Positive colonies for Tau P216A-P219A in pBSK was screened through colony PCR (C) and also confirmed through sequencing (D).

3.8 Mutagenesis of Tau P233A-P236A

Seventh PXXP motifs is formed by P233 and P236 in Tau. Both the proline partners were mutated to alanine to create the double mutant. P233 and P236 were mutated to alanine by inverse PCR using the mutagenic primers (mentioned in page no. 44, Table 1). Tau in pBSK construct was amplified with mutagenic primers for creating the P233A-P236A point mutations. This amplified plasmid was digested with DpnI enzyme for digesting the parental strands. This PCR product was transformed into XL-B competent cells and positive colonies was screened through colony PCR and double digestion. Point mutation was also confirmed through sequencing (figure 32).

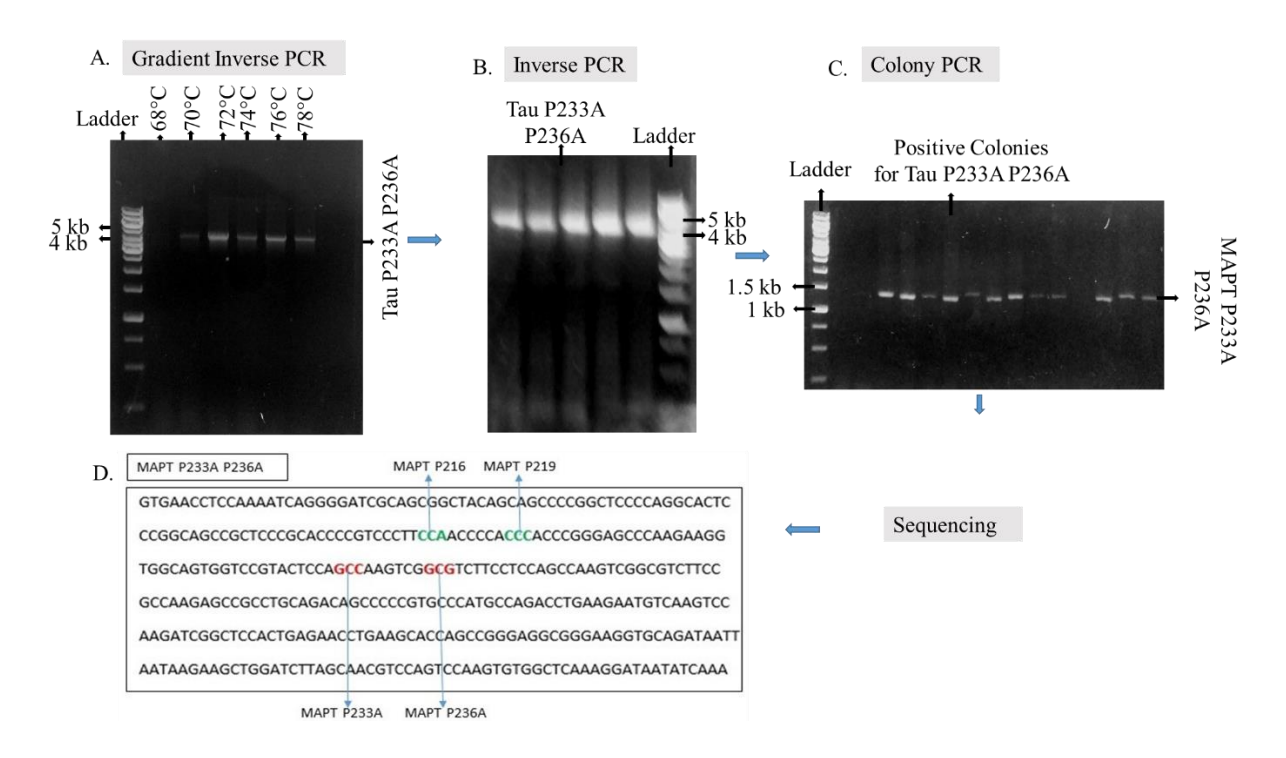


Figure 32. Mutagenesis of Tau P233A-P236A. The plasmid containing Tau in pBSK was amplified through inverse PCR (A and B). Positive colonies for Tau P233A-P236A in pBSK were screened through colony PCR (C) and also confirmed through sequencing (D).

3.9 Subcloning of the mutated Tau and Fyn Construct into pUAST-attB vector

After mutating the Tau and Fyn construct in smaller pBSK and pcDNA vectors, we cloned them into *Drosophila* specific pUAST-attB vector for generating the transgenic lines expressing human Tau and Fyn kinase.

3.10 Subcloning of the Tau P216A into pUAST-attB vector

Tau P216A was amplified from pBSK vector containing the mutated Tau P216A with the help of the WT Tau primers. This amplified Tau construct was digested with the EcoRI and XbaI enzymes and ligated into pUAST-attB vector digested with same pair of restriction enzymes. Ligated product was transformed into XL-B competent cells and positive colonies were screened through colony PCR. Tau P216A positive colonies were cultured and isolated plasmid was also confirmed through double digestion for the presence of the insert. After confirmation, this construct in pUAST-attB vector was used for generating the transgenic *Drosophila* lines through microinjection (figure 33).

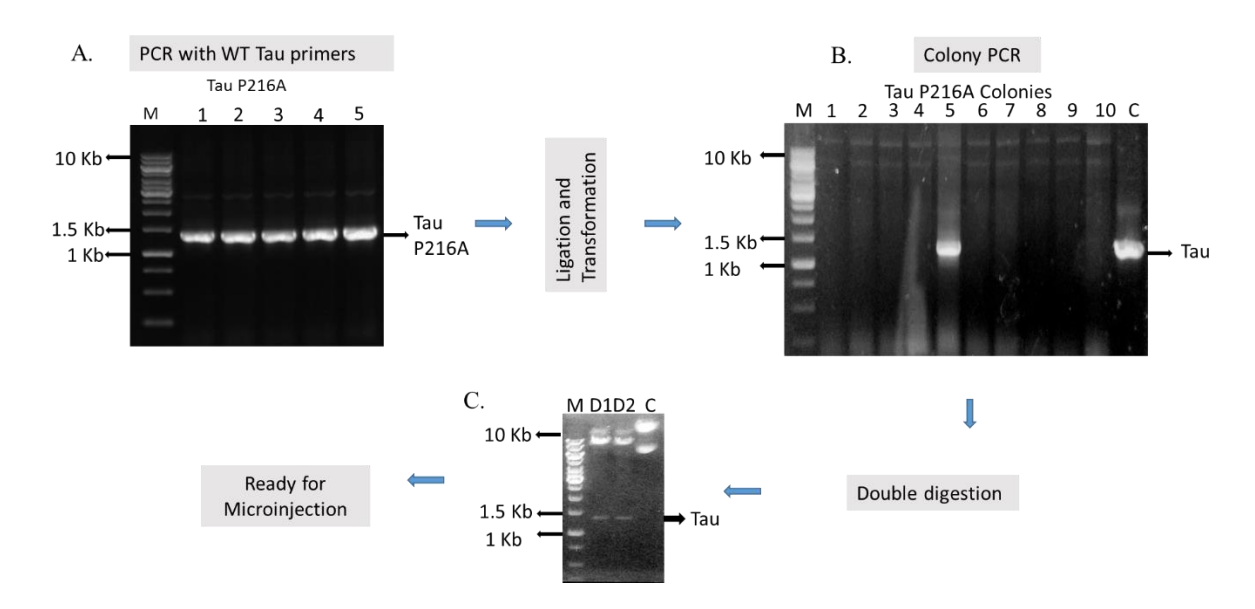


Figure 33. Subcloning of the Tau P216A into pUAST-attB vector. The plasmid containing Tau P216A in pBSK was amplified with WT Tau primers to amplify Tau P216A (A). This mutated Tau ligated into pUAST-attB vector and transformed into XL-B competent cells. Positive colonies were screened through colony PCR (B). Isolated plasmid with Tau P216A was also confirmed through double digestion (C).

3.11 Subcloning of the Tau P219A into pUAST-attB vector

Tau P219A was amplified from pBSK vector containing the mutated Tau P219A with the help of the WT Tau primers. This amplified Tau construct was digested with the EcoRI and XbaI enzymes and ligated into pUAST-attB vector digested with same pair of restriction enzymes. Ligated product was transformed into XL-B competent cells and positive colonies were screened through colony PCR. Tau P219A positive colonies were cultured and isolated plasmid was also confirmed through double digestion for the presence of the insert. After confirmation, this construct in pUAST-attB vector was used for generating the transgenic *Drosophila* lines through microinjection (figure 34).

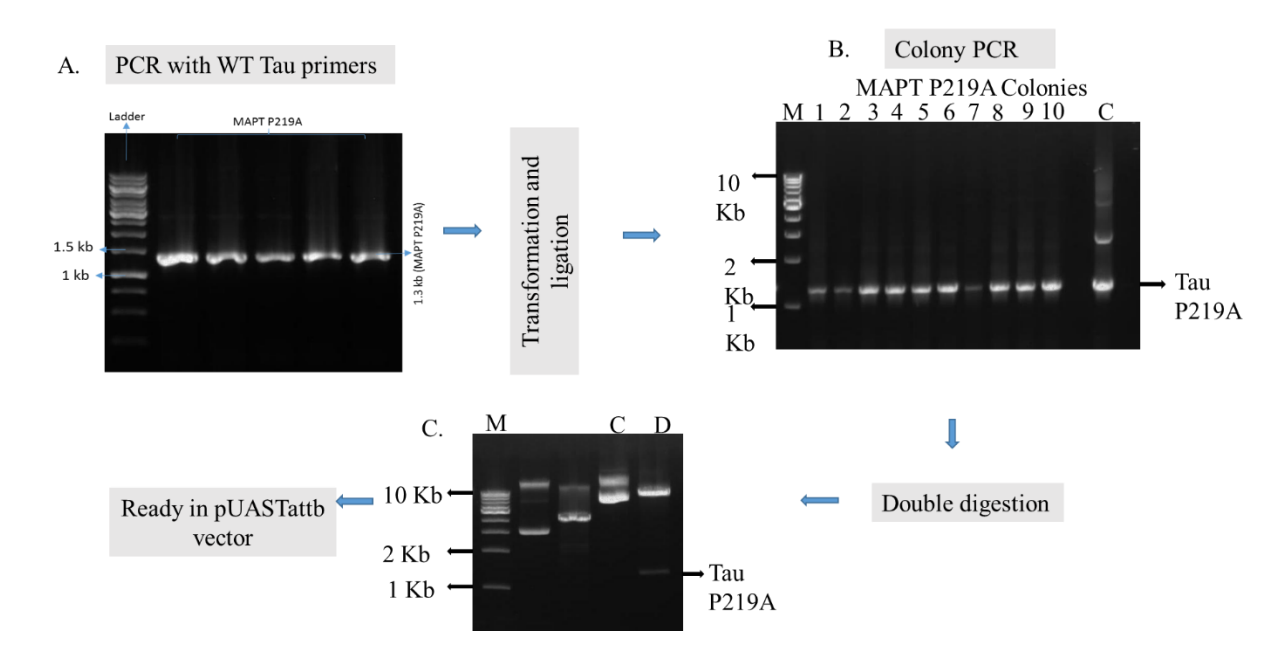


Figure 34. Subcloning of the Tau P219A into pUAST-attB vector. The plasmid containing Tau P219A in pBSK was amplified with WT Tau primers to amplify Tau P219A (A). This mutated Tau ligated into pUAST-attB vector and transformed into XL-B competent cells. Positive colonies were screened through colony PCR (B). Isolated plasmid with Tau P219A was also confirmed through double digestion (C).

3.12 Subcloning of the Tau P233A into pUAST-attB vector

Tau P233A was amplified from pBSK vector containing the mutated Tau P233A with the help of the WT Tau primers. This amplified Tau construct was digested with the EcoRI and XbaI enzymes and ligated into pUAST-attB vector digested with same pair of restriction enzymes. Ligated product was transformed into XL-B competent cells and positive colonies were screened through colony PCR. Tau P233A positive colonies were cultured and isolated plasmid was also confirmed through double digestion for the presence of the insert. After confirmation, this construct in pUAST-attB vector was used for generating the transgenic *Drosophila* lines through microinjection (figure 35).

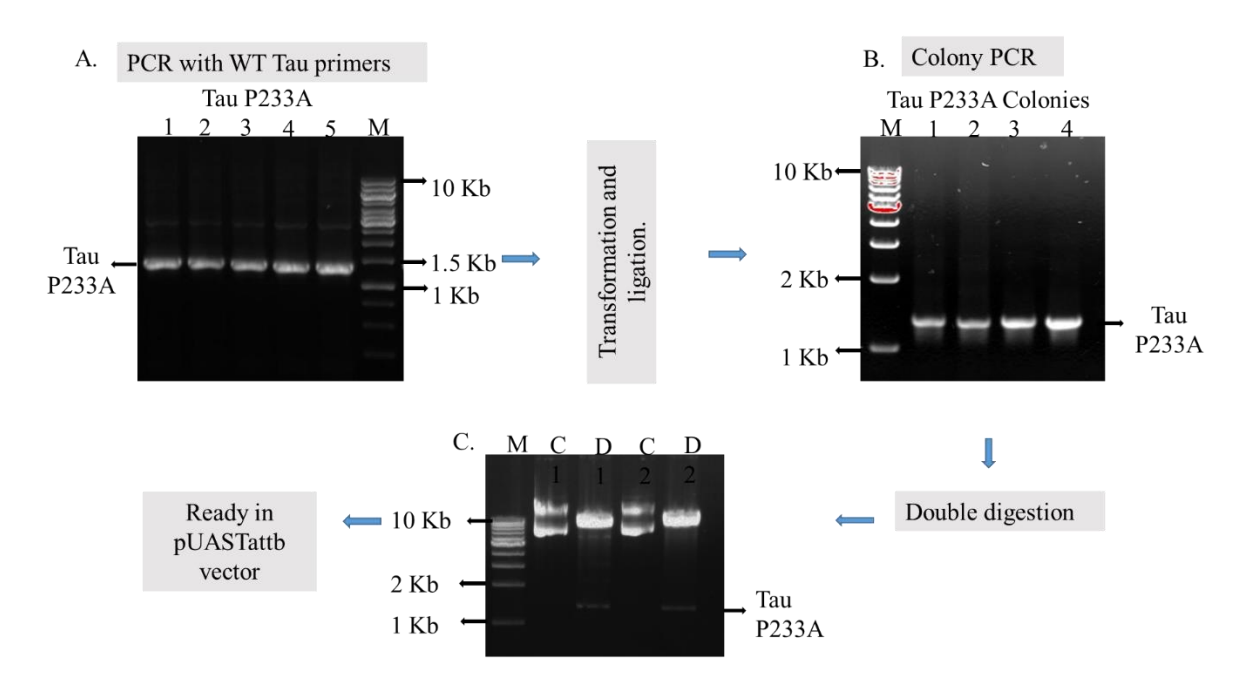


Figure 35. Subcloning of the Tau P233A into pUAST-attB vector. The plasmid containing Tau P233A in pBSK was amplified with WT Tau primers to amplify Tau P233A (A). This mutated Tau ligated into pUAST-attB vector and transformed into XL-B competent cells. Positive colonies were screened through colony PCR (B). Isolated plasmid with Tau P233A was also confirmed through double digestion (C).

3.13 Subcloning of the Tau P236A into pUAST-attB vector

Tau P236A was amplified from pBSK vector containing the mutated Tau P236A with the help of the WT Tau primers. This amplified Tau construct was digested with the EcoRI and XbaI enzymes and ligated into pUAST-attB vector digested with same pair of restriction enzymes. Ligated product was transformed into XL-B competent cells and positive colonies were screened through colony PCR. Tau P236A positive colonies were cultured and isolated plasmid was also confirmed through double digestion for the presence of the insert. After confirmation, this construct in pUAST-attB vector was used for generating the transgenic *Drosophila* lines (figure 36).

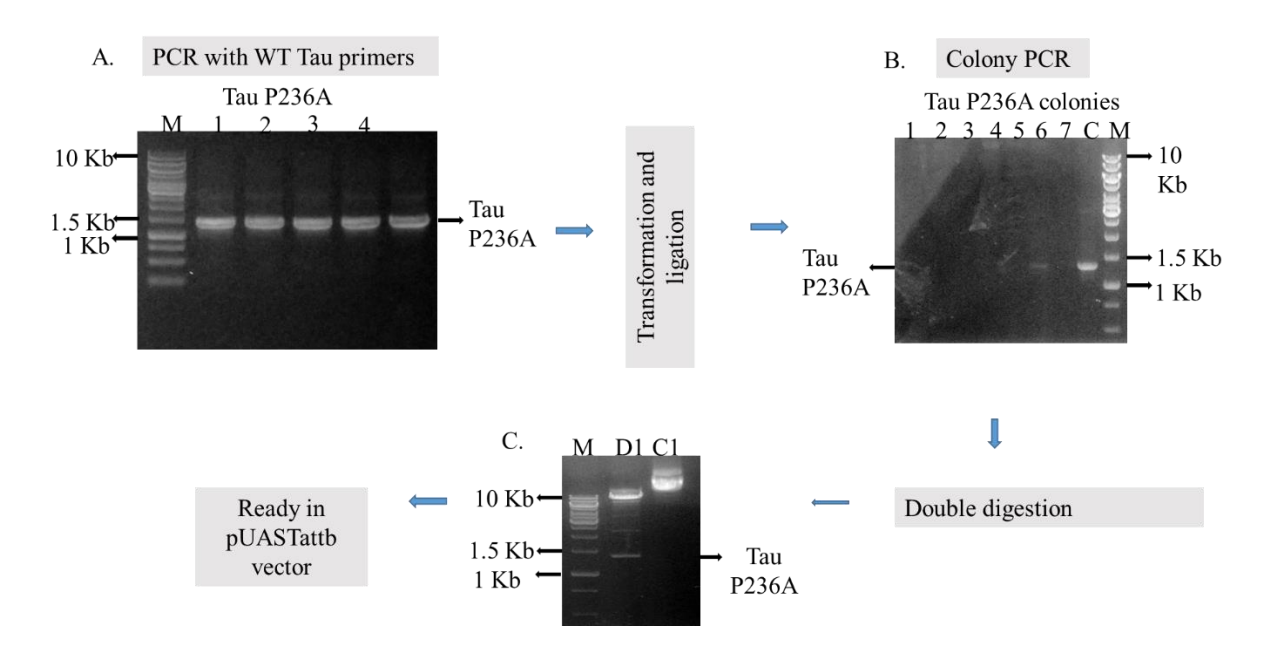


Figure 36. Subcloning of the Tau P236A into pUAST-attB vector. The plasmid containing Tau P233A in pBSK was amplified with WT Tau primers to amplify Tau P236A (A). This mutated Tau ligated into pUAST-attB vector and transformed into XL-B competent cells. Positive colonies were screened through colony PCR (B). Isolated plasmid with Tau P236A was also confirmed through double digestion (C).

3.14 Subcloning of the Tau P216A-P219A into pUAST-attB vector

Double mutants containing Tau P216A-P219A were also cloned into pUAST-attB vector through same protocol. Tau P216A-P219A was amplified from pBSK vector containing the mutated Tau P216A-P219A with the help of the WT Tau primers. This amplified Tau construct was digested with the EcoRI and XbaI enzymes and ligated into pUAST-attB vector digested with same pair of restriction enzymes. Ligated product was transformed into XL-B competent cells and positive colonies were screened through colony PCR. Tau P216A-P219A positive colonies were cultured and isolated plasmid was also confirmed through double digestion for the presence of the insert. After confirmation, this construct in pUAST-attB vector was used for generating the transgenic *Drosophila* lines (figure 37).

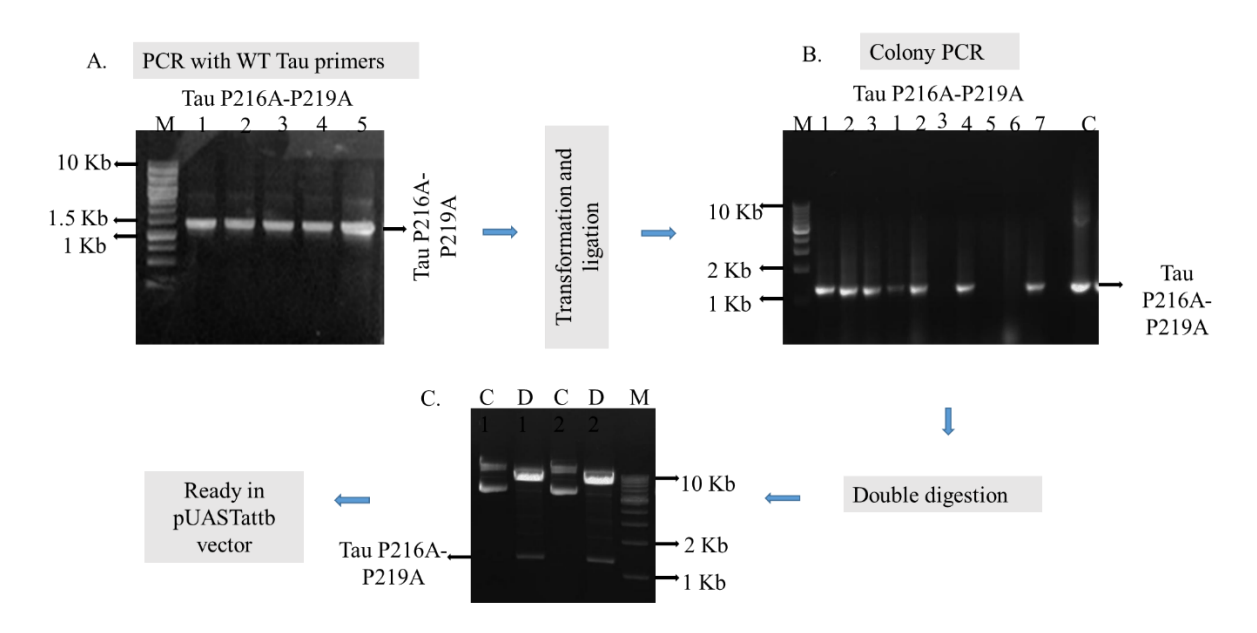


Figure 37. Subcloning of the Tau P216A-P219A into pUAST-attB vector. The plasmid containing Tau P216A-P219A in pBSK was amplified with WT Tau primers to amplify Tau P216A-P219A (A). This mutated Tau ligated into pUAST-attB vector and transformed into XL-B competent cells. Positive colonies were screened through colony PCR (B). Isolated plasmid with Tau P216A-P219A was also confirmed through double digestion (C).

3.15 Subcloning of the Tau P233A-P236A into pUAST-attB vector

Mutant containing Tau P233A-P236A was also cloned into pUAST-attB vector through same protocol. Tau P233A-P236A was amplified from pBSK vector containing the mutated Tau P233A-P236A with the help of the WT Tau primers. This amplified Tau construct was digested with the EcoRI and XbaI enzymes and ligated into pUAST-attB vector digested with same pair of restriction enzymes. Ligated product was transformed into XL-B competent cells and positive colonies were screened through colony PCR. Tau P233A-P236A positive colonies were cultured and isolated plasmid was also confirmed through double digestion for the presence of the insert. After confirmation, this construct in pUAST-attB vector was used for generating the transgenic *Drosophila* lines (figure 38).

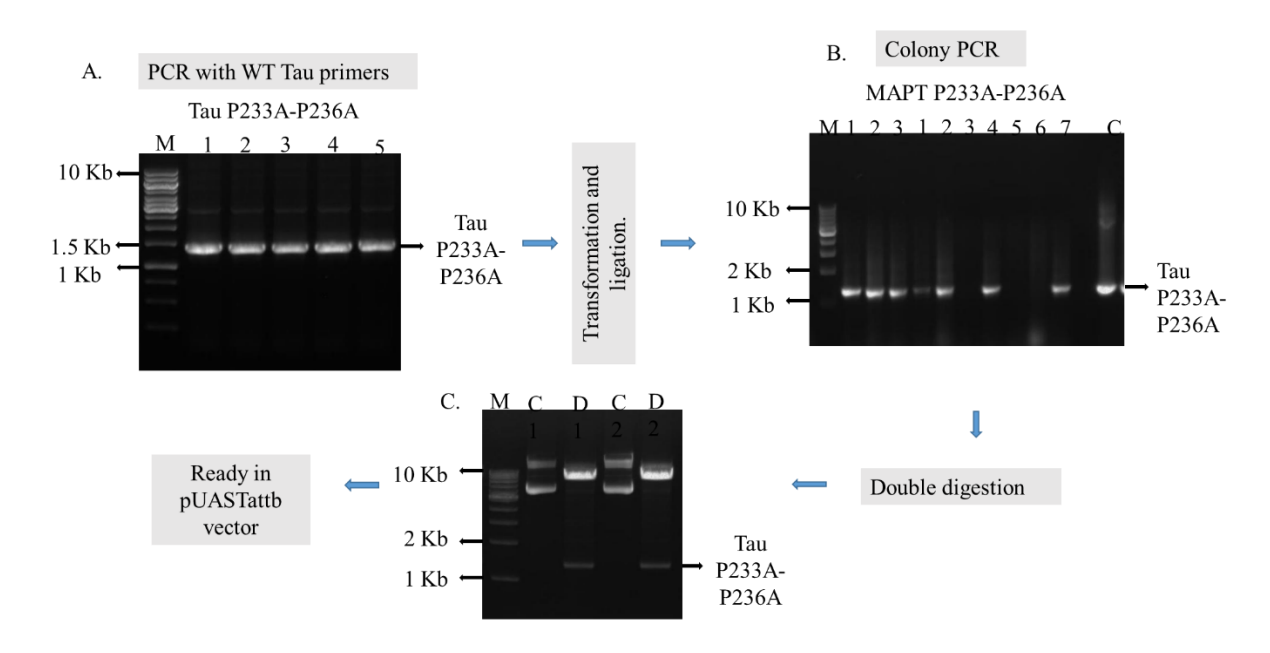


Figure 38. Subcloning of the Tau P233A-P236A into pUAST-attB vector. The plasmid containing Tau P233A-P236A in pBSK was amplified with WT Tau primers to amplify Tau P233A-P236A (A). This mutated Tau was ligated into pUAST-attB vector and transformed into XL-B competent cells. Positive colonies were screened through colony PCR (B). Isolated plasmid with Tau P233A-P236A was also confirmed through double digestion (C).

Summary of the constructs and mutants generated

Following constructs and mutants were generated in this study:

Table 2. Tau and Fyn mutants generated.

Sr. No	Construct Name	Mutation	Significance
1.	WT Tau	-	WT Tau
2.	Tau P216A	P216A	Part of the sixth PXXP motif
3.	Tau P219A	P219A	Part of the sixth PXXP motif
4.	Tau P216A-P219A	P216A-P219A	Sixth PXXP motif
5.	Tau P233A	P233A	Part of the seventh PXXP motif
6.	Tau P236A	P236A	Part of the seventh PXXP motif
7.	Tau P233A-P236A	P233A-P236A	Seventh PXXP motif
8.	Fyn	-	WT Fyn

3.16 Microinjection of the WT and mutated MAPT constructs into *Drosophila* embryos

For generating the transgenic *Drosophila* expressing human WT and mutated Tau protein, these constructs which we generated were microinjected into *Drosophila* embryos. We used Phi C31 integrase site specific integration system for inserting our construct at specific desired locus in *Drosophila* genome (Basler et al., 2007). We used Picoinjector PLI-90 from Harvard Apparatus for microinjection. Construct was diluted in injection buffer in 1:1 ratio and injected into less than 2 hours of age embryos.

Summary of the microinjections and transgenic flies we generated in this study:

Table 3. Transgenic flies generated.

S No	Construct Injected	Site of insertion	Chromosomal
	(In pUAST-attB vector)	(attP position)	Location
1.	WT Tau	86Fb	Chr 3
2.	Tau Y18F	86Fb	Chr 3
3.	Tau P216A	86Fb	Chr 3
4.	Tau P216A-P219A	86Fb	Chr 3
5.	WT Fyn	25C	Chr 2

We tried microinjections of the other remaining Tau and Fyn constructs also but they were not successful and will be done by the scholars in the lab. We moved ahead with these transgenic flies generated for this study after confirmation of the site-specific insertion.

3.17 Screening for transgenic flies after microinjections

For site specific insertions, we cloned the constructs in pUAST-attB vector. This pUAST-attB vector contains attB site for site-specific insertion, 5X UAS region for overexpression of the gene cloned and mini white gene (w) which helps in confirmation of the insertion in fly genome (Bischof et al., 2007). This pUAST-attB vector is microinjected into embryos of the attP landing site flies which have white eyes as they do not have functional white gene. Once the construct is inserted successfully at specific site after microinjection, mini white gene (in the construct) is expressed which will give red eye phenotype in the progeny. We used this red eye phenotype as a primary screening for the transgenic flies.

Microinjected embryos were kept at 18^oC in moist condition for proper healing, development and growth. Next day, hatched larvae were collected and transferred to food vials. Once the adult flies were eclosed, they were crossed with chromosome specific balancer

chromosome flies for screening. Initially the flies were screened for the reds eye colour. Redeyed flies from the cross were then molecularly confirmed for the site-specific insertion of the microinjected constructs with single fly PCR with flanking and WT Tau primers (as described in figure 15 and 16). For single-fly PCR crude extract of the red-eyed fly was prepared and PCR was done with flanking primers, WT Tau primers, attP landing site primers and rp49 control primers (figure 39). Single fly PCR confirmed the site-specific insertion of the construct.

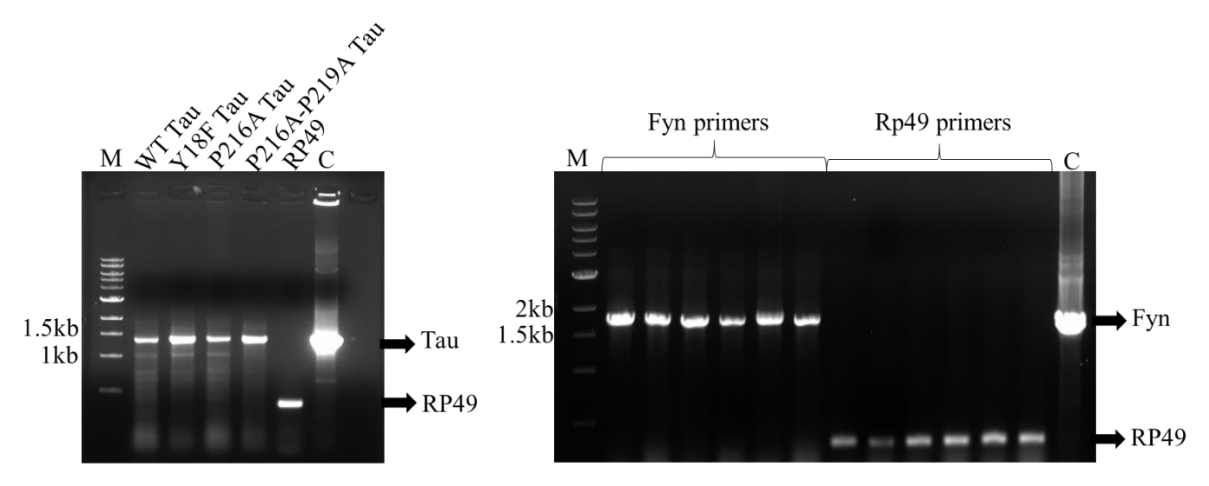


Figure 39. Single Fly PCR for Tau and Fyn transgenic flies. Single fly PCR for WT Tau and mutant Tau transgenic flies with WT Tau primers (A) and for Fyn transgenic fly with WT Fyn primers (B) confirming that Tau and Fyn transgene has been inserted in *Drosophila* genome.

We microinjected MAPT and Fyn constructs at different sites on different chromosomes to minimize the possible position effects. Once the insertion was confirmed through the SF PCR, we next confirmed the site-specific integration through SF PCR with attP site specific primers. We designed the primers such that forward primer will bind in the inserted construct whereas reverse primer will bind in the *Drosophila* genome region towards 3'end of the insertion site. Then we performed SF PCR which confirmed further that the microinjected Tau and Fyn constructs has been inserted at targeted specific sites (figure 40).

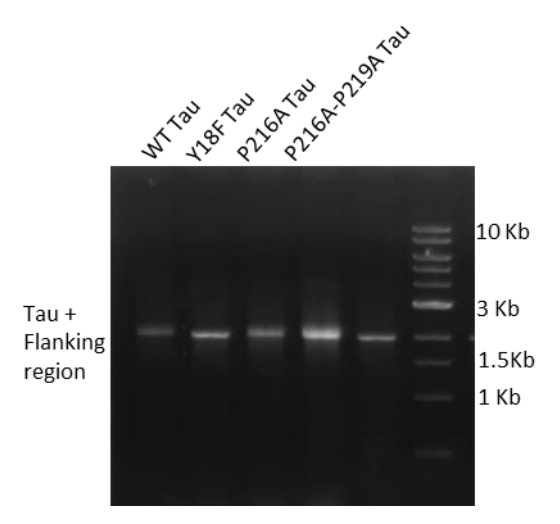


Figure 40. Single Fly PCR for site-specific integration of Tau and Fyn in generated transgenic flies. Reverse primers were designed from attP flanking region in *Drosophila* genome so that PCR amplification confirms the site-specific integration of the injected constructs.

To check the specificity of Tau primers used in the single-fly PCR to amplify transgenic human-Tau but not the endogenous drosophila Tau (dTau), we did PCR with attP landing site flies (BDSC Stock no 24749), wild type CantonS and generated WT Tau transgenic flies with attP primes and Tau primers. As expected there was no amplification in the CantonS and WT Tau transgenic flies with attP specific primers whereas attP site was amplified (figure 41) similarly there was amplification in attP landing site flies and wild type CantonS flies with Tau primers whereas Tau and Rp49 was amplified (figure 41). This confirms that the Tau primers are specific to human Tau only and does not amplify endogenous dTau.

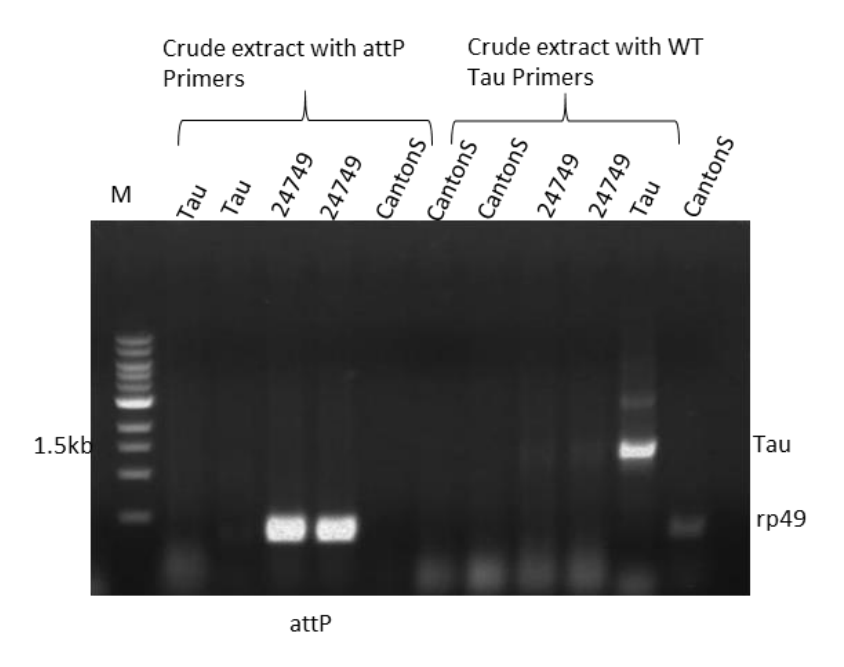


Figure 41. Tau primers are specific to transgene and does not amplify dTau. attP primers did not amplify attP in transgenic flies but amplifies attP in attP landing site flies. Also, there was no amplification in attP landing site flies and CantonS flies with Tau primers. Both of these furthers confirms our generated Tau transgenic flies.

3.18 Generation and confirmation of Tau and Fyn coexpression stocks

For expressing Tau and Fyn transgenes together in same fly we needed to generate the flies with both Tau and Fyn transgenes. For getting these flies, we crossed Tau and Fyn flies with specific second and third chromosome double balancer flies as mentioned in figure 42 and generated individual Tau and Fyn fly stock with balancer chromosomes.

First, we balanced chromosomes for both Tau and Fyn individual flies with balancer chromosomes on second and third chromosomes respectively. For generating this stock, virgin females, that are homozygous for Fyn and Tau have phenotypes like Wildtype (non-Cyo and non-Sb), are collected, and crossed with males from double-balancer, If/Cyo; MKRS/Tb stock (figure 42). Similarly, to make Fyn homozygous stock with third chromosome balancers (MKRS/Tb), Virgin females that are homozygous for Fyn and does not have any balancer, are collected, and crossed with males of double-balancer, If/Cyo; MKRS/Tb. In F1 generation we selected Tb larvae and discarded non-Tb larvae. Once the adult flies eclose from this Tb larvae we selected further for the presence of the MKRS and CyO wings with red eye (we called these flies as Fyn Stock 0). For next generation we did self-cross of this Fyn stock 0, and in the F2 generation we selected the flies with red eyes (for the presence of both alleles of Fyn) and

balancer third chromosome with MKRS and Tb (we labelled this fly stock as Fyn Stock A) (figure 42).

Similarly we made a stock with second chromosome balancer and Tau on third chromosome (Tau stock A), described for the Fyn stock. After getting both Tau and Fyn fly stocks with balancer chromosomes at third and second chromosomes respectively (Tau Stock A and Fyn Stock A), we crossed these two flies (Tau Stock A and Fyn stock A) and when we got F1 larvae, we collected Tb larvae and non-Tb larvae were discarded. After eclosion of adult flies for this Tb flies, we screened the progeny and collected CyO flies so that now this fly stock have Fyn/CyO; Tau/Tb genotype with both Tau and Fyn present in same fly. Later we also crossed these Fyn/CyO; Tau/Tb flies and collected homozygous stock for both Fyn and Tau transgene and final flies genotype is Fyn/Fyn; Tau/Tau (figure 42).

We followed same strategy and generated stocks for Fyn with WT Tau (Fyn/Fyn; Tau/Tau), Fyn with Tau Y18F (Fyn/Fyn; Tau Y18F/Tb), Tau P216A (Fyn/Fyn; Tau P216A/Tau P216A) and Tau P216A-P219A (Fyn/Fyn; Tau P216A-P219A/Tau P216A-P219A). We confirmed the Tau and Fyn transgenic stocks with the single fly PCR and western blotting.

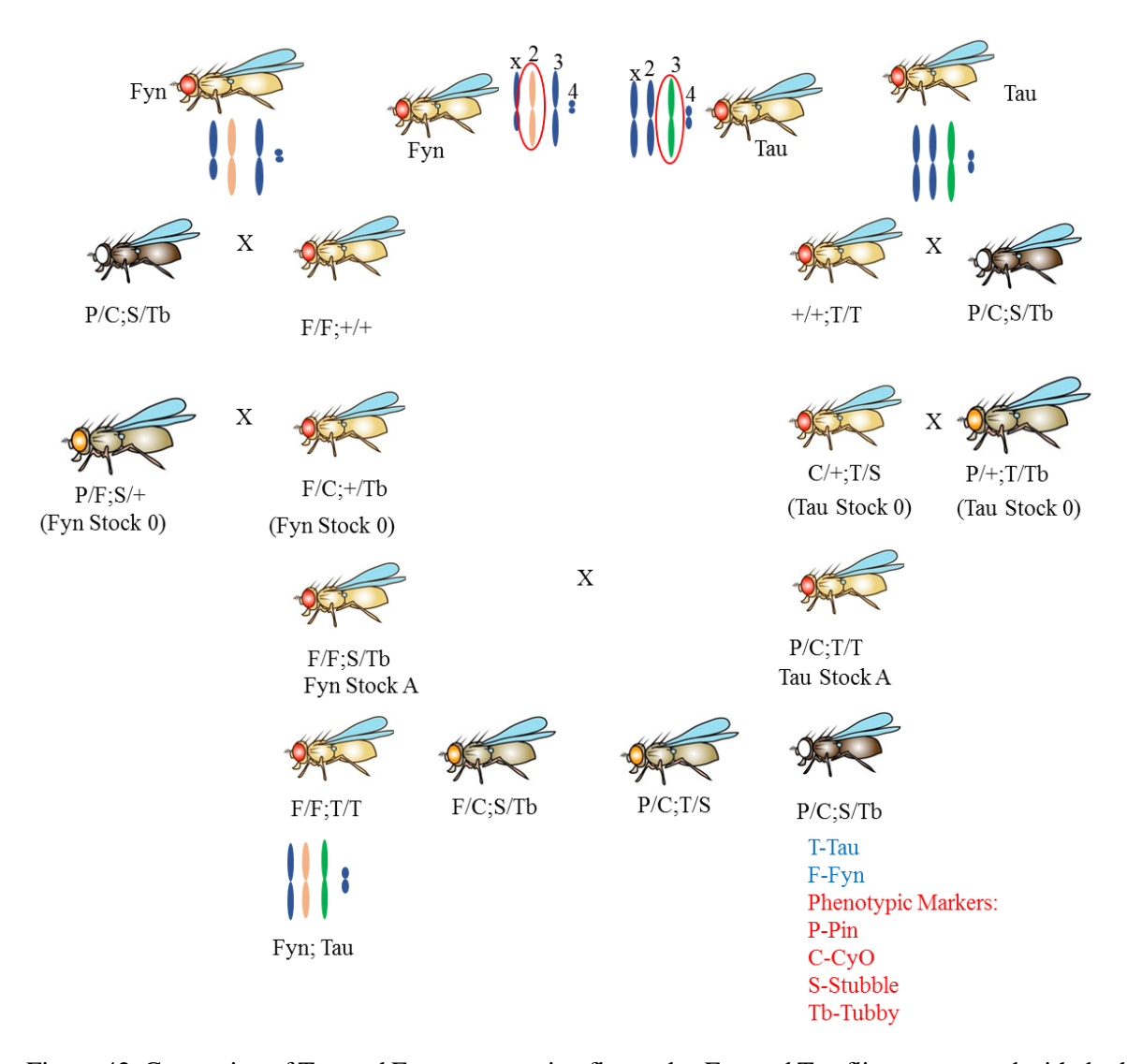
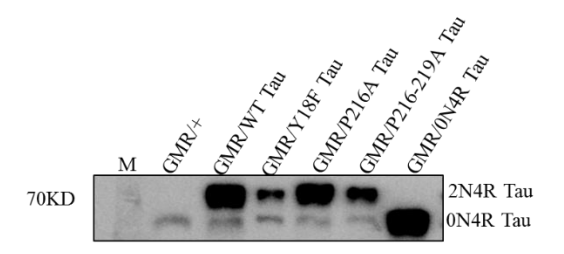
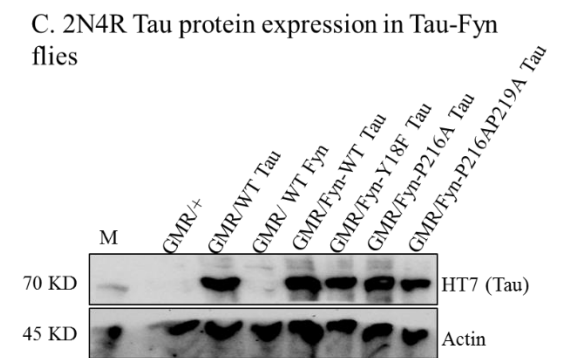


Figure 42. Generation of Tau and Fyn coexpression fly stocks. Fyn and Tau flies are crossed with double balancer flies (P-Pin, C- CyO, S-Stubble, and Tb- Tubby). In the next progeny, Fyn Stock 0 and Tau stock 0 is collected and self-crossed them to get the Fyn and Tau stock A. Followed by cross of the Fyn stock A and Tau stock A to get the final stock of Fyn/Fyn; Tau/Tau.

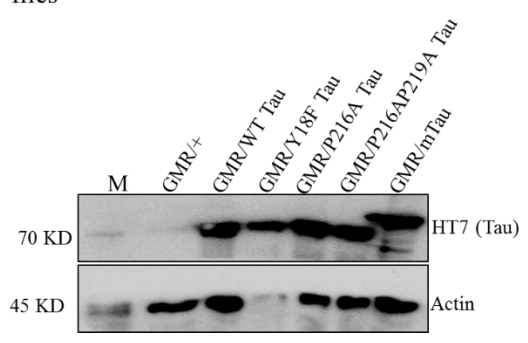
To confirm the expression of transgene in the in UAS-Tau and -Fyn transgenic flies, we performed SDS-PAGE and western blotting of the Tau and Fyn flies after crossing them to GMR-Gal4 driver. From the progeny flies, Heads were separated and crude protein extract was prepared from adult flies with RIPA buffer. Protein concentration was estimated with standard BCA protein estimation method and equal amount of protein was loaded in 10% SDS gel for separation. SDS gel was then transferred to PVDF membrane overnight at 4°C. After blocking the membrane, we probed the membrane with Tau, Fyn and actin primary antibodies. Western blotting further confirms the transgene expression in Tau and Fyn flies as both Tau and Fyn bands were present in transgenic flies only (figure 43).

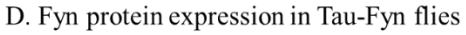
A. 2N4R Tau protein expression in transgenic flies





B. 2N4R Tau protein expression in transgenic flies





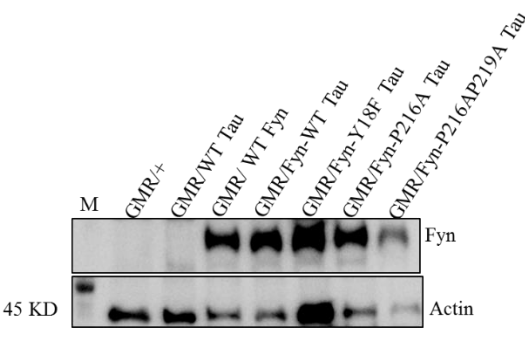


Figure 43. Western blot analysis for protein expression confirmation of generated Tau and Fyn transgenic flies. Tau bands were only present in WT and mutants of Tau flies (A and B). To confirm further whether generated flies are 2N4R Tau, we used 0N4R Tau flies as a positive control (A) and GMR/+ as a negative control. Tau and Fyn co-expressing flies western blotting also confirms the expression of both Tau and Fyn co-expression in same fly for both WT and mutants (C and D). Actin was used as loading control for all blots. Absence of Tau in Fyn flies and absence of Fyn in Tau flies also further confirms our generated transgenic flies (C and D).

Summary

We have successfully cloned 2N4R human Tau and Fyn in a cloning vector and performed site-directed mutagenesis through inverse PCR for the generation of Tau and Fyn mutants for studying the functional interaction of Tau and Fyn. Tau was mutated at Y18F, P216A, P219A, P216A-P219A, P233A, P236A, and P233A-P236A through site-directed mutagenesis. We have subcloned all the Tau and Fyn constructs (both wildtype and mutants) into fly specific pUAST-attB vector and microinjected them for getting site-specific insertions in *Drosophila* genome. Tau and its mutants microinjected at 86Fb insertion site in chromosome 3 and Fyn was microinjected at 25C insertion site in chromosome 2. We successfully generated

transgenic flies expressing WT-Tau, WT-Fyn, Tau Y18FTau, Tau P216ATau, and Tau P216A-P219ATau. Transgenic flies were then confirmed through genomic PCR and western blotting. Taken together, we have generated transgenic flies expressing Tau and its mutants, and Fyn to create a new *Drosophila* AD model expressing human Tau and Fyn transgenes, which can be used to study the functional interaction of Tau and Fyn to get new mechanistic insights into the Tau-mediated neurodegeneration.

Objective 2: Genetic analysis to understand the mechanism of Tau-Fyn mediated neurotoxicity.

After generating human WT and mutant Tau, WT Fyn, and Tau-Fyn transgenic flies we tried to investigate the synergistic effect of both Tau and Fyn coexpression on the Tau mediated toxicity in the *Drosophila* model.

3.19 WT and mutated Tau together with Fyn overexpression in *Drosophila* causes locomotor defects in aged flies

In the *Drosophila* models of neurodegeneration, defects in locomotion or climbing is a commonly observed phenotype of the several neurodegenerative diseases. As a first-hand assay, we started with analysing the effect of the Tau and Fyn coexpression on the climbing ability of *Drosophila*. We calculated the climbing index for each genotype on 1-day, 7-day, 14-day, 21-day and 28-day old flies. Climbing index is defined as the percentage of the flies crossing the 20 cm mark in 20 seconds.

We crossed UAS-Tau lines with Elav-gal4 for expressing Tau and Fyn in neurons and performed the climbing assay in cylindrical glass chamber divided into two-halves. We did not find any significant defects in the climbing ability of the flies up to 14 days with both Tau and Fyn expression (figure 44A-C). There was significant reduction in the climbing ability of the WT Tau (36.8%) flies at 21 days (figure 44D) which was further deteriorated in presence of Fyn (17.03%) (Compare WT Tau with Fyn-WT Tau, figure 44D) as compared to controls (52.75%). Tau P216A (37.75%) also reduced the climbing ability of the flies significantly (figure 44D, Tau P216A) which was further reduced in the presence of the Fyn (21.26%) (Compare Tau P216A with Fyn-Tau P216A, red circle and arrows) but presence of Fyn with Tau Y18F (30.63%) rescued the climbing defects slightly (compare Tau Y18F with Fyn-Tau Y18F, red circle and arrows). These results shows that WT Tau toxicity (36.08%) causes the age dependent decline in the climbing ability of the fly which is further deteriorated by the presence of Fyn (17.03%). Tau Y18A (30.63%) and Tau P216A (21.26%) mutants with Fyn co-expression has improved the locomotion by blocking the Fyn mediated phosphorylation or Fyn interaction to Tau (figure 44).

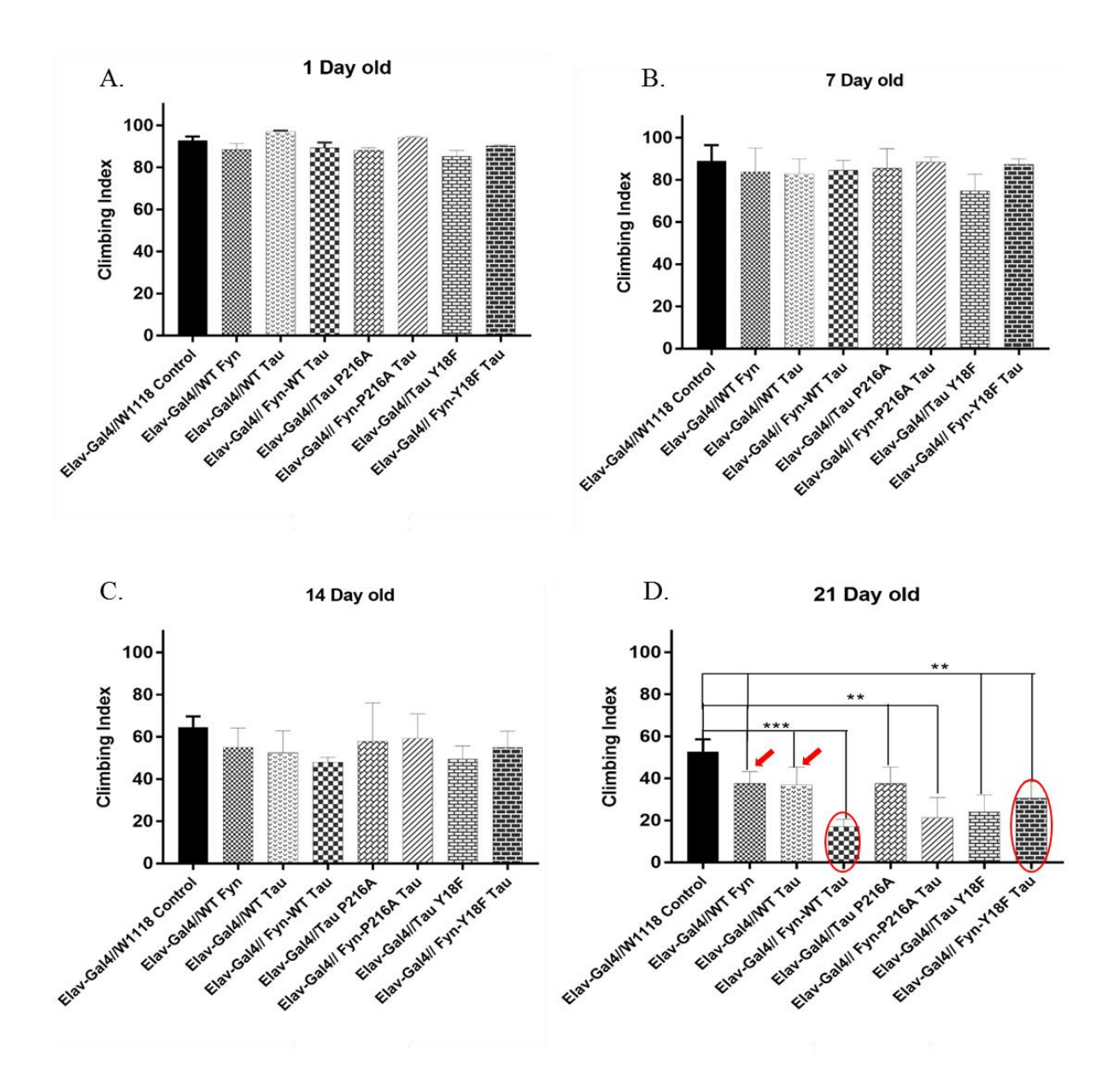


Figure 44. Tau and Fyn synergistically affect locomotion in an age-dependent manner. Age-dependent climbing Index was calculated for the flies expressing WT Tau, Tau P216A and Tau Y18F with Fyn coexpression. A. Climbing index of the 1-Day old flies. There was no significant difference observed in climbing index of WT-Tau, TauP216A and TauY18F Tau with Fyn coexpressing flies. B. Climbing index of the 7-day old flies. There was no significant difference observed in climbing index of WT Tau, Tau P216A and Tau Y18F with Fyn coexpressing flies. C. Climbing index of the 14-day old flies. There was no significant difference observed in climbing index of WT Tau, Tau P216A and Tau Y18F with Fyn coexpressing flies. D. Climbing index of the 21 days old flies. There was significant decrease in climbing index of WT Tau, Tau P216A and Tau Y18F with Fyn coexpressing flies. Fyn expression further deteriorated the climbing ability of the flies in both WT and P216A as well as Tau Y18F flies as compared to the age matched controls (compare red circles and red arrows). One-way ANOVA was

performed for calculating the p-value and significance. Data was analysed with Graph pad prism 8. N=3, n=20.

3.20 WT and mutated Tau and Fyn overexpression in *Drosophila* causes fused and disrupted ommatidia

Tau toxicity disrupts the ommatidia arrangement and leads to the degenerated eyes. To check the effect of the Fyn expression on the Tau toxicity we expressed Tau and Fyn in Drosophila eyes with GMR gal4. Nail print imprints can be used to study the outer surface of the fly eyes(Arya and Lakhotia, 2006). We performed age-dependent nail paint imprinting for analysing the ommatidia arrangement and eye surface morphology. Fyn expression increased the Tau toxicity in WT Tau (figure 45A2), as well as mutant Tau P216A (figure 45A4) and Tau Y18F (figure 45A6) flies. The regular array arrangement of ommatidia was disrupted in young age flies (1-day old) as well as old flies (30 days old). GMR-Gal4/+ and GMR/Fyn was used as a control. The severity of the toxicity was increased as the age progressed. The toxicity was result of the synergistic effect of the Tau and Fyn as there was very less or no disruption of the ommatidia in the WT Fyn (figure B2, C2 and D2), WT Tau (figure 45A2), Tau P216A (figure 45A4) and Tau Y18F (figure 45A6) flies without Fyn whereas the Tau and Fyn coexpression increased the Tau toxicity as in WT Tau-Fyn (compare figure 45A2 with figure 45A3), Tau P216A-Fyn (compare figure 45A4 with figure 45A5) and Tau Y18F-Fyn (compare figure 45A6 with figure 45A7). Overexpression of only Fyn did not cause any disruption of the ommatidia arrangement, whereas presence of Fyn along Tau with caused disruption of the ommatidia arrangement. We analysed the degeneration of the ommatidia in an age-dependent manner of 1-, 10-, 20- and 30-days old flies and found the consistent disruption of the ommatidia arrangement at all age points (figure 45A, 45B, 45C, 45D). These results shows that presence of Fyn exacerbates the Tau toxicity. Effect of the Tau and Fyn co-expression is rescued partially with Y18 and P216 mutants which blocks the Fyn-mediated phosphorylation or Fyn binding to Tau (figure 45).

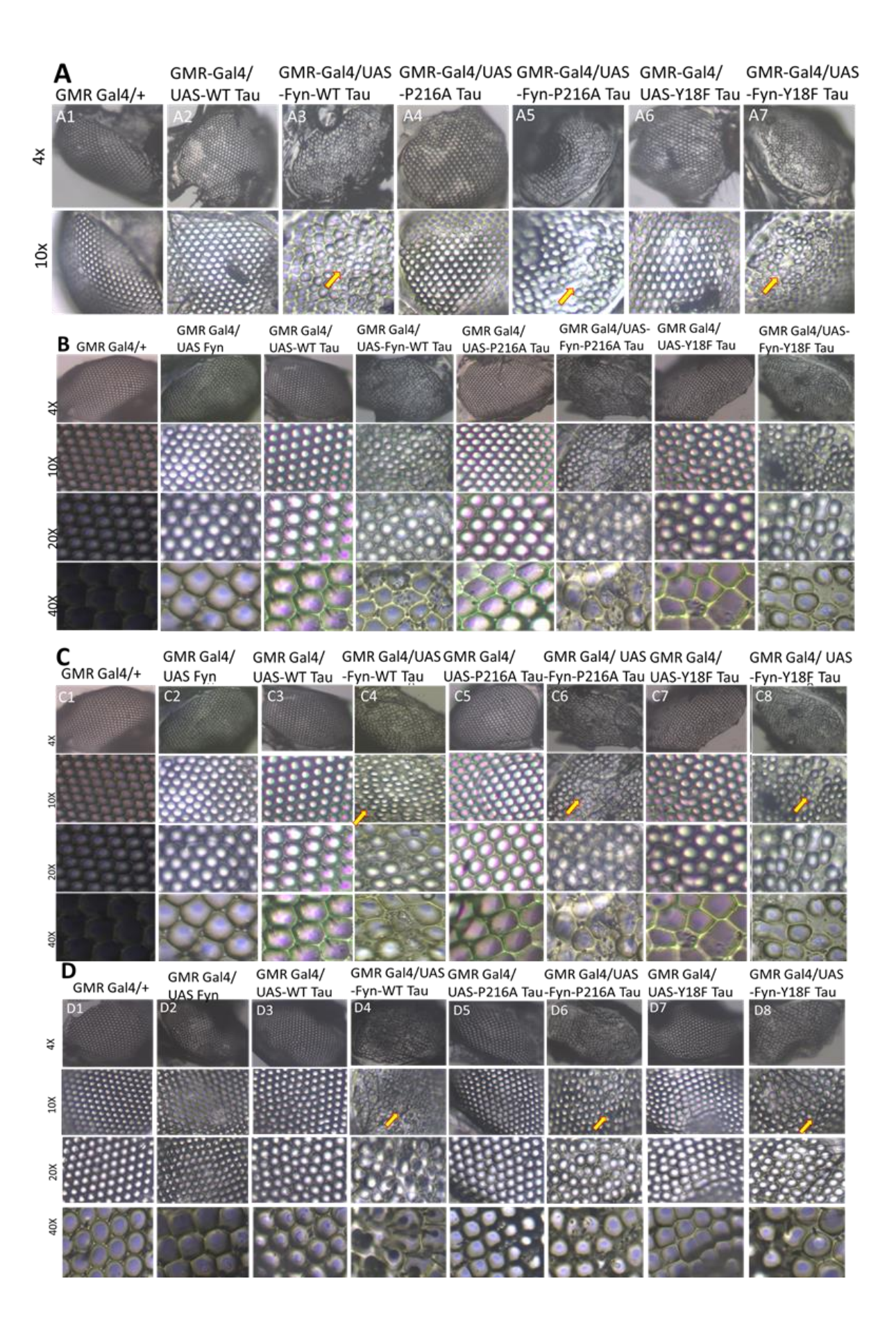
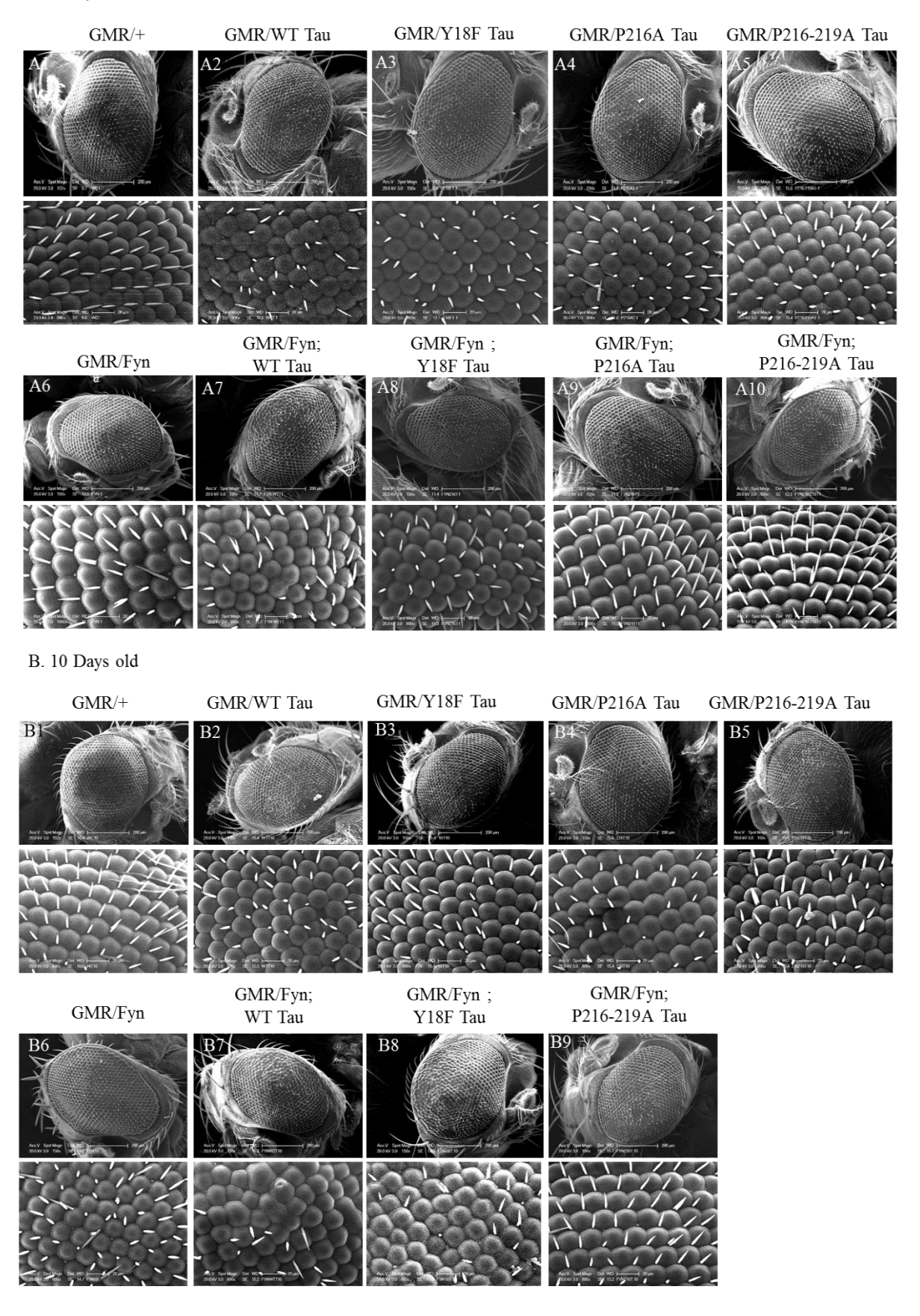


Figure 45. WT and mutated Tau and Fyn overexpression in Drosophila causes fused and disrupted ommatidia. A. Eye nail paint imprints of 1-day old flies expressing WT-Tau (A2), Tau P216A (A4) and Tau Y18F (A6) alone with Fyn coexpression (A3, A5 and A7 respectively). Above panel shows the images at 4X zoom and bottom panel shows same eye at 10X zoom. Yellow arrows indicates the zoomed area with degenerated eye ommatidia. B. Eye nail paint imprints of 10 days old flies expressing WT Tau (B3), Tau P216A (B5) and Tau Y18F (B7) alone with Fyn coexpression (B3, B6 and B7 respectively). Above panel shows the images at 4X zoom and bottom panels shows same eye at 10X, 20X and 40X zoom as indicated. C. Eye nail paint imprints of 20 days old flies expressing WT-Tau (C3), Tau P216A (C5) and Tau Y18F (C7) alone with Fyn coexpression (C4, C6 and C8 respectively). Above panel shows the images at 4X zoom and bottom panels show same eye at 10X, 20X and 40X as indicated. Yellow arrows indicates the zoomed area with degenerated eye ommatidia. D. Eye nail paint imprints of 30 days old flies expressing WT Tau (D3), Tau P216A (D5) and Tau Y18F (D7) alone with Fyn coexpression (D4, D6 and D8 respectively). Above panel shows the images at 4X zoom and bottom panels show same eye at 10X, 20X and 40X as indicated. Yellow arrows indicates the zoomed area with degenerated eye ommatidia. All images were taken with Olympus microscope and Infinity1 camera.

3.21 Tau overexpression in *Drosophila* causes rough eye and the loss of Inter Ommatidial Bristles

We found that overexpression of WT Tau causes the fusion and disruption of ommatidial arrangement. To confirm the Tau-mediated toxicity further and analysing the surface morphology of *Drosophila* eyes in our AD model, we have performed SEM. We crossed the Tau and Fyn flies with GMR-Gal4 driver and collected the progenies. Following this we performed SEM on 1-day and 10-day old flies, and counted the number IOBs (Inter ommatidial bristles). 1-day old flies expressing WT Tau (67.45%) show a decline in percentage of IOB, however it is increased in flies expressing mutant versions of Tau with mutations in the 6th PXXP motif (P216A (72.15%) and P216A-P219A (75.92%)) required for binding Fyn, and at Fyn phosphorylation site (Y18F (72.99%)). Flies co-expressing Fyn and Tau, Fyn; WT Tau (58.34%) and Fyn; Tau Y18F (51.54%) show higher decline in percentage of IoBs, but it is again rescued in flies lacking the Fyn interacting sites (Fyn; Tau P216A (70.42%) and Fyn; Tau P216A-P219A (76.25%)). We found that the flies expressing WT Tau (67.45%) and Fyn: WT Tau (58.34%) have very low percentage of IOBs compared to other genotypes. We also found that coexpression of Fyn with Tau Y18F (Fyn; Tau Y18F (51.54%)) have very low percentage of IOBs as comparable with WT Tau (67.45%) and Fyn; WT Tau (58.34%), which suggests that degeneration of bristles may be a result of Tau-Fyn interaction. These results suggest that Tau-Fyn physical interaction itself could result in the Tau toxicity even if Tau can't be phosphorylated at the Fyn target site. A similar trend is observed in 10-day old flies, the flies expressing WT Tau (53.76%) and Tau Y18F (49.73%) show intense rough eye phenotype with loss of bristles, ommatidial fusion, and misalignment of ommatidia as compared to the control flies (94.25%). However flies expressing Tau P216A (59.25%) and Tau P216A-P219A (60.78%) shows rescue from rough eye phenotype with increased percentage of IOBs compared to the flies expressing WT Tau (53.76%) and Tau Y18F (49.73%). In Fyn and Tau coexpression flies, Fyn; WT Tau (51.07%) and Fyn; Tau Y18F (42.09%) show more loss of bristles, however flies expressing Fyn; Tau P216A (62.21%) improved the percentage of ommatidia with IOBs (Percentages of ommatidia with IOBs were increased but shown statistically non-significant). Taking together, these results suggest that mutation in the Fyn interaction site (Tau P216A and Tau P216-P219A) rescues the photoreceptor neurons from Tau toxicity (figure 46).

A. 1 Day old



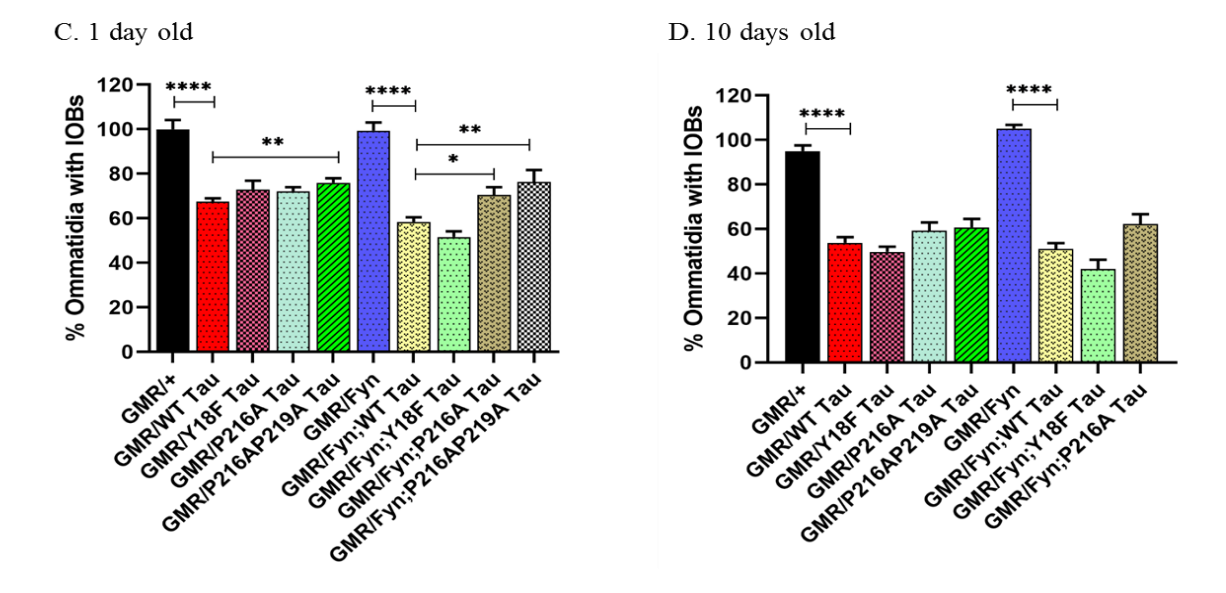


Figure 46. WT Tau overexpression in *Drosophila* causes rough eye and loss of Inter Ommatidial Bristles. A. Scanning electron micrographs of 1-day old flies expressing Tau and Fyn flies, lower panel shows the zoomed images of the top panel. A1-A5 SEM images of Tau and its mutants of 1 day old flies, A6-A10 are SEM images of Tau-Fyn flies as mentioned on top of image. B. SEM images of 10 days old flies of Tau expressing flies (B1-B5) and Tau-Fyn expressing flies (B6-B9), genotype is mentioned on top of each image. C. Quantification of percentage of ommatidia with IOBs of 1 day old flies. D. Quantification of percentage of ommatidia with IOBs of 10 days old flies. n=12-15 flies per genotype.

3.22 WT Tau mediated depletion in retinal neuron function is improved by reducing Fyn and Tau interaction (Tau P216A and Tau P216AP219A)

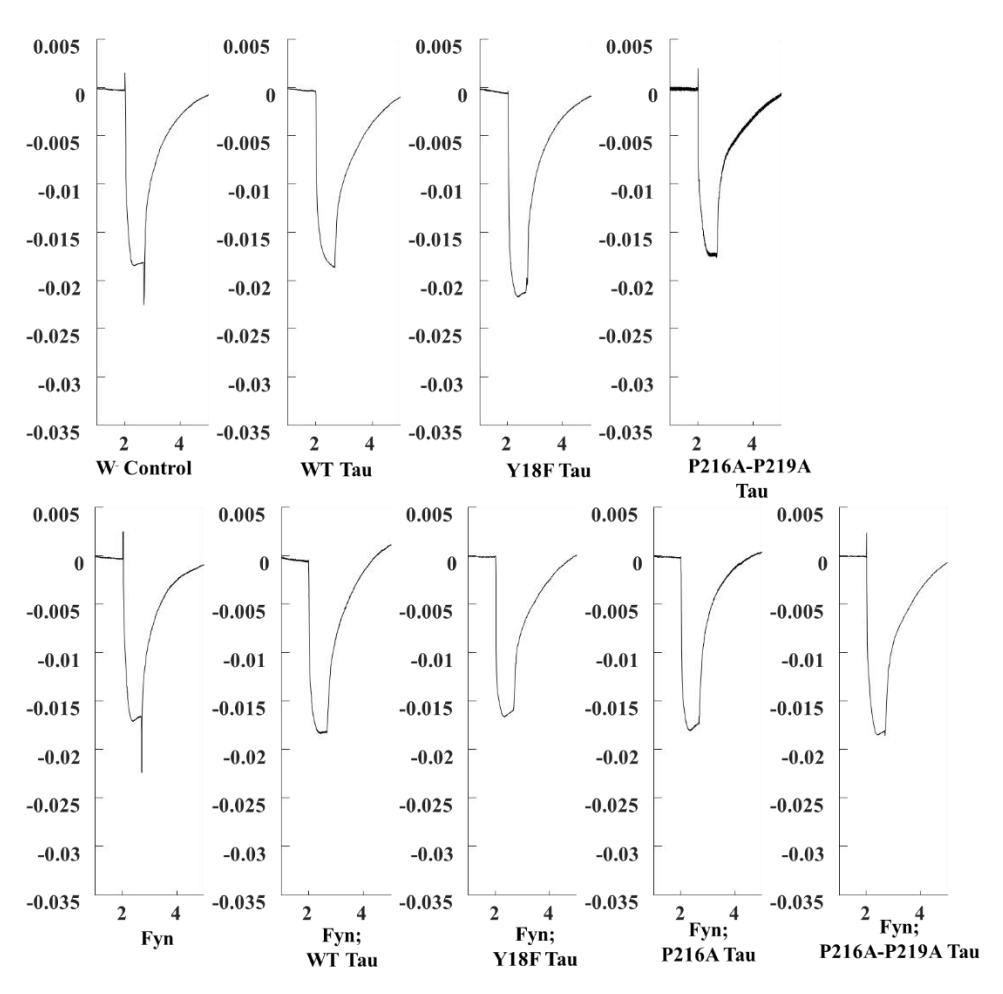
We found that Tau and Fyn coexpression leads to the disorganized and irregular array of arrangement of ommatidia in the adult flies. This disorganisation of the array of the ommatidia and loss of rhabdomeres may have functional loss of the retinal neurons of the flies expressing both Tau and Fyn, this functional loss of the retina can be monitored by the ERG (Belusic, 2011). *Drosophila* ERG has been an excellent model for studying the protein modifications and genetic interactions (Belusic, 2011). We checked the ERG for analysing the synergistic effect of the Tau and Fyn on the retinal neuron function as they are easily accessible. The ERG waveform consists of a sustained receptor potential, light-on and light-off transients. The receptor potential represents the depolarization in the photoreceptor cells(Alawi and Pak, 1971; Heisenberg, 1971). We evaluated the receptor potentials, lights-on and -off transients of the Tau and Fyn expressing adult flies in age dependent manner of 1-day, 10-day, 20-day and 30-day old flies.

We found that overexpression of WT Tau declined receptor potential significantly when compared with control flies respectively in 10-day (Controls 0.028V and WT Tau 0.012V), 20day (Controls 0.026V and WT Tau 0.015V) and 30-day old flies (Controls 0.020V and WT Tau 0.010V) (figure 47, comparison of transform of receptor potential graphs and black line (control) and red line (WT Tau)). Y18F Tau and Tau P216AP219A increased the receptor potential when compared with WT Tau flies at their respective age of 10-day (Tau Y18F 0.022V and Tau P216AP219A 0.019V vs WT Tau 0.012V), 20-day (Tau Y18F 0.015V and Tau P216AP219A 0.010V vs WT Tau 0.015V) and 30-day (Tau Y18F 0.011V and Tau P216AP219A 0.014V vs WT Tau 0.010V). Coexpression of Fyn and Tau also declined the receptor potential of the Fyn; WT Tau flies when compared with control flies or only Fyn flies in 10-day (Fyn; WT Tau 0.015V vs controls 0.027V and Fyn 0.015V), 20-day (Fyn; WT Tau 0.008V vs controls 0.026V and Fyn 0.015V) and 30-day old flies (Fyn; WT Tau 0.009V vs controls 0.020V and Fyn 0.013V). Similarly, Fyn; Y18F Tau and Fyn; Tau P216AP219A improved the receptor potential when compared with Fyn; WT Tau flies at their respective age of 10-day (Fyn; Tau Y18F 0.016V, Fyn; Tau P216A 0.018V and Fyn; Tau P216AP219A 0.013V vs Fyn; WT Tau 0.015V), 20-day (Fyn; Tau Y18F 0.011V, Tau P216A 0.016V and Fyn; Tau P216AP219A 0.008V vs Fyn; WT Tau 0.008V) and 30-day (Fyn; Tau Y18F 0.016V, Tau P216A 0.018V and Fyn; Tau P216AP219A 0.009V vs Fyn; WT Tau 0.009V). These results states that the decline in the receptor potential caused by overexpression of WT Tau and Fyn; WT Tau was improved by reducing the Tau and Fyn interaction through P216A mutation and through inhibiting the Y18 phosphorylation of Tau (figure 47, receptor potential graphs and traces).

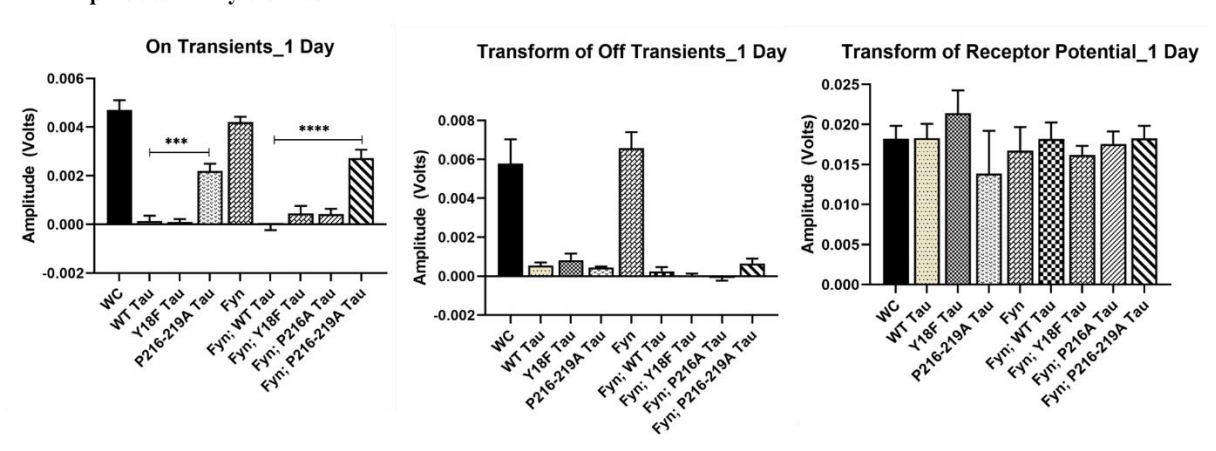
Further we also calculated the on transient and off transients. We did not observed any significant changes in the off transients in WT Tau and mutants its mutants, but we found that overexpression of WT Tau declined on transients significantly when compared with control flies respectively in 1-day (Controls 0.0047V and WT Tau 0.0001V), 10-day (Controls 0.01V and WT Tau 0.00001V), 20-day (Controls 0.007V and WT Tau 0.0009V) and 30-day old flies (Controls 0.0075V and WT Tau 0.0005V). Y18F Tau and Tau P216AP219A increased the on transients when compared with WT Tau flies at their respective age of in 1-day (Tau Y18F 0.0002V and Tau P216AP219A 0.002V vs WT Tau 0.0002V), 10-day (Tau Y18F 0.0007V and Tau P216AP219A 0.002V vs WT Tau 0.0001V), 20-day (Tau Y18F 0.001V and Tau P216AP219A 0.001V vs WT Tau 0.0009V) and 30-day (Tau Y18F 0.001V and Tau P216AP219A 0.003V vs WT Tau 0.0005V). Similarly, Fyn; Y18F Tau and Fyn; Tau P216AP219A improved the on transients when compared with Fyn; WT Tau flies at their respective age of 1-day (Fyn; Tau Y18F 0.0004V, Fyn; Tau P216A 0.0004V and Fyn; Tau P216AP219A 0.002V vs Fyn; WT Tau -0.0002V), 10-day (Fyn; Tau Y18F 0.005V, Fyn; Tau P216A 0.004V and Fyn; Tau P216AP219A 0.004V vs Fyn; WT Tau 0.002V), 20-day old on transients were non-significant (Fyn; Tau Y18F 0.005V, Tau P216A 0.005V and Fyn; Tau P216AP219A 0.001V vs Fyn; WT Tau 0.09V) and 30-day (Fyn; Tau Y18F 0.0032V, Tau P216A 0.0028V and Fyn; Tau P216AP219A 0.002V vs Fyn; WT Tau 0.002V). These results also suggests that the loss in the on transients caused by overexpression of WT Tau and Fyn; WT Tau was improved by reducing the Tau and Fyn interaction through P216A mutation and through inhibiting the Y18 phosphorylation of Tau (figure 47, on transients graphs and traces).

Comparison of ERG traces of 1-day old (black traces in fig47 E1), 10-day old (red traces in fig47 E1), 20-day old (green traces in fig47 E1) and 30-day old flies (blue traces in fig47 E1 show that there was decline in receptor potential in WT Tau and Fyn-WT Tau overexpression flies (traces became smaller as the flies aged) and this receptor potential was increased in Tau Y18F, P216A-P219ATau and Fyn-Tau P216ATau flies (red, green and blue traces are bigger that black traces). In consistent with the observations of IoB phenotypes in the SEM and the results of eye-nail-paint imprint assay, these results also further suggest that inhibiting the Tau and Fyn interaction reduces the Tau mediated toxicity in *Drosophila* model (figure 47).

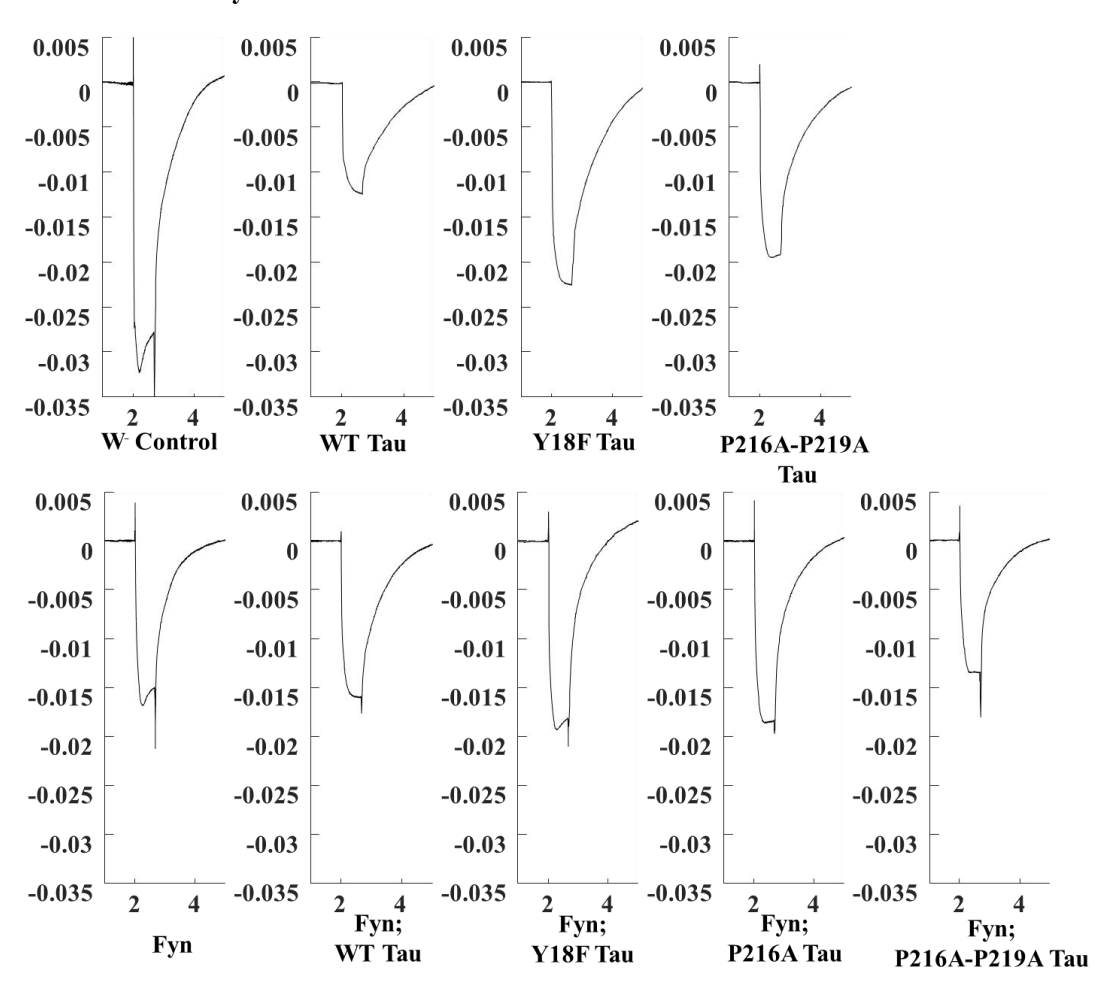
A1. Traces: 1 Day old flies



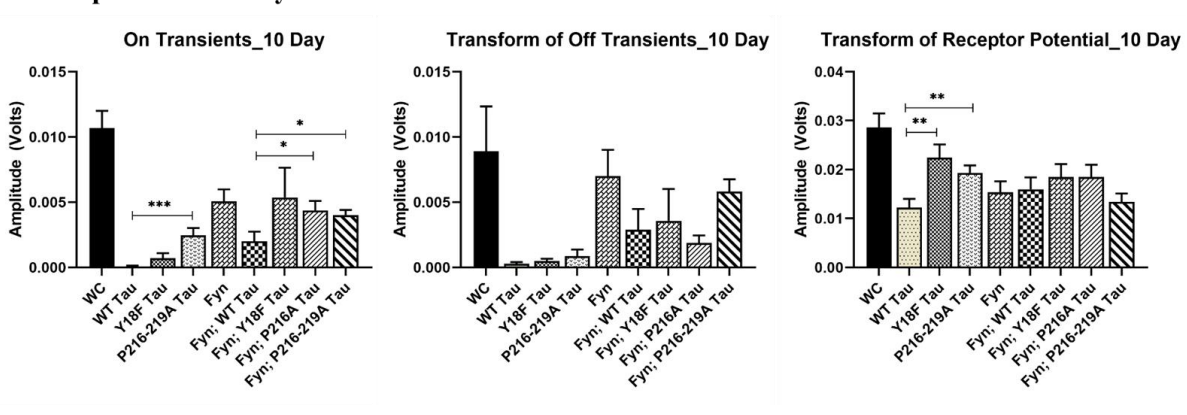
A2. Amplitudes: 1 Day old flies



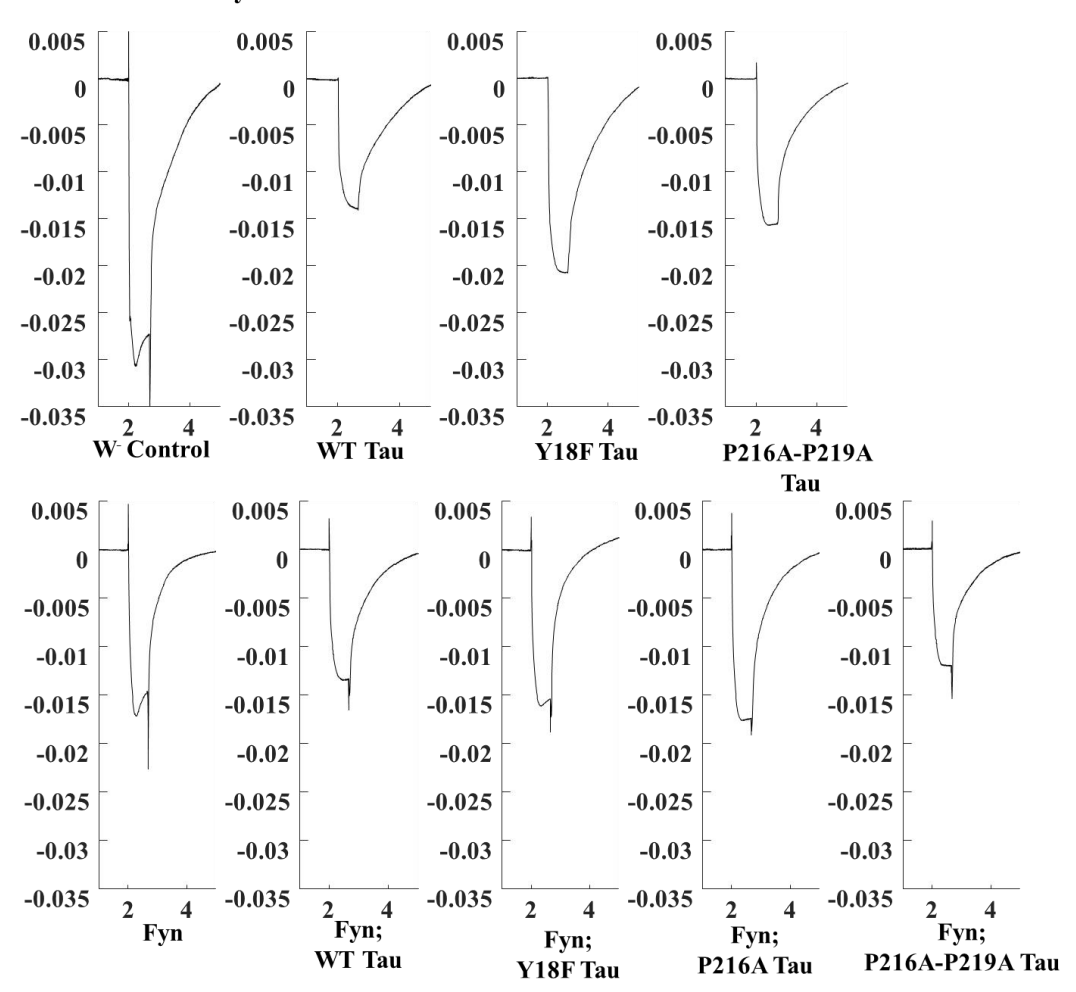
B1. Traces: 10 Days old flies



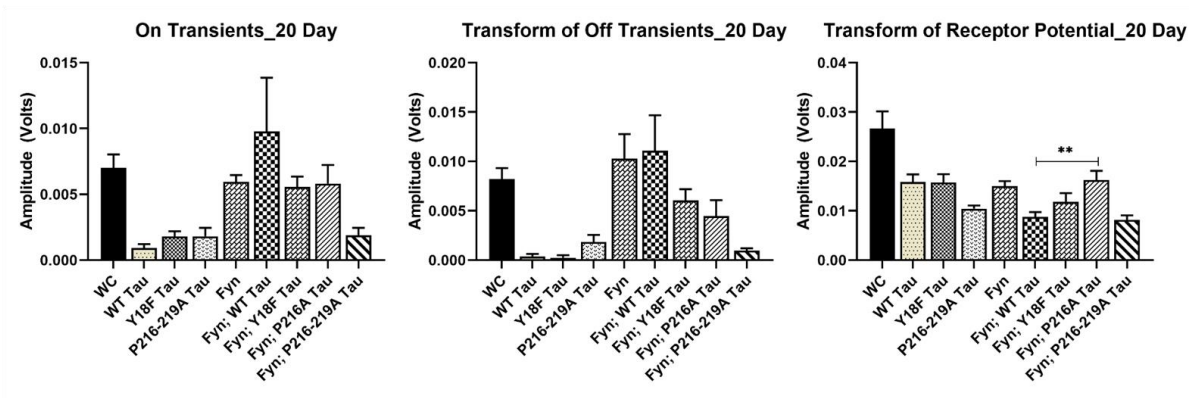
B2. Amplitudes: 10 Day old flies



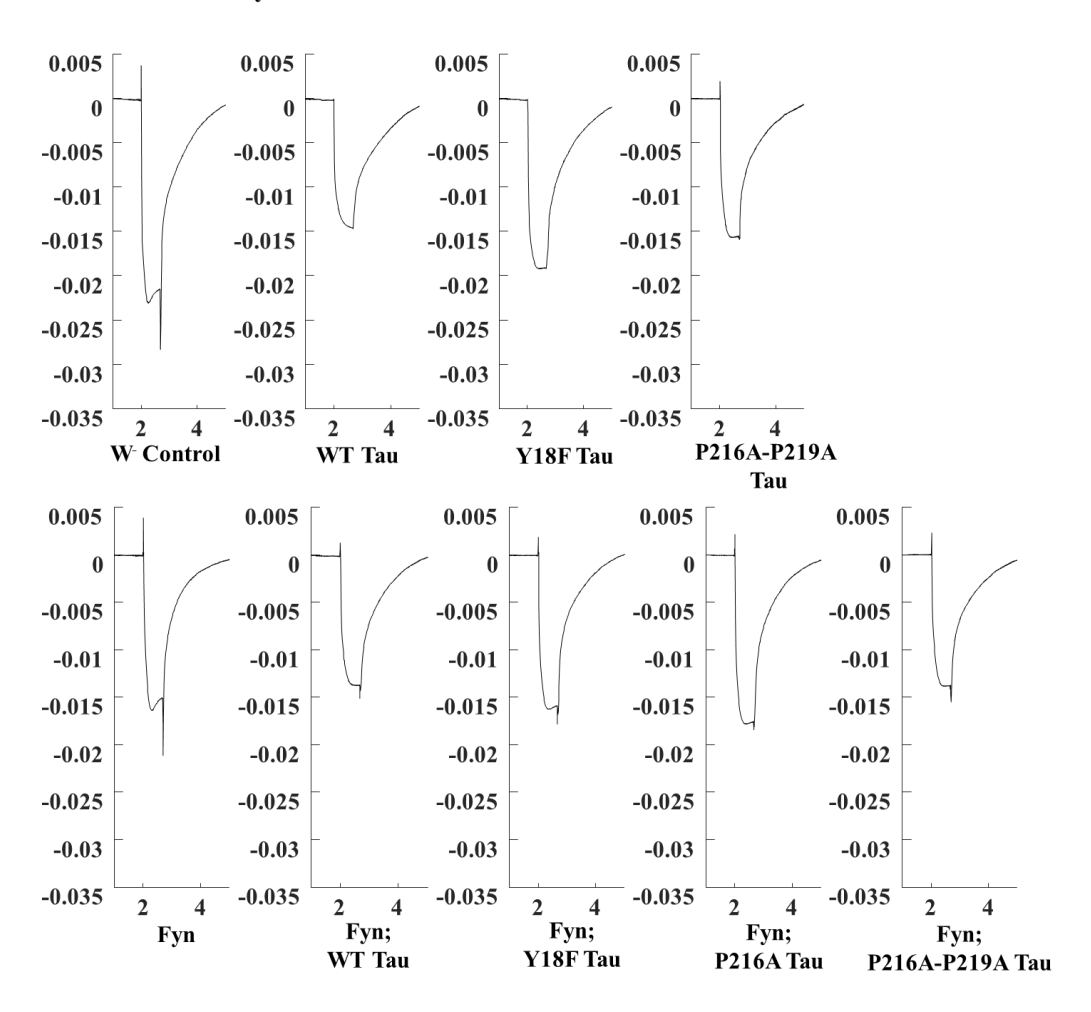
C1. Traces: 20 Days old flies



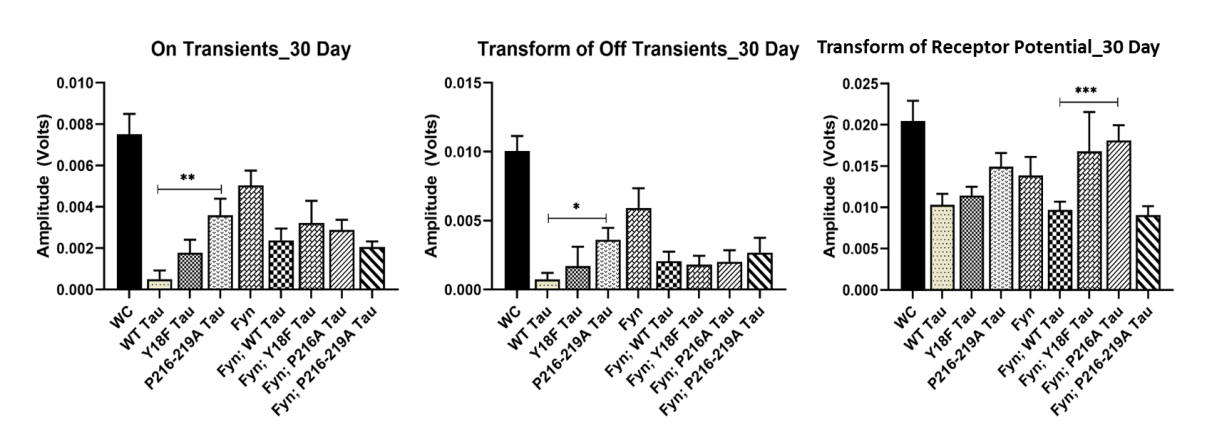
C2. Amplitudes: 20 Day old flies



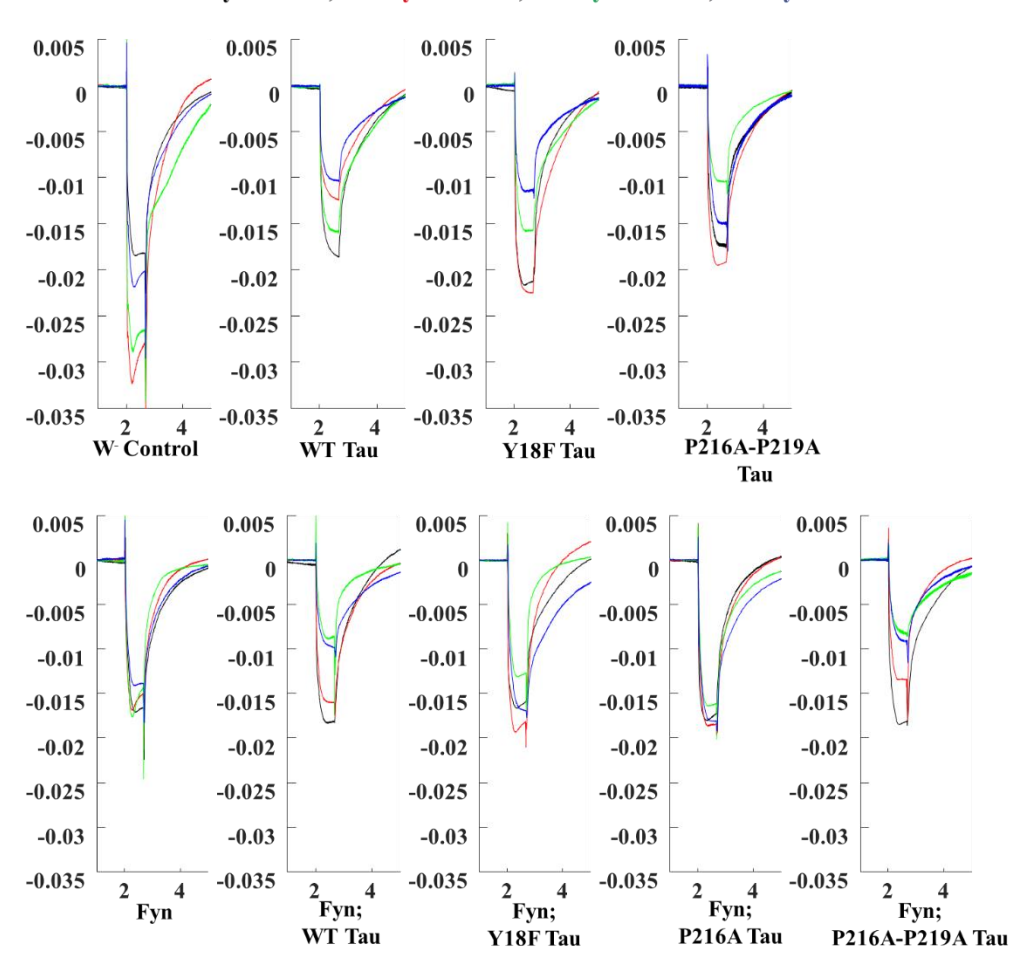
D1. Traces: 30 Days old flies



D2. Amplitudes: 30 Day old flies



E1.. Traces: 1 Day old flies, 10 Days old flies, 20 Days old flies, 30 Days old flies



E2. Amplitudes: 30 Day old flies

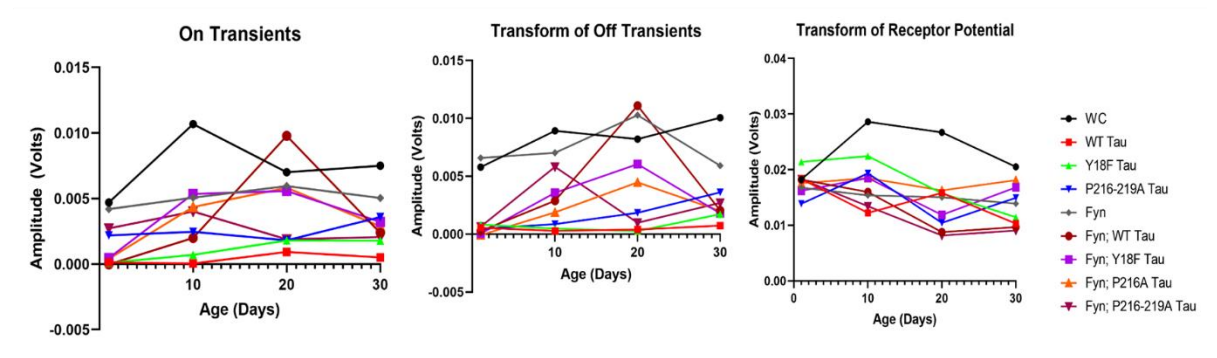


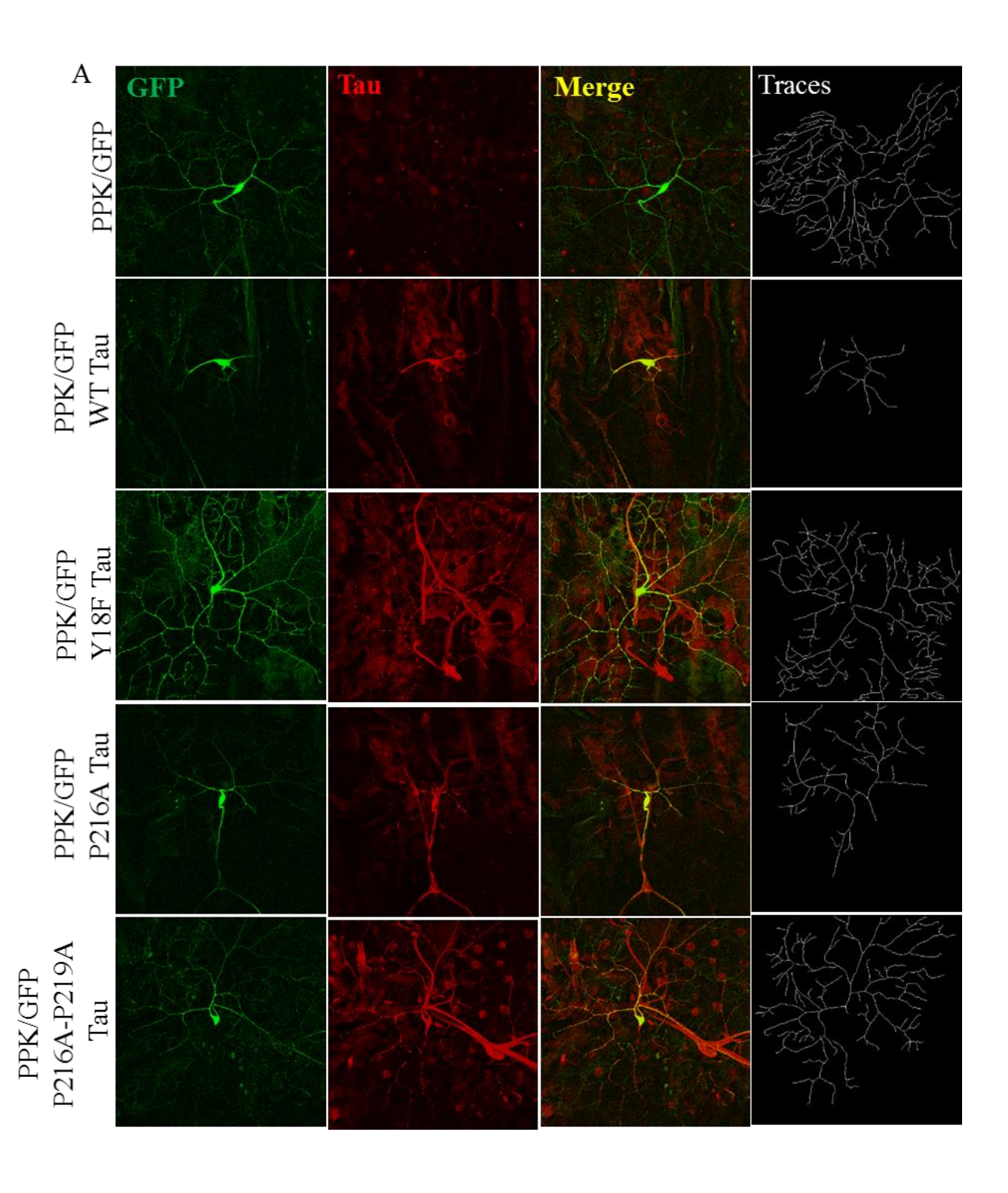
Figure 47. WT Tau and WT Tau-Fyn overexpression reduces the receptor potential between photoreceptor cells. Age dependent ERG were recorded for 1-day and 10-day, 20-day and 30-day old flies. A1 and A2: 1 day old flies ERG traces, off transients, on transients and receptor potential were quantified and analysed. B1 and B2, 10 day old flies ERG traces, off transients, on transients and receptor potential were quantified and analysed. C1 and C2, 20 day old flies ERG traces, off transients, on transients and receptor potential were quantified and analysed. D1 and D2, 30 day old flies ERG traces, off transients, on transients and receptor potential were quantified and analysed. E1 and E2,

Comparison of the 1-day (black) and 10-day (red), 20-day (green) and 30-day (blue) old traces of the recorded ERGs for Tau and Fyn expressing flies. n=10-15 flies per genotype.

3.23 WT and mutated Tau overexpression reduces C4da neurons dendritic arborization

Progressive death of the neurons is associated with AD and Tauopathies. Reduction in neuronal density and reduction in arborization of the dendrites has been found in AD brain (Falke et al., 2003). Proper arborization of the dendrites is important for incoming signal processing and transfer. Therefore, next we wanted to study the dendritic arborization in Tau and Tau-Fyn overexpressing flies. For studying the dendrites in *Drosophila*, C4da neurons has been widely used as model (Iseki et al., 2001; Sáchez-Soriano et al., 2007). We used C4da as our model to study the dendrites in third instar larvae. We used PPK-Gal4 driver for overexpression of Tau and Fyn transgenes in *Drosophila* larvae. To mark the dendrites of C4da neurons with PPK Gal4, we made a stable homozygous stock of UAS-GFP with PPK-Gal4 and crossed this stock with Tau transgenic flies.

We found that overexpression of WT Tau caused severe reduction in the arborization of the third instar larvae with total loss of distal dendrites, reduced dendritic length and branch numbers. WT Tau overexpression also significantly reduced the arbor surface area and lead to simplified dendritic arborization of C4da neurons. Whereas, when we blocked the phosphorylation of Tau at Y18 or reduced the Fyn interaction through P216A and Tau P216A-P219A, we found rescue in WT Tau overexpression effects as we found increased dendritic length (WT Tau (18μm) vs Tau Y18F (123μm), Tau P216A (60.03μm) and Tau P216219A (93.36μm)), increase in arbor surface area (WT Tau (28.90 μm²) vs Tau Y18F (121.14 μm²), Tau P216A (91.55 μ m²) and Tau P216219A (92.66 μ m²)), and also more number of branches (WT Tau (20.22 branches) vs Tau Y18F (186.6 branches), Tau P216A (68.66 branches) and Tau P216219A (125.62 branches)). Hence, reducing the Y18 phosphorylation of Tau and interaction with Fyn rescued the toxic effects of WT Tau overexpression and formed the complex and branched arborization of the C4da neurons. We also used Strahler analysis to check the branching pattern of the dendrites in Tau flies. We found that as compared to control, WT Tau overexpression leads to total loss of the tertiary and quaternary branches of the dendrites, In WT Tau overexpressing flies there were only primary and secondary dendrites where as if we reduce the Y18 phosphorylation of Tau we got all primary, secondary, tertiary and quaternary branches. Similarly, if we reduce the Fyn interaction through Tau P216A or Tau P21A-P219A, we found higher branching pattern. Strahler analysis also suggests that reduction in the Y18 phosphorylation of Tau or the Tau-Fyn interaction rescues the toxic effects of the WT Tau and increases the branching complexity leading to arborized dendrite of the neurons (figure 48).



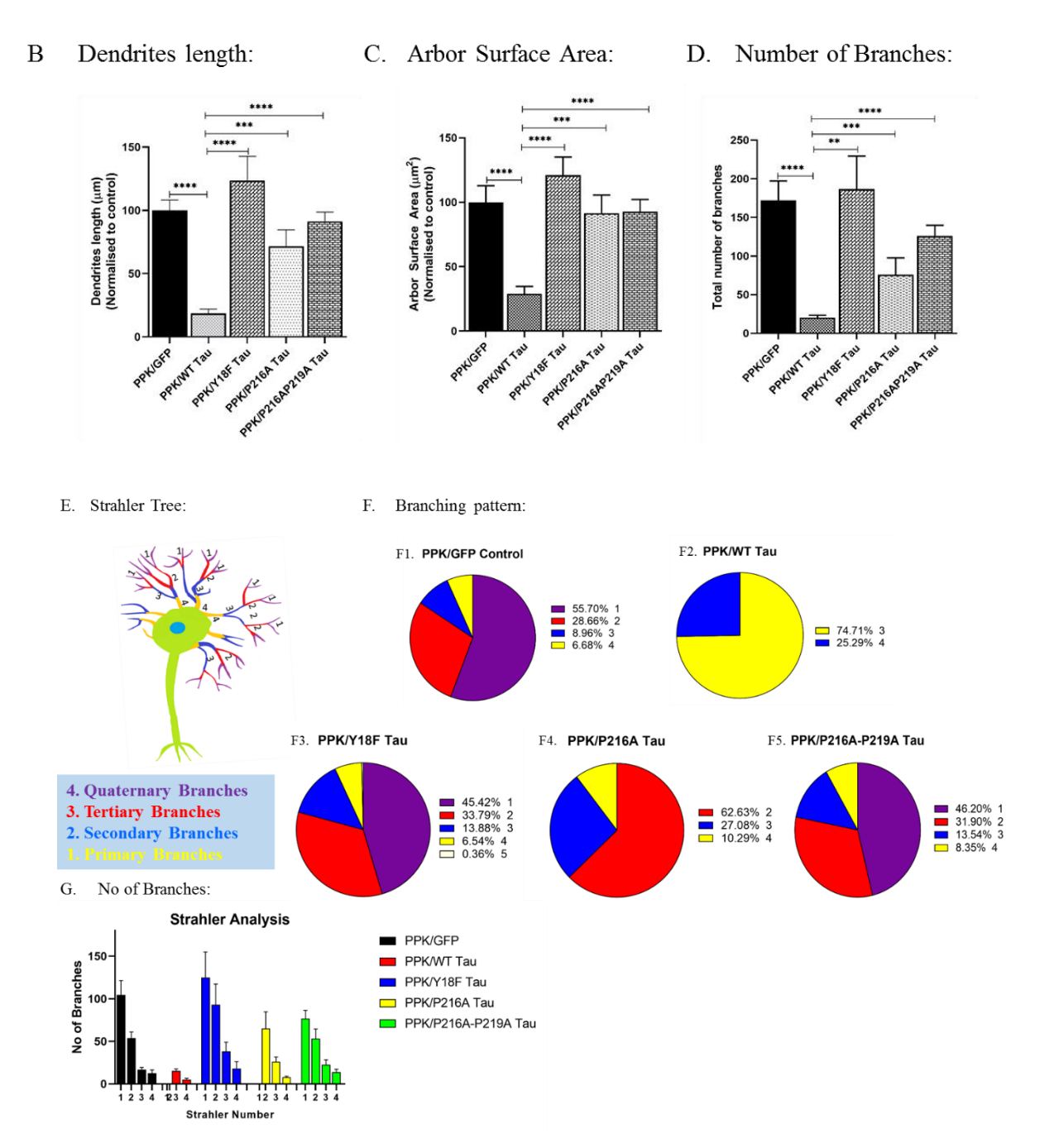


Figure 48. WT and mutated Tau overexpression reduces C4da neurons dendritic arborization and branching pattern. A. Confocal microscopy images of third instar larvae C4da neurons expressing WT Tau, Tau Y18F, Tau P216A and Tau P216A-P219A. C4da neurons are marked with PPK-Gal4; UAS-GFP (green) and stained for Tau (Red). Traces were drawn using neurite traces plugin in Fiji software as mentioned in methodology section. B. Quantification of the dendritic length, C. Arbor surface area and D. number of branches of the C4da neurons. Reducing the Y18 phosphorylation and Tau-Fyn interaction significantly increased the length of dendrites, arbor surface area and number of branches. E. Schematic of the Strahler tree and pattern of branches. F. Strahler analysis of the traces of the C4da neurons. F1-F5 branching pattern of the C4da neurons expressing GFP control (F1), WT Tau (F2), Tau Y18F (F3), Tau P216A (F4) and Tau P216A-P219A (F5). Strahler analysis revealed that WT Tau

overexpression reduced the branching complexity and only primary and secondary dendrites were present whereas Tau Y18F, Tau P216Aand Tau P216A-P219A significantly increased the branching complexity as tertiary and quaternary dendrites were also present were as comparable to controls. G. Bar graph representing total number in each Strahler number for all genotypes as mentioned. Student t-test was used for statistical analysis with graph pas prism 8.0. n= 10 neurons.

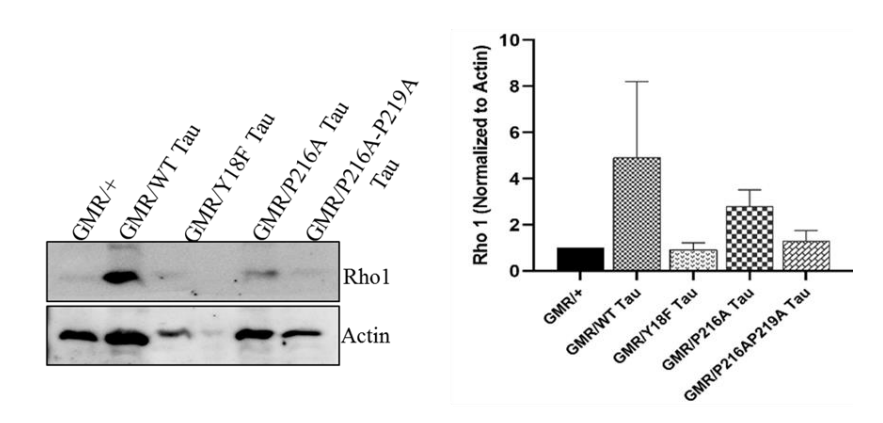
3.24 WT Tau overexpression affects Rho1 and Rac1 levels

We found that overexpression of WT Tau reduces the dendritic arborization of the C4da neurons. Structure and plasticity of dendritic spines be determined by the actin cytoskeleton and remodeling (Lei et al., 2016) We also know that effectors of the Rho and Rac signalling regulate actin cytoskeleton. Previous studies show that increased activity of Rho1 and decreased activity of Rac1 has been associated with the decreased branching pattern and simplified branching tree in neurons (Nakayama et al., 2000; Threadgill et al., 1997b). Also, these small Rho GTPases, Rho1 and Rac1 are important players in maintaining the cellular cytoskeleton through regulating the actin and microtubule rearrangements (Burridge and Wennerberg, 2004). Decreased expression and levels of Rac1 have also been found in the AD brain (Zhao et al., 2006) whereas Rho1 expression was found to be increased in mouse model of AD (Huesa et al., 2010). Though association of the Rho1 and Rac1 with the pathogenicity of AD is known, the role of these Rho family GTPases in Tau mediated toxicity is still unclear. Therefore, we wanted to check the levels of the Rho family GTPases Rho1 and Rac1 in Tau mediated neurodegeneration Tau.

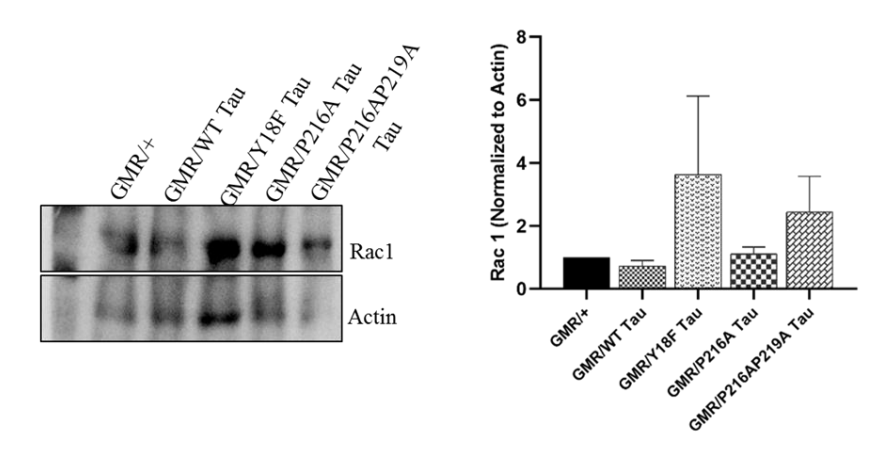
We crossed the Tau flies with GMR-Gal4, and progenies were collected. Heads were separated and crude protein extract was prepared as mentioned in methods section (2.2.14). After performing western blots, we found that overexpression of the WT Tau increased the Rho1 levels whereas decreased the levels of the Rac1. Densitometry analysis also show increased Rho1 (figure 49A, Rho1 levels normalised with actin controls as WT Tau (4.90), controls (1), Tau Y18F (0.91), Tau P216A (2.80) and Tau P216AP219A (1.30)) and decreased Rac1 (figure 49B, Rac1 levels normalised with actin controls as WT Tau (0.7), controls (1), Tau Y18F (3.62), Tau P216A (1.1) and Tau P216AP219A (2.44)) in WT Tau flies when compared with controls, Y18F and P216A, P216AP219A mutants of Tau. This hints that when we reduced the Y18 phosphorylation and Tau Fyn interaction through Tau P216A and Tau P216A-P219A the levels of Rho1 was decreased and Rac1 was increased which also supports our previous results and gives us a clue that abnormal expression or levels of Rho1 and Rac1 may be associated with Tau mediated toxicity in AD and Tauopathies. We also tried to check

the Rho1 and Rac1 levels in the Tau and Fyn coexpressing flies but the single repeat data was not significant to make any conclusion. This is the data for one repeat of the experiment, we are currently repeating the experiments for making any conclusive remark on this (figure 49).

A. WT Tau overexpression increases Rho1 levels



B. WT Tau overexpression decreases Rac1 levels



C. WT Tau and Fyn synergistically increases Rho1 levels

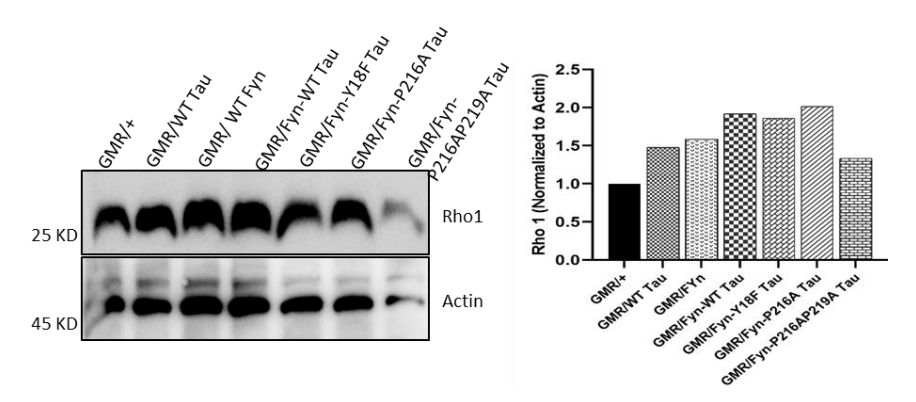


Figure 49. WT Tau overexpression affects Rho1 and Rac1 levels. A. Western blotting for Rho1 in Tau overexpression flies and quantification of the blot. B. Western blotting for Rac1 in Tau overexpression flies and quantification of the blot in B. C. Western blotting for Rho1 in Tau-Fyn coexpressing flies and quantification of the blot. For quantification of all blots, normalization was done to the control sample levels and values were plotted as bar graphs.

Summary

To summarize the results in the second objective, in our Tau AD model, WT Tau overexpression causes decline in the *Drosophila* locomotion in aged flies which is improved by reducing Fyn mediated phosphorylation of the Tau. Tau overexpression causes rough eye (nail paint imprinting assay), loss of IOBs (SEM analysis) and reduction in the synaptic transmission (ERG analysis) which is improved by reducing the Tau-Fyn interaction and Y18 phosphorylation of Tau by Fyn. Expression of WT Tau in C4da neurons decreases the dendritic length, dendritic surface area and number of the branches leading to the simplified branching complexity and reduced arborization, which can be rescued by reducing the phosphorylation of the Tau at Y18 as it significantly increases the branching complexity and arborization (Confocal microscopy and Strahler analysis of the C4da neurons). Initial experiments hint that WT Tau overexpression may perturb the Rho1 and Rac1 homeostasis by increasing the Rho1 levels and reducing the Rac1 levels but the experiment needs to be repeated for conclusive results.

Objective 3: Repurposing the drugs used in oncotherapy for checking the neuroprotective effects in *Drosophila* model of AD.

As a part of my research work in studying the mechanism of Tau and Fyn mediated neurodegeneration we have generated a model to study the Tau-mediated neurodegeneration. We wanted to leverage this AD or Tauopathy model to find new therapeutic compounds by drug repurposing. Drug repurposing and repositioning of established chemical compounds and drugs has been found to be cost effective, time saving and gave better treatment options. With the help of our lab collaborator Prof. Markus Zweckstetter, Max Planck Institute for Multidisciplinary Sciences, Gottingen, we procured eight different compounds used oncotherapy (modified from original ones) and checked for their protective effects on Tau mediated neurotoxicity using *Drosophila* as a model. These compounds have already shown positive effects in preventing Tau seeding and fibrillation in vitro and in cell models.

Note: As the compounds are being patented, in the interest of institutions and authors the chemical name of the compounds tested are not disclosed here as the data is not published yet. I have used specific numbers given to each compound from compound 1 to compound 8 for all the records and analysis here.

3.25 Drug Dosage and Treatment

As these are already established drugs that are being used in oncotherapy, their recommended doses for patients are already available. We selected the dosage recommended for human use and calculated the recommended concentration for flies and larvae according to the body weight of the third instar larvae, we called it as 'reference dose for the flies'. We used this reference dose concentration and two higher concentrations than reference dose, for the primary screening in larvae. We performed primary screening with these three different concentrations and selected the best one for further experiments. Following table represents the different concentrations we used in primary screening for each compound. The highlighted concentration (in bold) is the reference dose.

Table 4. Compounds and their concentrations used in primary screening.

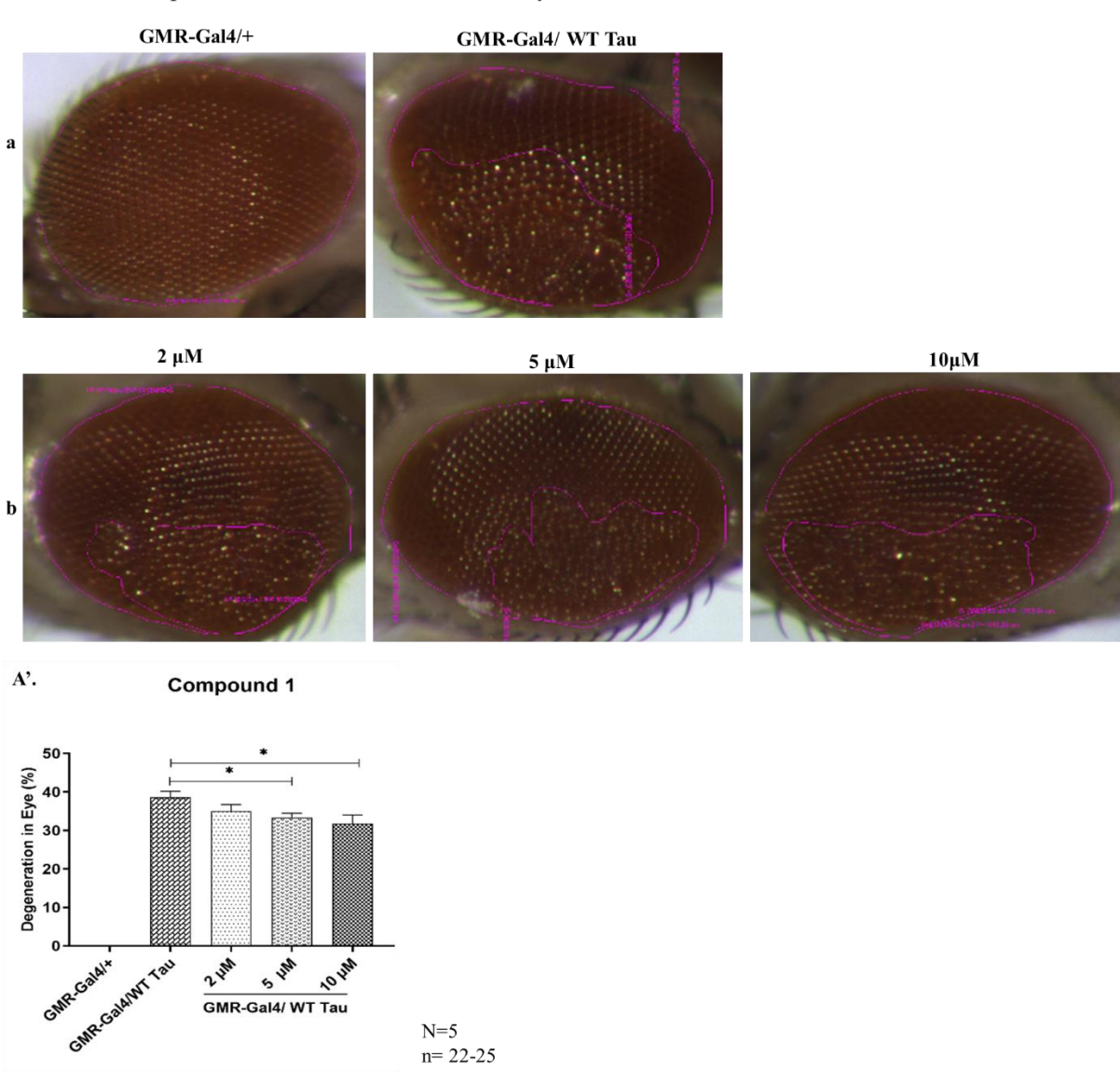
Sr. No	Compound	Concentrations used	
1.	Compound 1	2μM , 5μM, 10μM	
2.	Compound 2	1μΜ , 2μΜ, 5μΜ	
3.	Compound 3	18μΜ , 28μΜ, 84μΜ	
4.	Compound 4	7μM , 14μM, 20μM	
5.	Compound 5	10μΜ , 20μΜ, 30μΜ	
6.	Compound 6	25μM , 50μM, 100μM	
7.	Compound 7	05μM , 10μM, 15μM	
8.	Compound 8	15μM , 30μM, 44μM	

3.26 Screening of the compounds for protective effects on Tau toxicity

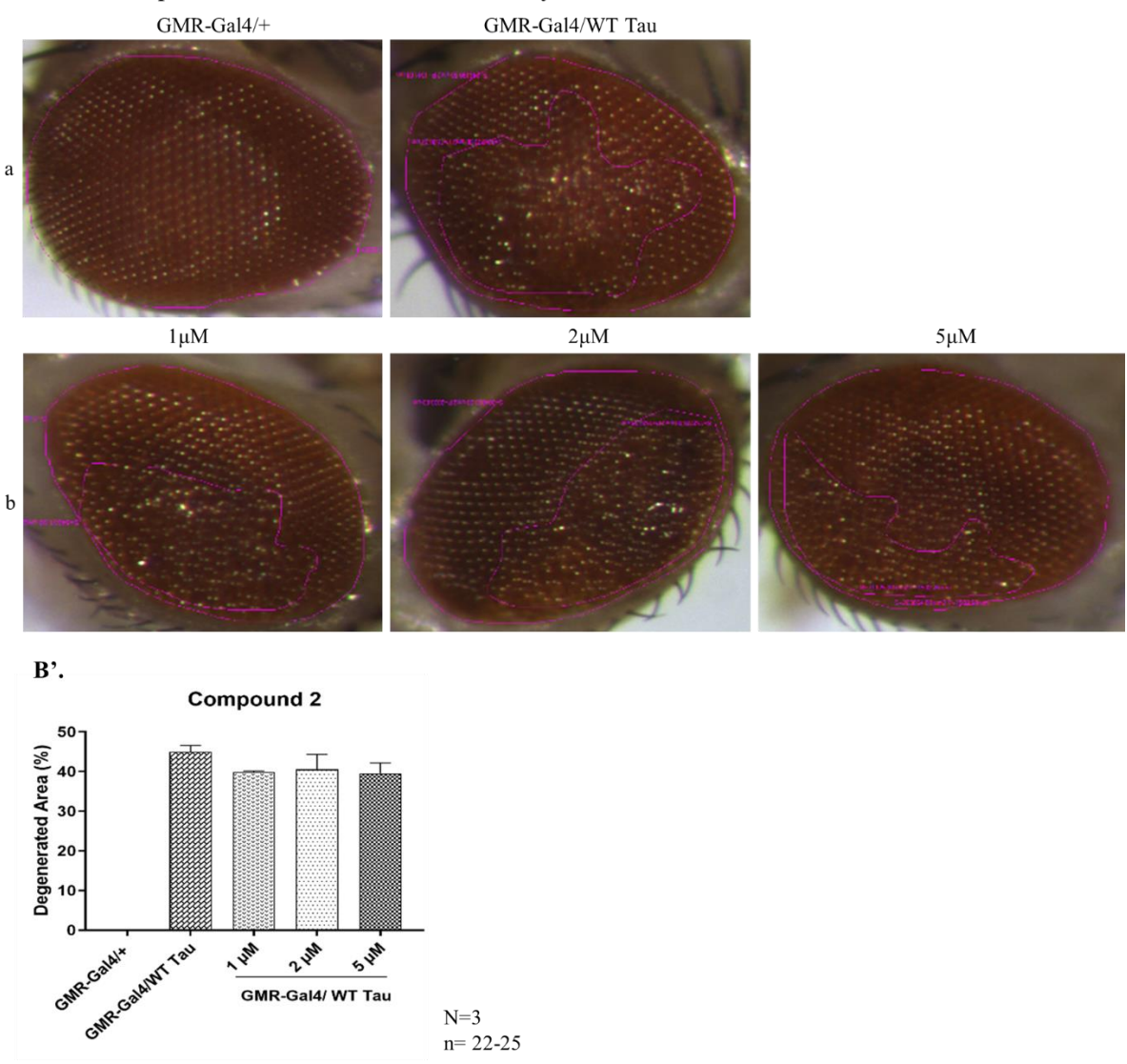
As a primary screening and for checking the effects of the compounds on the Tau toxicity, we overexpressed WT Tau in the *Drosophila* eyes with GMR-Gal4. Larvae were treated with different concentrations of the compound thrice at each instar stage. Once flies eclosed, we did imaging with light microscope and scanning electron microscope for analysing the eye surface morphology. WT Tau overexpression causes rough eye phenotype and fusion of ommatidia in very young flies. For getting initial expression of the effects of the compounds in the eye surface morphology we did full eye imaging and calculated the percentage of the degenerated (fused and rough ommatidia) surface area and compared among different concentrations of the compounds as well as controls. We found that WT Tau overexpression caused degeneration in eyes and treatment with compound 1 (WT Tau untreated (38.59%), 2μM (35.01%), 5μM (33.40%) and 10μM (31.76%)), compound 3 (WT Tau untreated (41.48%), 7μM (31.12%), 14μM (34.64%) and 20μM (32.95%)), compound 5 (WT Tau untreated (40.55%), 10μM (32.20%) and 20μM (30.30%)), compound 7 (WT Tau untreated (38.75%), 5μM (34.27%), 10μM (28.50%) and 15μM (28.80%)), and compound 8 (WT Tau untreated (40.41%), 15μM (32.16%), 30μM (29.82%) and 44μM (31.20%)), in the larval

stages significantly reduced the degenerated area in the adult eyes. This reduction in the percentage of the surface area after treatment states that Compounds 1, 3, 5, 7, and 8 treatment have protective effects against the WT Tau toxicity in *Drosophila* eyes (figure 50).

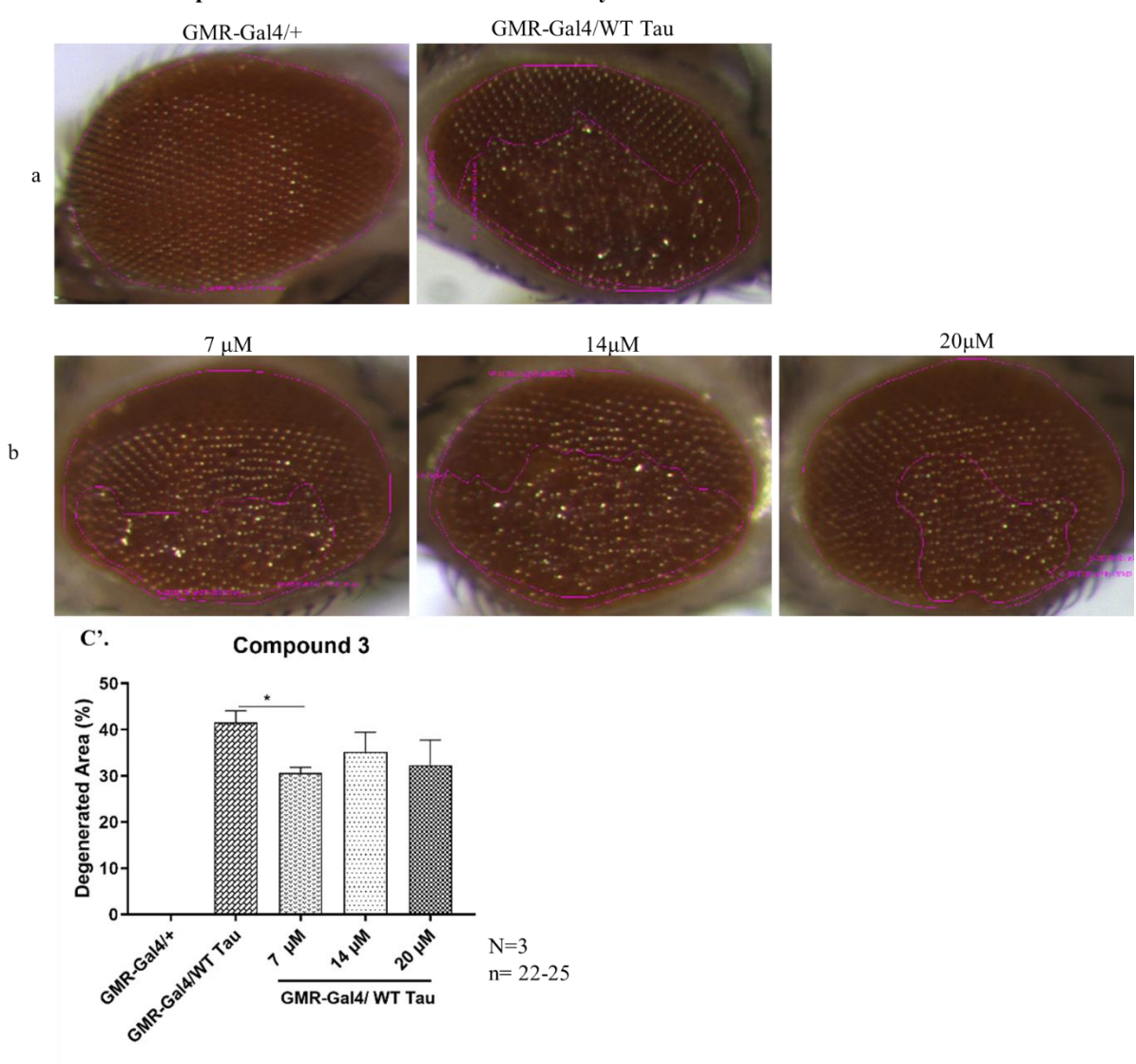
A. Effect of compound 1 treatment on WT Tau toxicity:



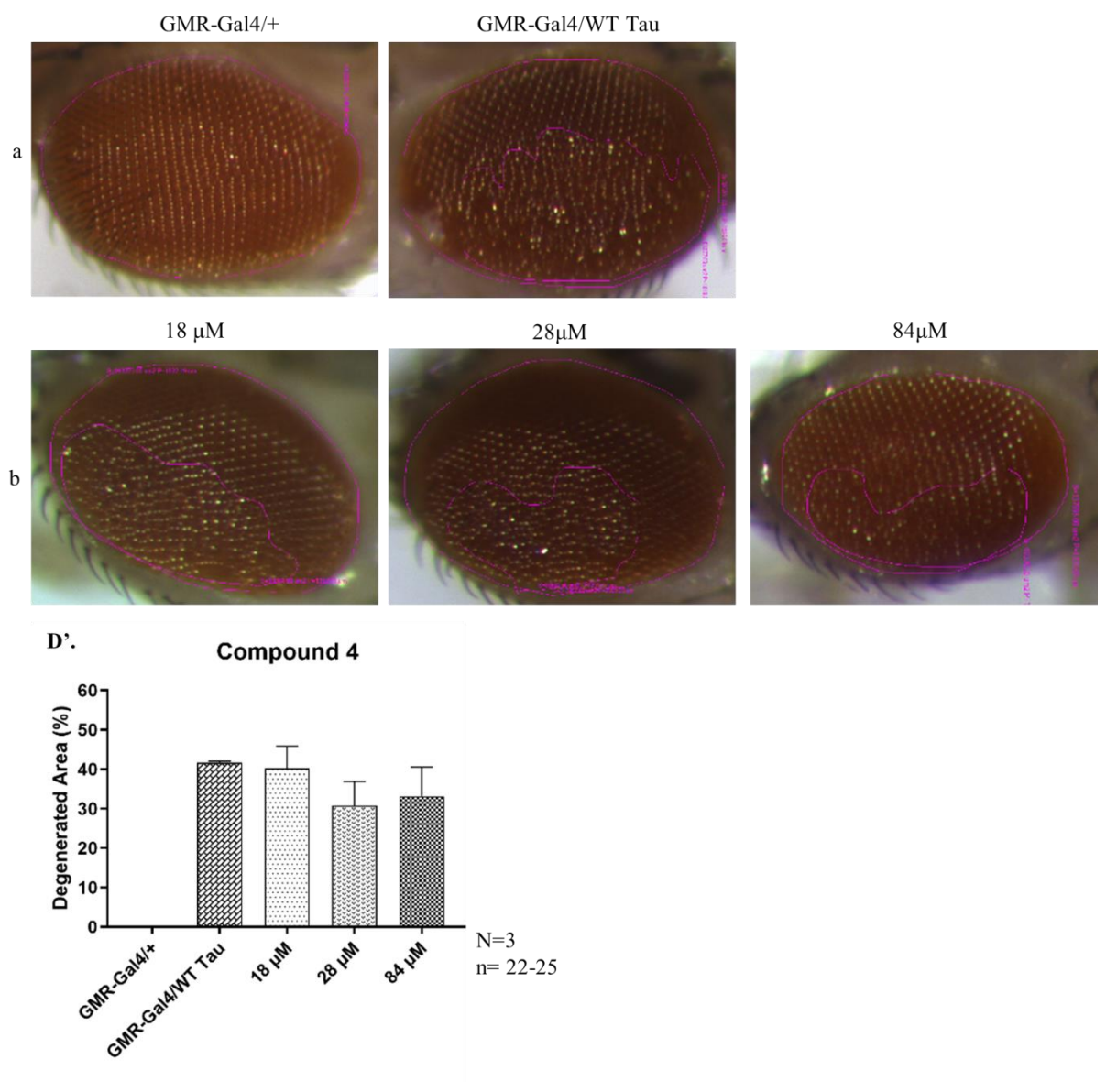
B. Effect of compound 2 treatment on WT Tau toxicity:



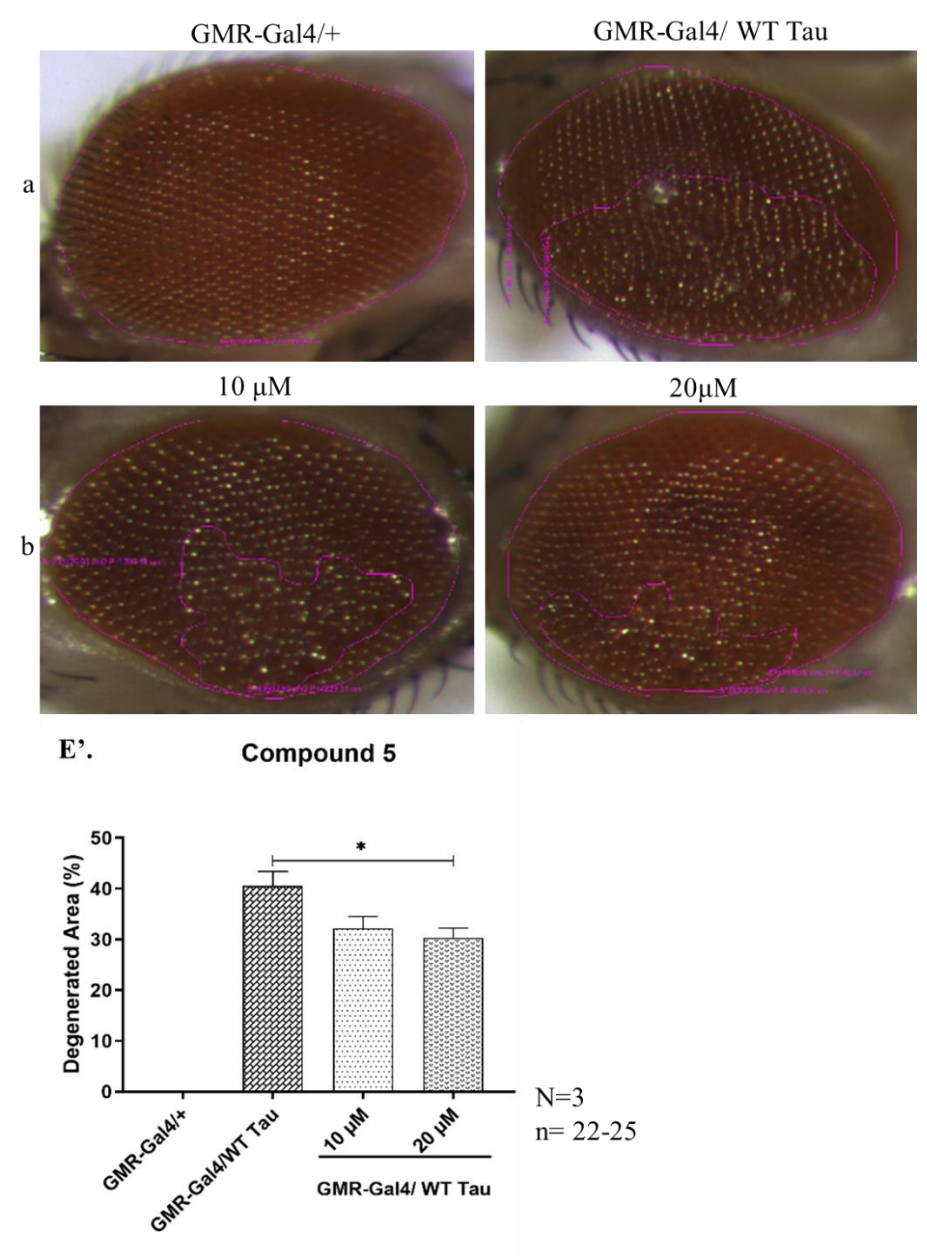
C. Effect of compound 3 treatment on WT Tau toxicity:



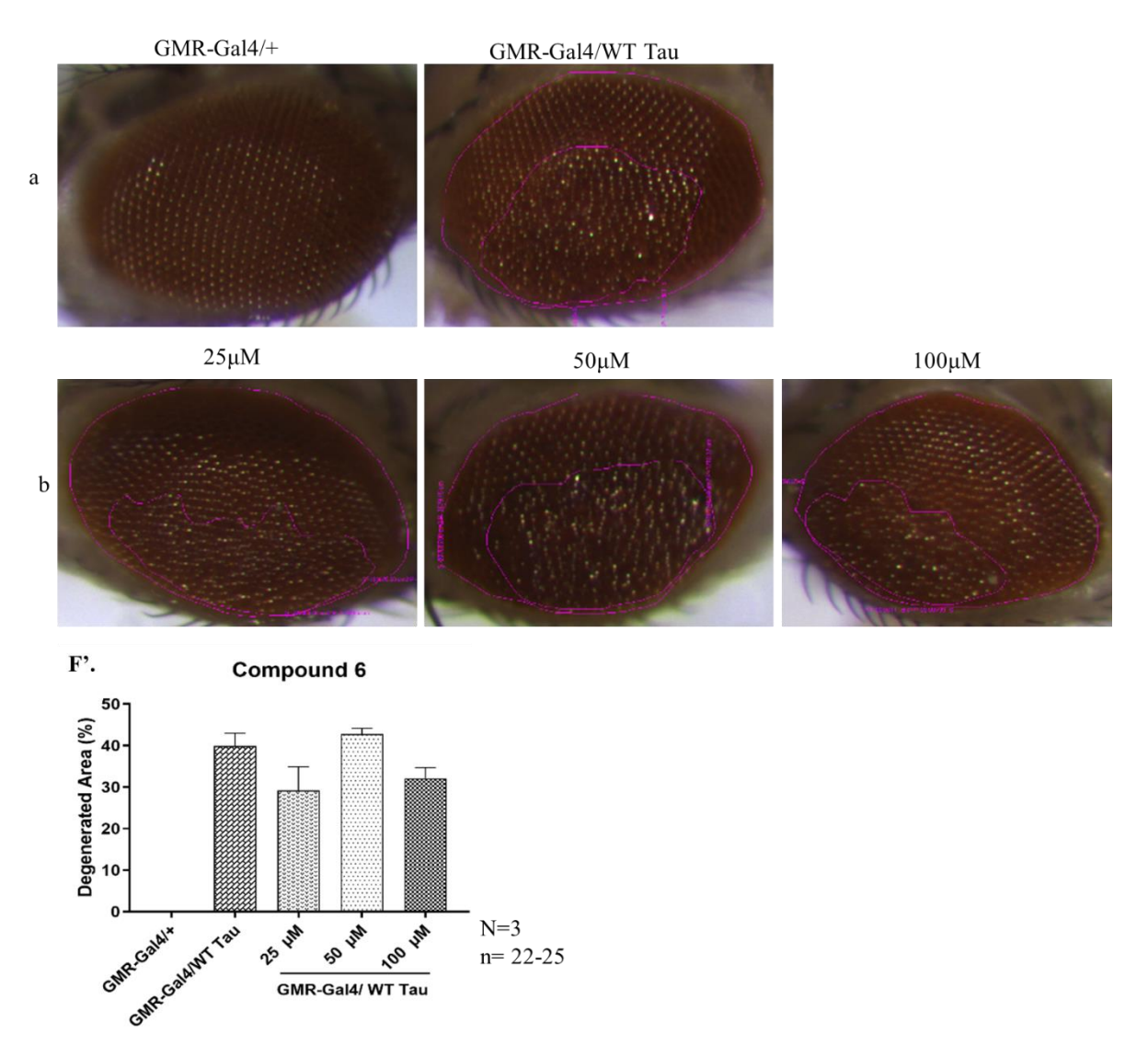
D. Effect of compound 4 treatment on WT Tau toxicity:



E. Effect of compound 5 treatment on WT Tau toxicity:

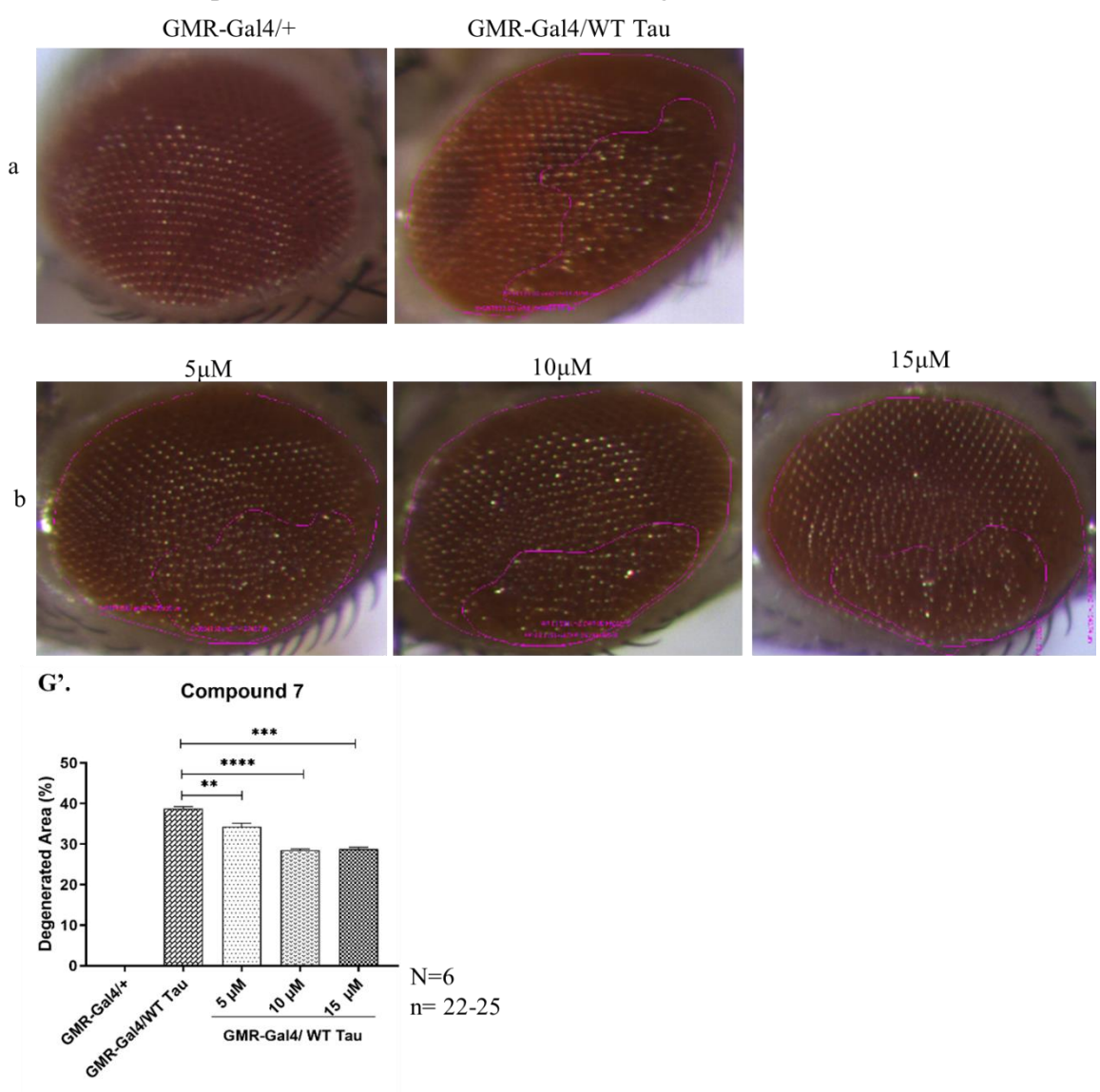


F. Effect of compound 6 treatment on WT Tau toxicity:



Contd.

G. Effect of Compound 7 treatment on WT Tau toxicity:



Contd.

H. Effect of compound 8 treatment on WT Tau toxicity:

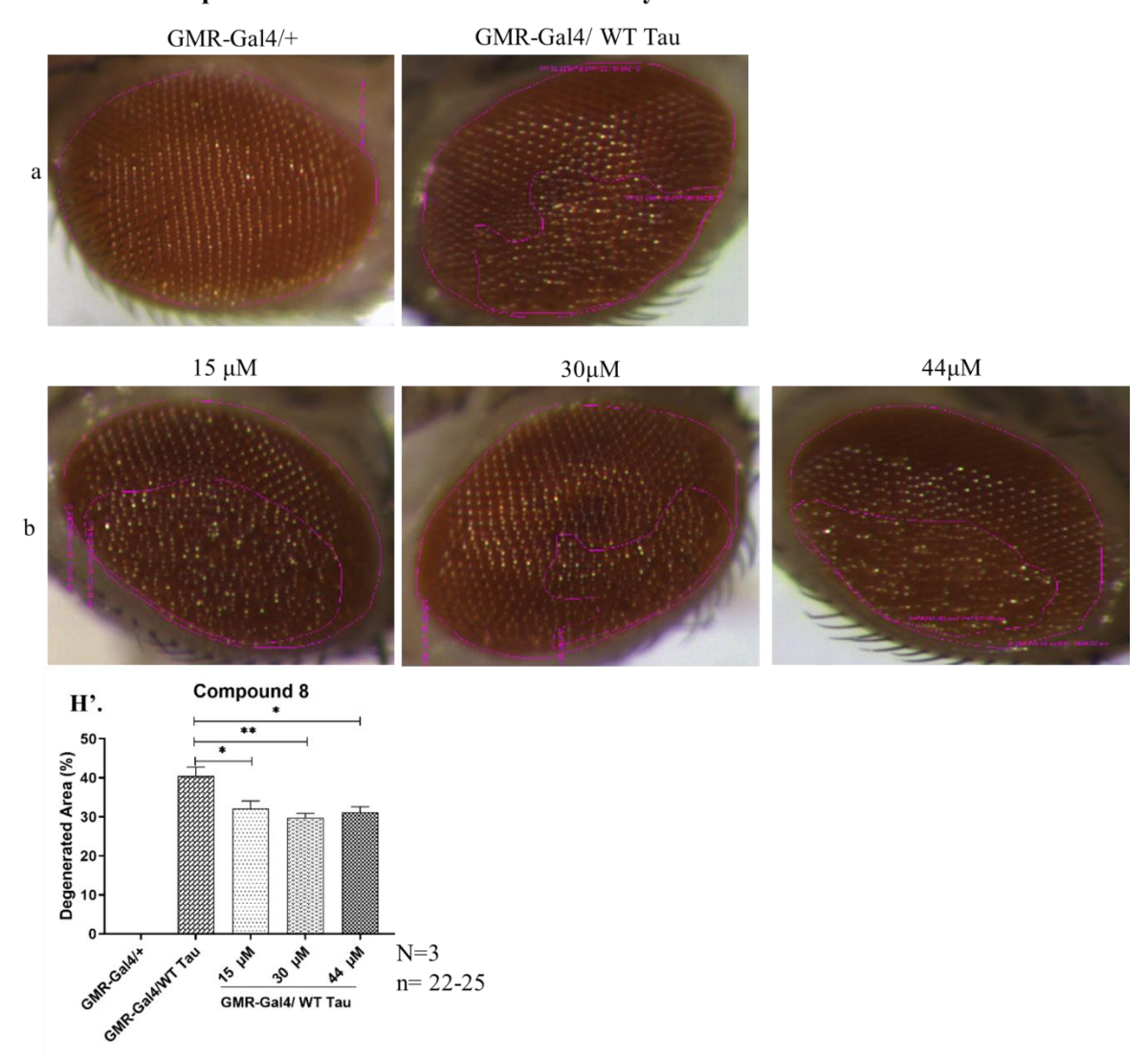


Figure 50. Full eyes light microscopy imaging of the compounds treated flies and control flies, a represents control and WT Tau untreated flies, and b represents WT Tau treated flies. A. Compound 1 treated flies eyes compared with control and untreated WT Tau flies. Total surface area and degenerated surface area is calculated and quantified as percentage in A'. B. Compound 2 treated flies eyes compared with control and untreated WT Tau flies. Total surface area and degenerated surface area is calculated and quantified as percentage in B'. C. Compound 3 treated flies eyes compared with control and untreated WT Tau flies. Total surface area and degenerated surface area is calculated and quantified as percentage in C'. D. Compound 4 treated flies eyes compared with control and untreated WT Tau flies. Total surface area and degenerated surface area is calculated and quantified as percentage in D'. E. Compound 5 treated flies eyes compared with control and untreated WT Tau flies. Total surface area and degenerated surface area is calculated and quantified as percentage in E'. F. Compound 6 treated flies eyes compared with control and untreated WT Tau flies. Total surface area and degenerated surface area is calculated and quantified as percentage in F'. G. Compound 7 treated flies eyes compared with control and untreated WT Tau flies. Total surface area is calculated and quantified as percentage in F'. G. Compound 7 treated flies eyes compared with control and untreated WT Tau flies. Total surface area is calculated and untreated WT Tau flies. Total surface area is calculated and untreated WT Tau flies. Total surface area is calculated and untreated WT Tau flies. Total surface area is calculated and untreated WT Tau flies. Total surface area is calculated and untreated WT Tau flies.

quantified as percentage in G'. H. Compound 8 treated flies eyes compared with control and untreated WT Tau flies. Total surface area and degenerated surface area is calculated and quantified as percentage in H'.

3.27 SEM to check the effects of drug compounds on degeneration of eye

To confirm the results of the primary screening with high resolution imaging, we have performed scanning electron microscopy (SEM) to see the protective effects of the compounds in treated and untreated flies. We chose one concentration which had the best significance values from the three concentrations we have used in the primary screening. Following tables summarizes the compounds and their concentrations we used for checking the retinal degeneration using SEM.

Table 5. Compounds used for SEM.

Sr No	Compound	Concentration for SEM
1.	Compound 1	10 μΜ
2.	Compound 3	20 μΜ
3.	Compound 5	20 μΜ
4.	Compound 8	30 μΜ
5.	Compound 7	10 μΜ

We did three treatments as described previously for light microscopy and 1-day old flies were fixed in 1 % formaldehyde followed by serial dehydration in 25%, 50%, 75% and 100% ethanol for 12 hours each. Dehydrated flies were fixed on the SEM stab and images were captured at 200X for complete eye.

SEM analysis confirmed the protective effects of the compounds on the WT Tau toxicity. We found that treatment with compound 1 (WT Tau untreated (40.73%), 10μM (33.33%)), compound 3 (WT Tau untreated (40.73%), 20μM (33.99%)), compound 5 (WT Tau untreated (40.73%), 20μM (34.63%)), compound 7 (WT Tau untreated (40.73%), 10μM (32.34%)) and 8 (WT Tau untreated (40.73%), 30μM (34.63%)) decreased the WT Tau toxicity in the *Drosophila* eyes with compound 7 and compound 1 being the most consistent and

significant (figure 51). We proceeded for functional studies to further quantify these protective effects of the compound's treatment on the WT Tau toxicity.

SEM Analysis of WT Tau flies treatments with compounds:

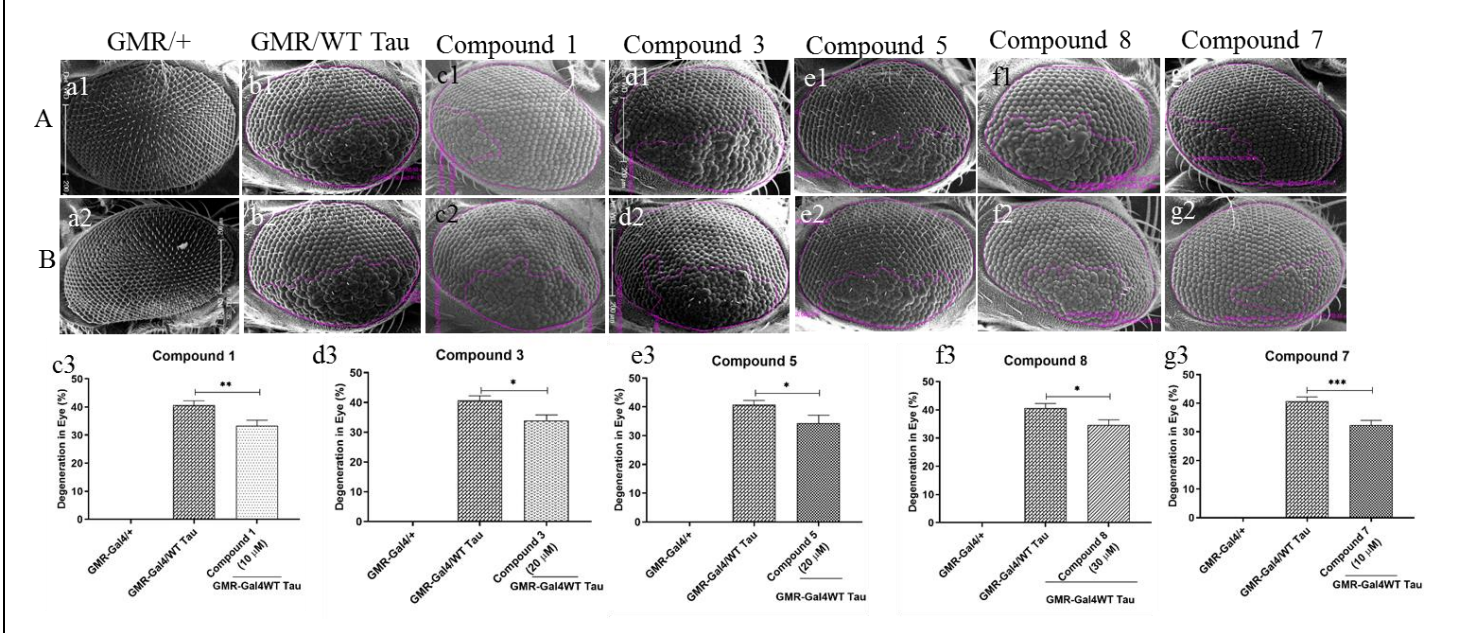


Figure 51. Scanning electron microscopy of the compounds treated flies and control flies, A and B represents duplicates. A. a1 and a2 represents the control and b1-b2 represents WT Tau untreated controls. Compound 1 treated (c1-c2) flies eyes compared with WT Tau untreated controls (b1 and b1) and percentage of the degenerated area is quantified in c3. Compound 3 treated (d1-d2) flies eyes compared with WT Tau untreated controls (b1 and b1) and percentage of the degenerated area is quantified in d3. Compound 5 treated (e1-e2) flies eyes compared with WT Tau untreated controls (b1 and b1) and percentage of the degenerated area is quantified in e3. Compound 8 treated (f1-f2) flies eyes compared with WT Tau untreated controls (b1 and b1) and percentage of the degenerated area is quantified in f3. Compound 7 treated (g1-g2) flies eyes compared with WT Tau untreated controls (b1 and b1) and percentage of the degenerated area is quantified in g3. 12-15 flies were analysed for each genotype and treatment.

3.28 Compounds treatment rescues Tau mediated neurodegeneration in retinal neurons (ERGs)

After SEM analysis we confirmed that five compounds have protective effects on the Tau neurotoxicity. These five compounds (Compound 1, 3, 5, 7 and 8) significantly reduced the degenerated surface area of the eye. Moving ahead, as a functional assay, we wanted to check the effects of these compounds treatment of the neuronal function. *Drosophila* ERG is a well-studied model for analysing genetic interactions, protein modification as well as for the functional loss of the photoreceptor cells (Belusic, 2011). Out of five compounds which we

analysed through SEM, we selected two best compounds and recorded the ERG from the treated flies to analyse the effect of the treatment on the synaptic transmission between photoreceptor cells and laminar neurons. Following table indicates the compounds and the concentration we used for the ERG of the treated flies.

Table 6. Compounds used for ERG.

Sr. No	Compound	Concentration
1.	Compound 7	10 μΜ
2.	Compound 8	30 μΜ

We orally fed the compound to the larvae as mentioned earlier in the methods section. Once the progeny was eclosed we collected the adult flies and recorded the ERGs. We analysed the on-transient, off-transient and receptor potentials from ERG recordings of control and treated flies. We found that the both compounds treatment significantly improved the ontransient in the treated flies which was significantly lost in the untreated WT Tau flies (WT Tau untreated (-0.00008V), compound 7 (0.001V), compound 8 (0.001V), and controls (0.005V)). Off-transients were also improved but statistically non-significant. Treatment with both compounds significantly increased the receptor potential of the WT Tau overexpressing flies as compared to untreated Tau flies (WT Tau untreated (0.011V), compound 7 (0.017V), compound 8 (0.018V), and controls (0.023V)). Taking together, we concluded that treatment with compound 7 and compound 8 significantly improves synaptic transmission between photoreceptor cells and laminar neurons. Finally, we provided in vivo evidences for the protective effects of the compound 7 and compound 8 on Tau mediated neurotoxicity in *Drosophila* eye model (figure 52).

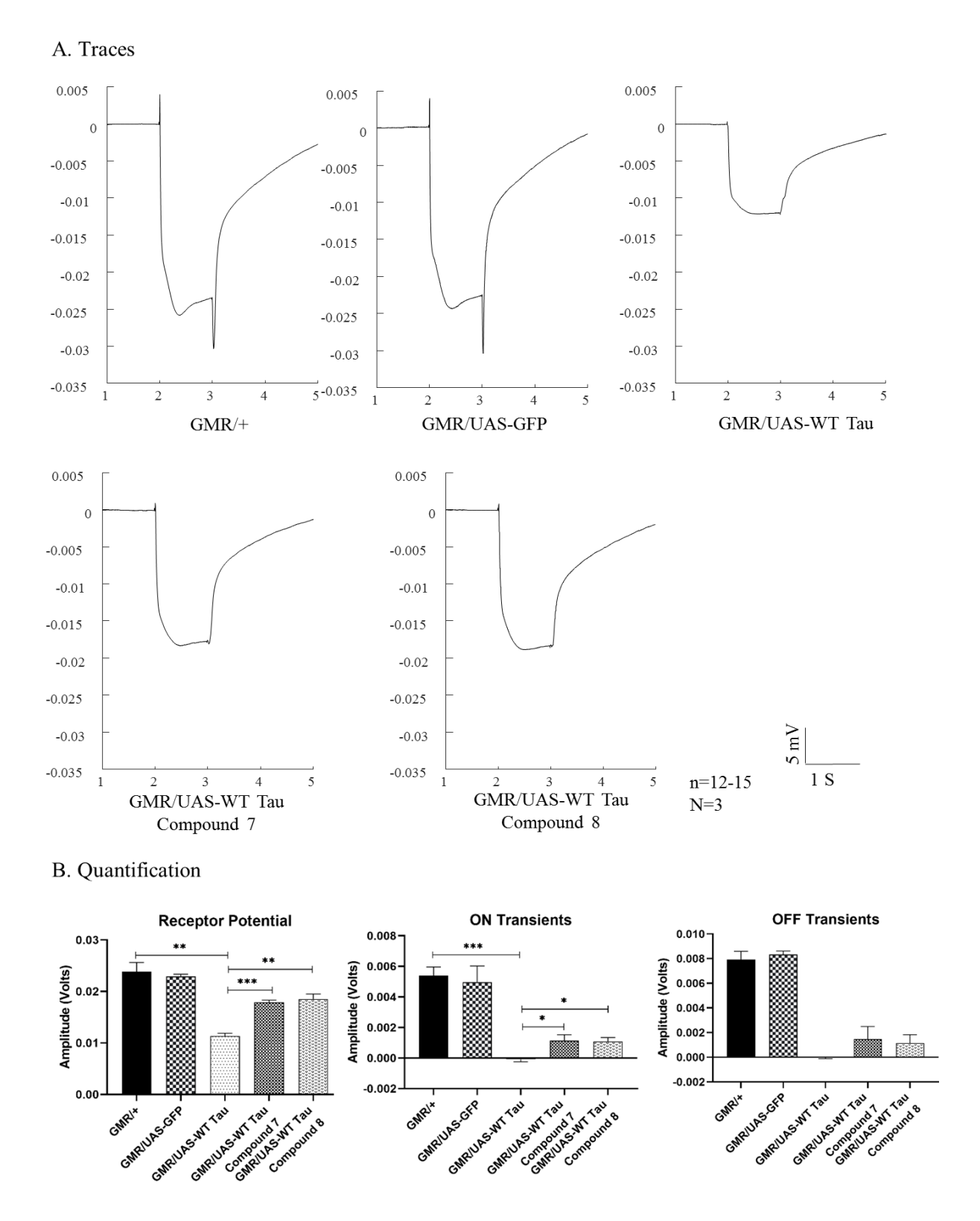


Figure 52. Compounds treatment rescues Tau mediated neurodegeneration in retinal neurons (ERGs). A. ERG traces of the GMR/+, GMR/GFP, GMR/UAS-WT Tau (upper panel) and ERG traces of the GMR/UAS-WT Tau treated with compound 7 and 8 (lower panel). B. Quantification of the receptor potential, on transients and off transients of the controls, untreated and compound 7 and 8 treated flies. GMR/+ and GMR/UAS-GFP were used as a positive control flies.

Summary

To summarize the results of the third objective of repurposing the drugs used in oncotherapy for checking the neuroprotective effects in *Drosophila* model of AD, we found that the treatment of compounds 1, 3, 5, 7 and 8 had significant reduction on the degenerated surface area of eyes in the primary screening. Accordingly, SEM analysis of the rough-eye phenotype recovery also confirmed that compounds 1, 3, 5, 7 and 8 reduce the Tau toxicity in eyes. To even precisely check the effect on the neuronal function we did ERGs on control and drug-treated flies and found significant increase in the Receptor potential and ON transient amplitudes in the flies treated with compounds 7 and 8. We provided extracellular recordings of retinal neurons, we conclude that compounds 7 and 8 have protective effects against Tau mediated neurotoxicity.

Chapter 4: Discussion

Alzheimer's disease is non-curable neurodegenerative disorder which progresses with aging. There is no treatment available for AD probably may be because the molecular players and their mechanism involved in AD progression are not well understood yet. The major pathological hallmarks of AD are the presence of amyloid- β (A β) plaques in the extracellular matrix and neurofibrillary tangles in the intracellular sides (Ittner and Ittner, 2018). A β plaques are formed due to improper processing of Amyloid Precursor Protein (APP) by the proteolytic enzymes β and γ secretase to produce A β peptides of different length, and A β 42 is considered to be more pathogenic (Kotzbauer et al., 2004). Neurofibrillary Tangles are formed due to abnormal phosphorylation of microtubule associated protein Tau (Grundke-Iqbal et al., 1986b).

There are many serine threonine kinases involved in Tau phosphorylation, and tyrosine kinase activation is the primary response for any cell activity. According to AD hypothesis, $A\beta$ accumulates in the extracellular side can trigger the downstream signal for Tau phosphorylation. This hyperphosphorylated Tau aggregates form paired helical filament and later forms neurofibrillary tangles. FTDP (Frontal Temporal Dementia with Parkinson) is another neurodegenerative disease caused by mutations in Tau. This observation brings the idea that not only $A\beta$ can cause neurodegeneration even Tau alone can cause neurodegeneration.

Fyn, an Src family kinase also interacts with Tau and phosphorylates at tyrosine 18, which has been found abnormally hyperphosphorylated in AD brain (Lee et al., 2004). Fyn interacts with Tau through its SH3 domain and phosphorylates tyrosine residues of Tau (Lee et al., 1998).

1. Generation of *Drosophila* model of AD: Generation of stable transgenic flies expressing Wild Type (WT) & mutated human Tau and Fyn for studying functional interaction.

The mechanism of Tau and Fyn interaction, the molecular players involved in the signalling cascade and their impact on AD pathogenicity is not well known. Therefore, we proposed to study the mechanism of Tau and Fyn interaction and the molecular players involved in the Tau mediated neurotoxicity. To study the functional interaction of Tau and Fyn, we decided to mutate the important interaction sites of Tau and Fyn, and checked their impact on Tau toxicity in *Drosophila*. Fyn interacts with Tau through its SH2 and SH3 domain and

binds to PXXP motifs in Tau (Lau et al., 2016; Usardi et al., 2011a). Therefore, we selected two PXXP motifs (6th and 7th PXXP motifs in Tau) which are important for binding of Fyn and the target site of the Fyn (Y18 in Tau) (figure 13) for creating site directed mutations, and humanised Drosophila model by overexpressing them. We mutated Tau Tyrosine-18 to Phenylalanine (Y18F); Proline 216 to Alanine (P216A) (figure 27); and Proline 216, 219 to Alanine 216, 219 (P216A-P219A) (figure 31). We also mutated the seventh PXXP motif of Proline 233 to alanine (P233A) (figure 29); Proline 236 to Alanine (P236A) (figure 30); and Proline 233, 236 to Alanine 233,236 (P233-236A) (figure 32). We used inverse PCR with mutagenic primers for creating the site-specific mutations in human Fyn kinase and Tau. Transformed colonies were screened through colony PCR and insert was further confirmed through double digestion of the isolated plasmid. Mutation at specific desired position was confirmed through the sequencing. For inserting the construct into *Drosophila* genome, we cloned Tau and Fyn constructs into *Drosophila* specific pUAST-attB vector (figure 34-39) and microinjected into Drosophila embryos (figure 15). After microinjecting the construct, embryos were cultured at lower temperature (18°C) for their proper healing and growth. Once flies were eclosed from injected larvae or pupa, they were screened for the transgenic flies. After eclosion of the injected flies, we did phenotypic screening through red eye phenotype for the presence of the white gene in the injected flies' progeny. Positive flies were also confirmed then through single fly PCR for genomic (figure 40) and site-specific integration (figure 41). We got transgenic flies for WT Tau, Tau Y18F, Tau P216A and Tau P216A-P219A. We confirmed the transgenic flies for protein expression through western blotting (figure 43) and confirmed the generation of our Drosophila AD and Tauopathies model with reduced interaction of Fyn (P216A and P216A-P219A Tau) and reduced phosphorylation of the Y18 (Tau Y18F flies), which is primary phosphorylation site of the Fyn kinase in AD condition.

To study the interaction between human Tau and Fyn in AD and synergistic effect of both Tau and Fyn on Tau mediated toxicity, we need to express both Tau and Fyn in same fly. To bring both Tau and Fyn in same fly, we brought both chromosomes carrying Tau and Fyn genes in same fly. We generated double transgenic *Drosophila* stock carrying Fyn;WT Tau, Fyn; Tau P216A, Fyn; Tau P216A-P219A and Fyn; Tau Y18F. We proceeded further and studied the synergistic effect of Tau and Fyn on Tau toxicity.

2. Genetic analysis to understand the mechanism of Tau-Fyn mediated neurotoxicity.

Overexpression of WT Tau in *Drosophila* model AD exhibits the impaired locomotion in adult flies (Prüßing et al., 2013). As a first-hand experiment to check the effect of Tau and Fyn functional interaction on Tau neurotoxicity in our transgenic flies, we analysed the age-dependent locomotion of the adult flies. We did not find any significant difference in young flies as most of the transgenic flies were able to climb up (figure 44A). We analysed age dependent locomotion at the age of 1-, 7-, 14-, and 21-day old animals. At the age of 14 days there was improvement (but statistically non-significant) in climbing ability of the flies expressing Y18F and Tau P216A (figure 44C) compared to WT-Tau expressing animals. In 21 days old flies, we found that overexpression of the WT Tau causes age dependent reduction in the fly locomotion which was improved by blocking the phosphorylation of Y18 by Fyn or Fyn interaction to Tau (figure 44D). We concluded that the overexpression of the WT Tau affects the climbing ability of flies and reduces the locomotion in adult aged flies which is improved by reducing the Y18 phosphorylation (Tau Y18F) and Tau-Fyn interaction (Tau P216A).

Drosophila eye has been a widely studied and used as a model for studying the neurodegeneration in flies (Bolus et al., 2020; Chan and Bonini, 2000; Prüßing et al., 2013). To check the effects of the WT Tau toxicity in WT and reduced Tau-Fyn interaction and Fyn mediated phosphorylation of Tau at Y18, we analysed the *Drosophila* eyes through nail paint imprinting assay and scanning electron microscopy (SEM). Nail polish imprints of eye creates the exact replica of the outer surface of the eye which can be used to study the degeneration (Arya and Lakhotia, 2006). We overexpressed the WT Tau, Tau Y18F and Tau P216A with and without Fyn overexpression in the retinal neurons by GMR-Gal4 driver and found that WT Tau overexpression caused rough eye phenotype (figure 45) which was increased by the presence of the Fyn. We analysed age dependent degeneration and concluded that presence of the Fyn was further deteriorating the ommatidia arrangement (yellow arrows in Fyn presence with Tau) (figure 45). For quantifying the eye degeneration, we analysed the *Drosophila* eye through SEM. We counted the percentage of the ommatidia with IOBs as a measure of the degeneration in the neurons (Chen et al., 2011; Yeh et al., 2010). We found the loss of interommatidial bristles due to neurodegeneration which was rescued partially by blocking the Fynmediated phosphorylation at Y18 (Tau Y18F) and Fyn interaction to Tau (Tau P216A-P219A) (figure 46A and C) in young adult flies. At the age of 10-day old in adult flies, there was improvement in percentage of ommatidia with IOBs but statistically non-significant. Taking

together SEM analysis tells that reduction in Fyn mediated hyperphosphorylation of Tau at Y18 and reduction in Fyn interaction with Tau significantly reduces the Tau mediated toxicity in *Drosophila* eye model.

Overexpression of Tau causes dysfunction of the retinal neurons which can be analysed through ERGs (Chiasseu et al., 2017; Dolph et al., 2014). We crossed WT and mutant Tau expressing flies with GMR-Gal4 and progenies were used for ERG. In consistent with established literature (Chiasseu et al., 2017; Chouhan et al., 2016), we found that overexpression of WT Tau reduces on transient, off transients and receptor potential (figure 47). Reducing the Fyn interaction with Tau (Tau P216A-P219A) significantly rescues the effect of the WT Tau and improves the on transients in both young and aged flies (figure47). This further supports that reducing the Fyn interaction with Tau reduces the Tau mediated neurotoxicity and the functional interaction of the Tau with Fyn is sufficient for inducing toxicity. In consistent with previous findings of that Fyn may induce the local somatic accumulation of the hyperphosphorylated Tau leading to toxicity (Li and Götz, 2017c; Yin et al., 2021).

Drosophila C4da neurons is a widely used model to study the pathogenetic mechanisms of neurodegeneration (Iseki et al., 2001; Sáchez-Soriano et al., 2007; Zschätzsch et al., 2014). Tau overexpression leads to the dendritic degeneration (Ittner and Ittner, 2018; Lars M Ittner et al., 2010; Thies and Mandelkow, 2007; Urbanska et al., 2008). To study the dendritic degeneration, we have overexpressed Tau and its mutants in the C4da (dendritic arborization) neurons with PPK-Gal4, and found that WT Tau overexpression leads to the total loss of distal dendrites and less or no arborization (figure 48 A). Blocking the Fyn mediated phosphorylation at Y18 and Fyn interaction to Tau rescued the toxic effects of the Tau as seen by quantification of dendritic lengths (figure 48B), dendritic arbor surface area (figure 48C) and number of dendritic branches (figure 48C). To analyze the branching complexity and arborization of the neurons we used Strahler analysis, and found that as consistent with previous quantification, blocking the Fyn mediated Tau phosphorylation (Tau Y18F) and reducing the Tau interaction with Fyn (Tau P216A and Tau P216A-P219A) significantly increases the branching pattern of the neurons (figure 48F). WT Tau overexpression resulted in the loss of tertiary and quaternary dendrites (figure 48F2 and 48G) whereas Tau Y18F (figure 48F3) and Tau P216A (figure 48F4), Tau P216A-P219A (figure 48F5) overexpression had increased number of the tertiary and quaternary dendrites (figure 45F, 48G) compared to the WT Tau expression alone. Tau is

important for translocation of the Fyn to the dendrites (Lars M. Ittner et al., 2010c), in consistent with this, probably absence of the Fyn interaction with Tau and Fyn mediated Y18 phosphorylation, did not allow translocation of the overexpressed Tau to the dendrites which lead to the normal arborization of the neurons. Currently we are repeating and checking the effects C4da neurons arborization in the Fyn overexpression also which will help us for better understanding of the effect of functional interaction of Tau and Fyn in Tau mediated neurotoxicity.

To study the downstream signalling cascade or pathways and their molecular players affected by the Tau and Fyn mediated dendritic degeneration, we wanted to check the levels of the Rho family GTPases Rho1 and Rac1 as their levels are altered in AD brain (Zhao et al., 2006) and AD mouse model (Huesa et al., 2010), but their role in Tau neurotoxicity is not known. We studied the levels of the Rho1 and Rac1 GTPases in Tau and Fyn overexpressing flies. Till date we are repeating this experiment for final conclusions but in the initial experiment results we found a possible increase in the Rho1 (figure 49A) in Tau overexpressing flies which is reduced back to control levels when we inhibit the Fyn mediated Y18 phosphorylation (Tau Y18F) and reduce the Fyn interaction with Tau (Tau P216A and P216A-P219A Tau) (figure 49A). Although we did not find a possible significant change in the Rac1 levels when compared with the control (figure 49B) but the levels of Rac1 were increased more than control and Tau overexpression levels by inhibiting the Fyn mediated phosphorylation at Y18 (Tau Y18F) and Fyn interaction to Tau (Tau P216A and P216A-P219A Tau) (figure 49B). In one attempt of the experiment with Fyn and Tau overexpressing flies, we got a hint that there may be an increase in the Rho1 protein levels which are reduced when the Tau and Fyn interaction is reduced (figure 49C). These initial results gave us a glimpse of increased Rho1 levels and simultaneously reduction in the Rac1 levels in Tau mediated neurotoxicity which may be leading to the disintegrated cytoskeleton and degeneration of the neurons. We are repeating the experiments and blotting for Rho1 and Rac1 for supporting our initial observations and conclusions.

3. Repurposing the drugs used in oncotherapy for checking the neuroprotective effects in *Drosophila* model of AD.

For checking the effects of the drugs used in oncotherapy on the Tau toxicity, we overexpressed WT Tau in the *Drosophila* eyes with GMR Gal4. Age synchronized larvae were treated with different concentrations of the compounds thrice, at each instar stage as mentioned

in section 2.2.18 of materials and methods. For getting initial expression of the effects of the compounds in the eye surface morphology and primary screening of the compounds, we did full eye imaging and calculated the percentage of the degenerated (fused and rough ommatidia) surface area with the help of Infinity Analyze software, and compared among different concentrations of the compounds as well as controls (figure 50). We found that compound 1 (figure 50A and A'), compound 3(figure 50C and C'), compound 5 (figure 50E and E'), compound 7 (figure 50G) and compound 8 (figure 50H) treatment in the larval stages significantly reduced the degenerated area in the eyes. To confirm it further, we did scanning electron microscopy (SEM) imaging for analysing the surface morphology of the compound treated and untreated flies (figure 51). We chose one concentration which had the best significance values from the three we used in the light microscopy (Table no.5). SEM analysis further confirmed the protective effects of the compounds on the WT Tau toxicity. We found that compound 1 (figure 51c1, c2 and c3), compound 3 (figure 51d1, d2 and d3), compound 5 (figure 51e1, 51e2 and 51e3), compound 7 (figure 51g1, 51g2 and 51g3) and compound 8 (figure 51f1, 51f2 and 51f3), decreased the Tau mediated toxicity in the *Drosophila* eyes. But we found that the compound 7 and compound 8 being the most consistent and had significant reduction in the Tau neurotoxicity. To further study these protective effects of these two compounds (compound 7 and compound 8) treatment on the WT Tau toxicity on neuronal functions we recorded the Electroretinograms (ERGs) and checked the synaptic transmission between photoreceptor cells and retinal laminar neurons (figure 52). We found that compound 7 and compound 8 significantly increased the receptor potential and on-transients in WT Tau overexpressing flies (figure 52B). As these compounds are already established and being used in oncotherapy, our *in vivo* evidences for the protective effects on the Tau toxicity will help in progress of these compounds for repurposing them as a possible treatment strategy for the AD and Tauopathies.

Chapter 5: Conclusions

We successfully generated *Drosophila* AD models for studying the pathogenic role of Y18 phosphorylation of Tau, and Fyn interaction in Tau-Fyn mediated neurodegeneration in AD. WT Tau overexpression reduced the *Drosophila* locomotion in aged flies, causes rough eye, loss of IOBs and reduction in the synaptic transmission which is improved by reducing the Fyn interaction and Y18 phosphorylation of Tau. WT Tau overexpression in C4da neurons simplified branching complexity and reduced arborization which is rescued by reducing the phosphorylation of the Tau at Y18 and Fyn interaction. WT Tau overexpression may disturb the Rho1 and Rac1 homeostasis by increasing the Rho1 levels and reducing the Rac1 levels as an effector downstream pathway of Tau and Fyn mediated neurodegeneration in AD. Also, we screened 8 onco-therapeutic compounds and found that compound 7 and compound 8 has protective effects against Tau mediated toxicity.

Our study highlights the pathogenic role of one single tyrosine phosphorylation of Y18 and Fyn binding to Tau in Tau mediated neurodegeneration in AD.

APPENDIX

Matlab program codes for processing ERG recording data

Following matlab programs were used for analysing the ERG recordings using matlab software. Three different codes were written to read the data, processing of the data and exporting the graphs and data sheets.

```
%To analyse EAG
STRAINS={'WC'
                   %Short form for types.
        'WTT'
       'Y18F'
       'P216219T'
       'Fyn'
       'FWTT'
       'F18T'
       'F216T'
       'F216219T'}
% Age File name Genotype
                                                  Type in shortfom
                              Date
Used for check Age
                         Repeat
% 1 Day WC1 1
              Control Aug 06, 2011, Sat WC
                                                                      1
Fs=10000;
[NUMs TXT MSC]=xlsread('Tau_Fyn','Tau_Fyn'); %Reading the XL sheet
% NUMs=NUMs(:,end-2:end);
                                                    %Making sure the last
% three columns are used
NUMs=NUMs';
             %Reshaping the matrix
% ROOTf='D:\files\Ravi Kant\ERGs\ERGs For Compounds\' %Root folder
ROOTf='D:\files\Ravi Kant\ERGs in SLS\RKY May 2023\mat files\'
for n=1:size(TXT,1) %Over all sets
 if NUMs(1,n) == 1 %If the recording is to be used.
     try
      [X] = read_data_tet_setup_multi([ROOTf TXT{n,4} '/experiment/'
TXT{n,2}],6,10,1,[]); %Read the file.
     catch
      trv
       [X] = read data tet setup multi([ROOTf TXT{n,4} '/experiment/'
TXT\{n,2\}], 6, 9, 1, []); %Read the file for 9 trial case.
```

```
catch
       clear X; %To take care of non uniform trial lengths like on May
07
       for trl=1:10
         X tmp= read data tet setup multi([ROOTf TXT{n,4} '/experiment/'
TXT{n,2}],6,10,1,setdiff((1:10),trl));
         X(trl,:)=X_tmp(1:15*15000);
       end
      end
     end
   N trl=10;
   X=heka read([ROOTf TXT{n,2}],N trl);
   X=X'/10;
     X=(X*5/(2^15))/1000; %Sacling to convert the integers from the DAQ to
voltage
   X=X-median(X(:,1:19000)')'*ones(1,size(X,2)); %Removing the based line
shift by sbtracting the baseline
   X=filtfilt(ones(12,1)/2,1,X')'; %Smoothening the waveform
   [GD]=check traces and mean(X,10000:19000,Fs,25); %Check if the waveform
is OK
   title(FLE); %Showing the file name details
   if length(GD) == 1
       MN=X(GD,:);
   else
       MN=mean(X(GD,:)); %Mean of the good trials
   end
   axis([1 7 -0.05 0.01]);
   ONon=round (30000*10/15)+10000;
   ONoff=round(31500*10/15)+10000;
   RPon=round(40500*10/15)+10000;
   RPoff=round(43500*10/15)+10000;
   OFFon=round(45000*10/15)+10000;
   OFFoff=round(47250*10/15)+10000;
   [ONRESP(n) IDX] = max(MN(ONon:ONoff));
                                          %Findind the nean ON
   plot((ONon+IDX-1)/Fs,ONRESP(n),'yo'); %Ploting the ON response value
and locations
    [RP(n)] = mean(MN(RPon:RPoff));
                                           %Mean receptor potential
```

```
plot((round(52750*10/15))/Fs,RP(n),'yo');
                                                                                                                                                                                                                                                    %Indicating the
receptor potential value
                                                                                                                                                                                                            %Finding the OFF response
                  [OFFRESP(n) IDX] = min(MN(OFFon:OFFoff));
                 plot((OFFon+IDX-1)/Fs,OFFRESP(n),'yo'); %Indicating the mean OFF
response
                 OFFRESP(n) = OFFRESP(n) - RP(n);
                                                                                                                                                                     %Calculating the OFF
reponse from receptor potential
             % INs=input('1 if NOT OK, else press ENTER'); %if the traces and
calculations are OK
                 INs=[];
            if isempty(INs) & ~isempty(GD)
                                                                                                                                                                                                                                                                         %If ERG is OK
                          GDset(n)=1;
                                                                                                                                                                                                        %Mark as OK
                          try %Try concatenating
 \texttt{GOOD}\{\texttt{find}(\texttt{strcmp}(\texttt{TXT}\{\texttt{n},5\},\texttt{STRAINS})), \texttt{NUMs}(\texttt{2},\texttt{n}), \texttt{NUMs}(\texttt{3},\texttt{n})\} = [\texttt{GOOD}\{\texttt{find}(\texttt{strcmp}(\texttt{n},5),\texttt{n})\} = [\texttt{GOOD}(\texttt{num}(\texttt{num}(\texttt{num}(\texttt{num}(\texttt{num}(\texttt{num}(\texttt{num}(\texttt{num}(\texttt{num}(\texttt{num}(\texttt{num}(\texttt{num}(\texttt{num}(\texttt{num}(\texttt{num}(\texttt{num}(\texttt{num}(\texttt{num}(\texttt{num}(\texttt{num}(\texttt{num}(\texttt{num}(\texttt{num}(\texttt{num}(\texttt{num}(\texttt{num}(\texttt{num}(\texttt{num}(\texttt{num}(\texttt{num}(\texttt{num}(\texttt{num}(\texttt{num}(\texttt{num}(\texttt{num}(\texttt{num}(\texttt{num}(\texttt{num}(\texttt{num}(\texttt{num}(\texttt{num}(\texttt{num}(\texttt{num}(\texttt{num}(\texttt{num}(\texttt{num}(\texttt{num}(\texttt{num}(\texttt{num}(\texttt{num}(\texttt{num}(\texttt{num}(\texttt{num}(\texttt{num}(\texttt{num}(\texttt{num}(\texttt{num}(\texttt{num}(\texttt{num}(\texttt{num}(\texttt{num}(\texttt{num}(\texttt{num}(\texttt{num}(\texttt{num}(\texttt{num}(\texttt{num}(\texttt{num}(\texttt{num}(\texttt{num}(\texttt{num}(\texttt{num}(\texttt{num}(\texttt{num}(\texttt{num}(\texttt{num}(\texttt{num}(\texttt{num}(\texttt{num}(\texttt{num}(\texttt{num}(\texttt{num}(\texttt{num}(\texttt{num}(\texttt{num}(\texttt{num}(\texttt{num}(\texttt{num}(\texttt{num}(\texttt{num}(\texttt{num}(\texttt{num}(\texttt{num}(\texttt{num}(\texttt{num}(\texttt{num}(\texttt{num}(\texttt{num}(\texttt{num}(\texttt{num}(\texttt{num}(\texttt{num}(\texttt{num}(\texttt{num}(\texttt{num}(\texttt{num}(\texttt{num}(\texttt{num}(\texttt{num}(\texttt{num}(\texttt{num}(\texttt{num}(\texttt{num}(\texttt{num}(\texttt{num}(\texttt{num}(\texttt{num}(\texttt{num}(\texttt{num}(\texttt{num}(\texttt{num}(\texttt{num}(\texttt{num}(\texttt{num}(\texttt{num}(\texttt{num}(\texttt{num}(\texttt{num}(\texttt{num}(\texttt{num}(\texttt{num}(\texttt{num}(\texttt{num}(\texttt{num}(\texttt{num}(\texttt{num}(\texttt{num}(\texttt{num}(\texttt{num}(\texttt{num}(\texttt{num}(\texttt{num}(\texttt{num}(\texttt{num}(\texttt{num}(\texttt{num}(\texttt{num}(\texttt{num}(\texttt{num}(\texttt{num}(\texttt{num}(\texttt{num}(\texttt{num}(\texttt{num}(\texttt{num}(\texttt{num}(\texttt{num}(\texttt{num}(\texttt{num}(\texttt{num}(\texttt{num}(\texttt{num}(\texttt{num}(\texttt{num}(\texttt{num}(\texttt{num}(\texttt{num}(\texttt{num}(\texttt{num}(\texttt{num}(\texttt{num}(\texttt{num}(\texttt{num}(\texttt{num}(\texttt{num}(\texttt{num}(\texttt{num}(\texttt{num}(\texttt{num}(\texttt{num}(\texttt{num}(\texttt{num}(\texttt{num}(\texttt{num}(\texttt{num}(\texttt{num}(\texttt{num}(\texttt{num}(\texttt{num}(\texttt{num}(\texttt{num}(\texttt{num}(\texttt{num}(\texttt{num}(\texttt{num}(\texttt{num}(\texttt{num}(\texttt{num}(\texttt{num}(\texttt{num}(\texttt{num}(\texttt{num}(\texttt{num}(\texttt{num}(\texttt{num}(\texttt{num}(\texttt{num}(\texttt{num}(\texttt{num}(\texttt{num}(\texttt{num}(\texttt{num}(\texttt{num}(\texttt{num}(\texttt{num}(\texttt{num}(\texttt{num}(\texttt{num}(\texttt{num}(\texttt{num}(\texttt{num}(\texttt{num}(\texttt{num}(\texttt{num}(\texttt{num}(\texttt{num}(\texttt{num}(\texttt{num}(\texttt{num}(\texttt{num}(\texttt{num}(\texttt{num}(\texttt{num}(\texttt{num}(\texttt{num}(\texttt{num}(\texttt{num}(\texttt{num}(\texttt{num}(\texttt{num}(\texttt{num}(\texttt{num}(\texttt{num}(\texttt{num}(\texttt{num}(\texttt{num}(\texttt{num}(\texttt{num}(\texttt{num}(\texttt{num}(\texttt{num}(\texttt{num}(\texttt{num}(\texttt{num}(\texttt{num}(\texttt{num}(\texttt{num}(\texttt{num}(\texttt{num}(\texttt{num}(\texttt{num}(\texttt{num}(\texttt{num}(\texttt{num}(\texttt{num}(\texttt{num}(\texttt{num}(\texttt{num}(\texttt{num}(\texttt{num}(\texttt{n
TXT\{n,5\}, STRAINS)), NUMs(2,n), NUMs(3,n)}; [ONRESP(n) RP(n) OFFRESP(n)];
%Storing response parameters in
GOODMN{find(strcmp(TXT{n,5},STRAINS)),NUMs(2,n),NUMs(3,n)}=[GOODMN{find(str
cmp(TXT\{n, 5\}, STRAINS)), NUMs(2, n), NUMs(3, n); MN];
                          catch % Else if it is the first set
GOOD\{find(strcmp(TXT\{n,5\},STRAINS)),NUMs(2,n),NUMs(3,n)\}(1,:)=[ONRESP(n)]
RP(n) OFFRESP(n)];
                                  GOODMN\{find(strcmp(TXT\{n,5\},STRAINS)),NUMs(2,n),NUMs(3,n)\}(1,:)=MN;
                 else
                         GDset(n)=0;
                 end
         end
end
figure(2)
clf
subplot(311);
MN1s=[];
SEM1s=[];
MN2s=[];
SEM2s=[];
MN3s=[];
SEM3s=[];
cnt=0; %Total number of bars
```

```
DAYS=[1 10 20 30];
% SEM2all=[];
% for n=1:size(GOOD,1) %Over phenotype
    for m=1:size(GOOD,2) %Over age
      for k=1:size(GOOD, 3) %Over culture repeats
        SEM2all(end+1,1:3) = [n m k];
응
      if ~isempty(GOOD{n,m,k})
ջ
      SEM2all(end, 4:3+size(GOOD{n,m,k}(:,2),1))=GOOD{n,m,k}(:,2)';
      else
응
        [n m k]
응 응
          SEM2all(end, 1) = 0;
      end
응
      if ~isempty(GOOD{n,m,k})
응
        MN1s=[MN1s mean(GOOD{n,m,k}(:,1))];
응
        SEM1s = [SEM1s std(GOOD\{n, m, k\}(:, 1))/size(GOOD\{n, m, k\}(:, 1), 1)^0.5];
        MN2s = [MN2s mean(GOOD{n,m,k}(:,2))];
        SEM2s = [SEM2s std(GOOD{n,m,k}(:,2))/size(GOOD{n,m,k}(:,2),1)^0.5];
        MN3s = [MN3s mean(GOOD{n,m,k}(:,3))];
        SEM3s = [SEM3s std(GOOD{n,m,k}(:,3))/size(GOOD{n,m,k}(:,3),1)^0.5];
        cnt=cnt+1;
        XLABELS{cnt}=[STRAINS{n} 'd' num2str(DAYS(m)) 'r' num2str(k)];
%Geenrating xlabel for bars for each condition
      end
      end
    end
% end
% bar(MN1s)
% save -ascii SEM2all.txt SEM2all
SEM2ON=[];
SEM2RP=[];
SEM2OFF=[];
for n=1:size(GOOD,1) %Over phenotype
  for m=1:size(GOOD,2) %Over age
    for k=1:size(GOOD,3) %Over culture repeats
      SEM2ON (end+1,1:3) = [n m k];
      SEM2RP(end+1,1:3) = [n m k];
      SEM2OFF (end+1,1:3) = [n m k];
    if ~isempty(GOOD{n,m,k})
      SEM2ON(end, 4:3+size(GOOD{n,m,k}(:,2),1))=GOOD{n,m,k}(:,1)';
```

```
SEM2RP(end, 4:3+size(GOOD\{n,m,k\}(:,2),1))=GOOD\{n,m,k\}(:,2)';
      SEM2OFF (end, 4:3+size (GOOD \{n, m, k\} (:, 2), 1)) = GOOD \{n, m, k\} (:, 3)';
    else
      [n m k]
        SEM2all(end, 1) = 0;
    end
    if ~isempty(GOOD{n,m,k})
      MN1s=[MN1s mean(GOOD{n,m,k}(:,1))];
      SEM1s = [SEM1s std(GOOD\{n, m, k\}(:, 1))/size(GOOD\{n, m, k\}(:, 1), 1)^0.5];
      MN2s = [MN2s mean(GOOD{n,m,k}(:,2))];
      SEM2s = [SEM2s \ std(GOOD\{n,m,k\}(:,2))/size(GOOD\{n,m,k\}(:,2),1)^0.5];
      MN3s = [MN3s mean(GOOD{n,m,k}(:,3))];
      SEM3s = [SEM3s std(GOOD{n,m,k}(:,3))/size(GOOD{n,m,k}(:,3),1)^0.5];
      cnt=cnt+1:
      XLABELS{cnt}=[STRAINS{n} 'd' num2str(DAYS(m)) 'r' num2str(k)];
%Geenrating xlabel for bars for each condition
    end
    end
  end
end
bar (MN1s)
save -ascii SEM2ON.txt SEM2ON;
save -ascii SEM2RP.txt SEM2RP;
save -ascii SEM2OFF.txt SEM2OFF;
 bar([mean(GOOD{1,1}(:,1)) mean(GOOD{2,1}(:,1)) mean(GOOD{3,1}(:,1)) 
mean (GOOD{4,1}(:,1))...
      mean(GOOD{1,2}(:,1)) mean(GOOD{2,2}(:,1)) mean(GOOD{3,2}(:,1))
mean(GOOD\{4,2\}(:,1))]');
hold on;
errorbar(MN1s, SEM1s, '.');
% errorbar([mean(GOOD{1,1}(:,1)) mean(GOOD{2,1}(:,1)) mean(GOOD{3,1}(:,1))
mean (GOOD{4,1}(:,1))...
      mean(GOOD\{1,2\}(:,1)) mean(GOOD\{2,2\}(:,1)) mean(GOOD\{3,2\}(:,1))
mean (GOOD{4,2}(:,1))]',...
      [std(GOOD{1,1}(:,1))/size(GOOD{1,1}(:,1),1)^0.5]
std(GOOD\{2,1\}(:,1))/size(GOOD\{2,1\}(:,1),1)^0.5...
      std(GOOD{3,1}(:,1))/size(GOOD{3,1}(:,1),1)^0.5
std(GOOD\{4,1\}(:,1))/size(GOOD\{4,1\}(:,1),1)^0.5...
      std(GOOD\{1,2\}(:,1))/size(GOOD\{1,2\}(:,1),1)^0.5
std(GOOD{2,2}(:,1))/size(GOOD{2,2}(:,1),1)^0.5...
```

```
std(GOOD{3,2}(:,1))/size(GOOD{3,2}(:,1),1)^0.5
std(GOOD\{4,2\}(:,1))/size(GOOD\{4,2\}(:,1),1)^0.5]','.');
title('ON')
subplot(312);
bar (MN2s);
 bar([mean(GOOD{1,1}(:,2)) mean(GOOD{2,1}(:,2)) mean(GOOD{3,1}(:,2)) 
mean(GOOD{4,1}(:,2))...
      mean(GOOD\{1,2\}(:,2)) mean(GOOD\{2,2\}(:,2)) mean(GOOD\{3,2\}(:,2))
mean(GOOD\{4,2\}(:,2))]');
hold on;
errorbar(MN2s,SEM2s,'.');
% errorbar([mean(GOOD{1,1}(:,2)) mean(GOOD{2,1}(:,2)) mean(GOOD{3,1}(:,2))
mean (GOOD{4,1}(:,2))...
      mean(GOOD\{1,2\}(:,2)) mean(GOOD\{2,2\}(:,2)) mean(GOOD\{3,2\}(:,2))
mean (GOOD{4,2}(:,2))]',...
      [std(GOOD{1,1}(:,2))/size(GOOD{1,1}(:,2),1)^0.5]
std(GOOD{2,1}(:,2))/size(GOOD{2,1}(:,2),1)^0.5...
      std(GOOD{3,1}(:,2))/size(GOOD{3,1}(:,2),1)^0.5
std(GOOD\{4,1\}(:,2))/size(GOOD\{4,1\}(:,2),1)^0.5...
      std(GOOD\{1,2\}(:,2))/size(GOOD\{1,2\}(:,2),1)^0.5
std(GOOD\{2,2\}(:,2))/size(GOOD\{2,2\}(:,2),1)^0.5...
      std(GOOD{3,2}(:,2))/size(GOOD{3,2}(:,2),1)^0.5
std(GOOD\{4,2\}(:,2))/size(GOOD\{4,2\}(:,2),1)^0.5]','.');
title('RP')
subplot(313);
bar (MN3s);
% bar([mean(GOOD{1,1}(:,3)) mean(GOOD{2,1}(:,3)) mean(GOOD{3,1}(:,3))
mean (GOOD{4,1}(:,3))...
     mean(GOOD\{1,2\}(:,3)) mean(GOOD\{2,2\}(:,3)) mean(GOOD\{3,2\}(:,3))
mean (GOOD{4,2}(:,3))]');
hold on:
errorbar(MN3s,SEM3s,'.');
% errorbar([mean(GOOD{
% errorbar([mean(GOOD{1,1}(:,3)) mean(GOOD{2,1}(:,3)) mean(GOOD{3,1}(:,3))
mean (GOOD{4,1}(:,3))...
      mean(GOOD\{1,2\}(:,3)) mean(GOOD\{2,2\}(:,3)) mean(GOOD\{3,2\}(:,3))
mean (GOOD{4,2}(:,3))]',...
      [std(GOOD{1,1}(:,3))/size(GOOD{1,1}(:,3),1)^0.5]
std(GOOD\{2,1\}(:,3))/size(GOOD\{2,1\}(:,3),1)^0.5...
      std(GOOD{3,1}(:,3))/size(GOOD{3,1}(:,3),1)^0.5
std(GOOD\{4,1\}(:,3))/size(GOOD\{4,1\}(:,3),1)^0.5...
```

```
std(GOOD{1,2}(:,3))/size(GOOD{1,2}(:,3),1)^0.5
std(GOOD{2,2}(:,3))/size(GOOD{2,2}(:,3),1)^0.5...
      std(GOOD{3,2}(:,3))/size(GOOD{3,2}(:,3),1)^0.5
      std(GOOD{4,2}(:,3))/size(GOOD{4,2}(:,3),1)^0.5]','.')
set(gca,'xticklabel',{[]})
for n=1:length(XLABELS)
    hd=text(n,-0.035,XLABELS\{n\});
    set(hd,'Rotation',90);
end
%set(gca,'XTickLabel',XLABELS)
% bar([mean(GOOD{1}(:,3)) mean(GOOD{2}(:,3)) mean(GOOD{3}(:,3))
mean(GOOD\{4\}(:,3))]);
% hold on;
% errorbar([mean(GOOD{1}(:,3)) mean(GOOD{2}(:,3)) mean(GOOD{3}(:,3))
mean(GOOD{4}(:,3))],...
          [std(GOOD{1}(:,3))/size(GOOD{1}(:,3),1)^0.5]
std(GOOD{2}(:,3))/size(GOOD{2}(:,3),1)^0.5...
      std(GOOD{3}(:,3))/size(GOOD{3}(:,3),1)^0.5
std(GOOD{4}(:,3))/size(GOOD{4}(:,3),1)^0.5],'.');
figure(3)
clf
figure(5)
clf;
figure(4)
clf
CLRs=jet(size(GOODMN,1)*size(GOODMN,2));
CLRlst=['krgb'];
for m=1:size(GOODMN,1)
    for n=1:size(GOODMN,2)
       MNtmpplt=0;
       cnttmp=0;
       MNtmpplt all=[];
       for k=1:size(GOODMN,3)
         if (size(GOODMN\{m,n,k\},1)>1)
           MNtmpplt=MNtmpplt+mean(GOODMN{m,n,k});
           MNtmpplt all=[MNtmpplt all;mean(GOODMN{m,n,k})];
           cnttmp=cnttmp+1;
         end
       end
       figure(3)
```

```
subplot(size(GOODMN,1), size(GOODMN,2), size(GOODMN,2) * (m-1)+n);
       plot((0:length(MNtmpplt)-1)/15000,MNtmpplt all','b');
       hold on
       plot((0:length(MNtmpplt)-1)/15000,MNtmpplt/cnttmp,'r');
       axis([1 5 -0.035 0.005]);
       if n==1
           ylabel(STRAINS{m});
       end
       if m==1
           title(num2str(DAYS(n)));
       end
       figure(5)
       subplot(size(GOODMN,1), size(GOODMN,2), size(GOODMN,2) * (m-1)+n);
       plot((0:length(MNtmpplt)-1)/15000,MNtmpplt/cnttmp,'r');
       axis([1 5 -0.035 0.005]);
       figure(4)
         subplot(size(GOODMN,1),1,m);
응
       subplot(1, size(GOODMN, 1), m);
       hold on
       plot((0:length(MNtmpplt)-1)/15000,MNtmpplt/cnttmp,CLRlst(n));
       axis([1 5 -0.035 0.005]);
    end
end
% for m=1:size(GOODMN,1)
      for n=1:size(GOODMN,2)
         plot((0:size(X,2)-1)/15000,GOODMN\{m,n\}','Color',CLRs((m-1)))
1) *size(GOODMN,2)+n,:));
         hold on
      end
% end
% legend(XLABELS);
```

Matlab code for reading Heka file:

```
function [X]=heka_read(FNM,N_trl)
eval(['load ''' FNM '.mat'';']);
[Bn An]=iirnotch([50]/5000,1/5000);
% [B A]=butter(2,[100]/5000);
for n=1:N_trl
    try
```

```
eval(['X(:,' num2str(n) ')=filtfilt(Bn,An,Trace_1_1_' num2str(n)
'_1(:,2));'])
    catch
        eval(['X(:,' num2str(n) ')=filtfilt(Bn,An,Trace_1_2_' num2str(n)
'_1(:,2));'])
    end
end
% plot((0:size(y,1)-1)/10000,y,'b')
% hold on
% plot((0:size(y,1)-1)/10000,mean(y'),'r')
```

Matlab program code to check traces and mean:

```
%Function to examine traces like EAG, LFP and finding good trials aftre
%removing DC.
%[GD]=check traces and mean(X,WINDOW,Fs,THRESH)
       -> Vector containing the list of good trials
응GD
       -> Matrix whose rows are the trials
%WINDOW -> The index of the points to be used for subtracting the mean.
       -> Sampling frequency
%THRESH -> Scalng for threshold for comparing median with SD. Use 3 by
%default
function [GD]=check traces and mean(X,WINDOW,Fs,THRESH)
     MED=median(mean(X(:,WINDOW))); %Takin median of trials in the window
     GD=find(abs(mean(X(:,WINDOW)')-
MED) < THRESH * median (std(X(:, WINDOW)'))); % Find if any points is greater
than the median (true) std *THRESH
   MED=median(X); %Takin median of trials
    GD=find(max(abs(X-
ones(size(X,1),1)*MED)')<THRESH*median(std(X(:,WINDOW)'))); %Find if any
points is greater than the median (true) std *THRESH
   figure(124)
   plot((0:size(X,2)-1)/Fs,X','b');
   hold on;
   plot((0:size(X,2)-1)/Fs,median(X),'r');
   try
     plot((0:size(X,2)-1)/Fs,(X(GD,:)),'k');
      plot((0:size(X,2)-1)/Fs,mean(X(GD,:)),'g');
```

catch

end

MN=mean(X(find(GD),:));
 xlabel('Time (sec)');
 ylabel('Variable (V)');

axis([1 7 -0.03 0.01]);

REFERENCES

- Aguilar, B.J., Zhu, Y., Lu, Q., 2017. Rho GTPases as therapeutic targets in Alzheimer's disease. Alzheimer's Res. Ther. 9, 1–10. https://doi.org/10.1186/s13195-017-0320-4
- Alawi, A.A., Pak, W.L., 1971. On-transient of insect electroretinogram: Its cellular origin. Science (80-.). 172, 1055–1057. https://doi.org/10.1126/science.172.3987.1055
- Arya, R., Lakhotia, S.C., 2006. A simple nail polish imprint technique for examination of external morphology of Drosophila eyes. Curr. Sci. 90, 1179–1180.
- Baloyannis, S.J., 2009. Dendritic pathology in Alzheimer's disease. J. Neurol. Sci. 283, 153–157. https://doi.org/10.1016/j.jns.2009.02.370
- Basler, K., Bischof, J., Maeda, R.K., Hediger, M., 2007. An optimized transgenesis system for Drosophila using germ-line-specific □ C31 integrases.
- Basurto-Islas, G., Luna-Muñoz, J., Guillozet-Bongaarts, A.L., Binder, L.I., Mena, R., García-Sierra, F., 2008. Accumulation of aspartic acid421- and glutamic acid 391-cleaved tau in neurofibrillary tangles correlates with progression in Alzheimer disease. J. Neuropathol. Exp. Neurol. 67, 470–483. https://doi.org/10.1097/NEN.0b013e31817275c7
- Belusic, G., 2011. ERG in Drosophila, in: Electroretinograms. InTech. https://doi.org/10.5772/21747
- Bhaskar, K., Hobbs, G.A., Yen, S.-H., Lee, G., 2010. Tyrosine phosphorylation of tau accompanies disease progression in transgenic mouse models of tauopathy. Neuropathol. Appl. Neurobiol. 36, 462–77. https://doi.org/10.1111/j.1365-2990.2010.01103.x
- Bhaskar, K., Yen, S.H., Lee, G., 2005. Disease-related modifications in tau affect the interaction between Fyn and tau. J. Biol. Chem. 280, 35119–35125. https://doi.org/10.1074/jbc.M505895200
- Bischof, J., Maeda, R.K., Hediger, M., Karch, F., Basler, K., 2007. An optimized transgenesis system for Drosophila using germ-line-specific C31 integrases. Proc. Natl. Acad. Sci. 104, 3312–3317. https://doi.org/10.1073/pnas.0611511104
- Boggon, T.J., Eck, M.J., 2004. Structure and regulation of Src family kinases. Oncogene 23, 7918–7927. https://doi.org/10.1038/sj.onc.1208081

- Bolognin, S., Lorenzetto, E., Diana, G., Buffelli, M., 2014. The Potential Role of Rho GTPases in Alzheimer's Disease Pathogenesis. Mol. Neurobiol. 50, 406–422. https://doi.org/10.1007/s12035-014-8637-5
- Bolus, H., Crocker, K., Boekhoff-Falk, G., Chtarbanova, S., 2020. Modeling Neurodegenerative Disorders in Drosophila melanogaster. Int. J. Mol. Sci. 2020, Vol. 21, Page 3055 21, 3055. https://doi.org/10.3390/IJMS21093055
- Bondi, M.W., Edmonds, E.C., Salmon, D.P., 2017. Alzheimer's Disease: Past, Present, and Future. J. Int. Neuropsychol. Soc. 23, 818. https://doi.org/10.1017/S135561771700100X
- Bordji, K., Becerril-Ortega, J., Nicole, O., Buisson, A., 2010. Activation of extrasynaptic, but not synaptic, NMDA receptors modifies amyloid precursor protein expression pattern and increases amyloid-β production. J. Neurosci. 30, 15927–15942. https://doi.org/10.1523/JNEUROSCI.3021-10.2010
- Borin, M., Saraceno, C., Catania, M., Lorenzetto, E., Pontelli, V., Paterlini, A., Fostinelli, S., Avesani, A., Fede, G. Di, Zanusso, G., Benussi, L., Binetti, G., Zorzan, S., Ghidoni, R., Buffelli, M., Bolognin, S., 2018. Rac1 activation links tau hyperphosphorylation and Aß dysmetabolism in Alzheimer's disease. Acta Neuropathol. Commun. 6, 1–17. https://doi.org/10.1186/s40478-018-0567-4
- Braak, H., Braak, E., 1991. Neuropathological stageing of Alzheimer-related changes. Acta Neuropathol. 82, 239–259. https://doi.org/10.1007/BF00308809/METRICS
- Bramblett, G.T., Goedert, M., Jakes, R., Merrick, S.E., Trojanowski, J.Q., Lee, V.M.Y., 1993. Abnormal tau phosphorylation at Ser396 in alzheimer's disease recapitulates development and contributes to reduced microtubule binding. Neuron 10, 1089–1099. https://doi.org/10.1016/0896-6273(93)90057-X
- Buée, L., Bussière, T., Buée-Scherrer, V., Delacourte, A., Hof, P.R., 2000. Tau protein isoforms, phosphorylation and role in neurodegenerative disorders. Brain Res. Rev. https://doi.org/10.1016/S0165-0173(00)00019-9
- Bulbarelli, A., Lonati, E., Cazzaniga, E., Gregori, M., Masserini, M., 2009. Pin1 affects Tau phosphorylation in response to Aβ oligomers. Mol. Cell. Neurosci. 42, 75–80. https://doi.org/10.1016/j.mcn.2009.06.001
- Burridge, K., Wennerberg, K., 2004. Rho and Rac take center stage. Cell 116, 167-179.

- https://doi.org/10.1016/S0092-8674(04)00003-0
- Caillet-Boudin, M.L., Buée, L., Sergeant, N., Lefebvre, B., 2015. Regulation of human MAPT gene expression. Mol. Neurodegener. 10, 1–14. https://doi.org/10.1186/s13024-015-0025-8
- Cappelletti, G., Tedeschi, G., Maggioni, M.G., Negri, A., Nonnis, S., Maci, R., 2004. The nitration of τ protein in neurone-like PC12 cells. FEBS Lett. 562, 35–39. https://doi.org/10.1016/S0014-5793(04)00173-5
- Chabrier, M.A., Blurton-Jones, M., Agazaryan, A.A., Nerhus, J.L., Martinez-Coria, H., LaFerla, F.M., 2012. Soluble Aβ promotes wild-type tau pathology in vivo. J. Neurosci. 32, 17345–17350. https://doi.org/10.1523/JNEUROSCI.0172-12.2012
- Chan, H.Y.E., Bonini, N.M., 2000. Drosophila models of human neurodegenerative disease. Cell Death Differ. 2000 711 7, 1075–1080. https://doi.org/10.1038/sj.cdd.4400757
- Chen, H., Firestein, B.L., 2007. RhoA Regulates Dendrite Branching in Hippocampal Neurons by Decreasing Cypin Protein Levels. J. Neurosci. 27, 8378. https://doi.org/10.1523/JNEUROSCI.0872-07.2007
- Chen, R.J., Chang, W.W., Lin, Y.C., Cheng, P.L., Chen, Y.R., 2013. Alzheimer's amyloid-β oligomers rescue cellular prion protein induced tau reduction via the Fyn pathway. ACS Chem. Neurosci. https://doi.org/10.1021/cn400085q
- Chen, S., Li, B., Grundke-Iqbal, I., Iqbal, K., 2008. I1PP2A affects Tau phosphorylation via association with the catalytic subunit of protein phosphatase 2A. J. Biol. Chem. 283, 10513–10521. https://doi.org/10.1074/jbc.M709852200
- Chen, Y., Yang, M., Deng, J., Chen, X., Ye, Y., Zhu, L., Liu, J., Ye, H., Shen, Y., Li, Y., Rao, E.J., Fushimi, K., Zhou, X., Bigio, E.H., Mesulam, M., Xu, Q., Wu, J.Y., 2011. Expression of human FUS protein in Drosophila leads to progressive neurodegeneration. Protein Cell 2, 477–486. https://doi.org/10.1007/S13238-011-1065-7
- Chévez-Gutiérrez, L., Bammens, L., Benilova, I., Vandersteen, A., Benurwar, M., Borgers, M., Lismont, S., Zhou, L., Van Cleynenbreugel, S., Esselmann, H., Wiltfang, J., Serneels, L., Karran, E., Gijsen, H., Schymkowitz, J., Rousseau, F., Broersen, K., De Strooper, B., 2012. The mechanism of γ-Secretase dysfunction in familial Alzheimer disease. EMBO J. 31, 2261–2274. https://doi.org/10.1038/EMBOJ.2012.79

- Chiasseu, M., Alarcon-Martinez, L., Belforte, N., Quintero, H., Dotigny, F., Destroismaisons, L., Vande Velde, C., Panayi, F., Louis, C., Di Polo, A., 2017. Tau accumulation in the retina promotes early neuronal dysfunction and precedes brain pathology in a mouse model of Alzheimer's disease. Mol. Neurodegener. 12, 1–20. https://doi.org/10.1186/s13024-017-0199-3
- Chin, J., Palop, J.J., Puoliväli, J., Massaro, C., Bien-Ly, N., Gerstein, H., Scearce-Levie, K., Masliah, E., Mucke, L., 2005. Fyn kinase induces synaptic and cognitive impairments in a transgenic mouse model of Alzheimer's disease. J. Neurosci. 25, 9694–9703. https://doi.org/10.1523/JNEUROSCI.2980-05.2005
- Cho, J.-H., Johnson, G.V.W., 2003. Primed phosphorylation of tau at Thr231 by glycogen synthase kinase 3β (GSK3β) plays a critical role in regulating tau's ability to bind and stabilize microtubules. J. Neurochem. 88, 349–358. https://doi.org/10.1111/j.1471-4159.2004.02155.x
- Chouhan, A.K., Guo, C., Hsieh, Y.-C., Ye, H., Senturk, M., Zuo, Z., Li, Y., Chatterjee, S., Botas, J., Jackson, G.R., Bellen, H.J., Shulman, J.M., 2016. Uncoupling neuronal death and dysfunction in Drosophila models of neurodegenerative disease. Acta Neuropathol. Commun. 4, 62. https://doi.org/10.1186/s40478-016-0333-4
- Cochran, J.N., Hall, A.M., Roberson, E.D., 2014. The dendritic hypothesis for Alzheimer's disease pathophysiology. Brain Res. Bull. https://doi.org/10.1016/j.brainresbull.2013.12.004
- Congdon, E.E., Kim, S., Bonchak, J., Songrug, T., Matzavinos, A., Kuret, J., 2008. Nucleation-dependent tau filament formation: The importance of dimerization and an estimation of elementary rate constants. J. Biol. Chem. 283, 13806–13816. https://doi.org/10.1074/jbc.M800247200
- Cripps, D., Thomas, S.N., Jeng, Y., Yang, F., Davies, P., Yang, A.J., 2006. Alzheimer disease-specific conformation of hyperphosphorylated paired helical filament-Tau is polyubiquitinated through Lys-48, Lys-11, and Lys-6 ubiquitin conjugation. J. Biol. Chem. 281, 10825–10838. https://doi.org/10.1074/jbc.M512786200
- de Ruiter, J.P., Uylings, H.B.M., 1987. Morphometric and dendritic analysis of fascia dentata granule cells in human aging and senile dementia. Brain Res. 402, 217–229. https://doi.org/10.1016/0006-8993(87)90028-X

- Derkinderen, P., Scales, T.M.E., Hanger, D.P., Leung, K.Y., Byers, H.L., Ward, M.A., Lenz, C., Price, C., Bird, I.N., Perera, T., Kellie, S., Williamson, R., Noble, W., Van Etten, R.A., Leroy, K., Brion, J.P., Reynolds, C.H., Anderton, B.H., 2005. Tyrosine 394 is phosphorylated in Alzheimer's paired helical filament tau and in fetal tau with c-Abl as the candidate tyrosine kinase. J. Neurosci. 25, 6584–6593. https://doi.org/10.1523/JNEUROSCI.1487-05.2005
- Dolph, P., Nair, A., Raghu, P., 2011. Electroretinogram recordings of Drosophila. Cold Spring Harb. Protoc. 6. https://doi.org/10.1101/pdb.prot5549
- Dolph, P., Nair, A., Raghu, P., Dolph, P., Nair, A., Raghu, P., 2014. Electroretinogram Recordings of Drosophila Electroretinogram Recordings of Drosophila. https://doi.org/10.1101/pdb.prot5549
- Dowjat, W.K., Adayev, T., Kuchna, I., Nowicki, K., Palminiello, S., Hwang, Y.W., Wegiel, J., 2007. Trisomy-driven overexpression of DYRK1A kinase in the brain of subjects with Down syndrome. Neurosci. Lett. 413, 77. https://doi.org/10.1016/J.NEULET.2006.11.02
- DuBoff, B., Götz, J., Feany, M.B., 2012. Tau Promotes Neurodegeneration via DRP1 Mislocalization In Vivo. Neuron 75, 618–632. https://doi.org/10.1016/j.neuron.2012.06.026
- Duman, J.G., Blanco, F.A., Cronkite, C.A., Ru, Q., Erikson, K.C., Mulherkar, S., Saifullah, A. Bin, Firozi, K., Tolias, K.F., 2021. Rac-maninoff and Rho-vel: The symphony of Rho-GTPase signaling at excitatory synapses. Small GTPases 00, 1–34. https://doi.org/10.1080/21541248.2021.1885264
- Falke, E., Nissanov, J., Mitchell, T.W., Bennett, D.A., Trojanowski, J.Q., Arnold, S.E., 2003. Subicular dendritic arborization in Alzheimer's disease correlates with neurofibrillary tangle density. Am. J. Pathol. 163, 1615–1621. https://doi.org/10.1016/S0002-9440(10)63518-3
- Fang, E.F., Hou, Y., Palikaras, K., Adriaanse, B.A., Kerr, J.S., Yang, B., Lautrup, S., Hasan-Olive, M.M., Caponio, D., Dan, X., Rocktäschel, P., Croteau, D.L., Akbari, M., Greig, N.H., Fladby, T., Nilsen, H., Cader, M.Z., Mattson, M.P., Tavernarakis, N., Bohr, V.A., 2019. Mitophagy inhibits amyloid-β and tau pathology and reverses cognitive deficits in models of Alzheimer's disease. Nat. Neurosci. https://doi.org/10.1038/s41593-018-0332-

- Feijoo, C., Campbell, D.G., Jakes, R., Goedert, M., Cuenda, A., 2005. Evidence that phosphorylation of the microtubule-associated protein Tau by SAPK4/p38δ at Thr50 promotes microtubule assembly. J. Cell Sci. 118, 397–408. https://doi.org/10.1242/jcs.01655
- Flood, D.G., Buell, S.J., Horwitz, G.J., Coleman, P.D., 1987. Dendritic extent in human dentate gyrus granule cells in normal aging and senile dementia. Brain Res. 402, 205–216. https://doi.org/10.1016/0006-8993(87)90027-8
- Gan, L., Cookson, M.R., Petrucelli, L., La Spada, A.R., 2018. Converging pathways in neurodegeneration, from genetics to mechanisms. Nat. Neurosci. 2018 2110 21, 1300–1309. https://doi.org/10.1038/s41593-018-0237-7
- Gerbec, Z.J., Thakar, M.S., Malarkannan, S., 2015. The Fyn-ADAP axis: Cytotoxicity versus cytokine production in killer cells. Front. Immunol. 6. https://doi.org/10.3389/fimmu.2015.00472
- Gong, C.-X., Singh, T.J., Grundke-Iqbal, I., Iqbal, K., 1993. Phosphoprotein Phosphatase Activities in Alzheimer Disease Brain. J. Neurochem. 61, 921–927. https://doi.org/10.1111/j.1471-4159.1993.tb03603.x
- Gong, C., Liu, F., Iqbal, K., 2005. Post-translational modifications of tau protein in Alzheimer 's disease Review 813–838. https://doi.org/10.1007/s00702-004-0221-0
- Grueber, W.B., Jan, L.Y., Jan, Y.N., 2002. Tiling of the Drosophila epidermis by multidendritic sensory neurons. Development 129, 2867–2878. https://doi.org/10.1242/DEV.129.12.2867
- Grundke-Iqbal, I., Iqbal, K., Quinlan, M., Tung, Y.C., Zaidi, M.S., Wisniewski, H.M., 1986a.
 Microtubule-associated protein tau. A component of Alzheimer paired helical filaments.
 J. Biol. Chem. 261, 6084–6089. https://doi.org/10.1016/S0021-9258(17)38495-8
- Grundke-iqbal, I., Iqbal, K., Tung, Y., Zaidi, M.S., Wisniewski, H.M., 1986. Microtubule-associated Protein Tau 4, 6084–6089.
- Grundke-Iqbal, I., Iqbal, K., Tung, Y.C., Quinlan, M., Wisniewski, H.M., Binder, L.I., 1986b. Abnormal phosphorylation of the microtubule-associated protein tau (tau) in Alzheimer cytoskeletal pathology. Proc. Natl. Acad. Sci. U. S. A. 83, 4913–4917. https://doi.org/10.1073/PNAS.83.13.4913

- Gu, G.J., Wu, D., Lund, H., Sunnemark, D., Kvist, A.J., Milner, R., Eckersley, S., Nilsson, L.N.G., Agerman, K., Landegren, U., Kamali-Moghaddam, M., 2013. Elevated MARK2-dependent phosphorylation of tau in Alzheimer's disease. J. Alzheimer's Dis. 33, 699–713. https://doi.org/10.3233/JAD-2012-121357
- Guo, T., Noble, W., Hanger, D.P., 2017. Roles of tau protein in health and disease. Acta Neuropathol. 133, 665–704. https://doi.org/10.1007/s00401-017-1707-9
- Hanger, D.P., Anderton, B.H., Noble, W., 2009. Tau phosphorylation: the therapeutic challenge for neurodegenerative disease. Trends Mol. Med. 15, 112–119. https://doi.org/10.1016/j.molmed.2009.01.003
- Hardy, J., Selkoe, D.J., 2002. The amyloid hypothesis of Alzheimer's disease: Progress and problems on the road to therapeutics. Science (80-.). 297, 353–356. https://doi.org/10.1126/SCIENCE.1072994/ASSET/C4ED1918-4F2B-4649-BA69-684D0145F32B/ASSETS/GRAPHIC/SE2820694002.JPEG
- Heisenberg, M., 1971. Separation of receptor and lamina potentials in the electroretinogram of normal and mutant Drosophila. J. Exp. Biol. 55, 85–100.
- Horiguchi, T., Uryu, K., Giasson, B.I., Ischiropoulos, H., LightFoot, R., Bellmann, C., Richter-Landsberg, C., M-Y Lee, V., Trojanowski, J.Q., 2003. Nitration of Tau Protein Is Linked to Neurodegeneration in Tauopathies. https://doi.org/10.1016/S0002-9440(10)63462-1
- Horowitz, P.M., Patterson, K.R., Guillozet-Bongaarts, A.L., Reynolds, M.R., Carroll, C.A., Weintraub, S.T., Bennett, D.A., Cryns, V.L., Berry, R.W., Binder, L.I., 2004. Early N-terminal changes and caspase-6 cleavage of tau in Alzheimer's disease. J. Neurosci. 24, 7895–7902. https://doi.org/10.1523/JNEUROSCI.1988-04.2004
- Huesa, G., Baltrons, M.A., Gómez-Ramos, P., Morán, A., García, A., Hidalgo, J., Francés, S.,
 Santpere, G., Ferrer, I., Galea, E., 2010. Altered Distribution of RhoA in Alzheimer's
 Disease and AβPP Overexpressing Mice. J. Alzheimer's Dis. 19, 37–56.
 https://doi.org/10.3233/JAD-2010-1203
- Hye, A., Kerr, F., Archer, N., Foy, C., Poppe, M., Brown, R., Hamilton, G., Powell, J., Anderton, B., Lovestone, S., 2004. Glycogen synthase kinase-3 is increased in white cells early in Alzheimer's disease. Neurosci. Lett. 373, 1–4. https://doi.org/10.1016/j.neulet.2004.10.031

- Iqbal, K., Alonso, A.D.C., Gong, C.X., Khatoon, S., Pei, J.J., Wang, J.Z., Grundke-Iqbal, I., 1998. Mechanisms of neurofibrillary degeneration and the formation of neurofibrillary tangles. J. Neural Transm. Suppl. 169–180. https://doi.org/10.1007/978-3-7091-6467-9_15
- Iqbal, K., Grundke-Iqbal, I., 1991. Ubiquitination and abnormal phosphorylation of paired helical filaments in Alzheimer's disease. Mol. Neurobiol. 5, 399–410. https://doi.org/10.1007/BF02935561
- Iseki, E., Kato, M., Marui, W., Uéda, K., Kosaka, K., 2001. A neuropathological study of the disturbance of the nigro-amygdaloid connections in brains from patients with dementia with Lewy bodies. J. Neurol. Sci. 185, 129–134. https://doi.org/10.1016/S0022-510X(01)00481-6
- Ittner, A., Ittner, L.M., 2018. Dendritic Tau in Alzheimer's Disease. Neuron 99, 13–27. https://doi.org/10.1016/j.neuron.2018.06.003
- Ittner, Lars M, Ke, Y.D., Delerue, F., Bi, M., Gladbach, A., Eersel, J. Van, Wo, H., Chieng, B.C., Christie, M.J., Napier, I.A., Eckert, A., Staufenbiel, M., Hardeman, E., 2010. Dendritic Function of Tau Mediates Amyloid- b Toxicity in Alzheimer's Disease Mouse Models 387–397. https://doi.org/10.1016/j.cell.2010.06.036
- Ittner, Lars M., Ke, Y.D., Delerue, F., Bi, M., Gladbach, A., van Eersel, J., Wölfing, H., Chieng, B.C., Christie, M.J., Napier, I.A., Eckert, A., Staufenbiel, M., Hardeman, E., Götz, J., 2010a. Dendritic function of tau mediates amyloid-β toxicity in alzheimer's disease mouse models. Cell 142, 387–397. https://doi.org/10.1016/j.cell.2010.06.036
- Ittner, Lars M., Ke, Y.D., Delerue, F., Bi, M., Gladbach, A., van Eersel, J., Wölfing, H., Chieng, B.C., Christie, M.J., Napier, I.A., Eckert, A., Staufenbiel, M., Hardeman, E., Götz, J., 2010b. Dendritic function of tau mediates amyloid-β toxicity in alzheimer's disease mouse models. Cell 142, 387–397. https://doi.org/10.1016/j.cell.2010.06.036
- Ittner, Lars M., Ke, Y.D., Delerue, F., Bi, M., Gladbach, A., van Eersel, J., Wölfing, H., Chieng, B.C., Christie, M.J., Napier, I.A., Eckert, A., Staufenbiel, M., Hardeman, E., Götz, J., 2010c. Dendritic function of tau mediates amyloid-β toxicity in alzheimer's disease mouse models. Cell 142, 387–397. https://doi.org/10.1016/j.cell.2010.06.036
- Jaruszewski, K.M., Omtri, R.S., Kandimalla, K.K., 2012. Role of nanotechnology in the

- diagnosis and treatment of alzheimer's disease. Curr. Adv. Med. Appl. Nanotechnol. 107–124. https://doi.org/10.2174/978160805131111201010107
- Jin, M., Shepardson, N., Yang, T., Chen, G., Walsh, D., Selkoe, D.J., 2011. Soluble amyloid β-protein dimers isolated from Alzheimer cortex directly induce Tau hyperphosphorylation and neuritic degeneration. Proc. Natl. Acad. Sci. U. S. A. 108, 5819–5824. https://doi.org/10.1073/pnas.1017033108
- Johnson, G.V.W., Bailey, C.D.C., 2003. The p38 MAP kinase signaling pathway in Alzheimer's disease. Exp. Neurol. 183, 263–268. https://doi.org/10.1016/S0014-4886(03)00268-1
- Jones, S.B., Lu, H.Y., Lu, Q., 2004. Abl tyrosine kinase promotes dendrogenesis by inducing actin cytoskeletal rearrangements in cooperation with Rho family small GTPases in hippocampal neurons. J. Neurosci. 24, 8510–8521. https://doi.org/10.1523/JNEUROSCI.1264-04.2004
- Kerr, J.S., Adriaanse, B.A., Greig, N.H., Mattson, M.P., Zameel Cader, M., Bohr, V.A., Fang,
 E.F., 2017. Mitophagy and Alzheimer's disease: cellular and molecular mechanisms HHS
 Public Access. Trends Neurosci 40, 151–166. https://doi.org/10.1016/j.tins.2017.01.002
- Kimura, R., Kamino, K., Yamamoto, M., Nuripa, A., Kida, T., Kazui, H., Hashimoto, R., Tanaka, T., Kudo, T., Yamagata, H., Tabara, Y., Miki, T., Akatsu, H., Kosaka, K., Funakoshi, E., Nishitomi, K., Sakaguchi, G., Kato, A., Hattori, H., Uema, T., Takeda, M., 2007. The DYRK1A gene, encoded in chromosome 21 Down syndrome critical region, bridges between b-amyloid production and tau phosphorylation in Alzheimer disease. Hum. Mol. Genet. 16, 15–23. https://doi.org/10.1093/hmg/ddl437
- Klein, C., Kramer, E.M., Cardine, A.M., Schraven, B., Brandt, R., Trotter, J., 2002. Process outgrowth of oligodendrocytes is promoted by interaction of Fyn kinase with the cytoskeletal protein Tau. J. Neurosci. 22, 698–707. https://doi.org/10.1523/jneurosci.22-03-00698.2002
- Kobayashi, S., Tanaka, T., Soeda, Y., Almeida, O.F.X., Takashima, A., 2017. Local Somatodendritic Translation and Hyperphosphorylation of Tau Protein Triggered by AMPA and NMDA Receptor Stimulation. EBioMedicine 20, 120–126. https://doi.org/10.1016/j.ebiom.2017.05.012

- Koc, E.C., Miller-Lee, J.L., Koc, H., 2017. Fyn kinase regulates translation in mammalian mitochondria. Biochim. Biophys. Acta Gen. Subj. 1861, 1–5. https://doi.org/10.1016/j.bbagen.2016.12.004
- Kotzbauer, P.T., Giasson, B.I., Kravitz, A. V, Golbe, L.I., Mark, M.H., Trojanowski, J.Q., Lee, V.M., 2004. Fibrillization of a -synuclein and tau in familial Parkinson's disease caused by the A53T a -synuclein mutation 187, 279–288. https://doi.org/10.1016/j.expneurol.2004.01.007
- Krämer-Albers, E.M., White, R., 2011. From axon-glial signalling to myelination: The integrating role of oligodendroglial Fyn kinase. Cell. Mol. Life Sci. 68, 2003–2012. https://doi.org/10.1007/s00018-010-0616-z
- Kuszczyk, M., Gordon-Krajcer, W., Lazarewicz, J.W., 2009. Homocysteine-induced acute excitotoxicity in cerebellar granule cells in vitro is accompanied by PP2A-mediated dephosphorylation of tau. Neurochem. Int. 55, 174–180. https://doi.org/10.1016/j.neuint.2009.02.010
- Landino, L.M., Skreslet, T.E., Alston, J.A., 2004. Cysteine oxidation of tau and microtubule-associated protein-2 by peroxynitrite: Modulation of microtubule assembly kinetics by the thioredoxin reductase system. J. Biol. Chem. 279, 35101–35105. https://doi.org/10.1074/jbc.M405471200
- Lau, D.H.W., Hogseth, M., Phillips, E.C., Neill, M.J.O., Pooler, A.M., Hanger, D.P., 2016. Critical residues involved in tau binding to fyn: implications for tau phosphorylation in Alzheimer's disease. Acta Neuropathol. Commun. 1–13. https://doi.org/10.1186/s40478-016-0317-4
- Lebouvier, T., Scales, T.M.E., Hanger, D.P., Geahlen, R.L., Lardeux, B., Reynolds, C.H., Anderton, B.H., Derkinderen, P., 2008. The microtubule-associated protein tau is phosphorylated by Syk. Biochim. Biophys. Acta Mol. Cell Res. 1783, 188–192. https://doi.org/10.1016/j.bbamcr.2007.11.005
- Lee, G., 2005. Tau and src family tyrosine kinases. Biochim. Biophys. Acta Mol. Basis Dis. https://doi.org/10.1016/j.bbadis.2004.09.002
- Lee, G., Newman, S.T., Gard, D.L., Band, H., Panchamoorthy, G., 1998. Tau interacts with src-family non-receptor tyrosine kinases. J. Cell Sci. 111 (Pt 2, 3167–77.

- Lee, G., Thangavel, R., Sharma, V.M., Litersky, J.M., Bhaskar, K., Fang, S.M., Do, L.H., Andreadis, A., Van Hoesen, G., Ksiezak-Reding, H., 2004. Phosphorylation of Tau by Fyn: Implications for Alzheimer's Disease. J. Neurosci. 24, 2304–2312. https://doi.org/10.1523/JNEUROSCI.4162-03.2004
- Lefebvre, T., Ferreira, S., Dupont-Wallois, L., Bussière, T., Dupire, M.J., Delacourte, A., Michalski, J.C., Caillet-Boudin, M.L., 2003. Evidence of a balance between phosphorylation and O-GlcNAc glycosylation of Tau proteins A role in nuclear localization. Biochim. Biophys. Acta Gen. Subj. 1619, 167–176. https://doi.org/10.1016/S0304-4165(02)00477-4
- Lei, W., Omotade, O.F., Myers, K.R., Zheng, J.Q., 2016. Actin Cytoskeleton in Dendritic Spine Development and Plasticity. Curr. Opin. Neurobiol. 39, 86. https://doi.org/10.1016/J.CONB.2016.04.010
- Leroy, K., Yilmaz, Z., Brion, J.P., 2007. Increased level of active GSK-3β in Alzheimer's disease and accumulation in argyrophilic grains and in neurones at different stages of neurofibrillary degeneration. Neuropathol. Appl. Neurobiol. 33, 43–55. https://doi.org/10.1111/j.1365-2990.2006.00795.x
- Lesort, M., Jope, R.S., Johnson, G.V.W., 1999. Insulin transiently increases tau phosphorylation: Involvement of glycogen synthase kinase-3β and Fyn tyrosine kinase. J. Neurochem. 72, 576–584. https://doi.org/10.1046/j.1471-4159.1999.0720576.x
- Li, C., Götz, J., 2017a. Somatodendritic accumulation of Tau in Alzheimer's disease is promoted by Fyn-mediated local protein translation. EMBO J. 36, e201797724. https://doi.org/10.15252/embj.201797724
- Li, C., Götz, J., 2017b. Somatodendritic accumulation of Tau in Alzheimer's disease is promoted by Fyn-mediated local protein translation. EMBO J. 36, 3120–3138. https://doi.org/10.15252/embj.201797724
- Li, C., Götz, J., 2017c. Somatodendritic accumulation of Tau in Alzheimer's disease is promoted by Fyn-mediated local protein translation. EMBO J. https://doi.org/10.15252/embj.201797724
- Li, S., Jin, M., Koeglsperger, T., Shepardson, N.E., Shankar, G.M., Selkoe, D.J., 2011. Soluble a β oligomers inhibit long-term potentiation through a mechanism involving excessive

- activation of extrasynaptic NR2B-containing NMDA receptors. J. Neurosci. 31, 6627–6638. https://doi.org/10.1523/JNEUROSCI.0203-11.2011
- Li, Z., Aizenman, C.D., Cline, H.T., 2002. Regulation of Rho GTPases by Crosstalk and Neuronal Activity In Vivo. Neuron 33, 741–750. https://doi.org/10.1016/S0896-6273(02)00621-9
- Liu, F., Shi, J., Tanimukai, H., Gu, Jinhua, Gu, Jianlan, Grundke-Iqbal, I., Iqbal, K., Gong, C.X., 2009. Reduced O-GlcNAcylation links lower brain glucose metabolism and tau pathology in Alzheimer's disease. Brain 132, 1820–1832. https://doi.org/10.1093/brain/awp099
- Liu, F., Zaidi, T., Iqbal, K., Grundke-Iqbal, I., Merkle, R.K., Gong, C.X., 2002. Role of glycosylation in hyperphosphorylation of tau in Alzheimer's disease. FEBS Lett. 512, 101–106. https://doi.org/10.1016/S0014-5793(02)02228-7
- Liu, G., Fiock, K.L., Levites, Y., Golde, T.E., Hefti, M.M., Lee, G., 2020. Fyn depletion ameliorates tauP301L-induced neuropathology. Acta Neuropathol. Commun. 8, 1–15. https://doi.org/10.1186/s40478-020-00979-6
- Liu, W., Zhao, J., Lu, G., 2016. miR-106b inhibits tau phosphorylation at Tyr18 by targeting Fyn in a model of Alzheimer's disease. Biochem. Biophys. Res. Commun. 478, 852–857. https://doi.org/10.1016/j.bbrc.2016.08.037
- Lustbader, J.W., Cirilli, M., Lin, C., Xu, H.W., Takuma, K., Wang, N., Caspersen, C., Chen, X., Pollak, S., Chaney, M., Trinchese, F., Liu, S., Gunn-Moore, F., Lue, L.F., Walker, D.G., Kappasamy, P., Zewier, Z.L., Arancio, O., Stern, D., Yan, S.S. Du, Wu, H., 2004.
 ABAD Directly Links Aβ to Mitochondrial Toxicity in Alzheimer's Disease. Science (80-.). 304, 448–452. https://doi.org/10.1126/science.1091230
- Mahmood, T., Yang, P.C., 2012. Western blot: Technique, theory, and trouble shooting. N. Am. J. Med. Sci. 4, 429–434. https://doi.org/10.4103/1947-2714.100998
- Mairet-Coello, G., Courchet, J., Pieraut, S., Courchet, V., Maximov, A., Polleux, F., 2013. The CAMKK2-AMPK Kinase Pathway Mediates the Synaptotoxic Effects of Aβ Oligomers through Tau Phosphorylation. Neuron 78, 94–108. https://doi.org/10.1016/j.neuron.2013.02.003
- Martin, L., Latypova, X., Terro, F., 2011. Post-translational modifications of tau protein:

- Implications for Alzheimer's disease. Neurochem. Int. 58, 458–471. https://doi.org/10.1016/j.neuint.2010.12.023
- Matsushima, S., Kuroda, J., Zhai, P., Liu, T., Ikeda, S., Nagarajan, N., Oka, S.I., Yokota, T., Kinugawa, S., Hsu, C.P., Li, H., Tsutsui, H., Sadoshima, J., 2016. Tyrosine kinase FYN negatively regulates NOX4 in cardiac remodeling. J. Clin. Invest. 126, 3403–3416. https://doi.org/10.1172/JCI85624
- McInnes, J., Wierda, K., Snellinx, A., Bounti, L., Wang, Y.C., Stancu, I.C., Apóstolo, N., Gevaert, K., Dewachter, I., Spires-Jones, T.L., De Strooper, B., De Wit, J., Zhou, L., Verstreken, P., 2018. Synaptogyrin-3 Mediates Presynaptic Dysfunction Induced by Tau. Neuron. https://doi.org/10.1016/j.neuron.2018.01.022
- Mehraein, P., Yamada, M., Tarnowska-Dziduszko, E., 1975. Quantitative study on dendrites and dendritic spines in Alzheimer's disease and senile dementia PubMed [WWW Document]. URL https://pubmed.ncbi.nlm.nih.gov/1155273/ (accessed 8.8.23).
- Melom, J.E., Littleton, J.T., 2011. Synapse development in health and disease. Curr. Opin. Genet. Dev. 21, 256–261. https://doi.org/10.1016/j.gde.2011.01.002
- Milnerwood, A.J., Gladding, C.M., Pouladi, M.A., Kaufman, A.M., Hines, R.M., Boyd, J.D., Ko, R.W.Y., Vasuta, O.C., Graham, R.K., Hayden, M.R., Murphy, T.H., Raymond, L.A., 2010. Early Increase in Extrasynaptic NMDA Receptor Signaling and Expression Contributes to Phenotype Onset in Huntington's Disease Mice. Neuron 65, 178–190. https://doi.org/10.1016/j.neuron.2010.01.008
- Miyamoto, T., Stein, L., Thomas, R., Djukic, B., Taneja, P., Knox, J., Vossel, K., Mucke, L., 2017. Phosphorylation of tau at Y18, but not tau- fyn binding, is required for tau to modulate NMDA receptor-dependent excitotoxicity in primary neuronal culture 1–19. https://doi.org/10.1186/s13024-017-0176-x
- Mondragón-Rodríguez, S., Trillaud-Doppia, E., Dudilot, A., Bourgeois, C., Lauzon, M., Leclerc, N., Boehm, J., 2012a. Interaction of endogenous tau protein with synaptic proteins is regulated by N-methyl-D-aspartate receptor-dependent tau phosphorylation. J. Biol. Chem. 287, 32040–32053. https://doi.org/10.1074/jbc.M112.401240
- Mondragón-Rodríguez, S., Trillaud-Doppia, E., Dudilot, A., Bourgeois, C., Lauzon, M., Leclerc, N., Boehm, J., 2012b. Interaction of endogenous tau protein with synaptic

- proteins is regulated by N-methyl-D-aspartate receptor-dependent tau phosphorylation. J. Biol. Chem. 287, 32040–32053. https://doi.org/10.1074/jbc.M112.401240
- Morishima-Kawashima, M., Hasegawa, M., Takio, K., Suzuki, M., Titani, K., Ihara, Y., 1993. Ubiquitin is conjugated with amino-terminally processed tau in paired helical filaments. Neuron 10, 1151–1160. https://doi.org/10.1016/0896-6273(93)90063-W
- Morita, A., Yamashita, N., Sasaki, Y., Uchida, Y., Nakajima, O., Nakamura, F., Yagi, T., Taniguchi, M., Usui, H., Katoh-Semba, R., Takei, K., Goshima, Y., 2006. Regulation of dendritic branching and spine maturation by semaphorin3A-fyn signaling. J. Neurosci. 26, 2971–2980. https://doi.org/10.1523/JNEUROSCI.5453-05.2006
- Nakayama, A.Y., Harms, M.B., Luo, L., 2000. Small GTPases Rac and Rho in the maintenance of dendritic spines and branches in hippocampal pyramidal neurons. J. Neurosci. 20, 5329–5338. https://doi.org/10.1523/JNEUROSCI.20-14-05329.2000
- Nakazawa, T., Komai, S., Tezuka, T., Hisatsune, C., Umemori, H., Semba, K., Mishina, M., Manabe, T., Yamamoto, T., 2001. Characterization of Fyn-mediated tyrosine phosphorylation sites on GluRe2 (NR2B) subunit of the N-methyl-D-aspartate receptor. J. Biol. Chem. 276, 693–699. https://doi.org/10.1074/jbc.M008085200
- Nguyen, T.H., Liu, J., Lombroso, P.J., 2002. Striatal enriched phosphatase 61 dephosphorylates Fyn at phosphotyrosine 420. J. Biol. Chem. 277, 24274–24279. https://doi.org/10.1074/jbc.M111683200
- Nimchinsky, E.A., Sabatini, B.L., Svoboda, K., 2002. Structure and function of dendritic spines. Annu. Rev. Physiol. 64, 313–353. https://doi.org/10.1146/ANNUREV.PHYSIOL.64.081501.160008
- Nisbet, R.M., Polanco, J.C., Ittner, L.M., Götz, J., 2015. Tau aggregation and its interplay with amyloid-β. Acta Neuropathol. https://doi.org/10.1007/s00401-014-1371-2
- Nygaard, H.B., van Dyck, C.H., Strittmatter, S.M., 2014. Fyn kinase inhibition as a novel therapy for Alzheimer's disease. Alzheimers. Res. Ther. 6, 8. https://doi.org/10.1186/alzrt238
- Palop, J.J., Chin, J., Roberson, E.D., Wang, J., Thwin, M.T., Bien-Ly, N., Yoo, J., Ho, K.O., Yu, G.Q., Kreitzer, A., Finkbeiner, S., Noebels, J.L., Mucke, L., 2007. Aberrant Excitatory Neuronal Activity and Compensatory Remodeling of Inhibitory Hippocampal

- Circuits in Mouse Models of Alzheimer's Disease. Neuron 55, 697–711. https://doi.org/10.1016/j.neuron.2007.07.025
- Parrish, J.Z., Emoto, K., Kim, M.D., Yuh, N.J., 2007. Mechanisms that Regulate Establishment, Maintenance, and Remodeling of Dendritic Fields. http://dx.doi.org/10.1146/annurev.neuro.29.051605.112907 30, 399–423. https://doi.org/10.1146/ANNUREV.NEURO.29.051605.112907
- Patrick, G.N., Zukerberg, L., Nikolic, M., De La Monte, S., Dikkes, P., Tsai, L.H., 1999. Conversion of p35 to p25 deregulates Cdk5 activity and promotes neurodegeneration. Nature 402, 615–622. https://doi.org/10.1038/45159
- Polleux, F., Morrow, T., Ghosh, A., 2000. Semaphorin 3A is a chemoattractant for cortical apical dendrites. Nature 404, 567–573. https://doi.org/10.1038/35007001
- Pool, M., Thiemann, J., Bar-Or, A., Fournier, A.E., 2008. NeuriteTracer: a novel ImageJ plugin for automated quantification of neurite outgrowth. J. Neurosci. Methods 168, 134–139. https://doi.org/10.1016/J.JNEUMETH.2007.08.029
- Pooler, A.M., Noble, W., Hanger, D.P., 2014. A role for tau at the synapse in Alzheimer's disease pathogenesis. Neuropharmacology 76, 1–8. https://doi.org/10.1016/j.neuropharm.2013.09.018
- Pope, W.B., Lambert, M.P., Leypold, B., Seupaul, R., Sletten, L., Krafft, G., Klein, W.L., 1994. Microtubule-associated protein tau is hyperphosphorylated during mitosis in the human neuroblastoma cell line SH-SY5Y. Exp. Neurol. 126, 185–194. https://doi.org/10.1006/exnr.1994.1057
- Poulsen, E.T., Iannuzzi, F., Rasmussen, H.F., Maier, T.J., 2017. An Aberrant Phosphorylation of Amyloid Precursor Protein Tyrosine Regulates Its Trafficking and the Binding to the Clathrin Endocytic Complex in Neural Stem Cells of Alzheimer 's Disease Patients 10. https://doi.org/10.3389/fnmol.2017.00059
- Prüßing, K., Voigt, A., Schulz, J.B., 2013. Drosophila melanogaster as a model organism for Alzheimer 's disease Drosophila melanogaster as a model organism for Alzheimer 's disease.
- Reyes, J.F., Reynolds, M.R., Horowitz, P.M., Fu, Y., Guillozet-Bongaarts, A.L., Berry, R., Binder, L.I., 2008. A possible link between astrocyte activation and tau nitration in

- Alzheimer's disease. Neurobiol. Dis. 31, 198–208. https://doi.org/10.1016/j.nbd.2008.04.005
- Reynolds, M.R., Berry, R.W., Binder, L.I., 2005. Site-specific nitration and oxidative dityrosine bridging of the τ protein by peroxynitrite: Implications for Alzheimer's disease. Biochemistry 44, 1690–1700. https://doi.org/10.1021/bi047982v
- Reynolds, M.R., Reyes, J.F., Fu, Y., Bigio, E.H., Guillozet-Bongaarts, A.L., Berry, R.W., Binder, L.I., 2006a. Tau nitration occurs at tyrosine 29 in the fibrillar lesions of Alzheimer's disease and other tauopathies. J. Neurosci. 26, 10636–10645. https://doi.org/10.1523/JNEUROSCI.2143-06.2006
- Reynolds, M.R., Reyes, J.F., Fu, Y., Bigio, E.H., Guillozet-Bongaarts, A.L., Berry, R.W., Binder, L.I., 2006b. Tau nitration occurs at tyrosine 29 in the fibrillar lesions of Alzheimer's disease and other tauopathies. J. Neurosci. 26, 10636–10645. https://doi.org/10.1523/JNEUROSCI.2143-06.2006
- Roberson, E.D., Halabisky, B., Yoo, J.W., Yao, J., Chin, J., Yan, F., Wu, T., Hamto, P., Devidze, N., Yu, G.-Q., Palop, J.J., Noebels, J.L., Mucke, L., 2011. Amyloid-/Fyn-Induced Synaptic, Network, and Cognitive Impairments Depend on Tau Levels in Multiple Mouse Models of Alzheimer's Disease. J. Neurosci. 31, 700–711. https://doi.org/10.1523/JNEUROSCI.4152-10.2011
- Rong, Y., Lu, X., Bernard, A., Khrestchatisky, M., Baudry, M., 2001. Tyrosine phosphorylation of ionotropic glutamate receptors by Fyn or Src differentially modulates their susceptibility to calpain and enhances their binding to spectrin and PSD-95. J. Neurochem. 79, 382–390. https://doi.org/10.1046/j.1471-4159.2001.00565.x
- Rudrabhatla, P., Pant, H.C., 2010. Phosphorylation-specific peptidyl-prolyl isomerization of neuronal cytoskeletal proteins by pin1: Implications for therapeutics in neurodegeneration. J. Alzheimer's Dis. 19, 389–403. https://doi.org/10.3233/JAD-2010-1243
- Russell, C.L., Mitra, V., Hansson, K., Blennow, K., Gobom, J., Zetterberg, H., Hiltunen, M., Ward, M., Pike, I., 2016. Comprehensive Quantitative Profiling of Tau and Phosphorylated Tau Peptides in Cerebrospinal Fluid by Mass Spectrometry Provides New Biomarker Candidates. J. Alzheimer's Dis. 55, 303–313. https://doi.org/10.3233/JAD-160633

- Ryoo, S.-R., Cho, H.-J., Lee, H.-W., Jeong, H.K., Radnaabazar, C., Kim, Y.-S., Kim, M.-J., Son, M.-Y., Seo, H., Chung, S.-H., Song, W.-J., 2008. Dual-specificity tyrosine(Y)-phosphorylation regulated kinase 1A-mediated phosphorylation of amyloid precursor protein: evidence for a functional link between Down syndrome and Alzheimer's disease. J. Neurochem. 104, 1333–1344. https://doi.org/10.1111/j.1471-4159.2007.05075.x
- Sáchez-Soriano, N., Tea, G., Whitington, P., Prokop, A., 2007. Drosophila as a genetic and cellular model for studies on axonal growth. Neural Dev. 2, 1–28. https://doi.org/10.1186/1749-8104-2-9
- Schwab, C., Demaggio, A.J., Ghoshal, N., Binder, L.I., Kuret, J., McGeer, P.L., 2000. Casein kinase 1 delta is associated with pathological accumulation of tau in several neurodegenerative diseases. Neurobiol. Aging 21, 503–510. https://doi.org/10.1016/S0197-4580(00)00110-X
- Schweers, O., Mandelkow, E.M., Biernat, J., Mandelkow, E., 1995. Oxidation of cysteine-322 in the repeat domain of microtubule-associated protein τ controls the in vitro assembly of paired helical filaments. Proc. Natl. Acad. Sci. U. S. A. 92, 8463–8467. https://doi.org/10.1073/pnas.92.18.8463
- Selkoe, D.J., Hardy, J., 2016. The amyloid hypothesis of Alzheimer's disease at 25 years. EMBO Mol. Med. 8, 595. https://doi.org/10.15252/EMMM.201606210
- Sergeant, N., Bretteville, A., Hamdane, M., Caillet-Boudin, M.L., Grognet, P., Bombois, S., Blum, D., Delacourte, A., Pasquier, F., Vanmechelen, E., Schraen-Maschke, S., Buée, L., 2008. Biochemistry of Tau in Alzheimer's disease and related neurological disorders. Expert Rev. Proteomics 5, 207–224. https://doi.org/10.1586/14789450.5.2.207
- Shane Arnold, C., Johnson, G.V.W., Cole, R.N., Dong, D.L.Y., Lee, M., Hart, G.W., 1996. The microtubule-associated protein tau is extensively modified with O- linked N-acetylglucosamine. J. Biol. Chem. 271, 28741–28744. https://doi.org/10.1074/jbc.271.46.28741
- Sherin K; John G., 1993. The protein tyrosine kinase fyn.pdf.
- Snyder, E.M., Nong, Y., Almeida, C.G., Paul, S., Moran, T., Choi, E.Y., Nairn, A.C., Salter, M.W., Lombroso, P.J., Gouras, G.K., Greengard, P., 2005. Regulation of NMDA receptor trafficking by amyloid-beta. Nat. Neurosci. 8, 1051–1058.

- https://doi.org/10.1038/NN1503
- Sontag, J.M., Nunbhakdi-Craig, V., White, C.L., Halpain, S., Sontag, E., 2012. The protein phosphatase PP2A/Bα binds to the microtubule-associated proteins Tau and MAP2 at a motif also recognized by the kinase Fyn: Implications for tauopathies. J. Biol. Chem. 287, 14984–14993. https://doi.org/10.1074/jbc.M111.338681
- Southard, E.E., 1910. ANATOMICAL FINDINGS IN SENILE DEMENTIA: A DIAGNOSTIC STUDY BEARING ESPECIALLY ON THE GROUP OF CEREBRAL ATROPHIES. Am. J. Psychiatry 66, 673-708–11. https://doi.org/10.1176/AJP.66.4.673
- Stojakovic, A., Chang, S.Y., Nesbitt, J., Pichurin, N.P., Ostroot, M.A., Aikawa, T., Kanekiyo, T., Trushina, E., 2021. Partial Inhibition of Mitochondrial Complex i Reduces Tau Pathology and Improves Energy Homeostasis and Synaptic Function in 3xTg-AD Mice.
 J. Alzheimer's Dis. 79, 335–353. https://doi.org/10.3233/JAD-201015
- Strahler, A. (1953) Revision of Hortons' Quantitative Factors in Erosional Terrain. Transactions, American Geophysical Union, 34, 345-365. References Scientific Research Publishing [WWW Document], n.d. URL https://www.scirp.org/(S(czeh2tfqw2orz553k1w0r45))/reference/referencespapers.aspx? referenceid=2183670 (accessed 5.27.23).
- Sun, X.Y., Tuo, Q.Z., Liuyang, Z.Y., Xie, A.J., Feng, X.L., Yan, X., Qiu, M., Li, S., Wang, X.L., Cao, F.Y., Wang, X.C., Wang, J.Z., Liu, R., 2016. Extrasynaptic NMDA receptor-induced tau overexpression mediates neuronal death through suppressing survival signaling ERK phosphorylation. Cell Death Dis. 7, e2449–e2449. https://doi.org/10.1038/cddis.2016.329
- Swatton, J.E., Sellers, L.A., Faull, Ã.R.L.M., Holland, A., Iritani, S., Bahn, S., 2004. Increased MAP kinase activity in Alzheimer's and Down syndrome but not in schizophrenia human brain 19, 2711–2719. https://doi.org/10.1111/j.1460-9568.2004.03365.x
- Takahashi, M., Tsujioka, Y., Yamada, T., Tsuboi, Y., Okada, H., Yamamoto, T., Liposits, Z., 1999a. Glycosylation of microtubule-associated protein tau in Alzheimer's disease brain. Acta Neuropathol. 97, 635–641. https://doi.org/10.1007/s004010051040
- Takahashi, M., Tsujioka, Y., Yamada, T., Tsuboi, Y., Okada, H., Yamamoto, T., Liposits, Z., 1999b. Glycosylation of microtubule-associated protein tau in Alzheimer's disease brain.

- Acta Neuropathol. 97, 635–641. https://doi.org/10.1007/s004010051040
- Talantova, M., Sanz-Blasco, S., Zhang, X., Xia, P., Akhtar, M.W., Okamoto, S.I.,
 Dziewczapolski, G., Nakamura, T., Cao, G., Pratt, A.E., Kang, Y.J., Tu, S., Molokanova,
 E., McKercher, S.R., Hires, S.A., Sason, H., Stouffer, D.G., Buczynski, M.W., Solomon,
 J.P., Michael, S., Powers, E.T., Kelly, J.W., Roberts, A., Tong, G., Fang-Newmeyer, T.,
 Parker, J., Holland, E.A., Zhang, D., Nakanishi, N., Chen, H.S.V., Wolosker, H., Wang,
 Y., Parsons, L.H., Ambasudhan, R., Masliah, E., Heinemann, S.F., Piña-Crespo, J.C.,
 Lipton, S.A., 2013. Aβ induces astrocytic glutamate release, extrasynaptic NMDA
 receptor activation, and synaptic loss. Proc. Natl. Acad. Sci. U. S. A. 110.
 https://doi.org/10.1073/PNAS.1306832110
- Tandon, A., Yu, H., Wang, L., Rogaeva, E., Sato, C., Chishti, M.A., Kawarai, T., Hasegawa, H., Chen, F., Davies, P., Fraser, P.E., Westaway, D., St George-Hyslop, P.H., 2003. Brain levels of CDK5 activator p25 are not increased in Alzheimer's or other neurodegenerative diseases with neurofibrillary tangles. J. Neurochem. 86, 572–581. https://doi.org/10.1046/j.1471-4159.2003.01865.x
- Tanimukai, H., Grundke-Iqbal, I., Iqbal, K., 2005. Up-Regulation of Inhibitors of Protein Phosphatase-2A in Alzheimer's Disease, The American Journal of Pathology. https://doi.org/10.1016/S0002-9440(10)62486-8
- Thies, E., Mandelkow, E.-M., 2007. Neurobiology of Disease Missorting of Tau in Neurons Causes Degeneration of Synapses That Can Be Rescued by the Kinase MARK2/Par-1. https://doi.org/10.1523/JNEUROSCI.4674-06.2007
- Threadgill, R., Bobb, K., Ghosh, A., 1997a. Regulation of dendritic growth and remodeling by Rho, Rac, and Cdc42. Neuron 19, 625–634. https://doi.org/10.1016/S0896-6273(00)80376-1
- Threadgill, R., Bobb, K., Ghosh, A., 1997b. Regulation of dendritic growth and remodeling by Rho, Rac, and Cdc42. Neuron 19, 625–634. https://doi.org/10.1016/S0896-6273(00)80376-1
- Tönnies, E., Trushina, E., 2017. Oxidative Stress, Synaptic Dysfunction, and Alzheimer's Disease. J. Alzheimer's Dis. 57, 1105–1121. https://doi.org/10.3233/JAD-161088
- Trepanier, C.H., Jackson, M.F., MacDonald, J.F., 2012. Regulation of NMDA receptors by the

- tyrosine kinase Fyn. FEBS J. 279, 12–19. https://doi.org/10.1111/j.1742-4658.2011.08391.x
- Um, J.W., Nygaard, H.B., Heiss, J.K., Kostylev, M.A., Stagi, M., Vortmeyer, A., Wisniewski, T., Gunther, E.C., Strittmatter, S.M., 2012. Alzheimer amyloid-β oligomer bound to postsynaptic prion protein activates Fyn to impair neurons. Nat. Neurosci. 15, 1227–1235. https://doi.org/10.1038/nn.3178
- Urbanska, M., Blazejczyk, M., Jaworski, J., 2008. Molecular basis of dendritic arborization. Acta Neurobiol. Exp. (Wars). 68, 264–288.
- Usardi, A., Pooler, A.M., Seereeram, A., Reynolds, C.H., Derkinderen, P., Anderton, B., Hanger, D.P., Noble, W., Williamson, R., 2011a. Tyrosine phosphorylation of tau regulates its interactions with Fyn SH2 domains, but not SH3 domains, altering the cellular localization of tau. FEBS J. 278, 2927–2937. https://doi.org/10.1111/j.1742-4658.2011.08218.x
- Usardi, A., Pooler, A.M., Seereeram, A., Reynolds, C.H., Derkinderen, P., Anderton, B., Hanger, D.P., Noble, W., Williamson, R., 2011b. Tyrosine phosphorylation of tau regulates its interactions with Fyn SH2 domains, but not SH3 domains, altering the cellular localization of tau. FEBS J. 278, 2927–2937. https://doi.org/10.1111/j.1742-4658.2011.08218.x
- Wang, J.Z., Grundke-Iqbal, I., Iqbal, K., 1996. Glycosylation of microtubule-associated protein tau: An abnormal posttranslational modification in Alzheimer's disease. Nat. Med. 2, 871–875. https://doi.org/10.1038/nm0896-871
- Wang, J.Z., Xia, Y.Y., Grundke-Iqbal, I., Iqbal, K., 2013. Abnormal hyperphosphorylation of tau: Sites, regulation, and molecular mechanism of neurofibrillary degeneration. J. Alzheimer's Dis. 33. https://doi.org/10.3233/JAD-2012-129031
- Wang, S., Tanzi, R.E., Li, A., 2019. Quantitative analysis of neuronal dendritic arborization complexity in Drosophila. J. Vis. Exp. 2019, 1–8. https://doi.org/10.3791/57139
- Wei, Z., Liu, H.T., 2002. MAPK signal pathways in the regulation of cell proliferation in mammalian cells. Cell Res. https://doi.org/10.1038/sj.cr.7290105
- Weingarten, M.D., Lockwood, A.H., Hwo, S.Y., Kirschner, M.W., 1975. A protein factor essential for microtubule assembly. Proc. Natl. Acad. Sci. U. S. A. 72, 1858–1862.

- https://doi.org/10.1073/pnas.72.5.1858
- Williams, D.W., Tyrer, M., Shepherd, D., 2000. Tau and tan reporters disrupt central projections of sensory neurons in Drosophila. J. Comp. Neurol. 428, 630–640. https://doi.org/10.1002/1096-9861(20001225)428:4<630::aid-cne4>3.0.co;2-x
- Williamson, R., Scales, T., Clark, B.R., Gibb, G., Hugh Reynolds, C., Kellie, S., Bird, I.N., Varndell, I.M., Sheppard, P.W., Everall, I., Anderton, B.H., 2002. Rapid tyrosine phosphorylation of neuronal proteins including tau and focal adhesion kinase in response to amyloid-β peptide exposure: Involvement of Src family protein kinases. J. Neurosci. 22, 10–20. https://doi.org/10.1523/jneurosci.22-01-00010.2002
- Witman, G.B., Cleveland, D.O.N.W., Weingarten, M.D., Kirschner, M.W., 1976. Tubulin requires tau for growth onto 73, 4070–4074.
- Xia, D., Götz, J., 2014. Premature lethality, hyperactivity, and aberrant phosphorylation in transgenic mice expressing a constitutively active form of Fyn. Front. Mol. Neurosci. 7, 1–11. https://doi.org/10.3389/fnmol.2014.00040
- Xia, D., Li, C., Götz, J., 2015. Pseudophosphorylation of Tau at distinct epitopes or the presence of the P301L mutation targets the microtubule-associated protein Tau to dendritic spines. Biochim. Biophys. Acta Mol. Basis Dis. 1852, 913–924. https://doi.org/10.1016/j.bbadis.2014.12.017
- Yadav, R.K., Gautam, D.K., Muj, C., Gajula Balija, M.B., Paddibhatla, I., 2021. Methotrexate negatively acts on inflammatory responses triggered in Drosophila larva with hyperactive JAK/STAT pathway. Dev. Comp. Immunol. 123, 104161. https://doi.org/10.1016/j.dci.2021.104161
- Yang, K., Belrose, J., Trepanier, C.H., Lei, G., Jackson, M.F., MacDonald, J.F., 2011. Fyn, a potential target for alzheimer's disease. J. Alzheimer's Dis. 27, 243–252. https://doi.org/10.3233/JAD-2011-110353
- Yao, X., Xian, X., Fang, M., Fan, S., Li, W., 2020. Loss of miR-369 Promotes Tau Phosphorylation by Targeting the Fyn and Serine/Threonine-Protein Kinase 2 Signaling Pathways in Alzheimer's Disease Mice. Front. Aging Neurosci. 11, 1–10. https://doi.org/10.3389/fnagi.2019.00365
- Yasojima, K., Kuret, J., Demaggio, A.J., McGeer, E., McGeer, P.L., 2000. Casein kinase 1

- delta mRNA is upregulated in Alzheimer disease brain. Brain Res. 865, 116–120. https://doi.org/10.1016/S0006-8993(00)02200-9
- Yeh, P.A., Chien, J.Y., Chou, C.C., Huang, Y.F., Tang, C.Y., Wang, H.Y., Su, M.T., 2010. Drosophila notal bristle as a novel assessment tool for pathogenic study of Tau toxicity and screening of therapeutic compounds. Biochem. Biophys. Res. Commun. 391, 510–516. https://doi.org/10.1016/j.bbrc.2009.11.089
- Yin, X., Zhao, C., Qiu, Y., Zhou, Z., Bao, J., Qian, W., 2021. Dendritic/Post-synaptic Tau and Early Pathology of Alzheimer's Disease. Front. Mol. Neurosci. 14, 1–9. https://doi.org/10.3389/fnmol.2021.671779
- Zempel, H., Mandelkow, E.M., 2012. Linking amyloid-β and tau: Amyloid-β induced synaptic dysfunction via local wreckage of the neuronal cytoskeleton. Neurodegener. Dis. 10, 64–72. https://doi.org/10.1159/000332816
- Zempel, H., Thies, E., Mandelkow, E., Mandelkow, E.M., 2010. Aβ oligomers cause localized Ca2+ elevation, missorting of endogenous Tau into dendrites, Tau phosphorylation, and destruction of microtubules and spines. J. Neurosci. 30, 11938–11950. https://doi.org/10.1523/JNEUROSCI.2357-10.2010
- Zhang, Y.J., Xu, Y.F., Chen, X.Q., Wang, X.C., Wang, J.-Z., 2005. Nitration and oligomerization of tau induced by peroxynitrite inhibit its microtubule-binding activity. FEBS Lett. 579, 2421–2427. https://doi.org/10.1016/j.febslet.2005.03.041
- Zhao, L., Ma, Q.L., Calon, F., Harris-White, M.E., Yang, F., Lim, G.P., Morihara, T., Ubeda, O.J., Ambegaokar, S., Hansen, J.E., Weisbart, R.H., Teter, B., Frautschy, S.A., Cole, G.M., 2006. Role of p21-activated kinase pathway defects in the cognitive deficits of Alzheimer disease. Nat. Neurosci. 2006 92 9, 234–242. https://doi.org/10.1038/nn1630
- Zhou, X.Z., Kops, O., Werner, A., Lu, P.J., Shen, M., Stoller, G., Küllertz, G., Stark, M., Fischer, G., Lu, K.P., 2000. Pin1-dependent prolyl isomerization regulates dephosphorylation of Cdc25C and Tau proteins. Mol. Cell 6, 873–883. https://doi.org/10.1016/S1097-2765(05)00083-3
- Zhu, X., Rottkamp, C.A., Boux, H., Takeda, A., Perry, G., Smith, M.A., 2000. Activation of p38 Kinase Links Tau Phosphorylation, Oxidative Stress, and Cell Cycle-Related Events in Alzheimer Disease. J. Neuropathol. Exp. Neurol. 59, 880–888.

https://doi.org/10.1093/jnen/59.10.880

Zschätzsch, M., Oliva, C., Langen, M., De Geest, N., Özel, M.N., Williamson, W.R., Lemon, W.C., Soldano, A., Munck, S., Hiesinger, P.R., Sanchez-Soriano, N., Hassan, B.A., 2014. Regulation of branching dynamics by axon-intrinsic asymmetries in Tyrosine Kinase Receptor signaling. Elife 3, 1–24. https://doi.org/10.7554/elife.01699

Investigating the mechanism of Tau and Fyn mediated neurodegeneration in Alzheimer's disease

by Ravi Kant Yadav

Indira Gandhi Memorial Library

HYDERABAD-500 046.

Submission date: 22-Aug-2023 12:14PM (UTC+0530)

Submission ID: 2149317037

File name: Thesis_RaviKant_IGM.pdf (9.78M)

Word count: 22042 Character count: 117500

Investigating the mechanism of Tau and Fyn mediated neurodegeneration in Alzheimer's disease

ORIGINALITY REPORT **/**% SIMILARITY INDEX **INTERNET SOURCES PUBLICATIONS** STUDENT PAPERS PRIMARY SOURCES scicrunch.org Internet Source Submitted to Universiti Sains Malaysia Student Paper www.science.gov Internet Source www.ncbi.nlm.nih.gov Internet Source www.jneurosci.org Internet Source kclpure.kcl.ac.uk Internet Source Adam I. Ramsaran, Ying Wang, Ali Golbabaei, Bi-ru Amy Yeung et al. "A shift in the mechanisms controlling hippocampal engram formation during brain maturation", Cold Spring Harbor Laboratory, 2023

Dr. MADHUBABU G.B.
Assistant Professor
Dept. of Biotechnology & Bioinformatics
School of Life Sciences
University of Hyderabad
Gachibowli, Hyderabad-500 046, India.

8	Lina Ma, Xuefan Jiang, Qiaoyi Huang, Wenxuan Chen, Huiqin Zhang, Hui Pei, Yu Cao, Huichan Wang, Hao Li. "Traditional Chinese medicine for the treatment of Alzheimer's disease: A focus on the microbiota-gut-brain axis", Biomedicine & Pharmacotherapy, 2023	<1%
9	dev.biologists.org	<1%
10	ses.library.usyd.edu.au	<1%
11	Kazama, H "Innervation and activity dependent dynamics of postsynaptic oxidative metabolism", Neuroscience, 20080303	<1%
12	Marilyn D. Resh. "Fyn, a Src family tyrosine kinase", The International Journal of Biochemistry & Cell Biology, 1998	<1%
13	"Tau Protein", Springer Nature, 2017 Publication	<1%
14	library.usask.ca Internet Source	<1%
15	bdsc.indiana.edu Internet Source	<1%

16	Fredrik Eriksson, W. David Culp, Robert Massey, Lars Egevad, Donita Garland, Mats A. A. Persson, Pavel Pisa. "Tumor specific phage particles promote tumor regression in a mouse melanoma model", Cancer Immunology, Immunotherapy, 2006	<1%
17	Madison Chilian, Karen Vargas Parra, Abigail Sandoval, Juan Ramirez, Wan Hee Yoon. "CRISPR/Cas9-mediated tissue-specific knockout and cDNA rescue using sgRNAs that target exon-intron junctions in Drosophila melanogaster", STAR Protocols, 2022	<1%
18	pure.manchester.ac.uk	1
	Internet Source	< 1 %
19		<1 _%
19	internet Source www.mdpi.com	<1% <1% <1%

Journal of Comparative Neurology, 01/19/1998

Publication

22	journals.biologists.com Internet Source	<1%
23	www.science.org	<1%
24	www.frontiersin.org Internet Source	<1%
25	Lorelei D. Shoemaker, Laurel F. Fuentes, Shauna M. Santiago, Breanna M. Allen et al. "Human brain arteriovenous malformations express lymphatic - associated genes", Annals of Clinical and Translational Neurology, 2014 Publication	<1%
26	Pilipiuk, J "Increased IP"3/Ca^2^+ signaling compensates depletion of LET-413/DLG-1 in C. elegans epithelial junction assembly", Developmental Biology, 20090301	<1%
27	Submitted to University of College Cork Student Paper	<1%
28	Yinquan Fang, Jianing Wang, Lemeng Yao, Chenhui Li, Jing Wang, Yuan Liu, Xia Tao, Hao Sun, Hong Liao. "The adhesion and migration of microglia to β -amyloid (A β) is decreased with aging and inhibited by Nogo/NgR	<1%

pathway", Journal of Neuroinflammation, 2018

Publication

Exclude quotes

On

Exclude matches

< 14 words

Exclude bibliography On